MAGNETOSTRATIGRAPHIC INVESTIGATIONS OF THE LOWER PALEOZOIC SYSTEM BOUNDARIES, AND ASSOCIATED PALEOGEOGRAPHIC IMPLICATIONS

Thesis by

Robert Lowell Ripperdan

In Partial Fulfillment of the Requirements
for the Degree of
Doctor of Philosophy

California Institute of Technology
Pasadena, California

1990

(submitted 20 March 1990)

Acknowledgements

It is, of course, impossible to properly acknowledge all of the individuals who have contributed to this work. Foremost consideration must be given to Dr. Joseph L. Kirschvink, whose enthusiastic guidance and patient friendship continue to become more valuable and appreciated. Special recognition must also be given to Dr. Clair C. Patterson, who remains an inspiration and shining example of scientific thought. Others from the Caltech community who should also receive special acknowledgement for their assistance in a multitude of ways include Dr. Leon T. Silver, Dr. Donald C. Burnett, Dr. Peter Goldreich, Dr. James Morgan, Dr. Craig Jones, Ms. Atsuko Kobayashi Kirschvink, Mrs. Fran Barnard, Ms. Cheryl Contopulous, and Mrs. Dorothy Coy McDougall.

It would be unwise to attempt to list everyone else who has provided support in their various ways during my tenure at Caltech; someone would certainly be omitted unintentionally, as should not be. To all who take the time to read these acknowledgements, and who have given their time on my behalf- your help and love have been much appreciated, and will not be forgotten.

Table of Contents

Dedicated to my parents,

to those who wish to answer

their own questions,

and to those eager for

the questions to be asked.

Abstract

Continued refinement of a global Geologic Timescale solely through increased precision of biostratigraphic correlations philosophically suffers from the inherent lack of a universal reference frame. Geomagnetic polarity reversals, which occur relatively rapidly and simultaneously on a global scale, can provide the necessary universal reference frame, provided the polarity reversals are correlated within a well-defined biostratigraphic framework and occur with a fairly distinctive pattern.

Magnetostratigraphic correlations across the Cambrian-Ordovician boundary interval indicate that normal polarity zones correlative to Late Cambrian conodont zones occur within sections from Texas, northern China, western Newfoundland, central Australia, and possibly Kazakhstan. These correlations strongly suggest that temporal differences may exist between sections in the absolute time value of key biostratigraphic horizons. There may also be very brief normal polarity zones correlative with Early Ordovician conodont and graptolite zonations, but those relationships have not yet been well-established.

Magnetostratigraphic correlations allow polarity to be unambiguously determined for the relevant continental unit, even in the absence of previous paleomagnetic investigation. Extension of this to Late Cambrian and Early Ordovician paleogeographic problems indicate that North China, and probably also South China, underwent approximately 90° counterclockwise rotation during the Cambrian, and were most likely attached to or very near the present northern margin of Australia during that time.

Paleomagnetic results from Upper Silurian through Middle Devonian carbonates of the Barrandian area, Czechoslovakia have at least three components of magnetization preserved within them. Two of the components appear to pass the fold test, indicating that they pre-date the deformation creating the basin, constrained to be not later than Late Carboniferous. Differences between the two components probably correspond to different times of acquisition, and may record rapid plate motion of the Bohemian Massif during the Middle Paleozoic.

Paleomagnetic results from Upper Ordovician to Lower Silurian carbonates from Anticosti Island, Quebec are not reliable because of the extremely weak magnetization of these rocks. Sharp increases in intensity during thermal demagnetization experiments may provide insight into the chemical changes which occur within carbonate rocks during thermal demagnetization, but at the present time those phenomenon are not well understood.

Chapter One Introduction

By the mid-1800's, nearly all of the currently recognized geologic systems had been defined, and the utility of fossils for long-range correlation and the demarcation of geologic time had already been well-established. Most of the systems were recognized as discrete units bounded by sharp changes in the fossil or rock record, and were thought to represent changes which affected the entire planet (probably reflecting the lingering influences of catastrophism, which viewed the geologic record as dominated by a series of widespread natural disasters, and Werner's Neptunist scheme, which considered the time relationships of a single locality to reflect universal events).

In retrospect, placing system boundaries at major breaks in the stratigraphic record was a prescription for dilemma. Under such a scheme, a portion of geologic time could not be defined by a physical point in rock within the type locality (Figure 1.1). As the body of stratigraphic knowledge increased, it became clear that other localities preserved stratigraphic levels which were absent from the type area, and problems arose as to which system best encompassed the intervening strata. Fossil zones which had clear system affinities in one area were found to correspond more closely to different systems in other areas when multiple groups of fossils were compared. Regional geologic timescales that could not be accurately correlated to each other became established. As geologic data accumulated on a global scale, and as geologists became interested in the rates and timing of wide-ranging phenomena such as glaciations and biological extinctions, it became clear that time-equivalent, or chronostratigraphic, marker horizons were necessary constraints for global correlations.

Under the auspices of the International Union of Geological Sciences' International Commission on Stratigraphy (ICS), the stratigraphic community has for the past 25 years been attempting to address many of these problems primarily by refining the biostratigraphic correlations used to construct the geologic time scale. Unfortunately, this strategy generally suffers from one philosophical pitfall: the potentially fallacious assumption that equivalent *horizon* correlations, such as the first or last occurrences of a particular taxa or changes in sea-level, also represent equivalent *time* correlations. In fact, equivalence of time can only be established using a chronometer universal within the reference frame being investigated. For the earth, only the physical laws and certain global physical properties

Figure 1.1. Hypothetical Silurian-Devonian boundary demonstrating the difference between a system boundary and a period boundary. Systems are physical units, and are completely defined by the type locality, despite a bounding unconformity. Periods are the abstract equivalents of systems, and cannot be precisely defined when an unconformity is used for a system boundary.

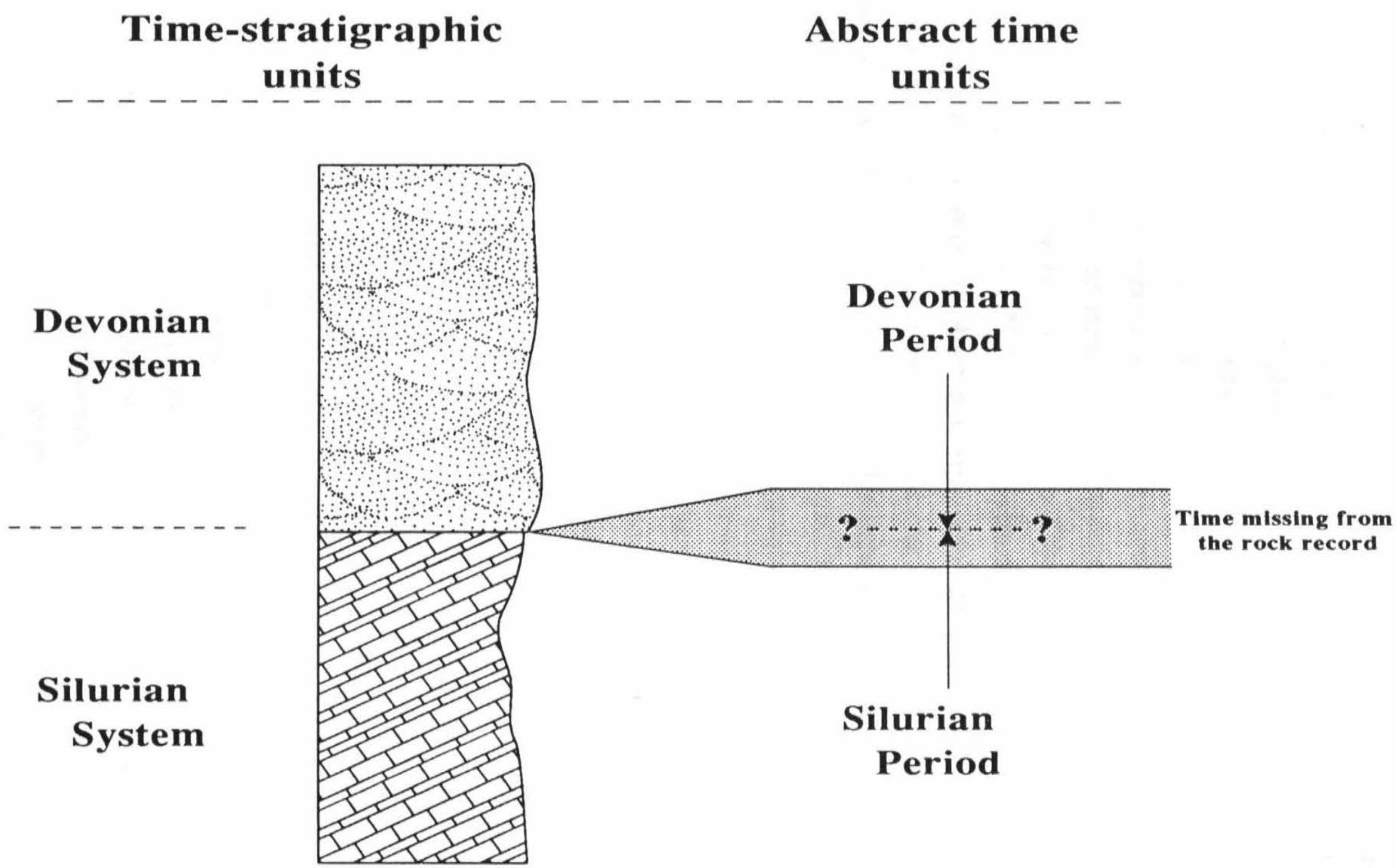
Time-stratigraphic units
Abstract time units
Devonian System
Silurian System
Devonian Period
Silurian Period
? ?
Time missing from the rock record

Figure 1.1

satisfy this requirement. Fossils are inadequate primarily because living organisms are influenced tremendously by their environment, and environments are subject to local changes that may not reflect a general planetary trend. Therefore, the time equivalence of fossil horizons in different localities needs to be demonstrated through another planetary clock before it can be considered reliable.

There are a plethera of planetary properties and physical laws which can be safely assumed to have everywhere the same value at the same time; examples include the obliquity of the planet's rotational axis to its orbit around the sun, the laws governing radioactive decay, and the length of the day. Unfortunately, virtually all of these properties and physical laws either leave no presently observable stratigraphic record of their value through time, or have changes so small as to be useful only for deducing very long term relationships. Radioactive decay can provide powerful insight into age relationships, but the preponderance of the fossil record lies within lithologies that are currently inaccessible to accurate radiochronology, and the associated error values for Paleozoic rocks (rocks older than about 230 million years) are too large to prove useful in establishing fine-scale stratigraphic relationships. However, one property of the earth leaves a readily observable record of its value in virtually all kinds of rocks, and, except for (geologically) very brief periods of time, has the same value simultaneously on a planetary scale: the polarity of the earth's magnetic dipole field.

Geomagnetic polarity stratigraphy, or magnetostratigraphy, involves determination of the earth's magnetic field polarity preserved in rocks. Polarity reversals of the earth's magnetic field are global events that probably take less than 10,000 years to complete (Harrison and Somayajulu 1966; Opdyke et al. 1973; many others). There is no evidence to suggest that normal and reversed polarities are simultaneously stable at the earth's surface, so that, except during the transitional periods of polarity changes or excursions, the geomagnetic field polarity is universal over the globe. Therefore, it is a logical conclusion that geomagnetic reversals can provide the necessary marker horizons useful for testing the chronostratigraphic significance of intercontinental biostratigraphic correlations.

Magnetostratigraphy has been widely applied to Cenozoic correlation problems for the past 20 years, and also to a lesser extent in Mesozoic correlations, but the technique has not previously been used for correlation problems involving the Lower Paleozoic except for the Precambrian-Cambrian boundary (Kirschvink 1978; Kirschvink and Rozanov 1984). One of the main reasons for this is the absence of marine magnetic anomalies older than Middle Jurassic: marine magnetic anomalies provide an ideal reference correlation for magnetostratigraphy, and without them correlations must originally be made to *define* a magnetic polarity reference scale rather than in conjunction with one. Also, even though the preservation of the geomagnetic field polarity is relatively insensitive to the rock type (the sole requirement being that a very minor amount of magnetic mineral be present), magnetostratigraphic correlations are most effectively made within a detailed biostratigraphic framework, which further compounds the difficulties in extending the technique to the Paleozoic: virtually all detailed Paleozoic biostratigraphies are found in either carbonate- or shale-rich sections, which are far from the most desirable lithologies for paleomagnetic work because they are often only weakly magnetic.

Overcoming the problems introduced by the use of weakly magnetic lithologies requires large numbers of samples, which increases the importance of identifying sample areas with the highest probabilities of success. However, the eligible candidates for sampling are greatly reduced by the need for a detailed biostratigraphic framework, and by the fact that older rocks have greater probabilities of having undergone levels of either metamorphorism or tectonization (or both) that may render them unsuitable for paleomagnetic work. Fortunately, an opportune side effect of the ICS effort to establish stratotype localities and precise boundary horizons for the geologic periods has been the detailed cataloguing of a large number of stratotype-quality sections from around the world. Many of the sections collected from during this study have been designated as global chronostratotypes by the ICS, or as potential chronostratotypes by the salient ICS boundary working group.

In addition to their potential for establishing chronostratigraphic relationships, magnetostratigraphic correlations provide important constraints for paleogeographic reconstructions. Many areas in the world have large gaps in the Paleozoic record, making construction of apparent polar wander paths (APWP), and quantitative constraints of paleogeographic positions, extremely difficult. Polarity stratigraphy allows the determination of hemisphere even in the complete absence of previous paleomagnetic work from the area, requiring only that one of the sections involved in the correlation comes from a continent with known polarity for that time interval. This proves to be invaluable when determining the paleogeographic positions of micro-continents, which often have limited stratigraphic records.

The identification of intercontinental chronostratigraphic horizons is essential for an accurate global view of the rates and timing of events in earth history. Magnetostratigraphy provides a unique correlation tool that is insensitive to the problems of lithologic facies or faunal endemism, and has a potential accuracy on the order of 10,000 years at reversal boundaries, while simultaneously providing valuable paleogeographic information.

Chapter Two **Methods of Investigation**

Magnetostratigraphic investigations using Paleozoic rocks face special problems that stem from the fact that the necessary detailed biostratigraphic framework almost always occurs within carbonate rocks. Carbonates are usually only weakly magnetized, so the use of a cryogenic magnetometer is necessary. Additionally, during thermal demagnetization experiments carbonates often display mineralogical alteration that obscures or obliterates the original magnetization (Lowrie and Heller 1982). Many modern carbonates lithologically similar to those used in these studies have magnetizations that are completely unblocked or obscured by mineralogical alteration at demagnetization temperatures around 400° Celsius (D. McNeill, pers. comm.). Carbonate rocks are also easily and strongly affected by weathering, and the effects of recrystallization on the existing magnetization are not presently well-understood. Yet another complication is the possibility that the magnetite occurring within a particular carbonate section is authigenic (McCabe et al. 1983).

Trying to overcome all of these problems often results in a paradox. The most desirable sections, those that have experienced very low temperatures of metamorphism or burial, often lack the structural complexity necessary to perform the fold test, making it impossible to constrain the age of the magnetization by this method. The best carbonate lithologies for paleomagnetic work are usually finer-grained platform limestones, which occur in a depositional regime generally lacking any conglomeratic units, thus making it impossible to establish the age of the magnetization through use of the conglomerate test. In the absence of any stability tests, then, the primary methods of assessing the reliability of results from sections are through applications of the consistency test and the reversal test. The reversal test has the inherent handicap that it is not applicable when a sample locality has only one polarity preserved, and is of limited validity when one polarity predominates over the other. The consistency test, which is based on the probability of similar magnetostratigraphic patterns arising in n number of sections through chance, is potentially the most powerful, and actually becomes stronger if one polarity predominates over another (although this increase has an upper bound; the test is useless if only one polarity is present). Since the probability rapidly becomes smaller as n becomes larger, a large number of sections (and samples) is desirable. This fact further strengthens the logic that period boundaries are the places to begin definition of a Lower Paleozoic magnetostratigraphic timescale.

2.1 Site and sample selections

Because carbonates are usually weakly magnetized, and often undergo mineralogical changes during thermal demagnetization, a great deal of care must be exercised in selecting sample areas. Ideal localities are those that have not experienced temperatures of burial or metamorphism exceeding the highest demagnetization temperature from which useful data can reasonably be expected to be obtained. For the purposes of this study a single criterion, the conodont alteration index (CAI), has been used to discriminate between desirable and undesirable sample localities. The CAI is a measure of the level of organic metamorphism occurring within the section (Epstein et al. 1977). Extrapolating the typical laboratory unblocking temperature back to Paleozoic times using time-temperature blocking relationships for magnetite (which is the dominant mineral carrying magnetic remanence in virtually all the rocks in this study), constrains the maximum conodont alteration indice (CAI) that permits elimination of thermal remagnetization as a likely source of the preserved direction (Figure 2.1). Generally, those relevant-aged sections exhibiting CAI values higher than 2.5 were not studied, on the grounds that the potential for the preserved directions being the result of thermal remagnetization is too high. CAI values for sections used in this study are given in Table 2.1

Diagenesis detrimental to paleomagnetic study often manifests itself in one or both of two forms: recrystallization of the surface material, with concomittant loss of the original direction; and development of iron oxides through secondary mineralization. Generally, both can be largely overcome by sampling the freshest exposures. However, in some localities this guideline proved to be insufficient, and results from these sites often reflected the influence of diagenesis.

A further complication is the possibility that the magnetite occurring within a particular carbonate section is authigenic (McCabe et al. 1983). In those studies that have identified authigenic magnetite, the mineral was found to be multi-domain and largely spheroidal in shape. To help identify those samples that may contain authigenic magnetite, IRM acquisition-AF demagnetization experiments were performed to characterize the magnetic mineralogy.

Once a site has been selected, the most important considerations for selecting samples are the freshness of exposure of the individual bed, the continuity of the outcrop, and the stratigraphic interval between samples in relation to the relevant biostratigraphic zones. Sampling intervals, which are given in Table 2.1, were generally as small as was logistically practical.

Figure 2.1 Comparison of conodont alteration indices (CAI) (after Epstein et al. 1977) with unblocking temperature-time curves for magnetite (after Pullaiah et al. 1975). Grey region indicates extrapolation of typical laboratory unblocking temperatures to plausible timescales of burial or metamorphism.

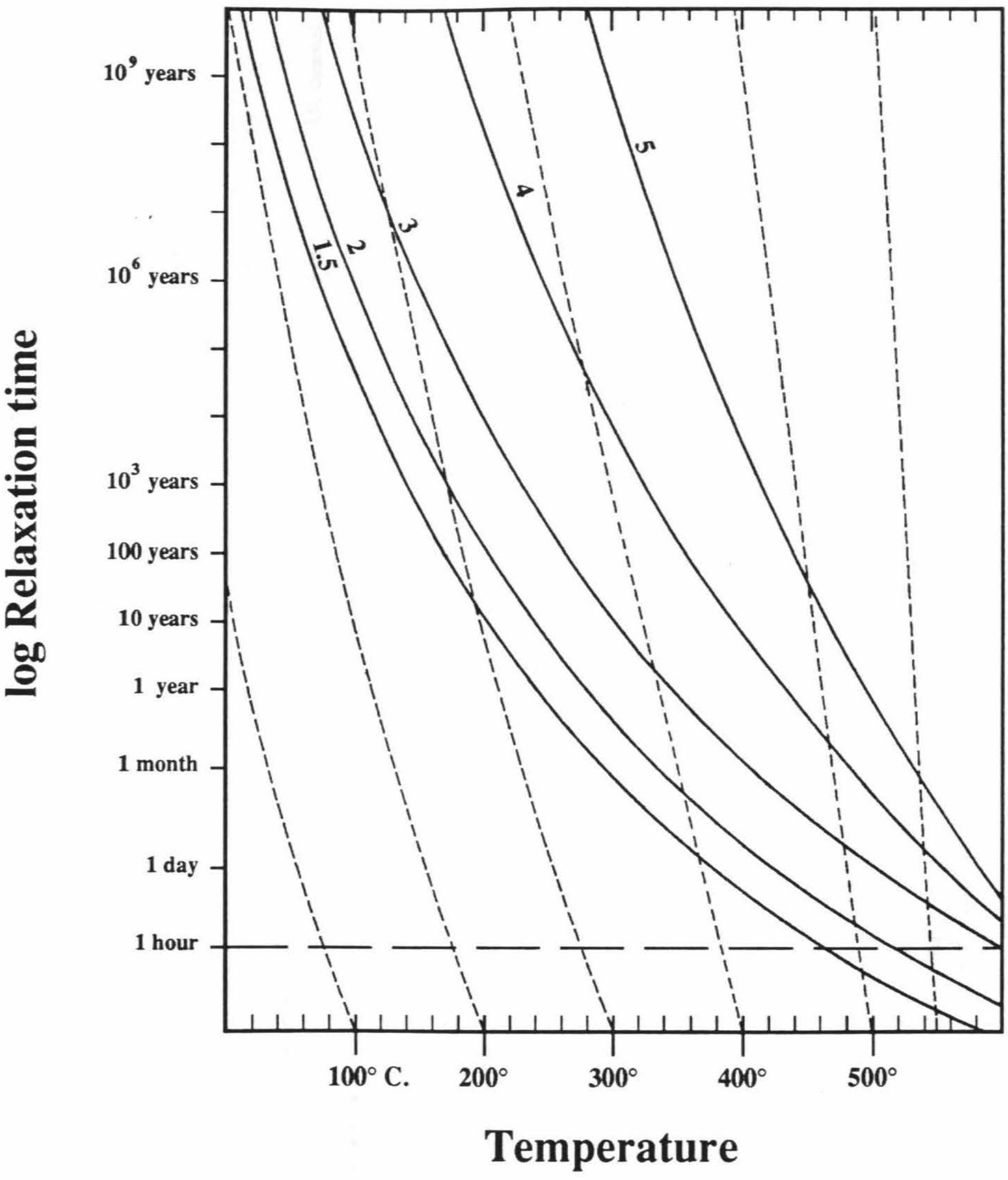
10⁹ years
10⁶ years
10³ years
100 years
10 years
1 year
1 month
1 day
1 hour
log Relaxation time
1.5
2
3
4
5
100° C.
200°
300°
400°
500°
Temperature

Table 2.1. General information for sample localities.

Locality and age	CAI	Collection technique	No. of sections	Total. no. of samples	Average interval	Field tests	Demagnetization techniques
*Malyi Karatau Range, Kazakhstan......Middle Cambrian-Earliest Ordovician. Collected July, 1984							
	1.0-1.5[1]	block	2	24	20 meters	fold	AF, thermal
Wilcox Pass, Alberta......Cambrian-Ordovician boundary. Collected July, 1985.							
	5.0+[2]	block	1	36	2 m.	-	(not analyzed)
Barrandian area, Czechoslovakia......Late Lochkovian-Early Gedinnian. Collected August, 1985.							
	2.0[3]	core	7	274	0.8 m.	fold	AF, thermal
*Yangtze Gorges area, China......Cambrian-Ordovician boundary. Collected September, 1985.							
	2.0[4]	core	1	75	0.6 m.	-	AF, thermal
Llano Uplift area, central Texas......Cambrian-Ordovician boundary. Collected June, 1986.							
	1.0-1.2[5]	core	2	92	1.3 m.	-	AF, thermal
Anticosti Island, Quebec, Canada......Late Ordovician-Early Silurian. Collected August, 1986.							
	1.0[6]	core	3	128	1.4 m.	congl.	AF, thermal
*Dayangcha, Jilin province, China......Cambrian-Ordovician boundary. Collected August, 1986.							
	1.5[7]	core	2	165	1.0 m.	-	AF, thermal
†Cow Head Group, western Newfoundland......Cambrian-Ordovician boundary. Collected September, 1986 and August, 1989.							
	1.5[8]	core,block	6	536	0.9 m.	congl., fold	AF, thermal
†Canadian Arctic archipelagao, Canada......Latest Ordovician-Early Devonian. Collected July, 1988.							
		core	2	187	35 m.	fold	(not analyzed)
Black Mountain, western Queensland, Australia......Cambrian-Ordovician boundary. Collected August, 1989.							
	1.0[9]	block	1	117	6.6 m.	-	thermal

* indicates sections collected by J.L. Kirschvink, California Institute of Technology, Pasadena, California.

† Work in progress.

References: [1]Apollonov et al. (1988), *Geological Magazine* **125**(4), p. 445-449; [2]J.L. Miller, pers. comm.; [3]G. Klapper, pers. comm.; [4]; [5]Miller et al. (1982) pp. 155-180 ***in*** The Cambrian-Ordovician boundary: sections, fossil distributions, and correlations; [6]C.R. Barnes, pers. comm.; [7]Chen et al. (1988). *Geological Magazine* **125**(4), p. 415-444; [8]Barnes, C.R. (1988), *Geological Magazine* **125**(4), p. 381-414; [9]B. Nicoll, pers. comm.

2.2 Sample collection techniques

There were two separate sample collection techniques employed during this investigation. One involved the collection of oriented block samples, with subsequent laboratory drilling of cores. The other employed a portable gas-powered drill (a specially-modified chain saw) equipped with diamond-tipped coring bits. The latter technique is much more rapid, eliminating the tedious step of drilling cores out of the blocks back in the laboratory, but it requires that a good supply of water be close by. Drilling also removes another source of error, since only one set of orientation measurements are required, instead of two. Most of the samples reported on here were collected as cores using either a McCullough or Pomeroy drill.

Sample orientations were determined in the field using both Brunton and (when possible) sun compasses. Standard procedure for both solar and magnetic orientation measurements involved placing a brass sleeve around the drilled core while it was still attached to the outcrop, and measuring the orientation of a plate orthogonal to the cylindrical axis of the core. By our convention, measurements with the Brunton compass were made with instrument north pointing to the right while facing the outcrop. Orientation marks were then placed on the core by running brass 'scritchers' down a thin gap at the top of the orienting sleeve, with the intention of leaving a distinctive sheen. Samples were labelled using "Sharpie" permanent ink pens, wrapped in paper, and labelled again. For most of this study, as an adopted convention sample labelling was done with the top of the core (that part nearest the edge of the outcrop) pointing to the left.

Block sampling was done with two conventions: Brunton measurements were done with compass north pointing to the right (as in core sampling), and measurements were made facing upslope. When possible, sun compass directions were also collected.

2.3 Laboratory preparation

Laboratory preparatory procedures involved converting block or core samples to a standard size for measurement in the magnetometer. Block samples required the drilling out of cores; this was done using a drill press modified to use coring bits. Orientations were then taken using the same equipment and techniques outlined above, with the added step that field orientations for the block were taken into account.

Before all other preparation steps, the cores had their brass orientation marks replaced by deep scratches, made using diamond-tipped scratching pens. Sample cores, which have a diameter of 2.5 cm, were cut to 2.5 cm in length using a Felker rock saw equipped with a stainless steel blade, and subsequently rinsed in a 4 N HCl bath until all ink marks were removed. After drying, the samples were labelled using Koh-i-noor opaque white ink. Broken samples were repaired using Zircar white cement. Reunification took place within a mu-metal shielded room, to eliminate the remanent magnetization associated with solidification of the cement (ZRM).

After final specimen preparation, the cores were placed within the shielded room and allowed to remain for at least one month before sample analysis, to facilitate loss of any viscous components of the natural remanence.

2.4 Sample analysis

2.4.1 Instrumentation

Paleomagnetic measurements were performed using an ScT cryogenic magnetometer with 2G SQUID electronics, interfaced to a dedicated Zenith XT-compatible or Apple IIe microcomputer controlling data collection and measurement procedures. Alternating-field demagnetization was done with a Schoenstedt model GSD-1 three-axis instrument. Thermal demagnetizations took place in a custom-built large-volume shielded oven.

Rock magnetic studies were performed on a 2G cryogenic magnetometer with 2G SQUID devices, interfaced to a (separate) dedicated XT-compatible microcomputer. Samples were crushed into 3-5 mm chunks, rinsed briefly in 1.2 N HCL, and placed within plastic vials, which served as sample holders during measurement procedures.

Excellent discussions concerning the principles utilized by the various types of magnetometers, including their construction and their relative strengths, and other instrumentation used in paleomagnetic research, can be found in Collinson (1983).

2.4.2 Demagnetization experiments

Both alternating-field (AF) and thermal demagnetization techniques were used on most samples. Typically, AF intensities did not exceed 15 mT (150 gauss) because of an anhysteretic remanent magnetization (ARM) that was pronounced above 15 mT. In most instances AF demagnetization procedures were controlled by microcomputer.

Thermal demagnetization yielded the more valuable information of the two demagnetization techniques used. Since carbonate rocks often do not give reliable results after heating at about 400° C., standard procedure was to perform thermal steps in 50° C. increments beginning with 100° C. up to 300° C., followed by 25° C. increments until the sample intensity decreased below the sensitivity of the instrument, about 10^{-5} Am^{-1} or increased by two orders of magnitude over the 200° C. measurement. (Using the 200° C. step as a basis for comparison eliminated the possible influence of magnetic components carried by goethite.) Heating times were generally one hour. For some samples, measurements were continued using higher temperatures despite fulfillment of one of the above criteria. However, there were no instances that suggested that these guidelines were unreliable as indicators that further data collection would be fruitless.

2.4.3. Rock magnetic studies

Rock magnetic studies used isothermal remanent magnetization (IRM) acquisition coupled with AF demagnetization. IRMs were induced using a custom-designed pulse-coil apparatus; typically, maximum IRM intensities attained were around 2 tesla. AF demagnetization was done with equipment manufactured by 2G Enterprises; maximum AF intensities were typically around 1 T. Both procedures were controlled by microcomputers.

A few experiments investigating the changes in rock magnetic properties with heating were undertaken. In these experiments, four splits, of approximately 1 gram each, were made from a single specimen; one split was unheated, and one each was heated for one hour at 150°, 300°, and 450° C. Each split then underwent identical protocols for IRM acquisition- AF demagnetization.

Magnetic mineral phases and sizes were estimated based on the shape of the IRM acquisition- AF demagnetization curves, and through use of the Lowrie-Fuller test (Lowrie and Fuller 1971; Cisowski 1981).

2.5 Data reduction

Data reduction was performed using the Macintosh-compatible QuickBasic program *Paleomag*, based on the principal component analysis techniques outlined in Kirschvink (1980) and developed at Caltech by Jones, Ripperdan, and Kirschvink (©1990).

Chapter Three Magnetostratigraphic results from the Cambrian-Ordovician boundary

Introduction

Agreement upon a horizon to represent the end of the Cambrian period has been difficult since the Cambrian system was first established by Adam Sedgewick in 1835. The original dispute (which is famous both for its participants, Sedgewick and his former student, Sir Roderick Murchison; and its acrimony, which ended in the dissolution of their long friendship) arose because the overlying Silurian, defined in southeastern Wales on biostratigraphic grounds by Murchison, had its base well below the top of Sedgewick's Cambrian system, which had been defined using the largely unfossiliferous strata in northwestern Wales. Their disagreement would not be resolved until 1879, when Charles Lapworth formally proposed a tripartite division of the Cambrian and Silurian strata, and defined the intermediate Ordovician system (Lapworth 1879).

Lapworth's own definition, which was solely on paleontologic grounds, placed the base of the Ordovician System at the base of the Lower Arenig Series in Wales, at the location of the change from Barrande's *'fauna primordiale'* to *'fauna seconde'*. However, correlation to other parts of the world indicated that the upper part of the Tremadoc Series in Wales should also be included in the Ordovician (Henningsmoen 1973). Much of this confusion was due to differences between Lapworth's personal definition of the Lower Arenig in Wales, and that of many other geologists Lapworth originally considered strata previously defined as Upper Tremadoc to be part of his Arenig Series. However, in 1902 Lapworth explicitly stated that 'the systematic base of the Ordovician System was *originally* drawn at the bottom of the Upper Tremadoc' (Henningsmoen 1973). Lapworth's placement of the Cambrian-Ordovician boundary at a major paleontological break, without direct specification of an individual representative taxon, further compounded the problem. Other workers outside Wales identified the change from the 'first' to 'second' faunas at stratigraphic levels ranging from the base of the (Lower) Tremadoc Series to the base of the Arenig Series (Figure 3.1). As a result, there has never been a universally recognized horizon representing the Cambrian-Ordovician boundary.

Under the guidance of the International Commission on Stratigraphy (ICS), the Cambrian-Ordovician Boundary Working Group (COBWG) has been seeking a biostratigraphic horizon suitable for unifying the various definitions for the Cambrian-Ordovician

Figure 3.1. The various levels at which the Cambrian-Ordovician boundary has been drawn in Britain and in Scandinavia (after Henningsmoen 1973).

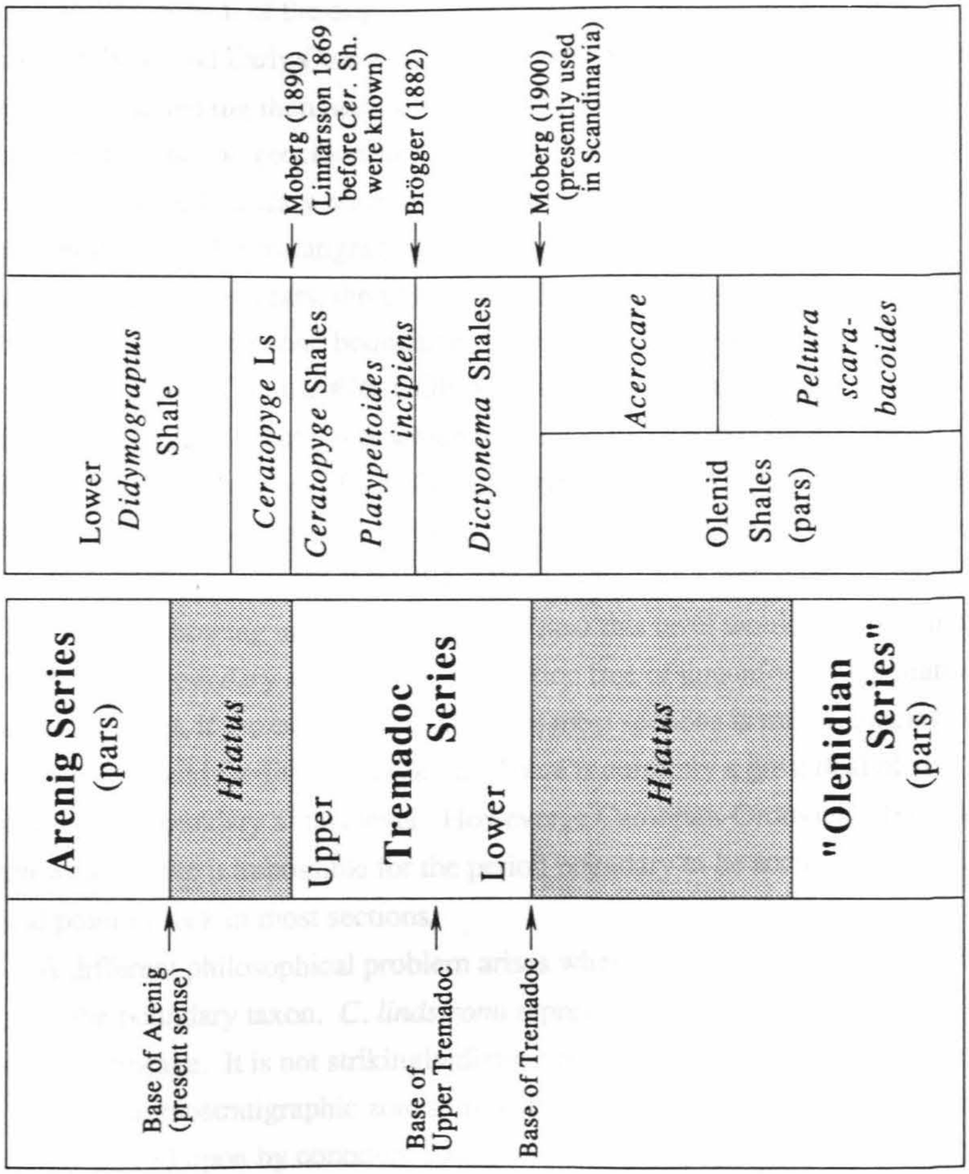
Britain
Scandinavia
Arenig Series
(pars)
Hiatus
Upper
Tremadoc
Series
Lower
Hiatus
"Olenidian
Series"
(pars)
Base of Arenig
(present sense)
Base of
Upper Tremadoc
Base of Tremadoc
Lower
Didymograptus
Shale
Ceratopyge Ls
Ceratopyge Shales
Platypeltoides
incipiens
Dictyonema Shales
Acerocare
Peltura
scara-
bacoides
Olenid
Shales
(pars)
Moberg (1890)
(Linnarsson 1869
before Cer. Sh.
were known)
Brögger (1882)
Moberg (1900)
(presently used
in Scandinavia)

Figure 3.1

boundary, to be located within a global stratotype section. Their efforts have concentrated on conodonts and graptolites, with current preference given to conodonts. Both groups are abundant and diverse in the boundary interval, with detailed biostratigraphic zonations (Miller 1988; Erdtmann 1988). Trilobites also serve as valuable correlation tools, and were an important component of the original definition of the base of the Ordovician, but most of the Late Cambrian and Early Ordovician faunas are apparently highly provincialized (Shergold 1988), making them unsuitable as global biochrons. Recent studies have also been undertaken into the geochemical (J. Wright) and paleomagnetic (this study) signatures occurring across the boundary horizon, in hopes of helping to establish the chronostratigraphic significance of biostratigraphic correlations.

For the past four years, the COBWG has focused principally on choosing between the base of two conodont zone boundaries, *Cordylodus proavus* and *Cordylodus lindstromi* (COBWG Circular #26; COBWG Circular #25), for the Cambrian-Ordovician boundary. The current debate over which horizon is more appropriate revolves around questions basic to the concept of a global stratotype. Many of the sections throughout the world have hiatuses interpreted by some to represent a eustatic sea level drop coincident with the base of *C. proavus* (Miller 1984). Establishing the Cambrian-Ordovician at this level in a section showing unconformities at or near this level would be most undesirable. Placement of the boundary at this level in a section free of unconformity or hiatus would be satisfactory; in fact, if the extent of the hiatus in most sections is minor, placing the boundary at this level could facilitate correlation. There is currently a great deal of support for establishing the boundary at this level. However, a Cambrian-Ordovician boundary at this horizon would make it impossible for the period boundary to be accurately correlated to a physical point in rock in most sections.

A different philosophical problem arises when considering *Cordylodus lindstromi* for use as the boundary taxon. *C. lindstromi* represents an intermediate member of an evolutionary lineage. It is not strikingly distinct from other members of the lineage also used to establish biostratigraphic zones; in fact, the taxonomy of *C. lindstromi* has not been universally agreed upon by conodont specialists. For many, it is difficult to support the establishment of a boundary at an observer-specific level. However, the *C. lindstromi* zone is much closer to the historical concept of the base of the Ordovician, which is essentially at the first appearance of nematophorous (planktonic) graptolites.

The results from this study strongly suggest that the first observed occurrences of *Cordylodus proavus* and *Cordylodus lindstromi* do not represent chronostratigraphic horizons. Unfortunately, little concern has been expressed over the chronostratigraphic significance of either of these biostratigraphic levels. A motion is currently under consideration by the COBWG that would allow re-introduction of candidate sections which are not amenable to magnetostratigraphy, thereby excluding the possibility of establishing their absolute time relationships with respect to other important sections. If the Cambrian-Ordovician *system* boundary is established within a section from which no magnetostratigraphic information can be obtained, it would mean that the Cambrian-Ordovician *period* boundary would remain uncorrelatable, since the time significance and relationships of the system boundaries in various parts of the world could not be established. It is hoped that this study demonstrates the importance of establishing the Cambrian-Ordovician boundary within a global stratotype that permits accurate determination of the magnetostratigraphy of the boundary interval, thereby allowing confident establishment of a chronostratigraphic boundary in other sections.

MAGNETOSTRATIGRAPHY OF THE CAMBRIAN-ORDOVICIAN BOUNDARY INTERVAL

Robert L. Ripperdan and Joseph L. Kirschvink
Division of Geological and Planetary Sciences
California Institute of Technology
Pasadena, California 91125 U.S.A.

M.K. Apollonov
Institute of Geological Sciences of the Academy of Sciences of the Kazakh SSR
Kalinina 69a, Alma-Ata 100, USSR

G.G. Ma, Z.C. Zhang
Yichang Institute of Geology and Mineral Resources
Yichang, Hubei, People's Republic of China

April 1990

Division Contribution #4482

Abstract

Magnetostratigraphic results from Cambro-Ordovician boundary-age sections in North America, China, Kazakhstan and Australia indicate that the Late Cambrian geomagnetic field had predominantly reverse polarity with short, highly correlative intervals of normal polarity within the Upper Cambrian conodont zones *Proconodontus muelleri, Proconodontus posterocostatus, and Cordylodus proavus.* This polarity pattern provides a globally isochronous framework for constraining intercontinental chronostratigraphic correlations. Other intervals of normal polarity occurring in younger strata are presently difficult to correlate.

These results also constrain polarity (with respect to North America and Australia) for the apparent polar wander paths of the North China block and Kazakhstan, placing Kazakhstan in the southern hemisphere and North China near the equator by the end of the Cambrian.

1. Introduction

The Cambrian-Ordovician boundary presents an excellent opportunity for magnetostratigraphic study primarily for two reasons: 1) the boundary interval has been recognized within many sections, providing a variety of lithologies to sample and increasing the likelihood of determining a workable polarity reversal stratigraphy, and 2) a diverse fauna of conodonts, graptolites and trilobites has been characterized from the boundary interval, establishing a detailed framework for correlation in a number of different facies and faunal provinces.

Fifteen sections at 7 different localities were investigated for their geomagnetic polarity stratigraphy (Figure 3.2). Of the sections studied critically by the Cambrian-Ordovician Boundary Working Group (COBWG), those in Kazakhstan, Texas, North and South China, western Newfoundland and central Australia have higher likelihoods for successful paleomagnetic research because they have low conodont alteration indices (CAI) (Table 3.1), indicating the sections have experienced low levels of thermal or burial metamorphism (Epstein *et al.* 1977). The sections near Dayangcha, (northern) China and the western Newfoundland Cow Head Group sections at Broom Point, Green Point, Martin

Figure 3.2. Sample localities. Abbreviations: WPA) Wilcox Pass, Alberta, Canada; LUT) Llano Uplift area, central Texas; CHN) Cow Head Group, western Newfoundland, Canada; KAZ) Malyi Karatau Range, Kazakhstan SSR; YGC) Yangtze Gorges area, Hubei province, China; DAY) Dayangcha, Jilin province, China; and BMA) Black Mountain, western Queensland, Australia.

Figure 3.2

Table 3.1. Conodont alteration indices for Cambro-Ordovician boundary-aged localities sampled for this study.

Locality	CAI	Average lab. blocking temp.*
Malyi Karatau Range, central Kazakhstan SSR	1.0-1.5[1]	400-500° C.
Yangtze Gorges area, Hubei province, China	2.0[2]	~300°
Llano Uplift area, central Texas, USA	1.0-1.2[3]	300-400°
Dayangcha, Jilin province, China	1.5[4]	350-450°
Cow Head area, western Newfoundland, Canada	1.5[5]	350-400°
Black Mountain, western Queensland, Australia	1.0[6]	400-450°

References: [1] Apollonov *et al.* 1988; [2]G.G. Ma, pers. comm.; [3]Miller *et al.* (1982); [4]Chen *et al.* (1988); [5]Barnes (1988); [6]R. Nicoll, pers. comm.

*Average laboratory blocking temperatures represent the temperatures at which the magnetic moment drops below 1.5×10^{-11} Am^2, or the magnetic moment increases by two or more orders of magnitude over the NRM.

Point, and St. Paul's Inlet are of particular importance because of their prominence as potential international stratotypes for the Cambrian-Ordovician boundary (COBWG 1985).

On its own, magnetostratigraphy is not generally useful in Paleozoic rocks. However, when used in conjunction with other stratigraphies, the technique can provide certain refinements. Geomagnetic field polarity is a property of the earth's deep interior, and in the absence of secondary effects, the polarity preserved in sediments is not sensitive to changes in facies, allowing different depositional environments to be correlated with high accuracy at reversal boundaries. Also, polarity reversals are globally isochronous events that take less than 10,000 years to complete. Magnetostratigraphy, therefore, is potentially useful as a tool whereby global biostratigraphic correlations can be made in a global chronostratigraphic framework without the difficulties imposed by facies-dependent or endemic faunas.

Another important benefit of magnetostratigraphy is the ability to resolve polarity ambiguities in the apparent polar wander paths (APWP) of continental blocks for which little or no previous paleomagnetic data exists. Paleomagnetic data alone cannot determine which hemisphere a continental block was in at the time of deposition, especially in blocks that may have undergone substantial rotations and plate motions. However, by correlating polarity patterns from areas where the APWP is well-known, such as North America and Australia, to places where the polarity has not previously been determined, like North China and Kazakhstan, the ancient geomagnetic field polarity can be established. This, in turn, constrains hemispheric relationships with respect to the reference APWP, facilitating paleogeographic reconstructions.

The major problem encountered in magnetostratigraphic research when using Paleozoic rocks is determining whether the preserved paleomagnetic directions have any relationship to the geomagnetic field at the time of deposition. There are a number of ways that the original magnetic directions can be lost; common examples include through diagenesis and thermal resetting. This problem is compounded by the lack of a geomagnetic polarity reference scale such as that preserved in marine magnetic lineations, which dates back only to the Middle Jurassic. Carbonate sections, the most logical choices for Paleozoic magnetostratigraphy because of their abundant fossils, are particularly difficult to work with: carbonate samples have a tendency to develop new minerals around 400° C. during thermal demagnetization experiments, with consequent loss of the original directions. Furthermore, two of the field tests for magnetic stability, the fold and conglomerate tests, are often not applicable in the carbonate sections most suited for magnetostratigraphic studies as determined by CAI, since one of the logical reasons for a low CAI is a lack of tectonic activity and one of the common features of a highly continuous section is a stable, low-energy environment of deposition. Because of these problems, it is most important that a number of sections that can be correlated accurately with fossils be studied, so that any internal consistency of the magnetostratigraphic data occurs within a tightly-constrained framework. This fact makes period boundaries, which are historically the time intervals most closely scrutinized by stratigraphers, logical places to begin assembling a geomagnetic polarity time scale for the Paleozoic.

2. Previous results

Previous paleomagnetic studies from rocks this old are few, and investigations with accurate knowledge of the age of the samples are even rarer. Watts *et al.* (1980), using Upper Cambrian carbonates and sandstones of the Wilberns Formation in the Llano Uplift area of central Texas, found that the polarity of their samples was predominantly reversed, with a short zone of mixed polarities possibly occurring within the upper part of the Cap Mountain Limestone (Figure 3.3). Studies by Khramov *et al.* (1965) and Rodionov (1966) from the Siberian platform determined large-scale polarity patterns in at least 10 Upper Cambrian and Lower Ordovician sections, but locating their results within the present biostratigraphic framework in Siberia is problematic, making correlation to the Cambrian-Ordovician boundary sections used in this study difficult.

Recent studies, by Prasad (1986) and Deutsch and Prasad (1987), using Cambrian-Ordovician carbonates in western Newfoundland, broadly identified the Lower Ordovician geomagnetic field as reversed polarity, with the Middle Ordovician showing normal polarity. Their work did not concentrate on the Cambrian-Ordovician boundary interval, and from their results it was impossible to construct a magnetic polarity stratigraphy across the boundary, but it suggested that polarity reversals might be preserved in the Cow Head Group.

Figure 3.3. Generalized magnetostratigraphic results of Watts *et al.* (1980) for Upper Cambrian units in the Llano Uplift area (after Watts *et al.* 1980). Results are constrained at the member level.

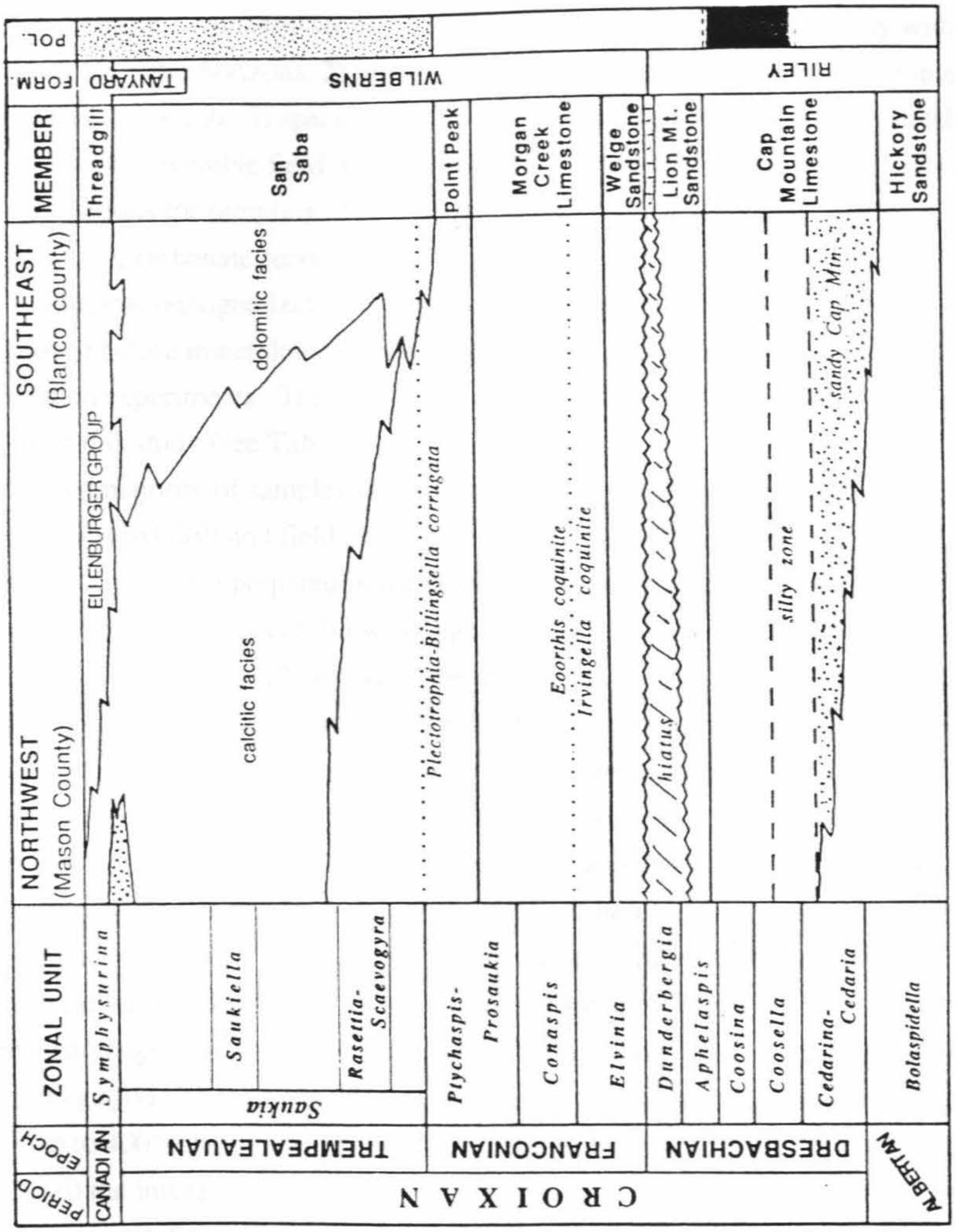

PERIOD
EPOCH
ZONAL UNIT
NORTHWEST (Mason County)
SOUTHEAST (Blanco county)
MEMBER
FORM.
POL.
CANADIAN
Symphysurina
Threadgill
TANYARD
ELLENBURGER GROUP
Saukia
Saukiella
Rasettia-Scaevogyra
TREMPEALEAUAN
calcitic facies
dolomitic facies
San Saba
WILBERNS
Ptychaspis-Prosaukia
Plectotrophia-Billingsella corrugata
Point Peak
Conaspis
FRANCONIAN
Eoorthis coquinite
Irvingella coquinite
Morgan Creek Limestone
Elvinia
Welge Sandstone
Dunderbergia
hiatus
Lion Mt. Sandstone
Aphelaspis
Coosina
DRESBACHIAN
Coosella
silty zone
Cap Mountain Limestone
RILEY
Cedarina-Cedaria
sandy Cap Mtn.
Bolaspidella
ALBERTAN
Hickory Sandstone
CROIXAN

3. Sampling strategy and techniques

Ideally, the following criteria should be met when collecting samples for magnetostratigraphic research from any section: 1) samples should be located precisely with respect to biostratigraphic horizons, 2) samples should be collected with as small an interval as is possible or reasonable, 3) special attention should be paid to prominent correlatable horizons, and 4) any possible field tests should be performed. Furthermore, the selection of carbonate sections for sampling should be based in part on the conodont alteration indice (when applicable); carbonate sections with CAIs of greater than 2.5 have a much higher potential for thermal remagnetization components (see Figure 3.4) that cannot be completely removed before mineralogical changes obliterate *in situ* directions during thermal demagnetization experiments. These selection criteria have been more or less fulfilled for the sections in this study (see Table 3.1).

The vast majority of samples were collected as 2.5 cm diameter cores using a portable gas-powered drill and field oriented with both magnetic and (when possible) sun compasses. Samples were prepared in the laboratory by trimming to 2.5 cm length with a Felker rock saw, followed by careful washing in 1.2N HCl to remove any stainless steel particles that may have been left behind by the drill bit or saw blade. All broken samples were glued using Zircar cement, with re-assembly taking place inside a mu-metal shielded room. Samples were measured using an ScT cryogenic magnetometer with 2G SQUID electronics, interfaced to a dedicated Zenith XT-compatible microcomputer, which controlled measurement procedures. Both alternating-field and thermal procedures were used on most samples during demagnetization experiments. Alternating-field demagnetization was done with a Schoenstedt model GSD-1 three-axis instrument. Alternating-field intensities were usually limited to below 15 millitesla (150 gauss) because of a prominent anhysteretic remanent magnetization (ARM) component that typically began to appear in samples at 20 mT (200 gauss). Thermal demagnetizations were usually carried out using 50° C. increments up to 400°, and then with smaller increments to the Curie point of magnetite (580° C.), until the intensity of the sample was less than 1.5×10^{-5} Am^{-1} (1.5×10^{-8} emu), or until the measured direction was demonstrably the result of mineralogical changes during heating. The primary criteria used for recognition of the latter were order-of-magnitude increases in intensity accompanied by random demagnetization trends when viewed in orthogonal and equal area projection. During subsequent data analysis, components of magnetization were identified using the principal component techniques outlined in

Figure 3.4. Comparison of CAI and log time-temperature curves for magnetite unblocking. CAI curves from Epstein *et al.* (1977); magnetite unblocking curves from Pullaiah *et al.* (1975). Comparisons of unblocking temperatures with organic metamorphism temperatures, indicated by CAI, are used to estimate the probability of the unblocked component being a thermal remanent magnetization (TRM). Under this scheme, for a sample bearing conodonts with CAI=2.5 and length of thermal event=10^8 years, the laboratory unblocking temperature necessary to rule out a TRM source for a component carried by magnetite is ~300° C.

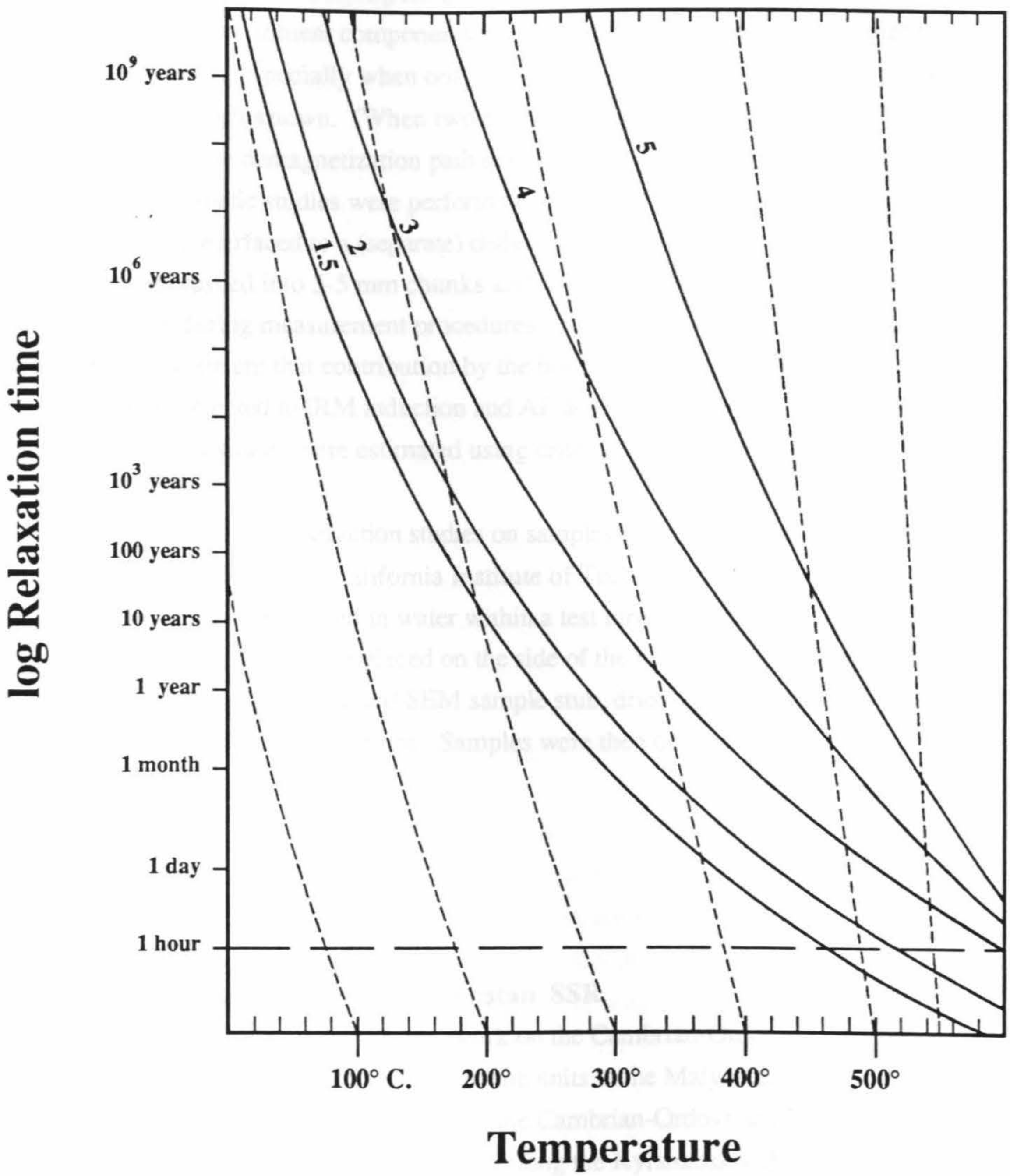
10^9 years
10^6 years
10^3 years
100 years
10 years
1 year
1 month
1 day
1 hour
log Relaxation time
5
4
3
2
1.5
100° C.
200°
300°
400°
500°
Temperature

Figure 3.4

Kirschvink (1980). For most of the samples in this study, single components could not be completely isolated by demagnetization. However, the trend of the demagnetization trajectory was often useful in identifying the polarity of the sample. Also, some measure of the consistency of the constituent components was gained by comparison of the poles of the least-squares planes, especially when only two components were present and one of the components was well-known. (When two components are being removed during demagnetization, the demagnetization path describes a plane in equal area projection.)

Rock magnetic studies were performed on a 2G cryogenic magnetometer with 2G SQUID devices, interfaced to a (separate) dedicated Zenith XT-compatible microcomputer. Samples were crushed into 3-5 mm chunks and placed within plastic vials, which served as sample holders during measurement procedures. The average sample weight was about 1 gram, enough to ensure that contribution by the holder to the total moment was negligible. Samples were subjected to IRM induction and AF demagnetization to obtain characteristic curves, and compositions were estimated using criteria outlined by King (1982) and Cisowski (1981).

Magnetic mineral extraction studies on samples from Batyrbay ravine were carried out by S.-B. R. Chang at the California Institute of Technology. Samples were ground into a coarse powder and placed in water within a test tube. Magnetite was then extracted with a cobalt-samarium magnet placed on the side of the test tube. After 1 day the sample was collected, placed on a standard SEM sample stub, dried, and AF demagnetized to reduce aggregation of magnetite grains. Samples were then observed using a scanning electron microscope.

4. Results

4.a. Malyi Karatau Range, Kazakhstan SSR

Our initial magnetostratigraphic work on the Cambrian-Ordovician boundary was done with 24 samples collected from limestone units in the Malyi Karatau Range of south-eastern Kazakhstan during the 1984 visit of the Cambrian-Ordovician Boundary Working Group. The sections at Batyrbay ravine and along the Kyrshabakty River are excellent candidates for magnetostratigraphy study because they contain nearly continuous sequences, have CAIs of 1.0-1.5 (Apollonov *et al.* 1988), and have been the objects of intense paleontologic investigation, the results of which are excellent biostratigraphic zonations based on both conodonts and trilobites. Also, sufficient structural complexity exists both within and between sections to perform fold tests.

An average of one sample per trilobite zone was collected from the middle of the Middle Cambrian to just below the base of the Ordovician, with most of the samples collected at trilobite zonal boundaries. Alternating-field and thermal demagnetization revealed two magnetic components, one of low coercivity and thermal stability with a direction very similar to that of the present-day geomagnetic field in Kazakhstan, and another two-polarity component dipping moderately downwards to the southwest (Figure 3.5; Table 3.2). The latter component passes the fold test (McElhinney 1964, McFadden and Jones 1981) at the 99% confidence level (Figure 3.6), indicating it was acquired before deformation of the area, interpreted to have begun in the Late Ordovician during formation of the Aksai structural belt (Abdulin *et al.* 1984). Comparison of unblocking temperatures for this component to the maximum metamorphic temperatures indicated by the regional CAI suggest that any contribution of a thermal remanent magnetization (TRM) to this component is insignificant.

Rock magnetic studies and mineral extractions indicate that the primary carrier of remanence is magnetite (Figure 3.7). Although other investigations have demonstrated the existence of authegenic magnetite in some limestones (McCabe *et al.* 1983), the formation of which could have preceded deformation while post-dating deposition, we found no evidence for a low-coercivity spheroidal fraction consistent with their findings. Coupled with the positive fold test and the low CAI of the region, this suggests that the high-stability component preserved in magnetite and isolated during thermal demagnetization is probably representative of the geomagnetic field at or immediately after the time of deposition.

The results from this preliminary suite of samples indicate that the geomagnetic field had predominantly single polarity from the Middle Cambrian *Ptychagnostus atavus* trilobite zone up through at least the base of the *Eoconodontus alisonae* conodont zone of the Upper Cambrian (Figure 3.8). This is in general agreement with the Upper Cambrian results of Watts *et al.* (1980) from the Llano Uplift area of central Texas, and on this basis the polarity was interpreted to be reverse. The youngest sample, taken from the *E. alisonae* (conodont)-*Lotagnostus hedini* (trilobite) zone boundary, about 5 meters below the first occurrence of *Cordylodus proavus* at Batyrbay, shows opposite (normal) polarity. Because only one sample of our original suite showed opposite polarity it was impossible to demonstrate conclusively that a reversal occurred at this level. However, recent studies by other investigators in Alma-Ata have both confirmed our original conclusion and

Figure 3.5. Typical demagnetization trend in orthogonal (left) and equal area projection for samples with reverse polarity. Sample CTZ 14.0, Kyrshabakty River section. In orthogonal projection, filled squares represent declination; empty squares represent inclination. Filled circles in equal area projection represent positive (down) inclinations. NRM=natural remanent magnetization.

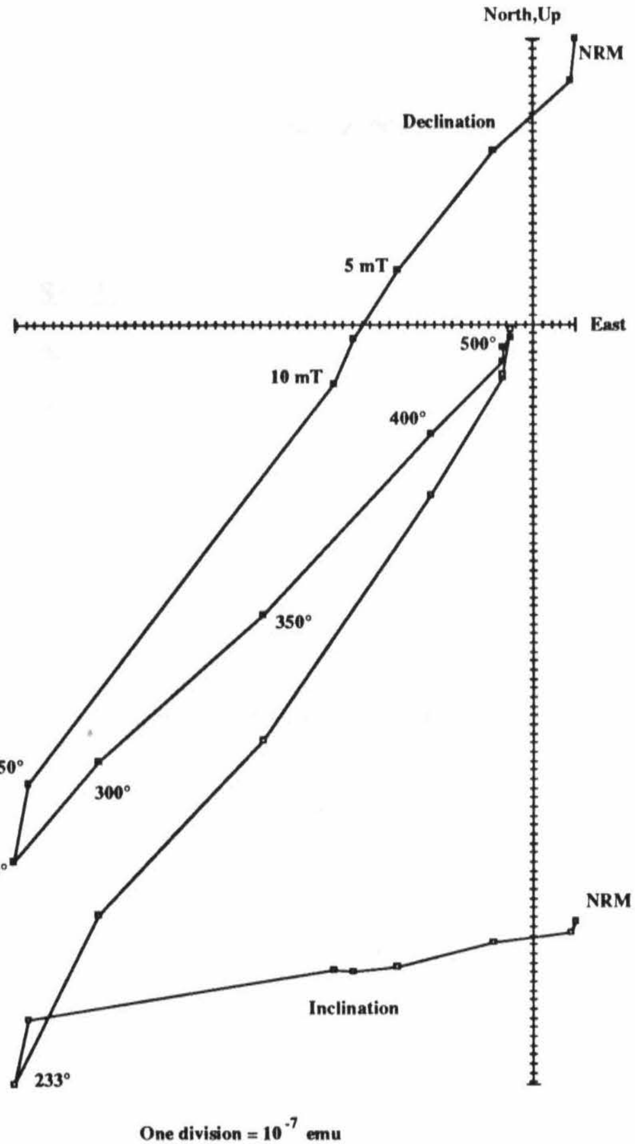

Malyi Karatau Range, Kazakhstan
Sample CTZ 14.0

Corrected for tilt of bedding

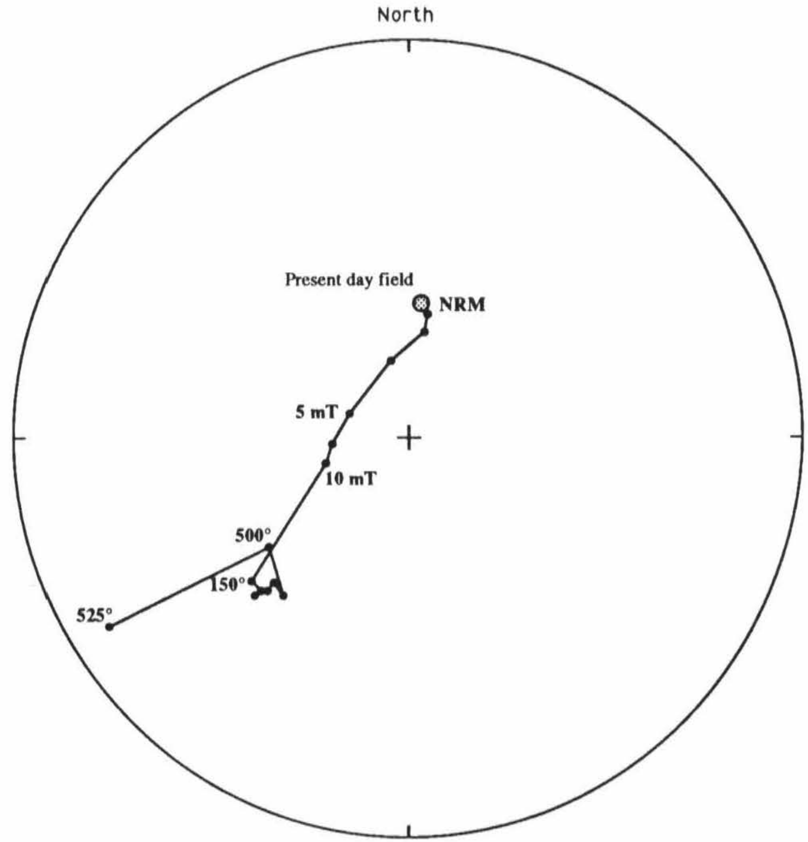

Figure 3.5

Table 3.2. Section mean directions, statistics, and pole positions for Upper Cambrian carbonates from the Malyi Karatau Range, southwestern Kazakhstan SSR.

				(Geographic)			(Tilt-corrected)							
Section	R_t	R_s	R_p	Decl	Incl	k	Decl	Incl	k	α_{95}	Pole Position		dm	dp
Both sections located at 43.5° N., 70.0° E.														
Batyrbay ravine	5	4	5	229°	-59°	17	229°	44°	18	19°	7° S.	27° E.	24°	15°
Kyrshabakty River	19	16	17	222°	-44°	8	221°	42°	41	6°	13° S.	32° E.	7°	5°
mean of both sections	24	20	22	223°	-47°	9	223°	43°	37	5°	11° S.	31° E.	6°	4°

R_t = total number of samples analyzed
R_s = total number of samples used to calculate statistics
R_p = total number of samples used for polarity interpretation
Decl = declination
Inc = inclination
k = the estimate of Fisher's precision parameter

α_{95} = associated radius of the cone of 95% confidence (McElhinny 1973)
dp and dm = semiminor and semimajor axes of the oval of 95% confidence around the poles

Figure 3.6. Characteristic directions isolated by least-squares analysis, in geographic and tilt-corrected coordinates. The directions pass the fold test of McElhinney (1964) at the 99% level ($k_2 / k_1 = 4.1$). Filled circles represent positive inclinations; shaded oval represents α_{95} circle of confidence.

Figure 3.7. Isothermal remanent magnetization (IRM) acquisition versus AF demagnetization of sample CTZ 14.0. Solid circles represent AF demagnetization of ARM (anhysteretic remanent magnetization).

Figure 3.8. Stratigraphic positions and polarity interpretation for samples from the Malyi Karatau Range, Kazakhstan SSR. (a) Kyrshabakty River section; (b) Batyrbay ravine section.

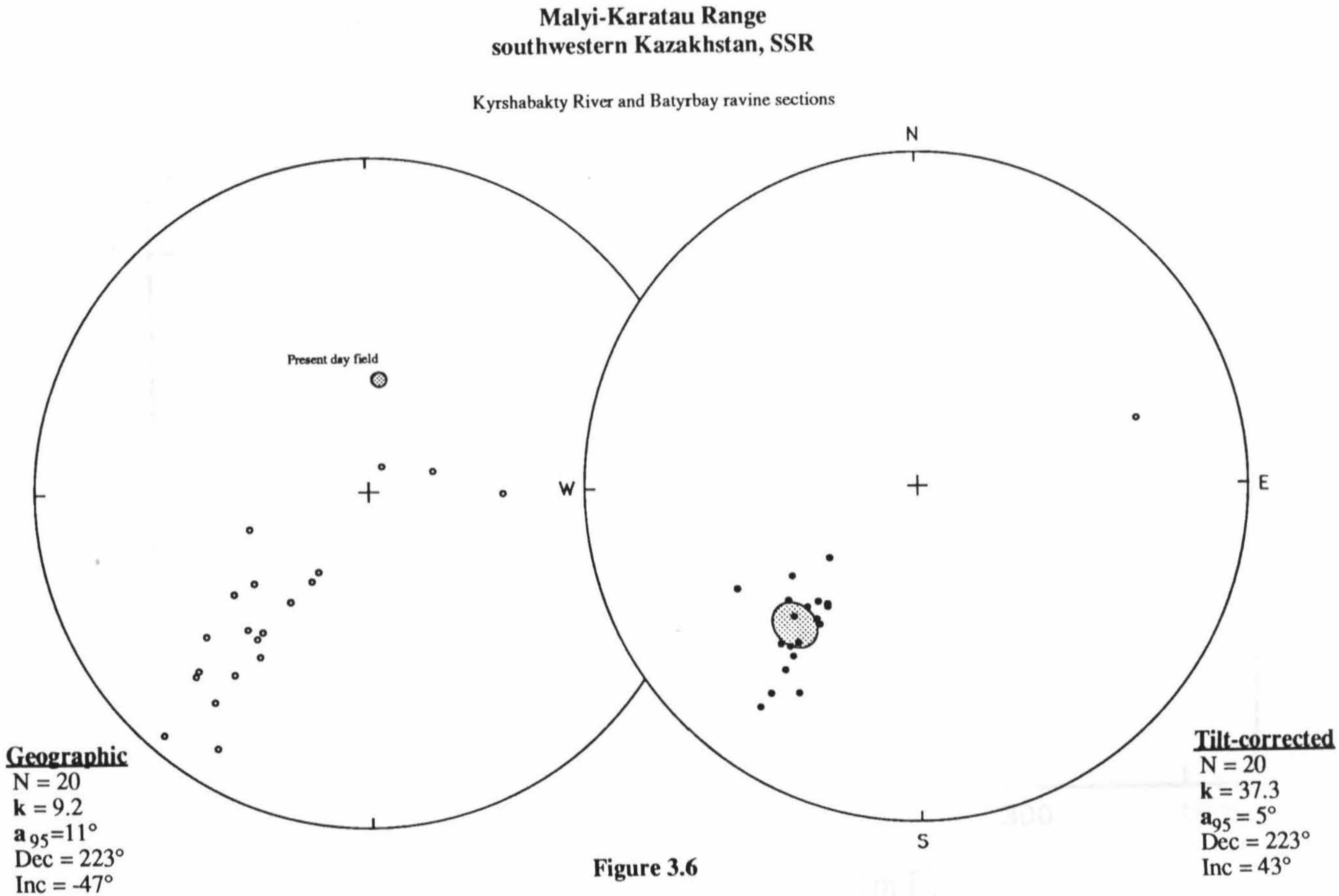
Malyi-Karatau Range
southwestern Kazakhstan, SSR
Kyrshabakty River and Batyrbay ravine sections
N
W
E
S
Present day field
Geographic
N = 20
k = 9.2
a 95=11°
Dec = 223°
Inc = -47°
Tilt-corrected
N = 20
k = 37.3
a95 = 5°
Dec = 223°
Inc = 43°

Figure 3.6

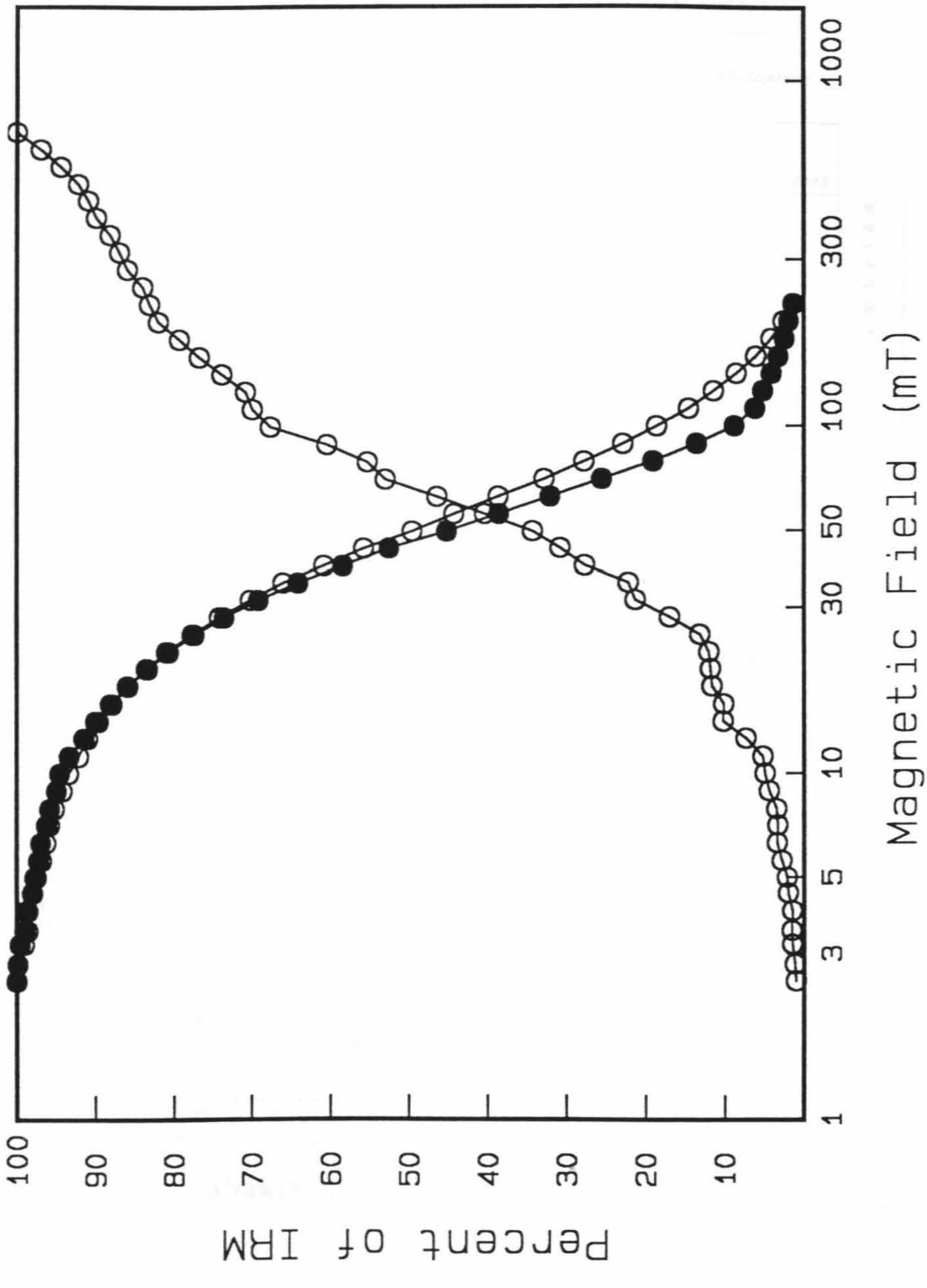
Percent of IRM
100
90
80
70
60
50
40
30
20
10
1
3
5
10
30
50
100
300
1000
Magnetic Field (mT)

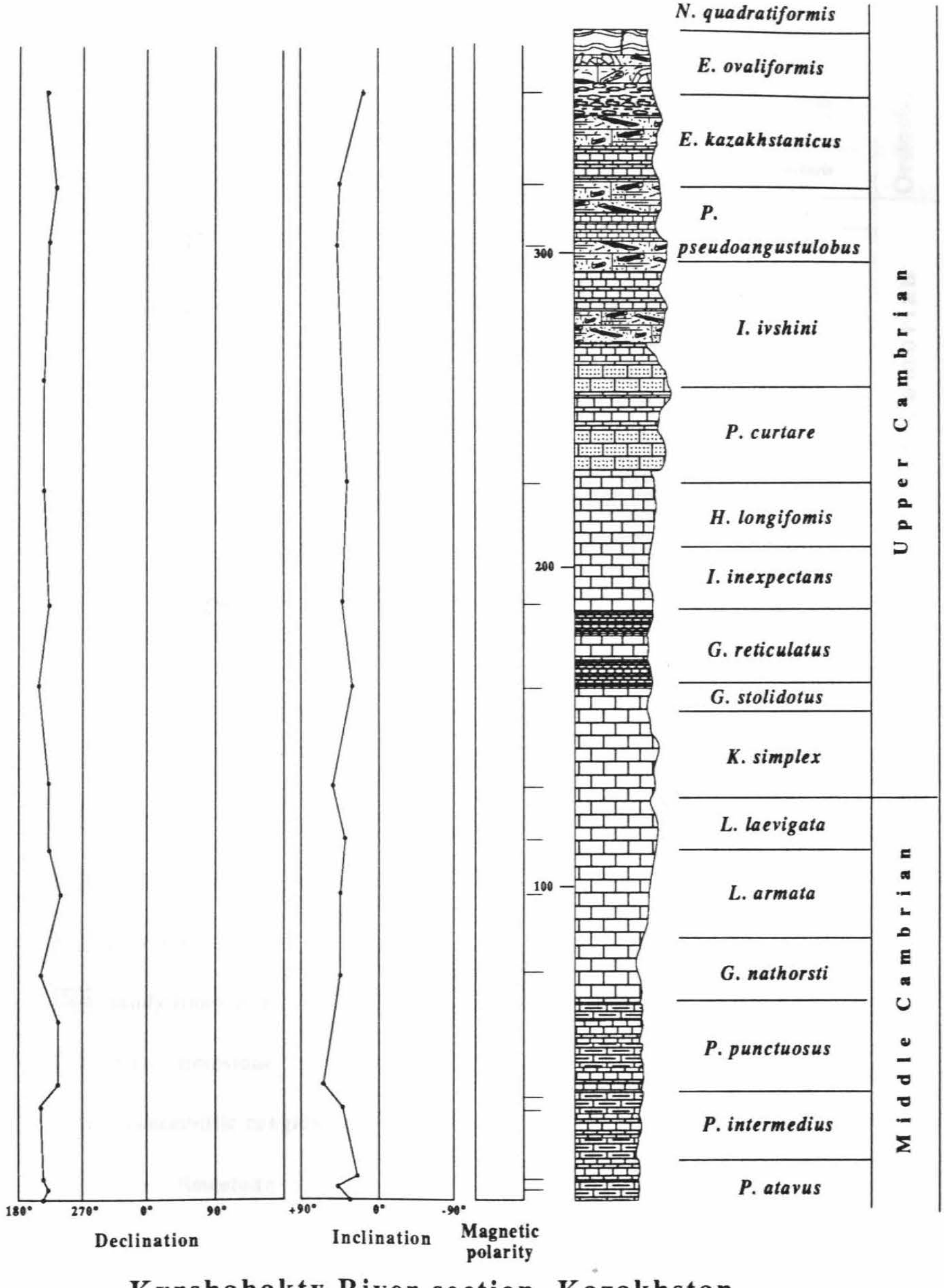

Kyrshabakty River section, Kazakhstan

Figure 3.8.a

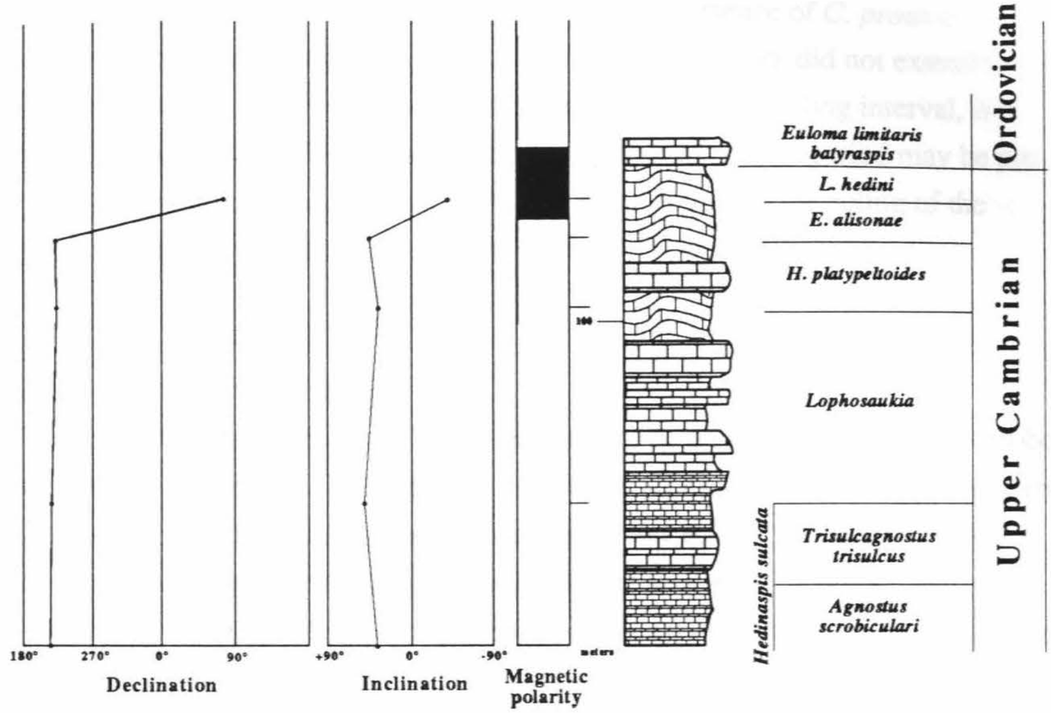

Batyrbay ravine, Kazakhstan

Figure 3.8.b

extended it, finding that a short period of normal polarity, beginning within the *E. alisonae* zone and ending a few meters above the lowest observed occurrence of *C. proavus*, is preserved at Batyrbay ravine (M. Apollonov, pers. comm.). Their work did not extend lower into the Upper Cambrian sequence, however, and because of the sampling interval, it is impossible to rule out the possibility that other short periods of normal period may be preserved within the sections reported on here. Present plans include re-sampling of the boundary section at Batyrbay ravine in August, 1990.

4.b. Llano Uplift Area, Texas

The Llano Uplift area in central Texas appeared to be a good place to try to corroborate the preliminary results from Kazakhstan. It is highly accessible, detailed conodont and trilobite biostratigraphies are in place, and the extremely low CAI of the area (1.0; Miller, pers. comm.) indicates the region has experienced little or no thermal alteration since deposition. Furthermore, the results from a previous paleomagnetic investigation in the area (Watts *et al.* 1980) suggested that the long period of predominantly single polarity observed in the Upper Cambrian rocks in Kazakhstan was also present in the Upper Cambrian rocks of the Llano Uplift.

Two sections, separated by about 1 kilometer (Figure 3.9) within the Threadgill Creek drainage, were sampled in June of 1985. The Lange Ranch section lies within the San Saba Member of the Wilberns Formation and extends upward into the overlying Threadgill Member of the Tanyard Formation. Excellent exposures begin about 23 meters below the Croixan-Canadian series boundary. The outcrops are composed primarily of interbedded coarse bioclastic, oolitic, and wavy-bedded nodular limestones, and are structurally simple, displaying very shallow dip and only two minor vertical faults. Samples taken from this section were precisely located within the local conodont biostratigraphy with the help of J.L. Miller.

The Threadgill Creek section is essentially the downward continuation of the Lange Ranch section, encompassing the lower members of the Wilberns Formation. Stratigraphic overlap of the two sections was obtained. Unfortunately, the Threadgill Creek section has, for much of its length, poorer exposures than the Lange Ranch section, and sample locations from here are generally less precise.

In spite of the many excellent aspects of these sections, they both have several drawbacks. The wet environment of central Texas and the Threadgill Creek drainage is

Figure 3.9. Sample localities within the Llano Uplift area (this study). Map symbols: Cr) Riley Formation; Cwwm) Welge Sandstone and Morgan Creek Limestone Members; Cwp) Point Peak Member; and Cws) San Saba Member, all of the Wilberns Formation; Ott) Threadgill Member of the Tanyard Formation; K) undifferentiated Cretaceous; QK) undifferentiated Quaternary to Cretaceous. Chevron pattern indicates location of traverse across outcrops. Horizontally ruled area is complexly faulted Cambrian and Ordovician strata. Modified from Miller *et al.* (1982).

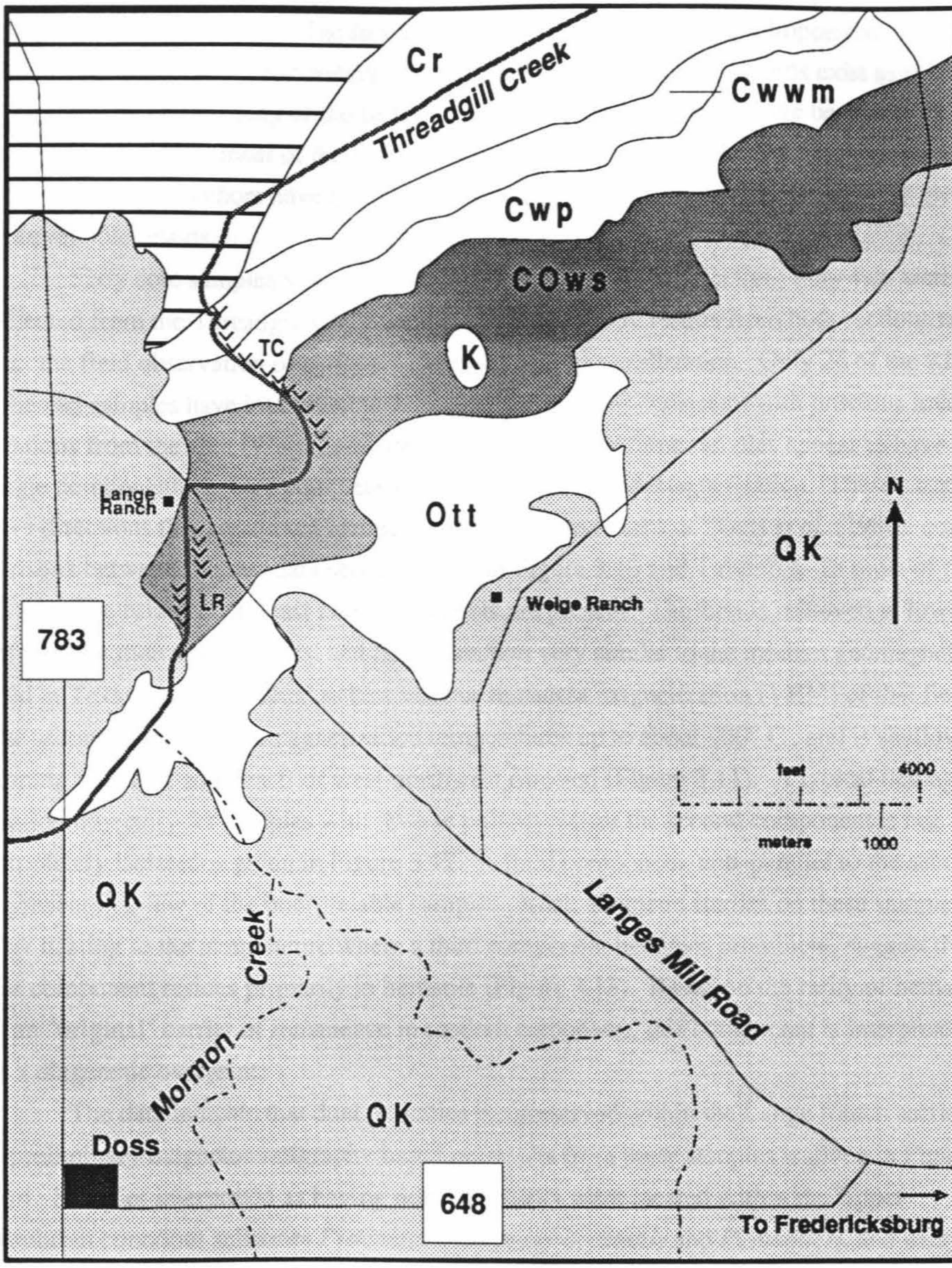
Cr
Threadgill Creek
Cwwm
Cwp
COws
K
TC
Lange Ranch
Ott
N
QK
LR
Weige Ranch
783
feet
4000
meters
1000
QK
Langes Mill Road
Creek
Mormon
QK
Doss
648
To Fredericksburg

Figure 3.9

highly conducive to diagenetic alteration and oxidation of magnetite, leading to loss of the original magnetic direction. The lack of structural complexity makes it impossible to perform a fold test for magnetic stability, and no breccia or conglomerate beds exist to perform a conglomerate test. Many of the beds within both sections appear to have been extensively recrystallized. Also, most of the limestone units are coarse-grained, while in previous studies the senior authors have found that finer-grained limestones have consistently given more reliable results.

Sixty core samples were collected from the Lange Ranch section; thiry-two were collected from the Threadgill Creek section. Paleomagnetic results from both sections reflect the field observation of surface weathering and recrystallization. Only 26 of the 92 collected samples have interpretable demagnetization paths consistent with previous investigations from the area (Watts *et al.* 1980). Of these, only three samples appear to have single components that are completely isolated by thermal demagnetization. These samples have directions that are almost identical to the previous results of Watts *et al.* (1980); comparisons between the two data sets are given in Figure 3.10 and Table 3.3. In most of the 26 samples, however, at least two components are present. The first is removed at low demagnetization temperatures, and has a direction very similar to the modern geomagnetic field in Texas; it is interpreted to be a viscous remanent magnetization (VRM) of that field. The second is stable at demagnetization temperatures up to about 400° C., and is shallowly-dipping and east-southeast- or west-northwest-directed (Figure 3.11). A typical demagnetization trajectory for samples with reverse polarity where the second component is not completely isolated is given in Figure 3.12. A third component, anti-parallel to the second, is present in a few of the interpretable samples. Rock magnetic studies on these samples, after heating to the temperature where a third component becomes prominent, suggest that this component resides primarily in hematite (Figure 3.13). Based on the rarity of hematite as an "original" carrier of remanence in modern carbonates, this component is interpreted to be a diagenetic overprint.

The data indicate that dual polarities are preserved within the Lange Ranch section. A preliminary magnetostratigraphy based on results from these samples is given in Figure 3.14. Samples interpreted as having normal polarity were located within the Upper Cambrian conodont subzones *Proconodontus posterocostatus* and *P. muelleri*, and near the base of the conodont zone *Cordylodus proavus*. Individual samples with normal polarity were also found higher in the section. Precise locations for the reversal boundaries are impossible to define; intervals between interpretable samples are too large. However, it

Figure 3.10. Comparison of characteristic directions from samples that appear to have had all other components completely removed by demagnetization, and site mean directions from Watts *et al.* (1980). Symbols as in Figure 3.7. Abbreviations for site mean directions : H1-H7, LBC) sites from the Hickory Member of the Riley Formation; C1-C3) sites from the Cap Mountain Limestone Member (n and r denote normal and reverse polarity); LM, K) sites from the Lion Mountain Sandstone Member; and SM, BC) sites from the Morgan Creek and Welge Members of the Wilberns Formation.

**Site-mean directions from Watts et al. (1980)
compared to
fully isolated characteristic directions
and the site-mean plane**

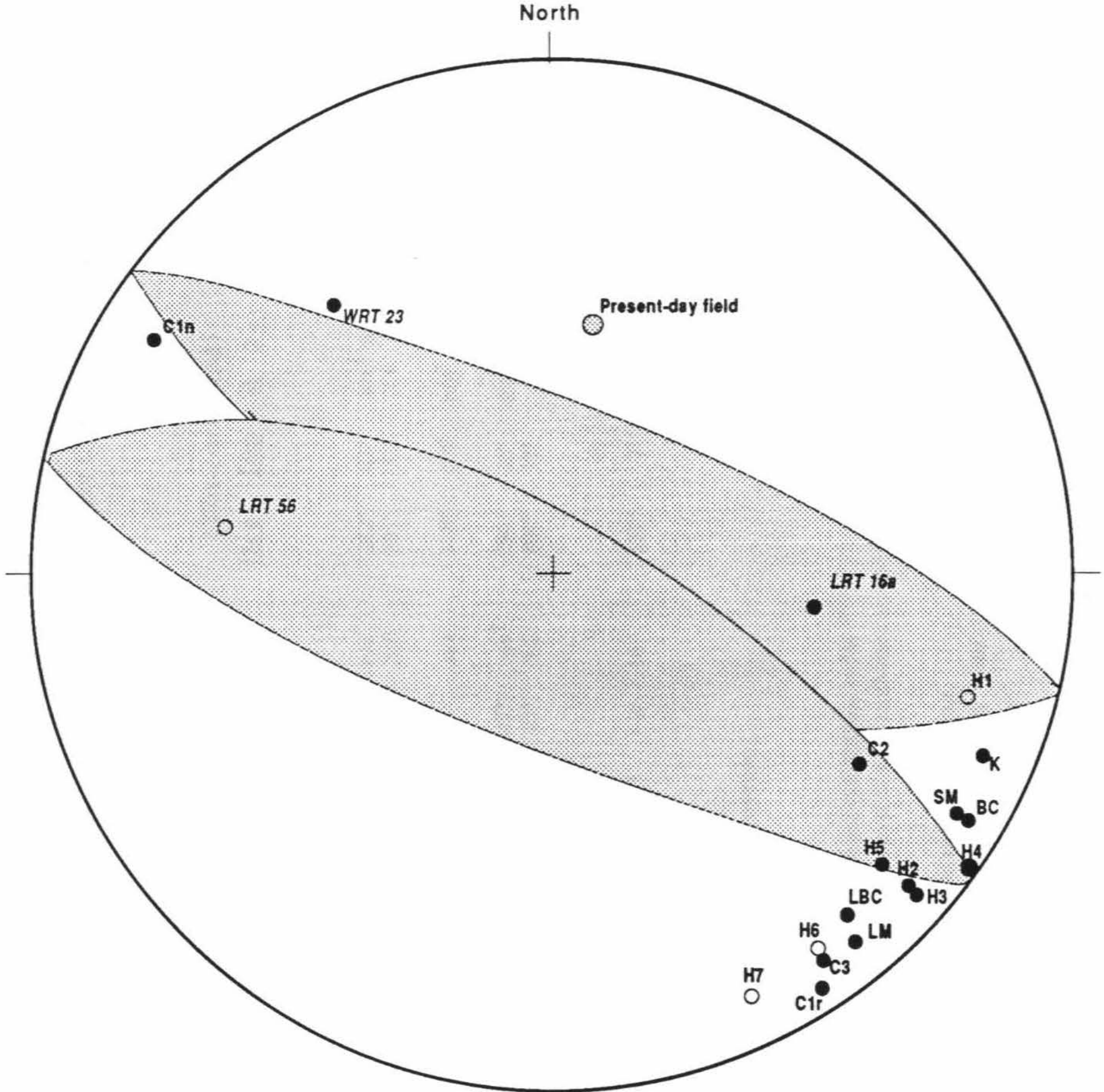

Figure 3.10

Table 3.3. Section mean directions, statistics, and pole positions for Upper Cambrian and Lower Ordovician carbonates of the Llano Uplift area, central Texas.

				(Geographic)			(Tilt-corrected)							
Section	R_t	R_s	R_p	Dec	Inc	k	Dec	Inc	k	α_{95}	Pole Position		dp	dm
Both sections located at 30.5° E., 99° W.														
Lange Ranch	60	2	18	278°	-42°	n/a†	282°	-43°	n/a†	n/a†	3° S.	144° E.	n/a†	n/a†
-poles to demagnetization planes			16	208°	26°	8.0	205°	22°	7.9	14°				
Welge Ranch	32	1	8	321°	33°	n/a†	318°	39°	n/a†	n/a†	52° N.	169° E.	n/a†	n/a†
mean of both sections	92	3	26	292°	-17°	n/a†	294°	-16°	n/a†	n/a†	16° N.	151° E.	n/a†	n/a†
-poles to demagnetization planes			23	206°	23°	9.2	204°	18°	9.0	11°				
Previous results (Watts et al. 1980)††														
-Morgan Creek-Welge	88	65	-	121°	-2°	16	121°	7°	20	4°	24° N.	151° E.	2°	4°

R_t = total number of samples analyzed
R_s = total number of samples used to calculate statistics
R_p = total number of samples used for polarity interpretation
Dec = declination
Inc = inclination
k = the estimate of Fisher's precision parameter
α_{95} = associated radius of the cone of 95% confidence (McElhinny 1973)
dp and dm = semiminor and semimajor axes of the oval of 95% confidence around the poles

†n/a= not applicable; insufficient data to warrant statistical analysis.
††Previous results reported only for the youngest unit sampled by Watts et al. (1980).

Figure 3.11. Poles to least-squares planes for samples having interpretable demagnetization trajectories, plotted in tilt-corrected coordinates. Symbols as in Figure 3.7.

Figure 3.12. Typical demagnetization trajectories for samples with reverse (a) and normal polarities. Symbols as in Figure 3.6.

Figure 3.13. Results of IRM induction-AF demagnetization studies on a sample heated to 450° C. The incomplete saturation above 300 mT during IRM induction suggests part of the remanence is carried by hematite or a similar high-coercivity mineral. (Goethite is not a likely candidate because the mineral breaks down at temperatures above ~100° C.)

Figure 3.14. Interpretative magnetic polarity stratigraphy for the Lange Ranch and Threadgill Creek sections. Normal polarity intervals are blackened. Intervals where no data was obtainable are shaded. Lithologic section and chronstratigraphy after Miller *et al.* 1982.

Llano Uplift area, central Texas

Poles to least-squares planes
of demagnetization trajectory

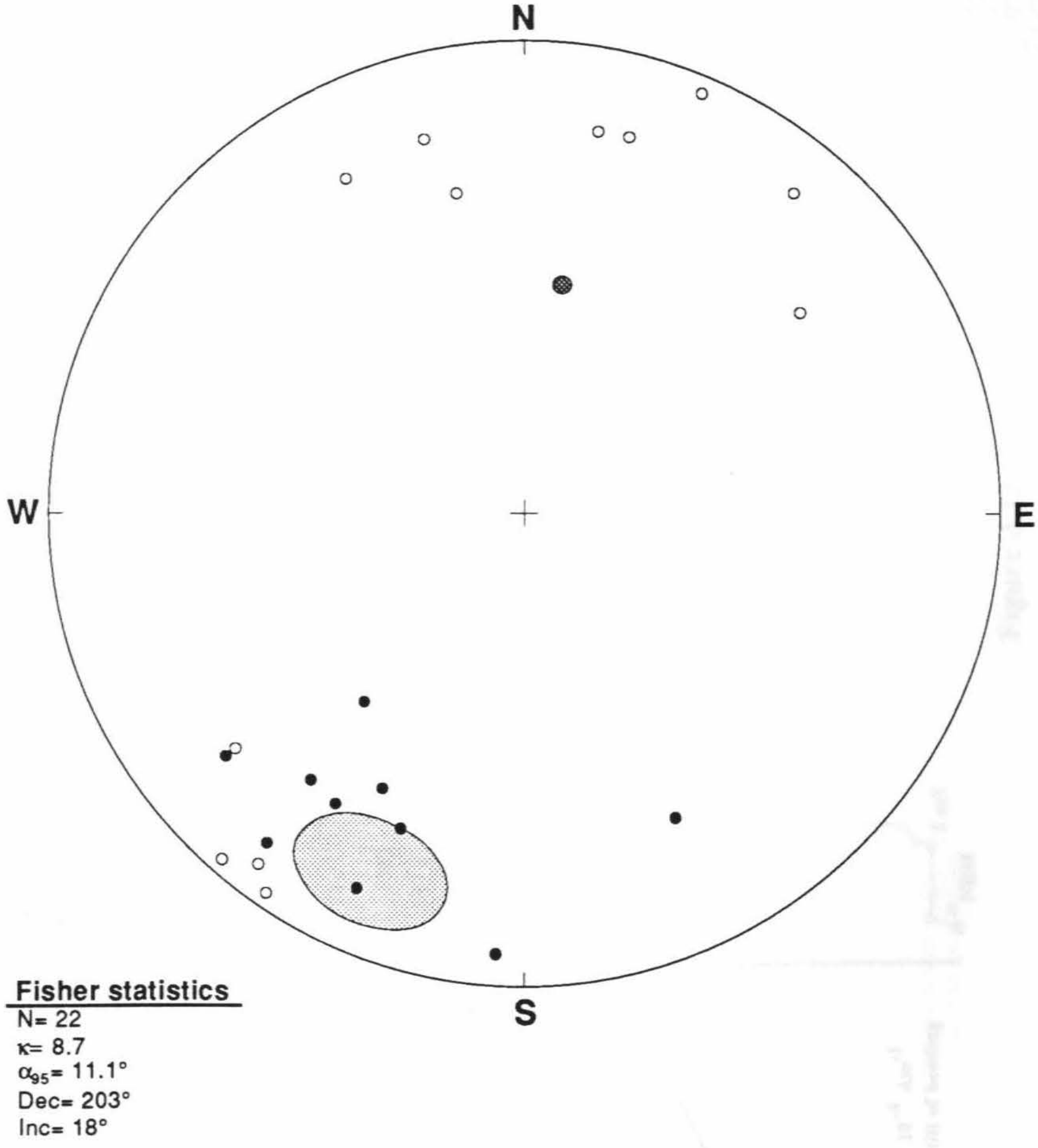

Progressive demagnetization of sample LRT 16.0b

Lange Ranch section

Llano Uplift area, Texas

Corrected for tilt of bedding

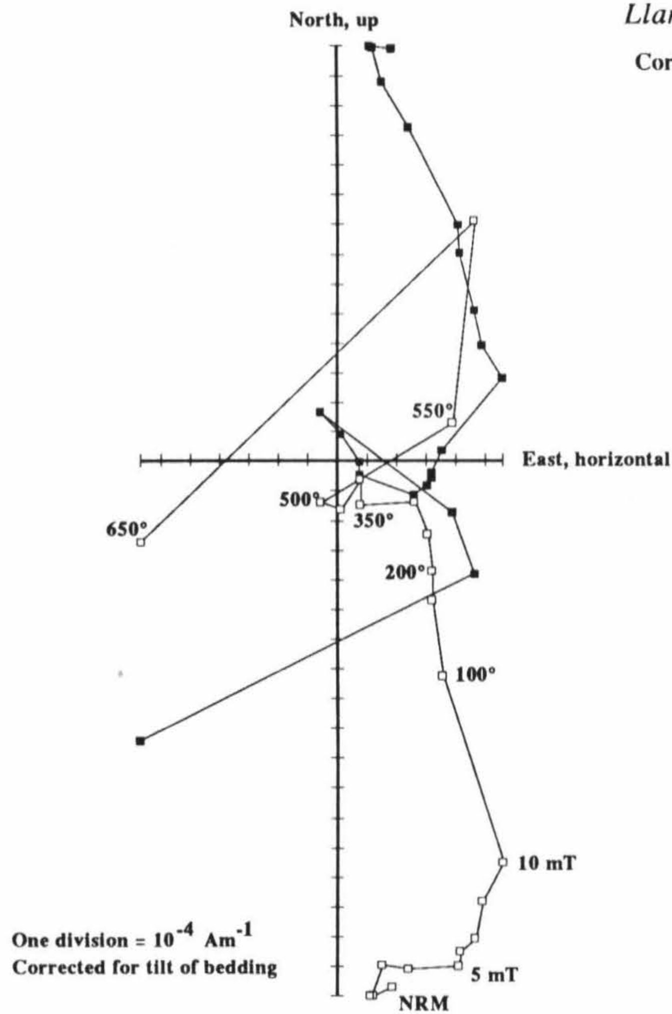

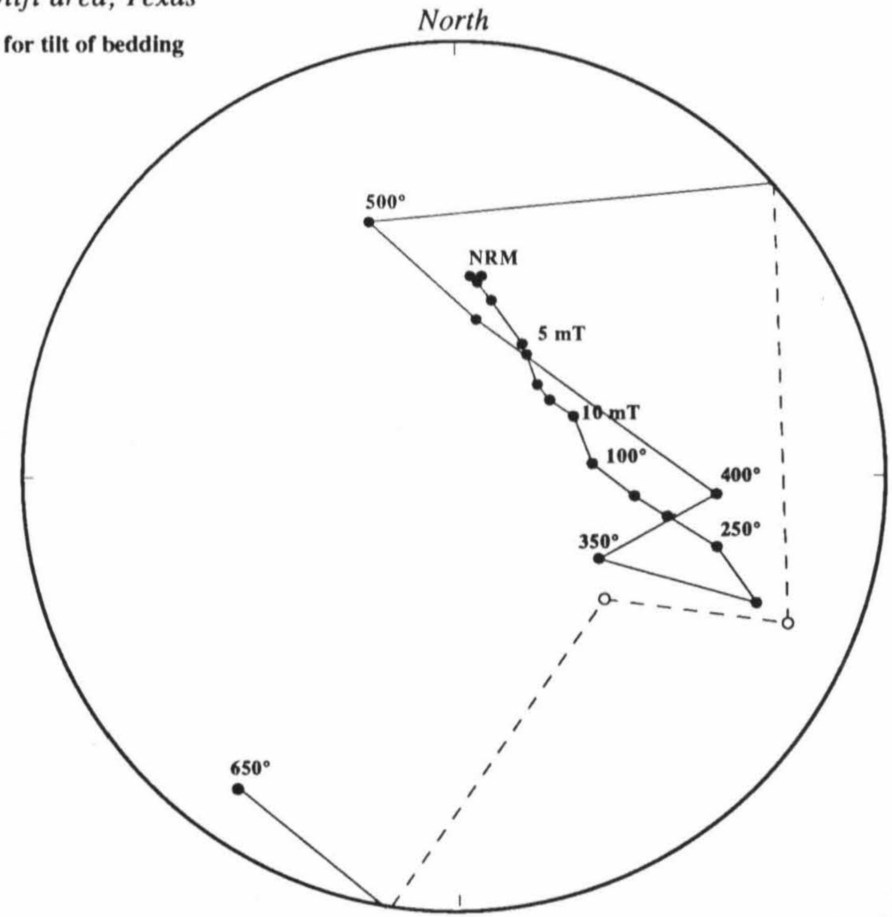

Figure 3.12.a

Progressive demagnetization of sample LRT 14.0

Lange Ranch section
Llano Uplift area, Texas
Corrected for tilt of bedding

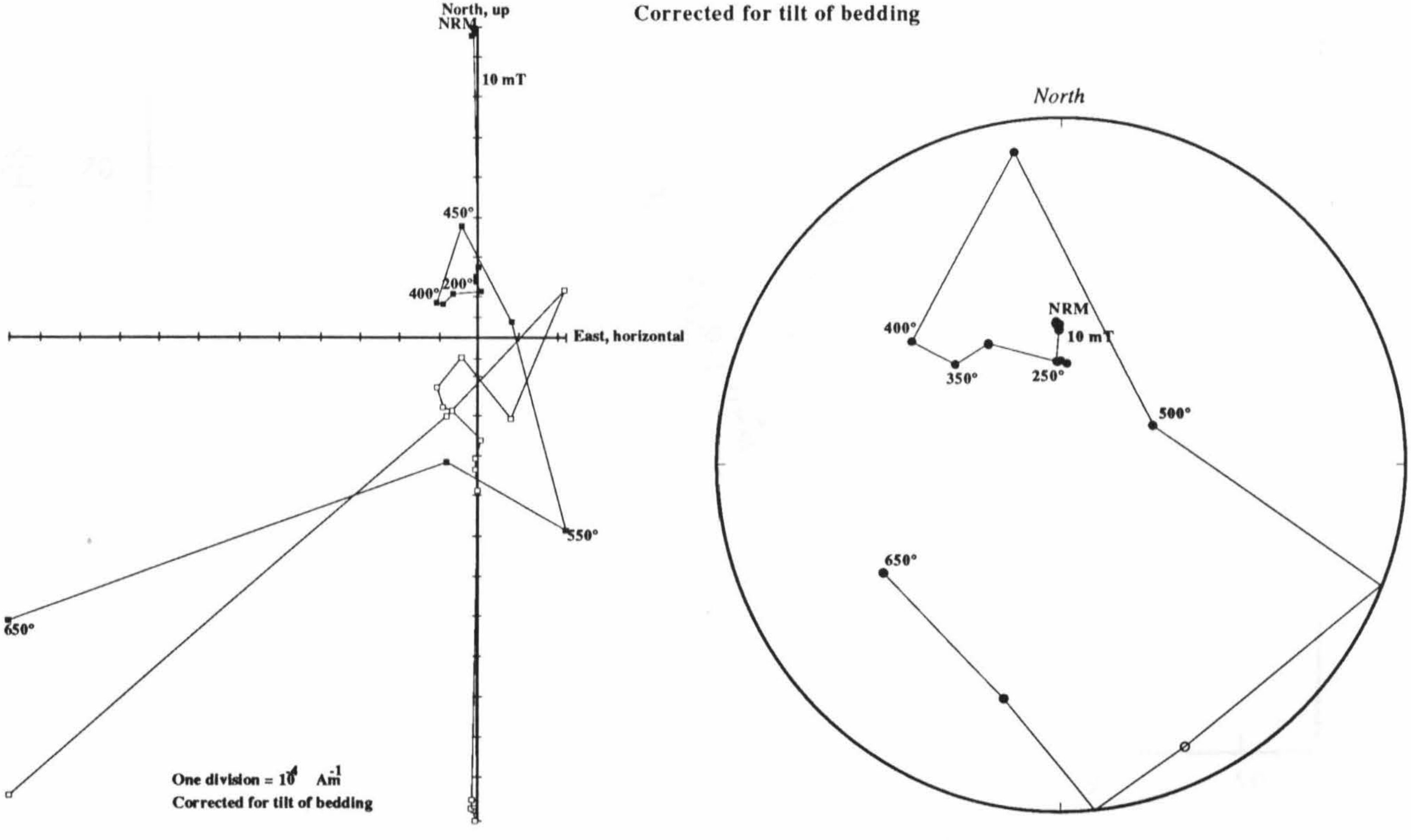

Figure 3.12.b

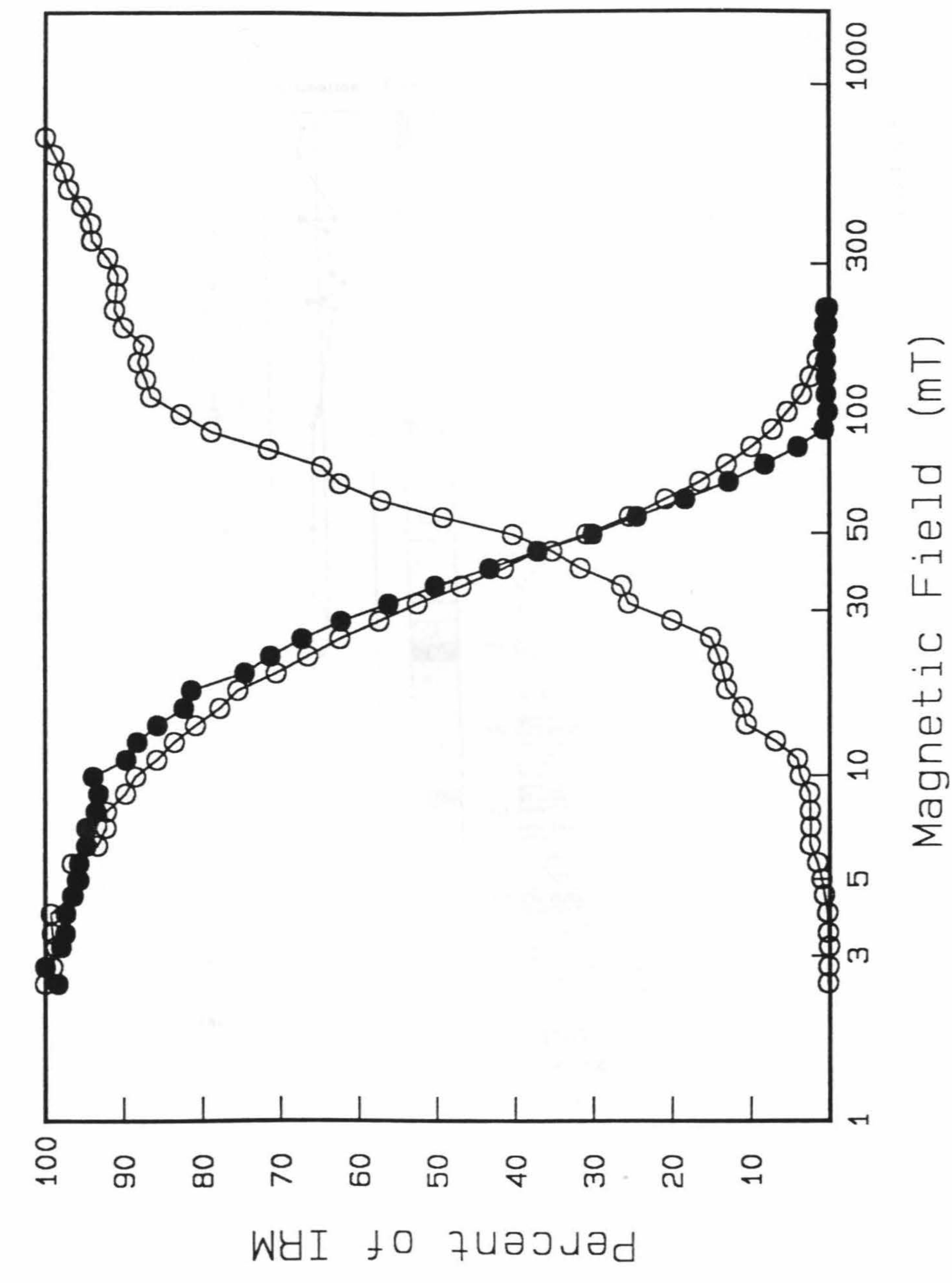
Percent of IRM
100
90
80
70
60
50
40
30
20
10
1
3
5
10
30
50
100
300
1000
Magnetic Field (mT)

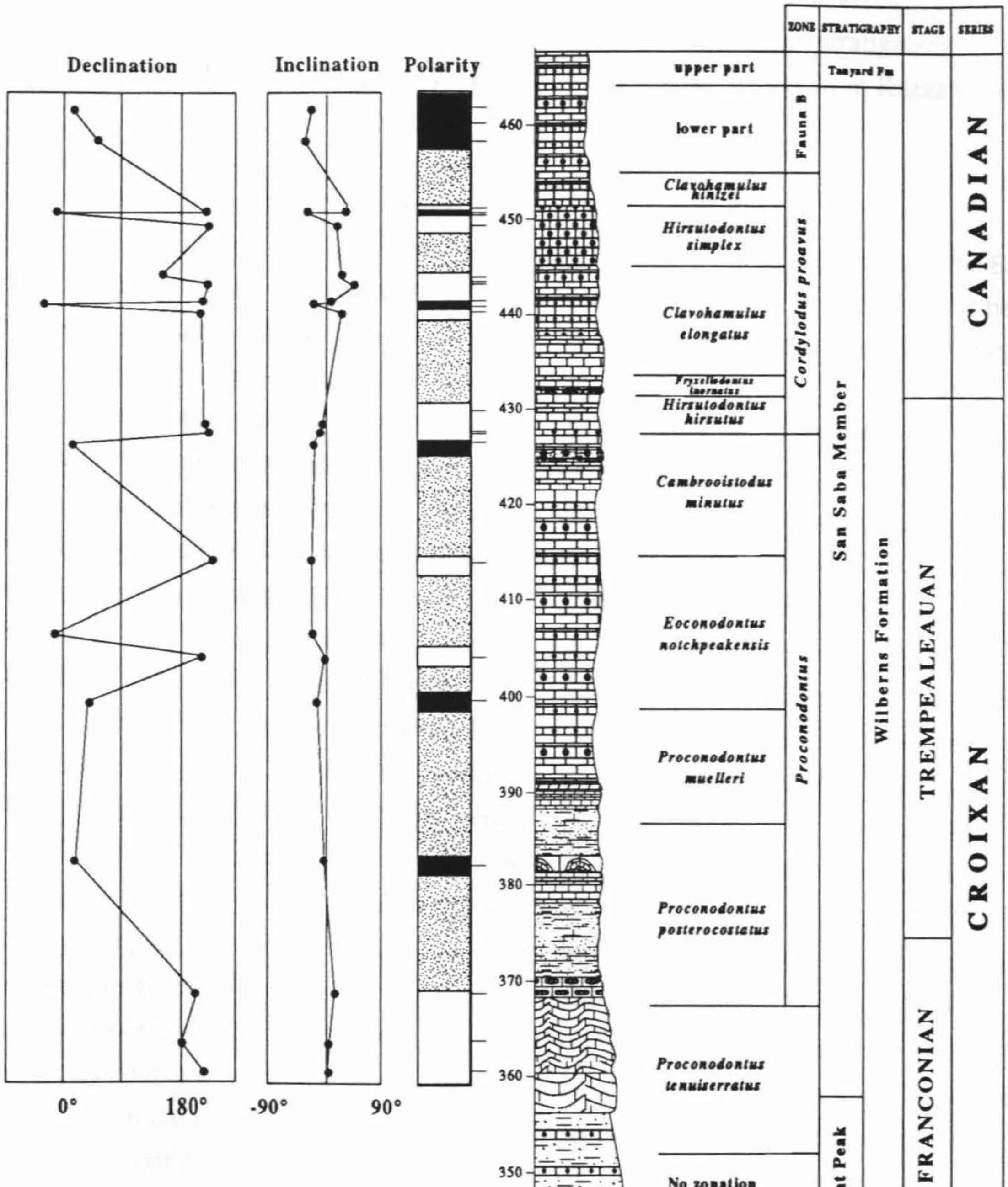
Declination
Inclination
Polarity
0°
180°
-90°
90°
ZONE
STRATIGRAPHY
STAGE
SERIES
upper part
lower part
Clavohamulus hintzei
Hirsutodontus simplex
Clavohamulus elongatus
Hirsutodontus hirsutus
Cambrooistodus minutus
Eoconodontus notchpeakensis
Proconodontus muelleri
Proconodontus posterocostatus
Proconodontus tenuiserratus
No zonation established
Fauna B
Cordylodus proavus
Proconodontus
Tanyard Fm
San Saba Member
Point Peak
Wilberns Formation
TREMPEALEAUAN
FRANCONIAN
CANADIAN
CROIXAN

Figure 3.14

appears that the intervals containing normal polarities are short, and that much of the Threadgill Creek section and the upper part of the Lange Ranch section are of predominantly reverse polarity, consistent with both the previous results from stratigraphically lower sections within the Llano Uplift, and the reconnaisance results from Kazakhstan.

4.c. East Yangtze Gorges, South China

Strata of Cambrian-Ordovician age are widespread and well-developed in the East Yangtze Gorges area. Because of the excellent exposure, a number of sections have been extensively studied. Many of the sections are rich in fossils and demonstrate fairly complete stratigraphic successions.

The Huanghuachang section is located in Hubei province on the north part of the Yangtze platform, about 25 km north of Yichang City. It is composed of a suite of highly fossiliferous carbonates showing continuous deposition within a single sedimentary facies. Seventy-five samples were collected from the section in September, 1985. Alternating-field and thermal demagnetization experiments yielded simple two-component demagnetization paths for 44 of these samples; a representative example is shown in Figure 3.15. One of the components is closely aligned to the present-day geomagnetic field, and is interpreted to be a VRM. The second, which in many samples was stable until the moment dropped to below 2×10^{-5} Am^{-1}, has moderate positive inclination and east-directed declination (Figure 3.16; Table 3.4). The lowermost two samples from this suite, near the lowest observed occurrence of *Cordylodus proavus*, appear to have a second component antiparallel to that of the remaining samples. Unfortunately, there were no other normal polarity samples identified, despite the fact that Early Ordovician normal polarity intervals are found in at least four other sections. It is possible, though unlikely, that the age assignment of this section is in error. Numerous studies (see Kent *et al.* 1987) have demonstrated that much of the South China block has experienced remagnetization to some degree, and at the present time, it is impossible to rule out remagnetization as an influence on the directions from this section.

4.d. Dayangcha, Jilin province, China

The Cambrian-Ordovician boundary-aged Xiaoyangqiao critical section, in Jilin province near Dayangcha, China (Figure 3.17), is one of the leading candidates for

Figure 3.15. Typical demagnetization trajectories for Lower Ordovician limestone from Huanghuachang. Symbols and projections as in Figure 3.6.

Figure 3.16. Equal area projection of characteristic directions obtained from the section near Huanghuachang. Symbols as in Figure 3.7.

Figure 3.17. Location map for the Dayangcha sections. Detailed site map from Chen *et al*. (1988).

Progressive demagnetization of sample HCO 65.1

Huanghuachang section

Yangtze Gorges area, Hubei Province, China

Corrected for tilt of bedding

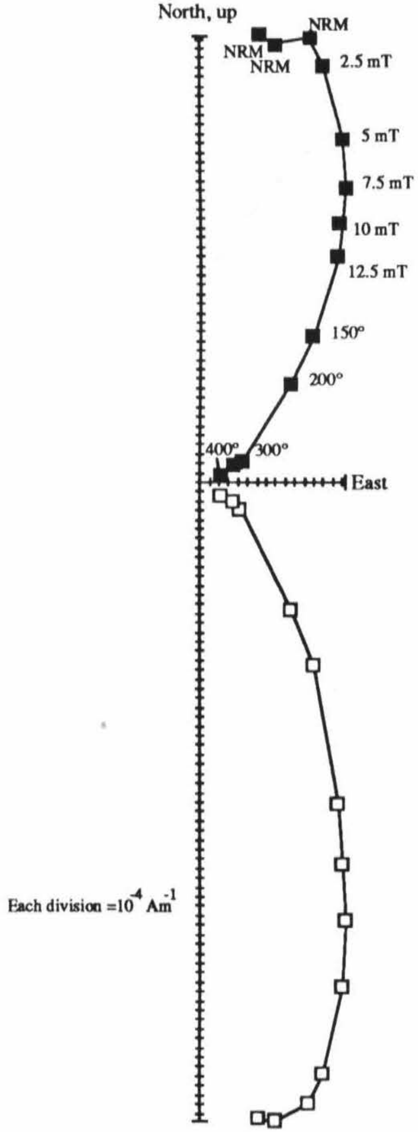

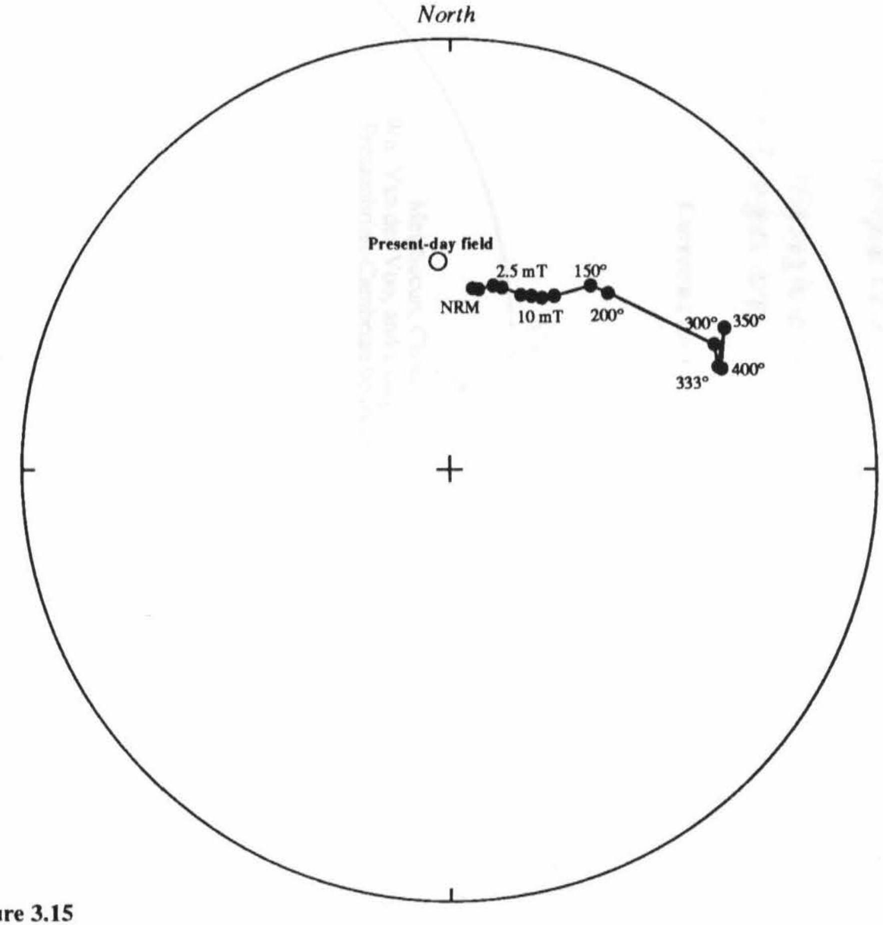

F igure 3.15

Characteristic directions isolated by principal component analysis

Huanghuachang section
Yangtze Gorges area, Hubei province, China

Corrected for tilt of bedding

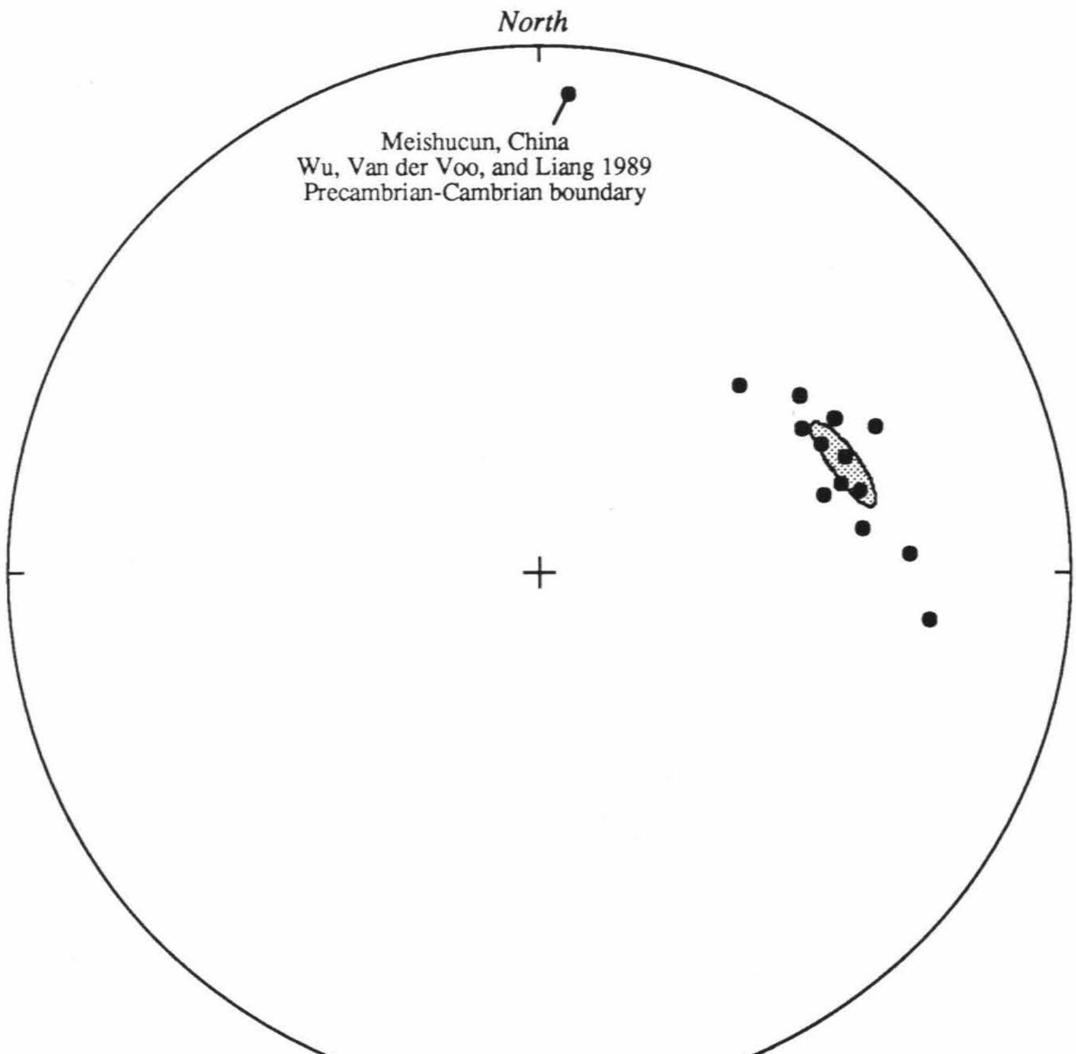

Figure 3.16

Table 3.4. Section mean directions, statistics, and pole positions for Upper Cambrian and Lower Ordovician carbonates near Dayangcha, China.

				(Geographic)			(Tilt-corrected)							
Section	R_t	R_s	R_p	Dec	Inc	k	Dec	Inc	k	α_{95}	Pole Position		dp	dm
Section located at 30.8° N., 111.2° E.														
Huanghuachang	75	14	28	61°	45°	48.7	70°	39°	45.5	6°	27° S.	11° E.	4°	7°
-demagnetization planes			19	230°	42°	10.9	217°	46°	10.5	11°				
Meishucun Precambrian-Cambrian boundary section (Wu *et al.* 1989)														
-Group B+C		57		4.0°	-9.1°	9	4.2°	7.1°	9	6.6°	69° S.†	90° E.†	-	-

R_t = total number of samples analyzed
R_s = total number of samples used to calculate statistics
R_p = total number of samples used for polarity interpretation
Dec = declination
Inc = inclination
k = the estimate of Fisher's precision parameter

α_{95} = associated radius of the cone of 95% confidence (McElhinny 1973)
dp and dm = semiminor and semimajor axes of the oval of 95% confidence around the poles
Note: the number of samples used to calculate statistics and the number of demagnetization planes will not necessarily sum to the number of samples used to interpret polarity. Some samples show excellent planar demagnetization trends which end in stable endpoints.

†Directions reflect this author's polarity interpretation, which is opposite that of Wu *et al.* 1989.

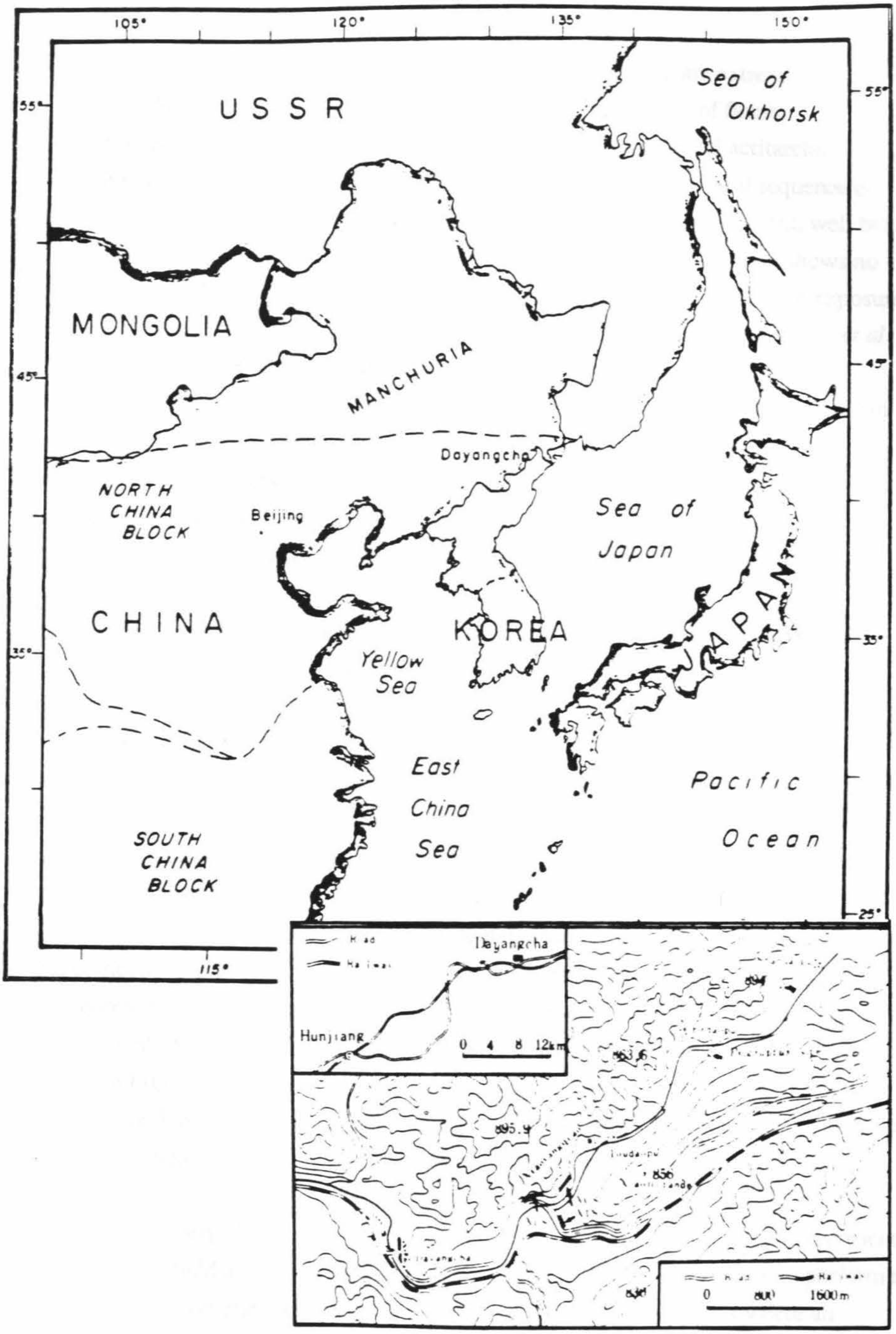
105°
120°
135°
150°
55°
45°
35°
25°
115°
USSR
Sea of Okhotsk
MONGOLIA
MANCHURIA
Dayangcha
NORTH CHINA BLOCK
Beijing
Sea of Japan
CHINA
KOREA
JAPAN
Yellow Sea
East China Sea
Pacific Ocean
SOUTH CHINA BLOCK
Dayangcha
Hunjiang
0 4 8 12km
895.9
856
0 800 1600m

designation as the international stratotype. The sections in this area are extremely important to understanding the boundary interval because of the rich diversities of fauna; biostratigraphic schemes exist for conodonts, trilobites, graptolites, and acritarchs.

Lithologically, the sections are comprised primarily of a rhythmical sequence of fine-grained carbonates deposited in a moderately deep outer shelf environment, well below the normal storm wave base (Chen *et al.* 1988). The entire boundary interval shows no break in sedimentation. The XCS section is free of faulting and folding, and the exposure is relatively fresh, although some weathering is evident. A CAI value of 1.5 (Chen *et al.* 1988) indicates the area has not been subjected to metamorphism.

The Xiaoyangqiao Critical and Lower Sections (XCS and XLS) were sampled in August, 1986, in conjunction with the visit of the Cambrian-Ordovician Boundary Working Group. A total of 165 core samples were collected from the two sections. Sample positions were highly constrained within the local bio- and litho- stratigraphies; sampling intervals were particularly small around the zonal bases of *C. proavus* and C. *lindstromi*. Although some of the samples showed evidence of the thin weathering rind present in the Dayangcha sections, most were from fresh exposure, and where possible, care was taken in the laboratory to ensure that the weathered portions of cores were not used during analysis.

All samples underwent AF and thermal demagnetization. As with other samples, the maximum AF intensities used did not exceed 15 mT. Thermal demagnetizations were performed in the usual manner up through the Curie point of magnetite, although for most samples, useful data was not obtained from steps above 450°. The data indicate the presence of a ubiquitous overprint component, interpreted as a VRM of the present day field, which was not completely removed by demagnetization. However, the contribution of this component to the total magnetization was sufficiently reduced to determine that a second component, with clearly antiparallel behavior, was present. No other components were identified. Representative examples of samples with normal and reversed polarities are given in Figures 3.18 and 3.19. Equal area projection of the poles to least-squares planes (Figure 3.20) strongly suggest that the second component is the same in all samples. There were no significant differences between the results from the XCS and the XLS (Table 3.55).

Unfortunately, demonstrating that the directions preserved in this section represent the geomagnetic field at the time of deposition is difficult. It was not possible to perform a fold test or a conglomerate test with these sections. Furthermore, in cases where an

Figure 3.18. Typical demagnetization trajectories for samples from the Xiaoyangqiao sections, showing reverse (a) and normal polarities.

Figure 3.19. Equal area projection of the poles to least-squares planes for samples from the sections near Dayangcha, China. Choice of pole to represent the plane is by a right-hand convention; with palm up and fingers pointed in the direction of demagnetization, thumb points towards pole.

Figure 3.20. Reversal test using mean directions of poles to demagnetization planes. Reverse polarity mean has been rotated 180° around an east-west axis for comparison with normal polarity mean. Overlap of α_{95} ovals of confidence indicates a positive reversal test, suggesting that the age of acquisition for the preserved directions is not significantly different.

Progressive demagnetization of sample XCS 97.0

Xiaoyangqiao critical section
Dayangcha, Jilin province, China

Corrected for tilt of bedding

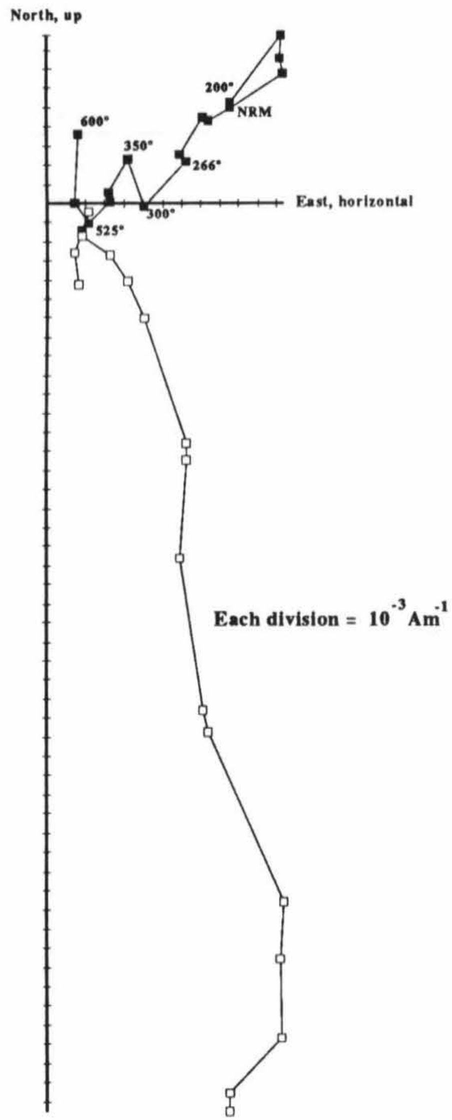

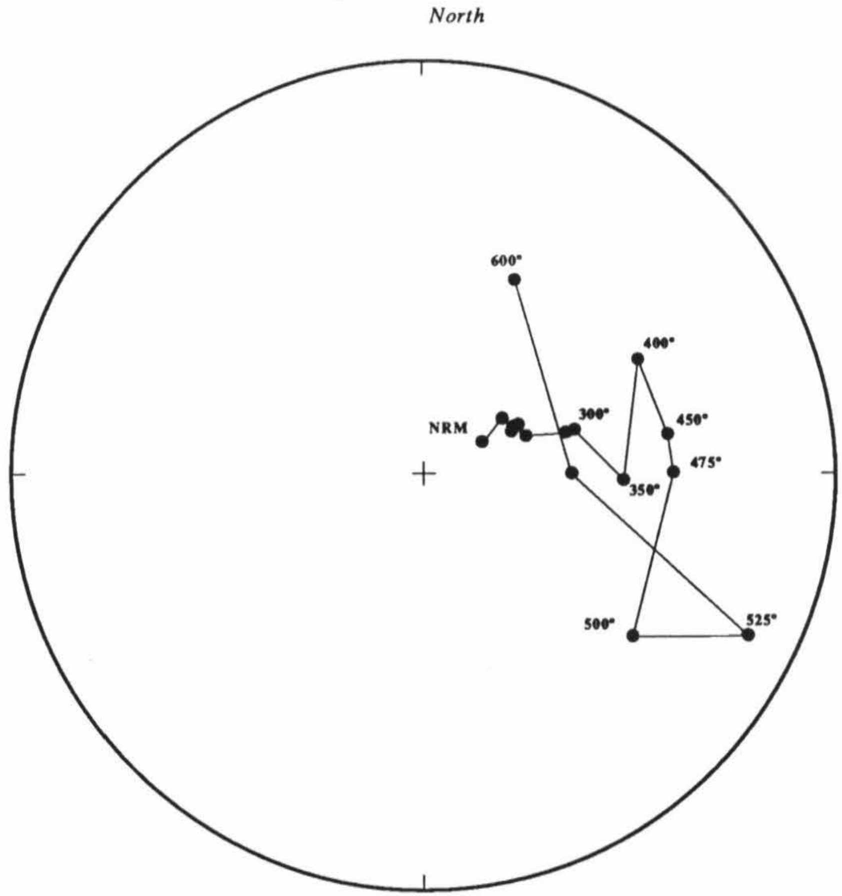

Figure 3.18.a

Progressive demagnetization of sample XCS 62.0

Xiaoyangqiao critical section
Dayangcha, Jilin province, China

Corrected for tilt of bedding

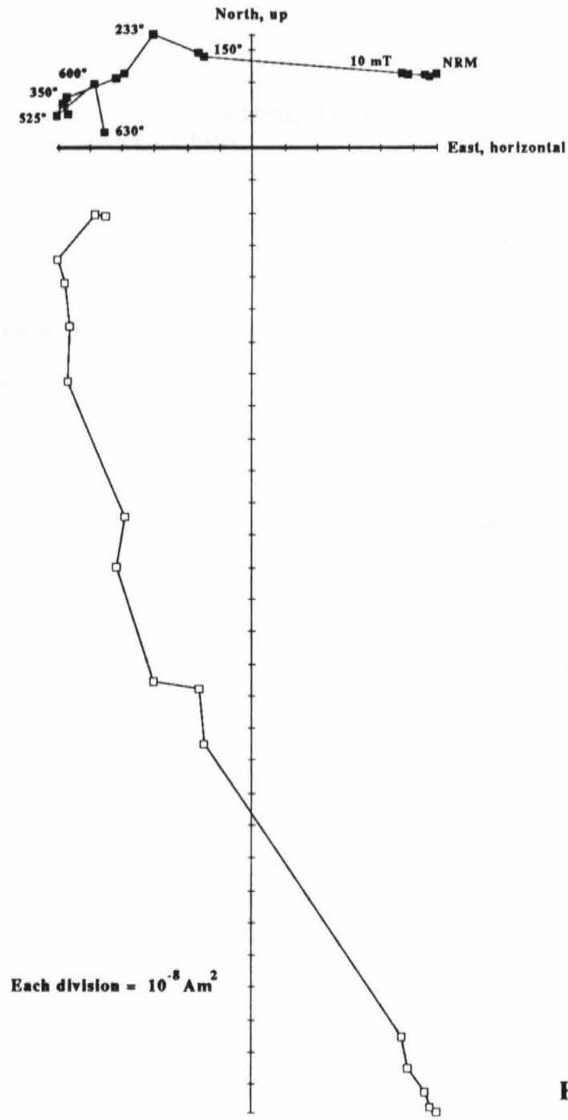

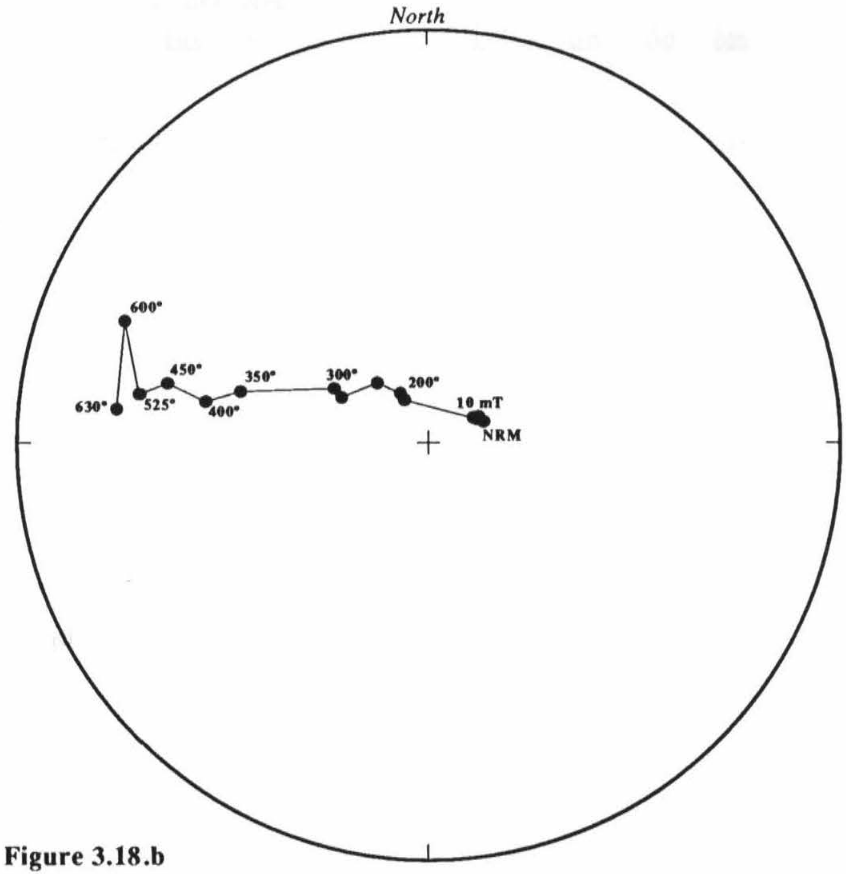

Figure 3.18.b

Table 3.5. Section mean directions, statistics, and pole positions for Upper Cambrian and Lower Ordovician carbonates near Dayangcha, China.

				(Geographic)			(Tilt-corrected)							
Section	R_t	R_s	R_p	**Dec**	**Inc**	**k**	**Dec**	**Inc**	**k**	α_{95}	**Pole Position**		δp	δm
Both sections located at 42.1°N., 126.7° E.														
Xiaoyangqiao Critical	130	4	71	271°	-14°	3.8	270°	17°	3.8	43°	6° N.	43° E.	23°	44°
-demagnetization planes			69	183°	28°	9.7	175°	8°	9.5	6°				
Xiaoyangqiao Low	35	-	16	-	-	-	-	-	-	-	-	-	-	-
-demagnetization planes			16	183°	29°	10.0	175°	7°	9.9	12°				
mean of all sections	165	4	90	-	-	-	-	-	-	-	-	-	-	-
-demagnetization planes				183°	28°	9.3	176°	8°	9.1	5°	-	-	-	-

R_t = total number of samples analyzed
R_s = total number of samples used to calculate statistics
R_p = total number of samples used for polarity interpretation
Decl = declination
Inc = inclination
k = the estimate of Fisher's precision parameter
α_{95} = associated radius of the cone of 95% confidence (McElhinny 1973)
δm and δp = meridinal and latitudinal axes of the oval of 95% confidence around the poles

Note: The number of samples used to calculate statistics and the number of demagnetization planes do not necessarily sum to the total number of samples used for polarity interpretation. Some samples showed excellent planar demagnetization trends which ended in stable, linear demagnetization trends.

Characteristic directions

Xiaoyangqiao Critical and Low sections
Dayangcha, Jilin province, China

Corrected for tilt of bedding

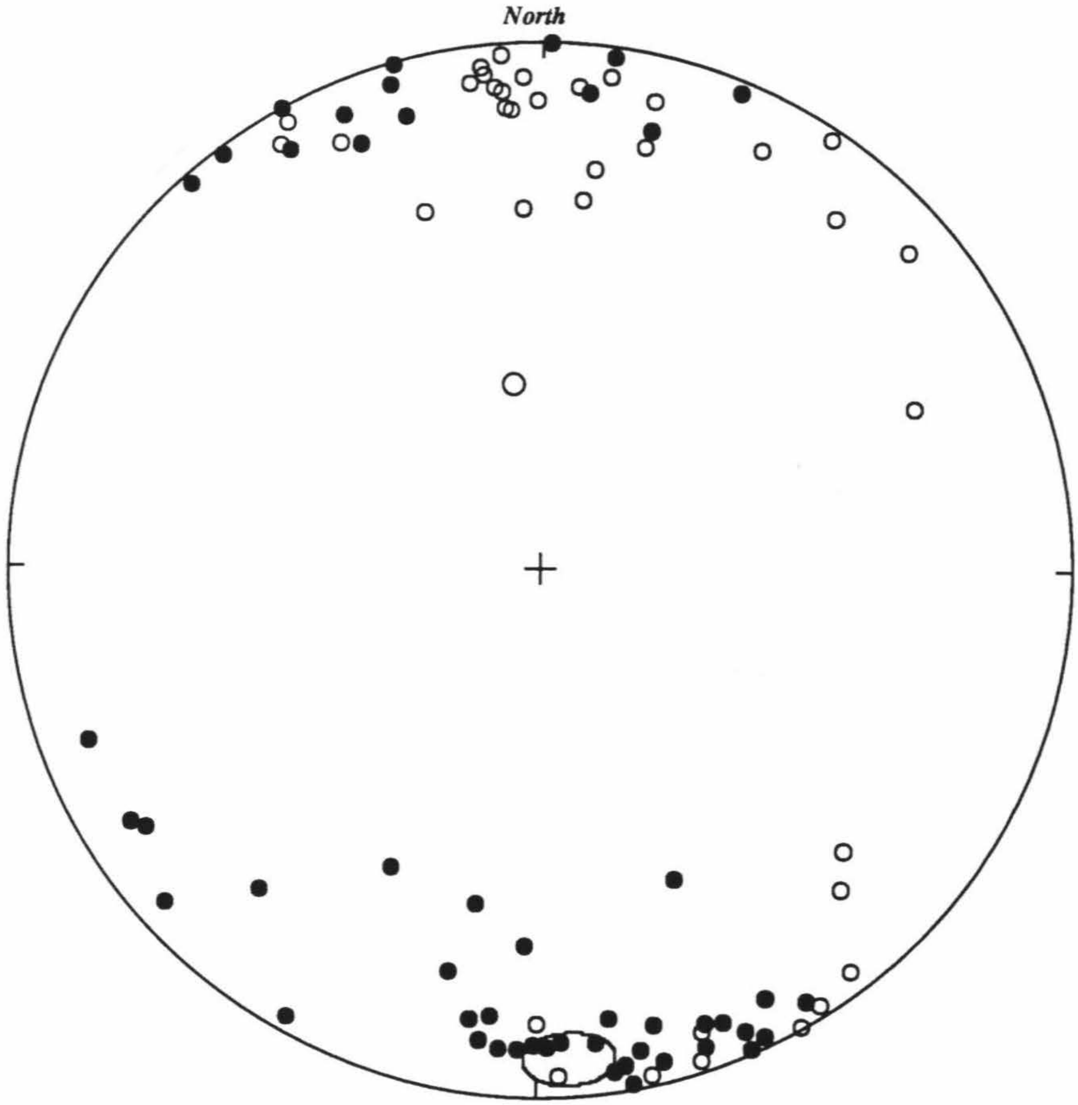

Figure 3.19

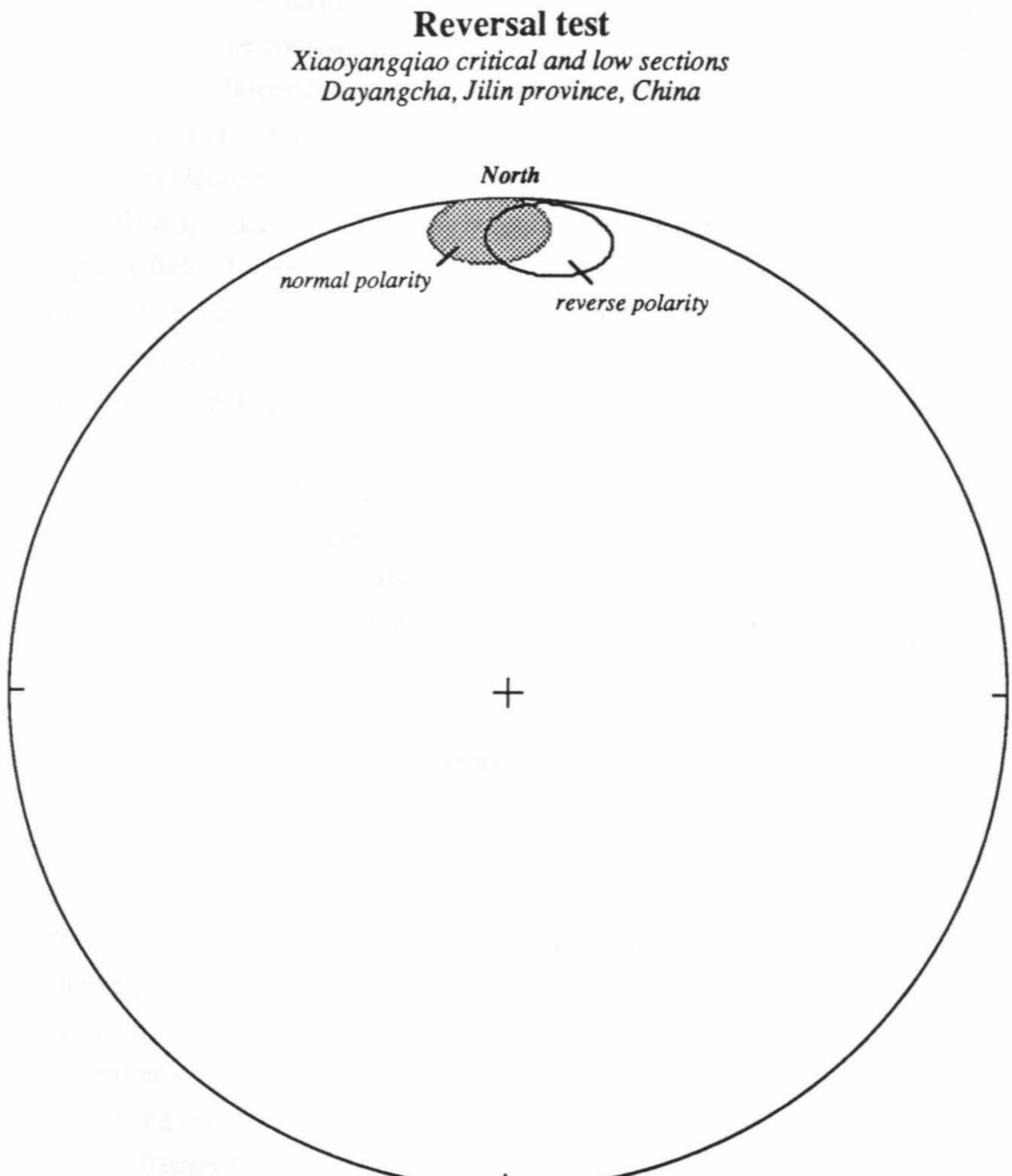
Reversal test
Xiaoyangqiao critical and low sections
Dayangcha, Jilin province, China
North
normal polarity
reverse polarity

Figure 3.20

compares two components instead of one, making a positive reversal test less reliable. It was not possible to perform a fold test or a conglomerate test with these sections. To make matters worse, there are no previous results from the North China Block for the Late Cambrian, leaving the consistency test as the only other means of assessing the nature of the magnetization. Intervals interpreted as normal polarity occur within the *Proconodontus posterocostatus* and *P. muelleri* subzones, and beginning at the base of the *Cordylodus proavus* zone (Figure 3.21), as in many of the other studied sections, arguing that the characteristic magnetization of the Xiaoyangqiao sections represents the depositional geomagnetic field. However, normal polarity appears to persist from the base of the *C. proavus* zone up through the *C. intermedius* zone to the base of the *C. lindstromi* zone. This is the only section studied to date that shows such a long interval of uninterrupted normal polarity at this level. Further study is needed to determine why this unique signature occurs.

Magnetostratigraphic correlation of the Upper Cambrian normal polarity intervals allows the Cambrian-Ordovician paleogeographic position of the North China block to be uniquely determined as oriented about 90° clockwise from its present position, and nearly equatorial. (A further discussion of the paleogeography of the North China block is given in Chapter 6.)

4.e. Cow Head area, western Newfoundland

The Cow Head Group, outcropping on the western coast of Newfoundland, provides a unique setting for magnetostratigraphic investigations because it possesses both large conglomeratic beds and extensive folding while displaying low CAI, maximizing the opportunity for performing magnetic stability tests while minimizing the possibility that thermal overprinting is a significant problem. The geologic setting of the Cow Head Group, i.e., that of a large submarine fan complex, allows collection in a variety of lithologies, and extremely detailed studies have identified a number of Cambrian-Ordovician sections preserving correlatable lithostratigraphic and biostratigraphic horizons (Noel and James 1986; Barnes 1988; many others). Furthermore, most of the sections are within Gros Morne National Park (declared as a World Heritage site in 1987), assuring both their protection and accessibility to legitimate scientific investigation.

While blessed with a number of positive aspects for paleomagnetic investigation, working with the Cow Head Group also has some special difficulties. The Cow Head Group makes up the northern portion of the Humber Allochthon and is locally highly de-

Figure 3.21. Geomagnetic polarity interpretation for the Xiaoyangqiao Critical (a) and Low sections near Dayangcha, Jilin Province, China. Stratigraphic column and biozonation from Chen (1986). Data points are poles to demagnetization planes. By convention, poles to the north represent normal polarity.

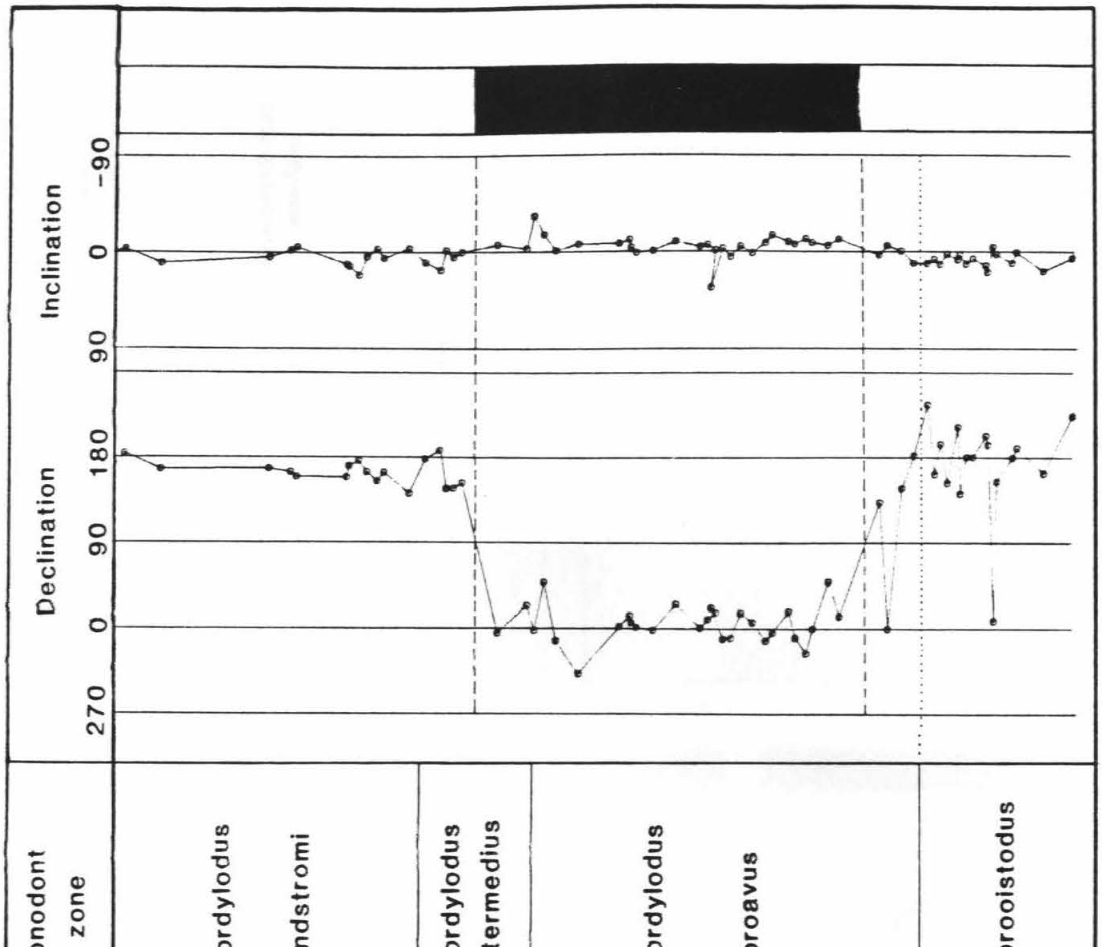
conodont zone
Cordylodus lindstromi
Cordylodus intermedius
Cordylodus proavus
Cambrooistodus
Declination
270
0
90
180
Inclination
90
0
-90
M
40
30
20
10

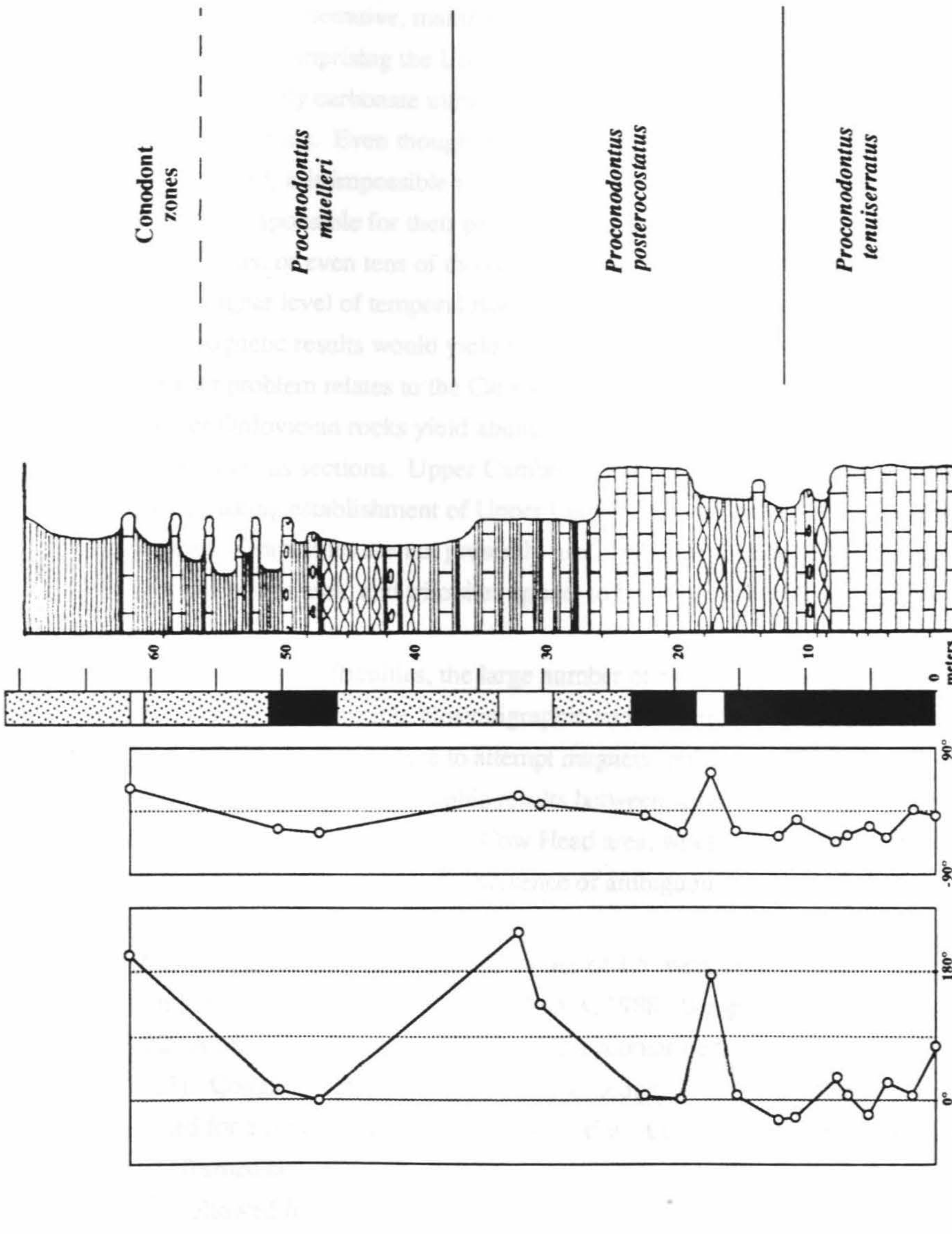
Conodont zones
Proconodontus muelleri
Proconodontus posterocostatus
Proconodontus tenuiserratus
60
50
40
30
20
10
0
meters
90°
-90°
Inclination
180°
0°
Declination

Figure 3.21.b

formed from the emplacement event, which has been interpreted to have begun in the Middle Ordovician. Deformations of this style have a high probability for rotational components that are non-penetrative, making interpretations of fold tests between sections difficult. Also, material comprising the Upper Cambrian and Lower Ordovician conglomeratic units are predominantly carbonate intraclasts that have been ripped off up-slope and shed down the submarine fan. Even though these blocks were probably fairly well-lithified before being reworked, it is impossible to discount the possibility that post-depositional diagenesis could be responsible for their preserved directions. If diagenesis occurred within a few thousand years, or even tens of thousands of years, the magnetic stratigraphy would still provide a higher level of temporal resolution than any other stratigraphic framework, but the paleomagnetic results would yield negative conglomerate tests.

Another problem relates to the Cambrian-Ordovician paleoecology of the Cow Head Group. Lower Ordovician rocks yield abundant faunas of conodonts, graptolites, and trilobites from various sections. Upper Cambrian units, however, are greatly impoverished in conodonts, making establishment of Upper Cambrian zonal boundaries impossible in the critical sections. Graptolites are not presently useful for biozonation in the Upper Cambrian rocks of this area, and trilobites appear to be rare in most of the Upper Cambrian sections.

In spite of these difficulties, the large number of sections and levels that can be correlated using widely-recognizable biostratigraphic and lithostratigraphic horizons makes the Cow Head Group an attractive place to attempt magnetic polarity stratigraphy. Demonstrable consistency of magnetostratigraphic results between sections within the group, and correlatability with sections outside the Cow Head area, would be powerful arguments for the reliability of the results, even in the presence of ambiguous fold and negative conglomerate tests.

A total of 6 sections, all with CAI values of 1.5, were collected from on two separate sampling trips, in September 1986 and August 1988. Sample localities are shown in Figure 3.22. A representative cross-section of the submarine fan complex was obtained (Figure 3.23). Conglomeratic units at Cow Head Ledge, Broom Point, and Green Point were collected for a conglomerate test. Bedding orientation differences permitted the fold test to be performed between sections, and the presence of highly deformed bedding at Broom Point allowed for micro-fold tests.

Figure 3.22. Sampling localities in the Cow Head Group, western Newfoundland, Canada.

Figure 3.23. Reconstructed depositional framework for the Cow Head Group. From James and Stevens (1986).

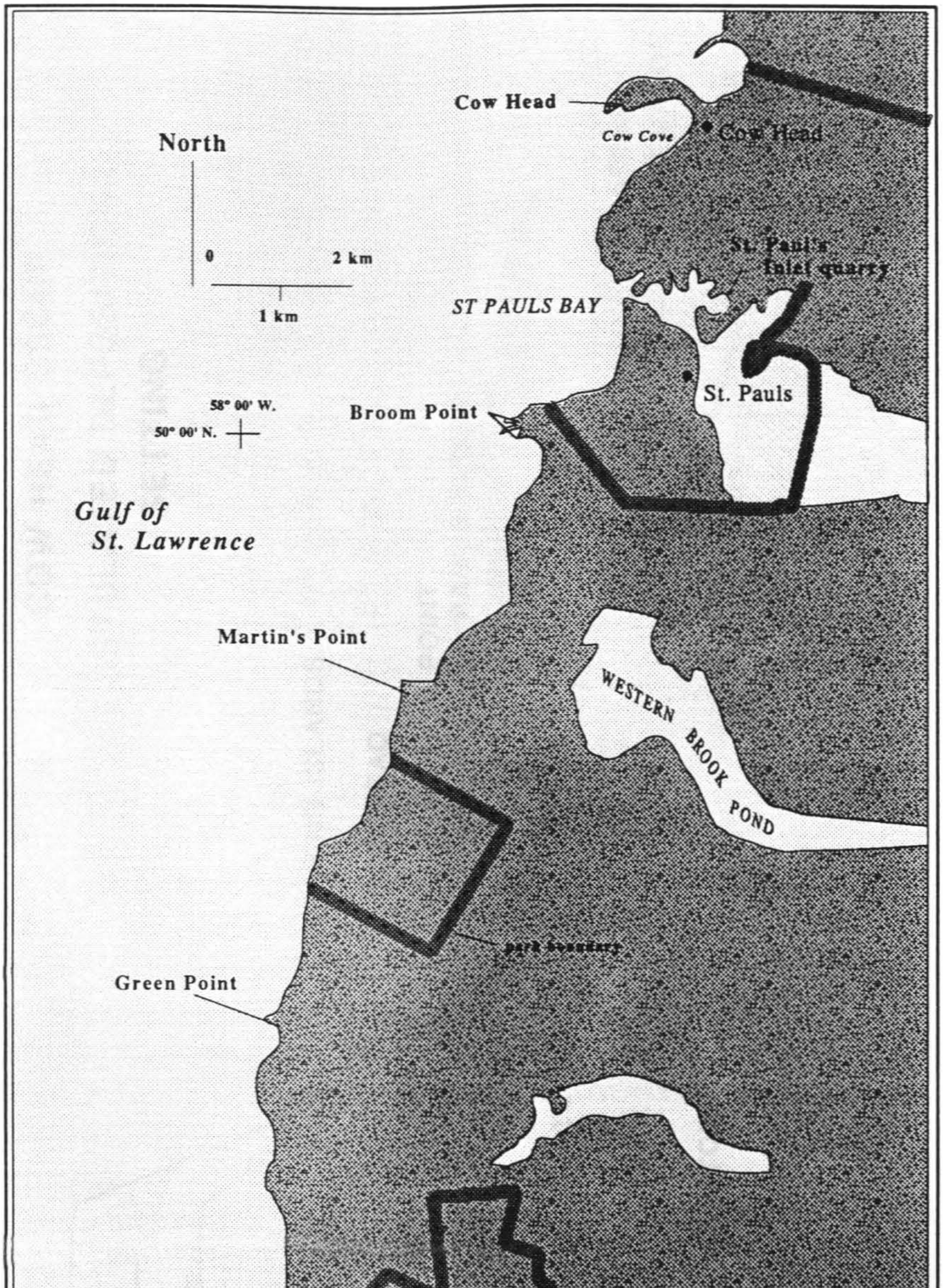
Cow Head
Cow Cove
Cow Head
North
0
2 km
1 km
St. Paul's
Inlet quarry
ST PAULS BAY
St. Pauls
58° 00' W.
50° 00' N.
Broom Point
Gulf of
St. Lawrence
Martin's Point
WESTERN BROOK POND
Green Point

Figure 3.22

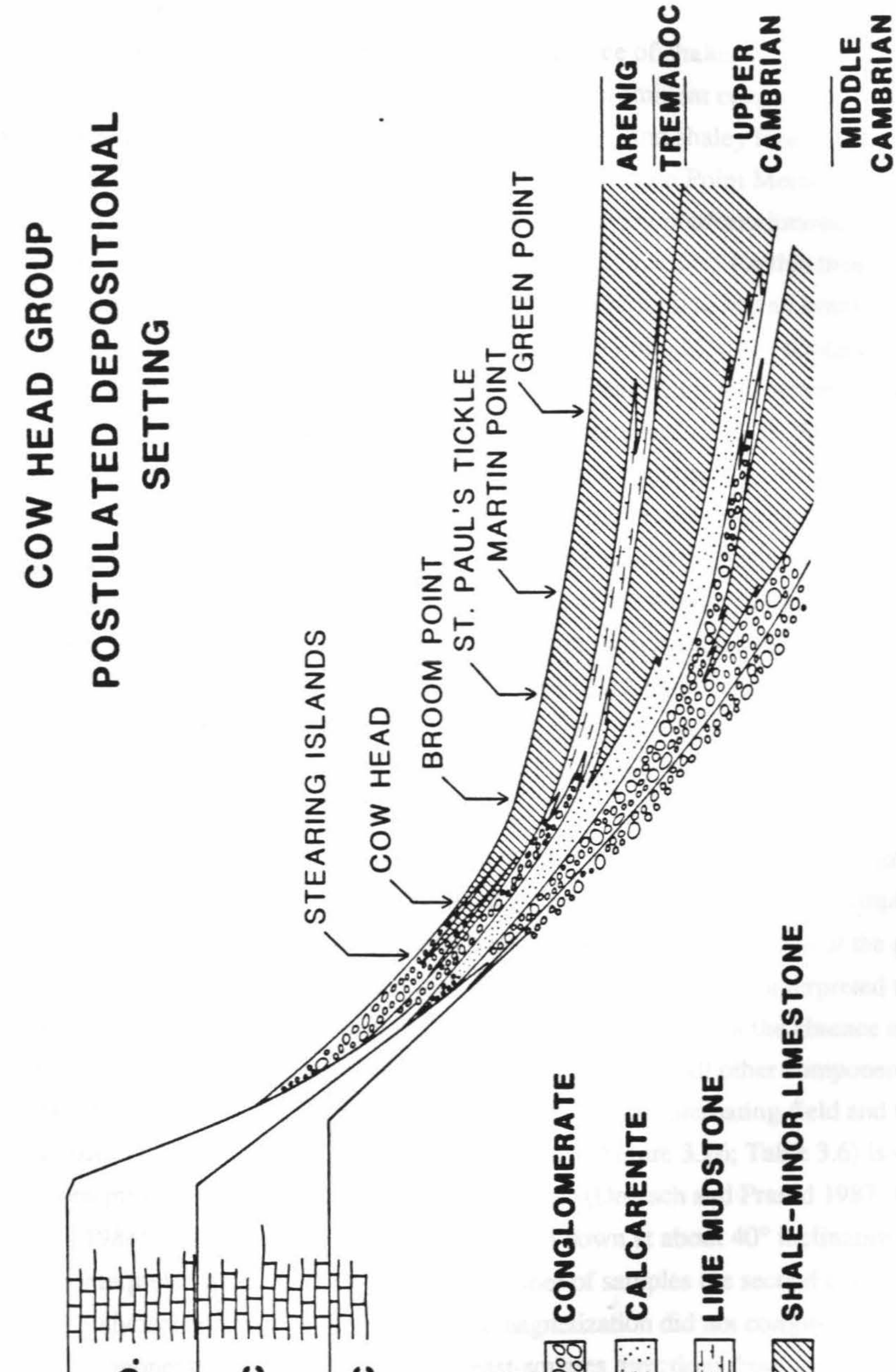
COW HEAD GROUP
POSTULATED DEPOSITIONAL
SETTING
STEARING ISLANDS
COW HEAD
BROOM POINT
ST. PAUL'S TICKLE
MARTIN POINT
GREEN POINT
ARENIG
TREMADOC
UPPER
CAMBRIAN
MIDDLE
CAMBRIAN
L.O.
U€
M€
CONGLOMERATE
CALCARENITE
LIME MUDSTONE
SHALE-MINOR LIMESTONE

4.e.1. Green Point

The Green Point section is comprised of a sequence of shales, shaley limestones, and limestones exposed along a wave-cut cliff, with two prominent conglomeratic beds within the Cambrian-Ordovician boundary interval. Shales and shaley limestones predominate in the lower part of the section, the Upper Cambrian Green Point Member, while the Lower Ordovician Broom Point Member is almost exclusively platform limestones. The section contains perhaps the world's finest assemblage of graptolites for this time interval (Erdtmann 1988). Unfortunately, most of the Green Point Member has an impoverished conodont fauna, but near the Green Point Member-Broom Point Member contact conodonts become more abundant (see Barnes 1988). Reported trilobite finds are extremely rare, especially in the Green Point Member, although recent comments by S.H. Williams (COBWG Circular #26) indicate they may be useful in the uppermost part of the section.

Magnetostratigraphic samples were collected from the section in September, 1986 and again in August, 1988. The first sampling traversed almost the entire section, from the lowest exposure of the Upper Cambrian up to the base of the Arenig Series. The second sampling concentrated on the interval between two prominent breccia units, approximately corresponding to the *Cordylodus intermedius* through *Cordylodus lindstromi* zones. For the first sampling, cores were taken using a portable drill, but with the establishment of Gros Morne National Park as a World Heritage site, no further mechanized collection was permitted, and block samples were taken in 1988.

Results of demagnetization experiments using the first suite of samples suggest the presence of at least two magnetic components in an overwhelming number of samples. Natural remanent magnetization (NRM) directions are nearly identical to that of the present-day geomagnetic field in western Newfoundland (Figure 3.24), and are interpreted to reflect a viscous remanent magnetization (VRM) component which, in the absence of any laboratory demagnetization, is usually strong enough to obscure all other components. This first component was often almost completely removed by alternating-field and thermal demagnetization (Figure 3.25). The second component (Figure 3.26; Table 3.6) is similar to directions previously identified as Lower Ordovician (Deutsch and Prasad 1987; Hall and Evans 1988) (Figure 3.27); i.e., southeastern and down at about 40° inclination for directions interpreted as reverse polarity. In a number of samples the second component was completely isolated, but for the majority, demagnetization did not completely remove the VRM component. Poles to the planes of least-squares directions from samples for which the second component could not be completely isolated, and those to the planar

Figure 3.24. Natural remanent magnetizations of samples from the Green Point section, demonstrating strong similarity to the present-day field direction in western Newfoundland.

Figure 3.25. Typical demagnetization trajectories in equal area (a,b) and orthogonal projection (c) for samples with reverse (a) and normal (b) polarities at Green Point, showing separation from the original NRM towards a direction trending southeast, with moderately positive inclination (for reverse polarity).

Figure 3.26. Equal area projection of characteristic directions isolated from the Green Point section.

Figure 3.27. Comparison, in equal area projection, of characteristic directions of samples from Green Point (this study), and previous directions identified from western Newfoundland.

Natural remanent magnetizations

Green Point section
Cow Head Group, western Newfoundland

Geographic coordinates

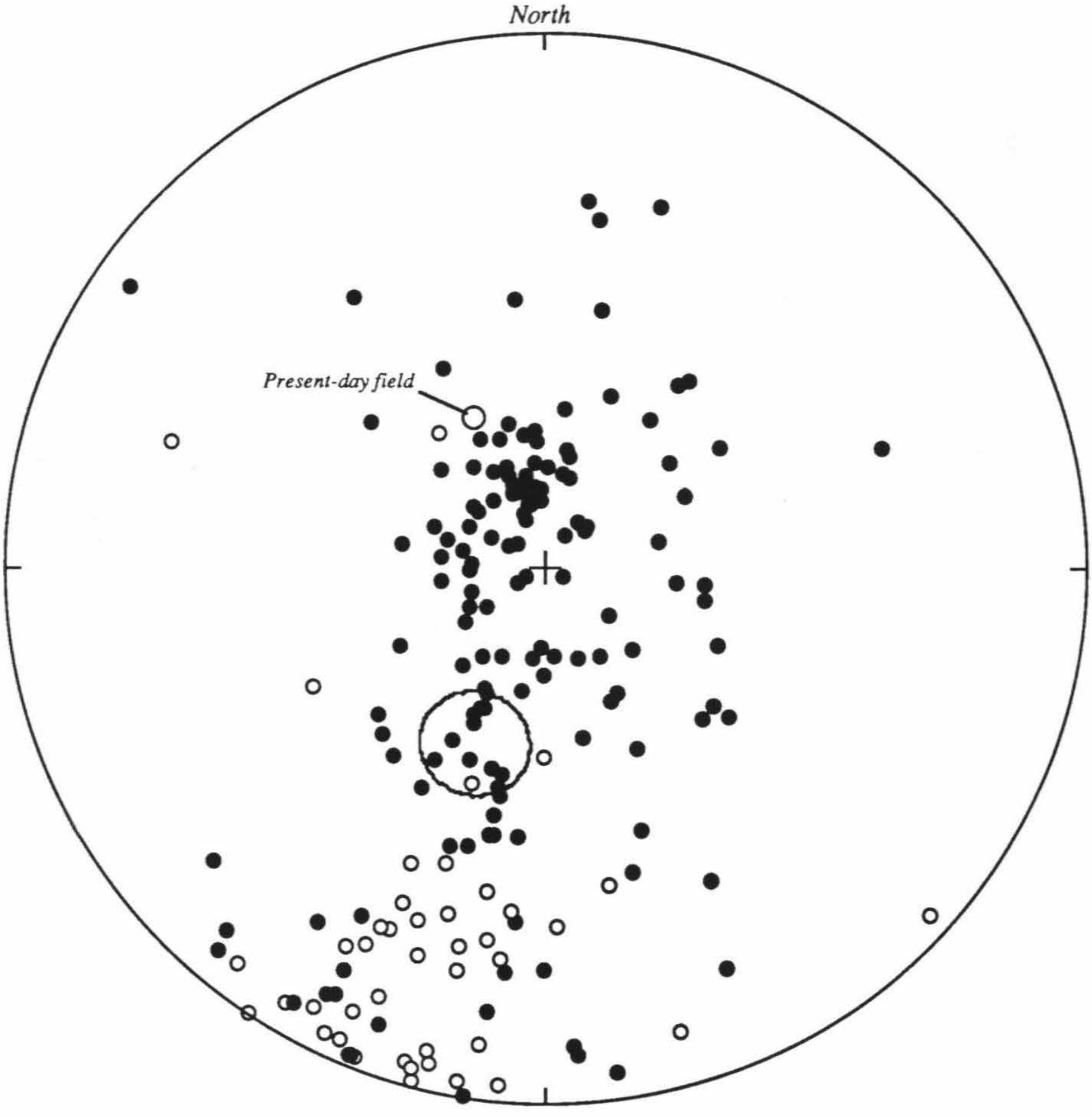

Figure 3.24

Progressive demagnetization of sample GPN 92.0

Green Point section
Cow Head Group, Newfoundland

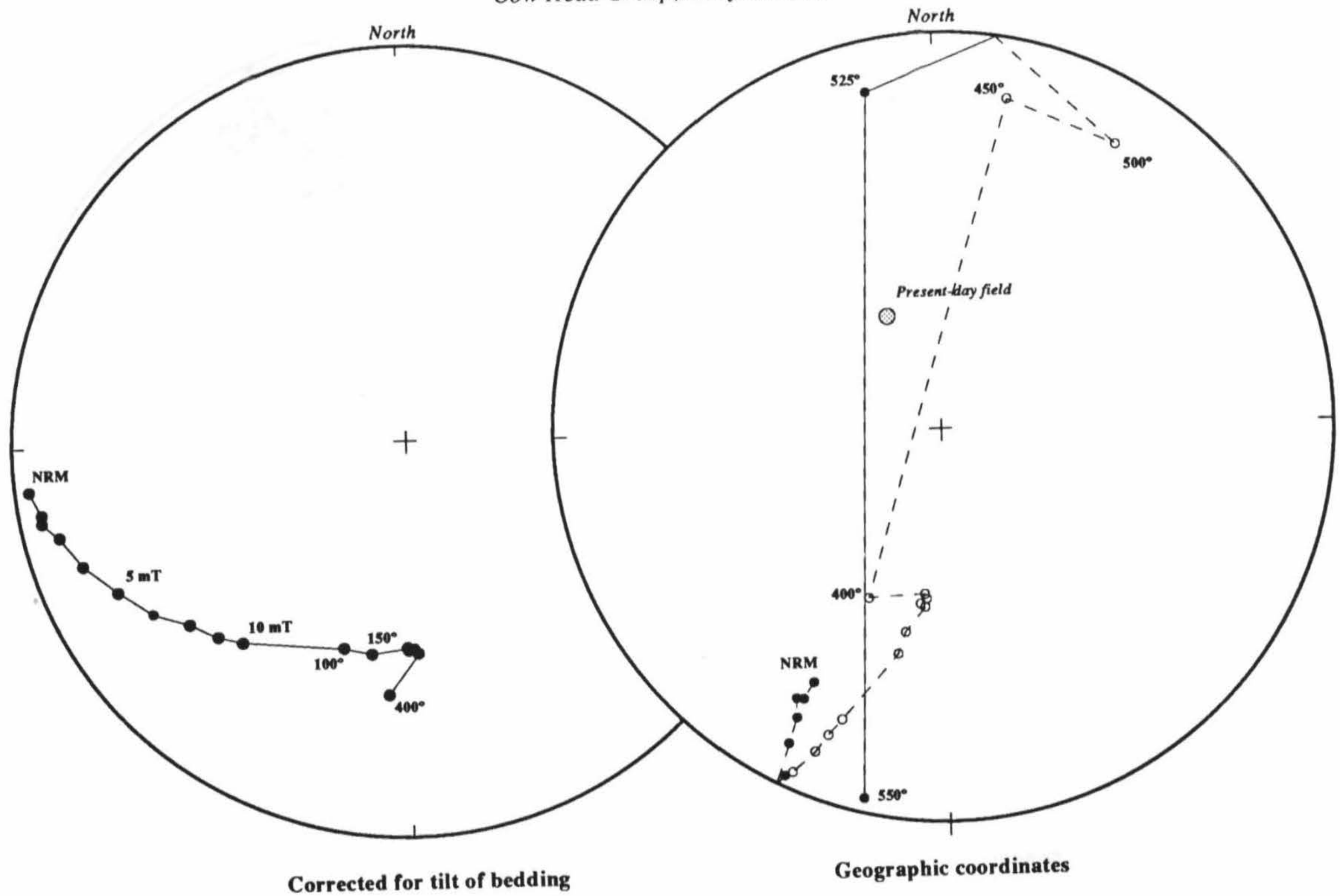

Figure 3.25.a

Progressive demagnetization of sample GPN 38.0

Green Point section

Cow Head Group, Newfoundland

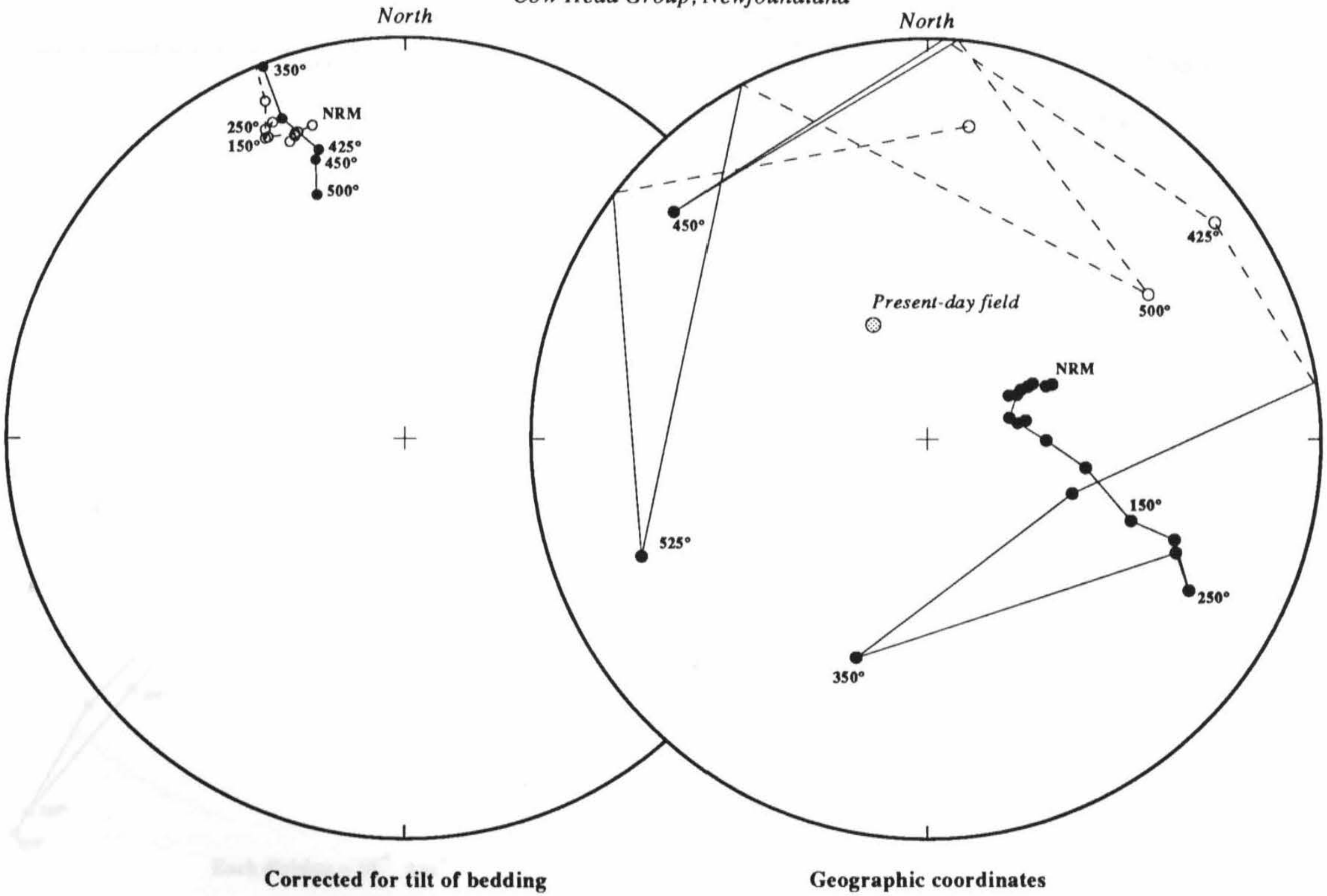

Figure 3.25.b

Progressive demagnetization of sample GPN 38.0

Green Point section
Cow Head Group, Newfoundland

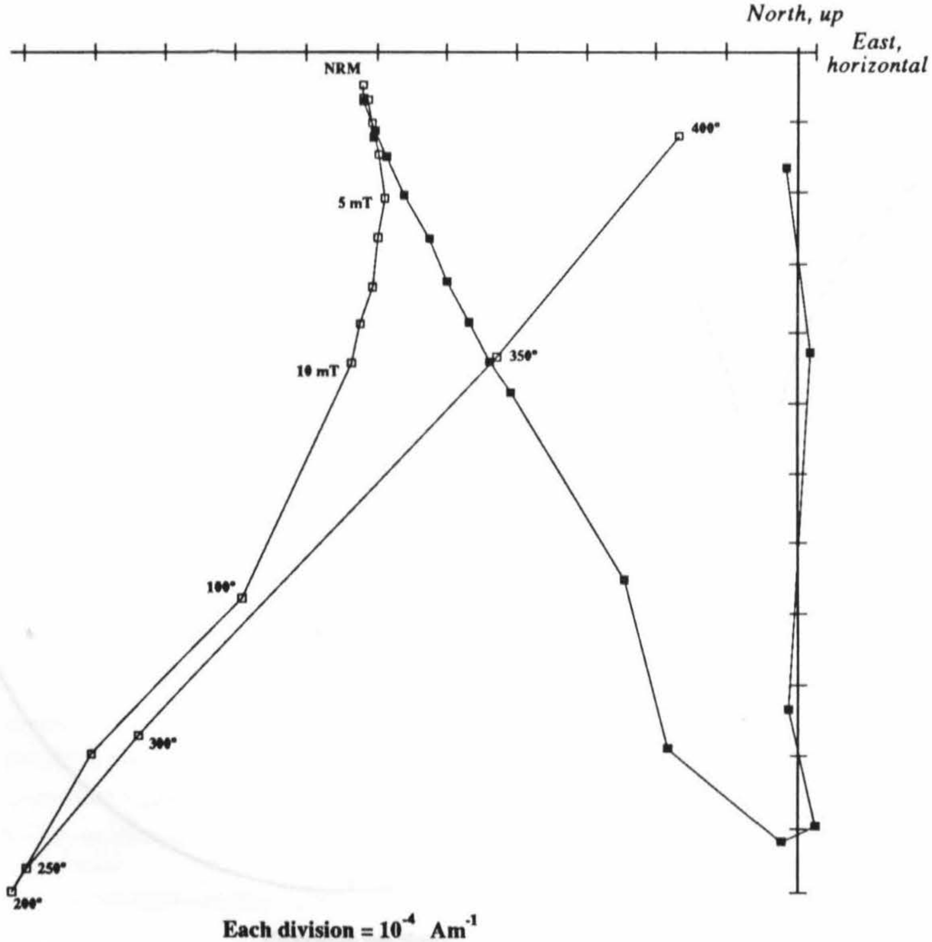

Progressive demagnetization of sample GPN 38.0

Green Point section
Cow Head Group, Newfoundland

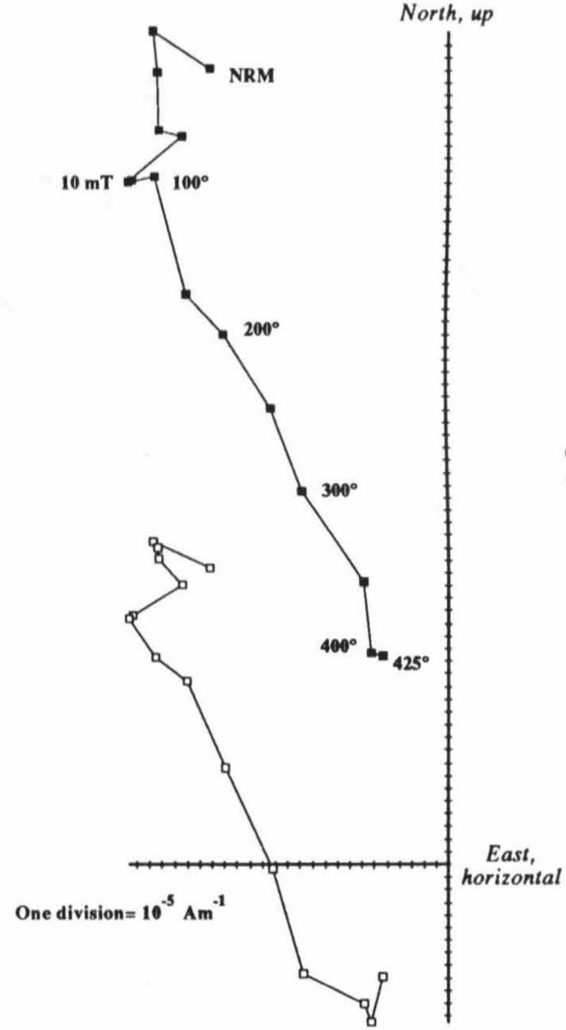

Figure 3.25.c

Characteristic directions

Green Point section
Cow Head Group, western Newfoundland

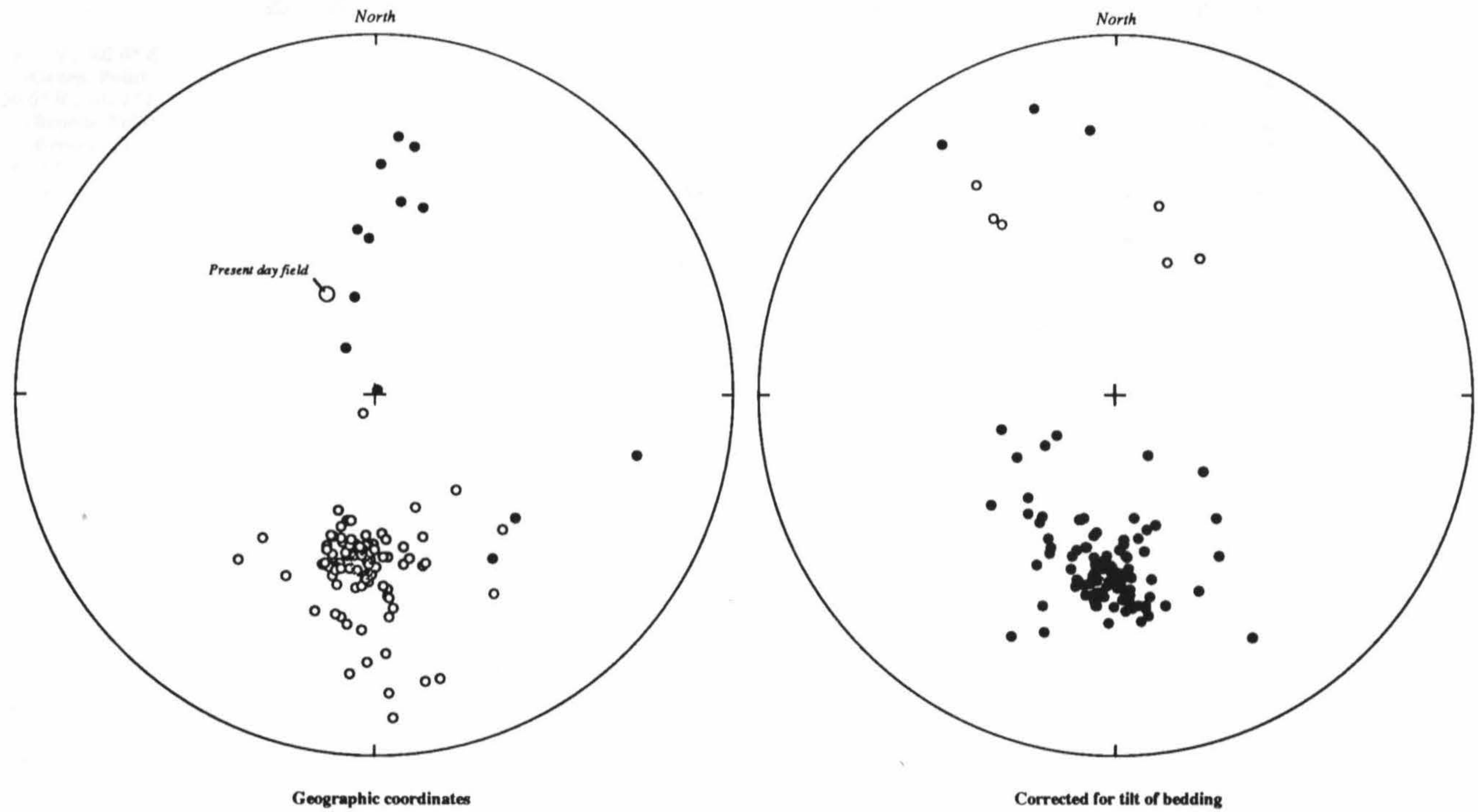

Figure 3.26

Table 3.6. Section mean directions, statistics, and pole positions for Upper Cambrian and Lower Ordovician carbonates from the Cow Head Group, western Newfoundland, Canada, along with selected previous results from western Newfoundland.

Section	R_t	R_s	R_p	(Geographic) Dec	(Geographic) Inc	(Geographic) κ	(Tilt-corrected) Dec	(Tilt-corrected) Inc	(Tilt-corrected) κ	(Tilt-corrected) α_{95}	Pole Position		δp	δm
49.7° N., 302.0° E.														
-Green Point	200	114	165	185°	-51°	20.8	182°	49°	20.3	3°	10° S.	60° W.	3°	4°
50.0° N., 302.2° E.														
-Broom Point North	97	26	72	145°	63°	16.5	159°	24°	15.1	7°	25° S.	35° W.	4°	8°
-Broom Point South	111	52	77	152°	73°	9.3	160°	15°	9.1	7°	30° S.	35° W.	4°	7°
50.1° N., 302.4° E.														
-St. Paul's Inlet quarry	34	19	25	167°	61°	9.4	153°	18°	9.3	12°	26° S.	28° W.	6°	12°
mean of all sections	442	211	339	171°	0°	5.3	170°	36°	8.3	4°	19° S.	48° W.	3°	5°
Deutsch and Prasad (1987)														
-St. George Group (A component)				151°	20°	120	148°	33°	80	3°	18° S.†	28° W.†	3°	5°
-Table Head Group (A component)				153°	29°	623	150°	41°	232	2°	13° S.†	31° W.†	3°	5°
Hall and Evans (1988)														
-St. George Group (A component)				nr	nr	nr	159°	35°	101	nr	nr	nr	-	-
-Table Head Group (site 2)				nr	nr	nr	148°	38°	43	5°	15° S.	28° W.	nr	nr

R_t = total number of samples analyzed
R_s = total number of samples used to calculate statistics
R_p = total number of samples used for polarity interpretation
Dec = declination
Inc = inclination

κ = estimate of Fisher's precision parameter

α_{95} = associated radius of the cone of 95% confidence (McElhinny 1973)

δm and δp = meridinal and latitudinal axes of the oval of 95% confidence around the poles
nr = not reported
†Polarity inverted from original reference.

Site-mean characteristic directions

Cow Head Group (this study) and previous results western Newfoundland, Canada

Corrected for tilt of bedding

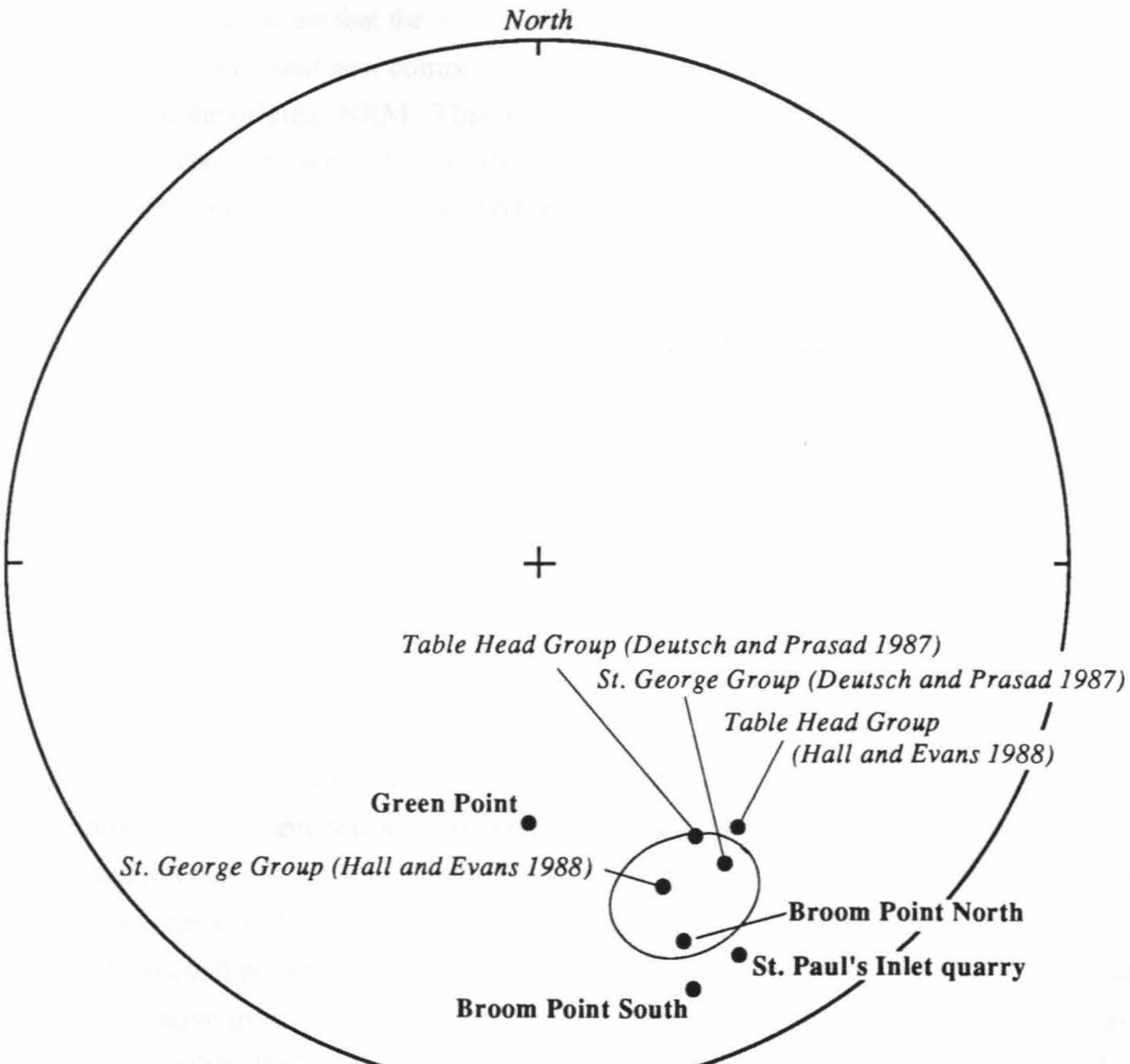

Figure 3.27

(two-component) portions of the demagnetization trends for samples from which the VRM component was completely removed, are virtually identical, indicating that the second component is probably the same in all samples.

A strong remagnetization component is present after thermal demagnetization at 400° C. in virtually all samples. Rock magnetic studies indicate that the mineral carrying the natural remanence (NRM) is magnetite, while the mineral carrying remanence at 450° C. and higher is predominantly hematite or another very high coercivity mineral. From this information it is concluded that the directions present after demagnetization temperatures higher than 400° represent new components acquired by chemical alteration, and are not components of the original NRM. This interpretation is consistent with results from modern-day carbonates, which frequently yield unreliable results above 400° C due to chemical alteration (D. McNeill, pers. comm.).

Magnetostratigraphic interpretation of the results from this section reveal two normal polarity intervals within the *Eoconodontus notchpeakensis or Cordylodus proavus* zone (Fig. 3.28). Within the overlying *C. intermedius* and *C. lindstromi* zones there are no samples that are conclusively of normal polarity, although there are two samples, separated by about 5 meters, which may possibly represent brief periods of normal polarity within the *C. lindstromi* zone.

Because of the extremely low conodont yields from units of the Martin Point Member (except for two samples from the large conglomerate comprising Bed 19) (Barnes 1988), no detailed Upper Cambrian conodont zonation has been established, making magnetostratigraphic correlation to other localities difficult. There are at least two plausible correlation schemes. The first suggests that the impoverished conodont faunas have severely obscured the first appearances of *C. proavus* , *C. caboti,* and *C. intermedius,* and that the upper normal polarity interval at Green Point correlates with normal polarity zones around the first occurrence of *C. proavus* at other localities. Under this hypothesis, the base of the *C. proavus* zone would be about 50 meters below Bed 19.

The second possibility presumes that Bed 19 was emplaced with enough erosion at its base to remove most of the *C. proavus* zone. Barnes (1988) argues that such a mechanism is implausible; Bed 19 sits upon a thin bed of limestone, arguing for a base that did not down-cut during emplacement. Under this scheme, the two normal polarity intervals would correlate with normal polarity intervals found at other localities in the *Proconodontus muelleri* and *P. posterocostatus* zones.

Figure 3.28. Magnetic polarity interpretation for Green Point. Lithologic section from James and Stevens (1986); biostratigraphy from Barnes (1988). Dashed text lower in the section indicates predicted biozone boundaries based on magnetostratigraphic correlation with sections outside the Cow Head Group.

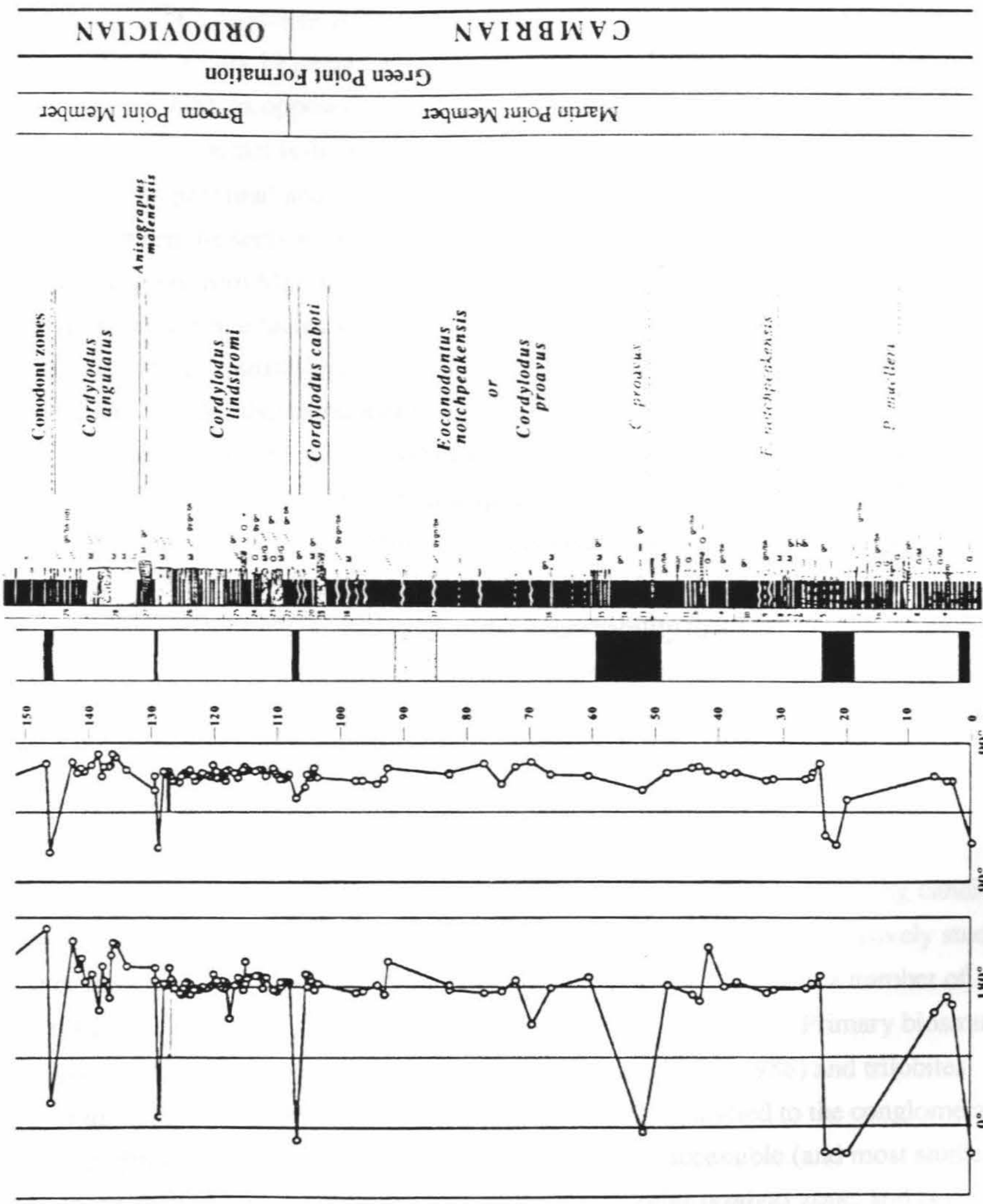
ORDOVICIAN
CAMBRIAN
Green Point Formation
Broom Point Member
Martin Point Member
Conodont zones
Cordylodus angulatus
Anisograptus matanensis
Cordylodus lindstromi
Cordylodus caboti
Eoconodontus notchpeakensis
or
Cordylodus proavus
meters
Inclination
Declination
90°
-90°
180°
0°

Unfortunately, resolving this question through collection of adequate numbers of conodonts from the lower part of the Green Point section appears unrealistic. Comparison with zonations in other sections is promising, but problematic. At Martin Point, the base of the *C. caboti* zone occurs 19 meters below the Martin Point Member-Broom Point Member contact (Barnes 1988), as opposed to 5 meters below at Green Point. However, the Martin Point-Broom Point contact is demonstrably diachronous (James and Stevens 1986, p. 74) between the more proximal and distal facies of the Cow Head Group, and may also be diachronous between the sections at Green Point and Martin Point. At the present time, the degree of collection from Martin Point does not permit an accurate estimate of the thickness of the *C. caboti* zone in a facies similar to that at Green Point, but at the St. Paul's Inlet quarry section, the *C. lindstromi*, *C. caboti*, and *C. proavus* zones are all of approximately the same thickness. Furthermore, assuming the time encompassed by the *C. proavus* zone is about 1 million years, and that the top of the C. proavus zone corresponds to Bed 19, the sedimentation rate required to have the first appearance of *C. proavus* 50 meters below Bed 19 is only 5 cm/1000 years. This seems quite reasonable; the sedimentation rate within the distal facies found at Green Point should have been fairly high (see Figure 3.22).

Because of the impoverished faunas, the improbability that Bed 19 was emplaced with significant erosion, and because the required sedimentation rate is quite realistic, correlation of the normal polarity interval in Beds 11-15 with the *C. proavus* zone is presently favored.

4.e.2. Broom Point North

The northern section at Broom Point was originally considered as a strong candidate for the Cambrian-Ordovician boundary global stratotype. The most intensively studied portion of the section consists predominantly of platform limestones, with a number of prominent conglomeratic units and highly deformed ribbon limestones. Primary biostratigraphic control for the section is based on both conodonts (Barnes 1988) and trilobites (Fortey *et al.* 1982), although trilobite recoveries are usually restricted to the conglomeratic units. Graptolites are also present. Unfortunately, the most accessible (and most studied) interval in the section begins above the base of the *Cordylodus proavus* zone, and perhaps even as high as the base of the *Cordylodus lindstromi* zone.

Ninety-seven core samples were collected from 88 levels in September, 1986 (10 samples were collected from a single wrinkled limestone unit as a micro-fold test), beginning in Bed 74 (see James and Stevens 1986). The directions of results from this section were similar to the results at Green Point, despite striking differences in the attitude of bedding between the two localities. Two components were obvious; one was similar to the present-day field in western Newfoundland, and the other very similar to the second component at Green Point (Figure 3.29; see also Table 3.6, Figure 3.27). The first component was removed by low levels of thermal demagnetization, and is interpreted to be a VRM. In a relatively high percentage of samples, the second component was completely isolated during thermal demagnetization. Equal area projection shows that the characteristic directions of this component (Figure 3.30) are highly consistent, particularly given this type of lithology, and compare well with other results from western Newfoundland, including Green Point.

Results from a micro-fold test, using a highly deformed limestone unit, were negative (Figure 3.31), demonstrating that the preserved directions were acquired after deformation. However, soft-sediment deformation of this type probably occurred immediately after deposition, since the folds do not interrupt the overlying bedding. Furthermore, when these directions are corrected for the present-tilt of bedding, they are identical to directions from other samples taken from non-deformed units, indicating the direction was acquired no later than the Middle Ordovician folding of the Cow Head Group. Therefore, the presence of a negative fold test from this section does not imply that a magnetic polarity stratigraphy from this section would not be representative of the field during (or immediately after) deposition, but simply that the direction preserved in the folded units was acquired after the folding took place.

Three very short normal polarity intervals have been identified within the Broom Point North section, although none of the three is defined by more than one sample (Figure 3.32). The lower two samples displaying normal polarity, which are both in the upper part of the *Cordylodus lindstromi* zone, each have adjacent 3-5 meter intervals with unstable magnetic properties. Both of these levels are unusual; there are very few other samples in this section that are apparently unstable. The lower occurs at virtually the same level as the reported first occurrence of the graptolite *Anisograptus matanensis*. The uppermost sample with normal polarity was the youngest sample collected from the section, and stratigraphically the highest collected from the Cow Head Group for this study.

4.e.3 Broom Point South

Samples were also collected from the Broom Point South section in September, 1986. The section contains many large conglomeratic units and at least two substantial un

Figure 3.29. Typical demagnetization trajectories in equal area (a) and orthogonal projection for samples with reverse polarity at Broom Point North.

Figure 3.30. Equal area projection of tilt-corrected characteristic directions of samples from the Broom Point North section. Decl.=156°, incl.=25°, κ= 25.3, α_{95}= 6°.

Figure 3.31. Equal area projection of characteristic directions obtained from Bed 74, a highly-deformed limestone unit within the Broom Point North section. Results yield a strongly negative fold test ($\kappa_{tilt\text{-}corrected}/\kappa_{geographic} = 4.1/55.4 = 0.07$), clearly indicating the preserved characteristic directions in this bed were acquired after the original soft-sediment deformation, but before Middle Ordovician folding of the Cow Head Group.

Figure 3.32. Magnetic polarity interpretation for the Broom Point North section. Stratigraphic column from James and Stevens (1986); biozonation from Barnes (1988).

Progressive demagnetization of sample BNN 8.0

Broom Point North section
Cow Head Group, western Newfoundland

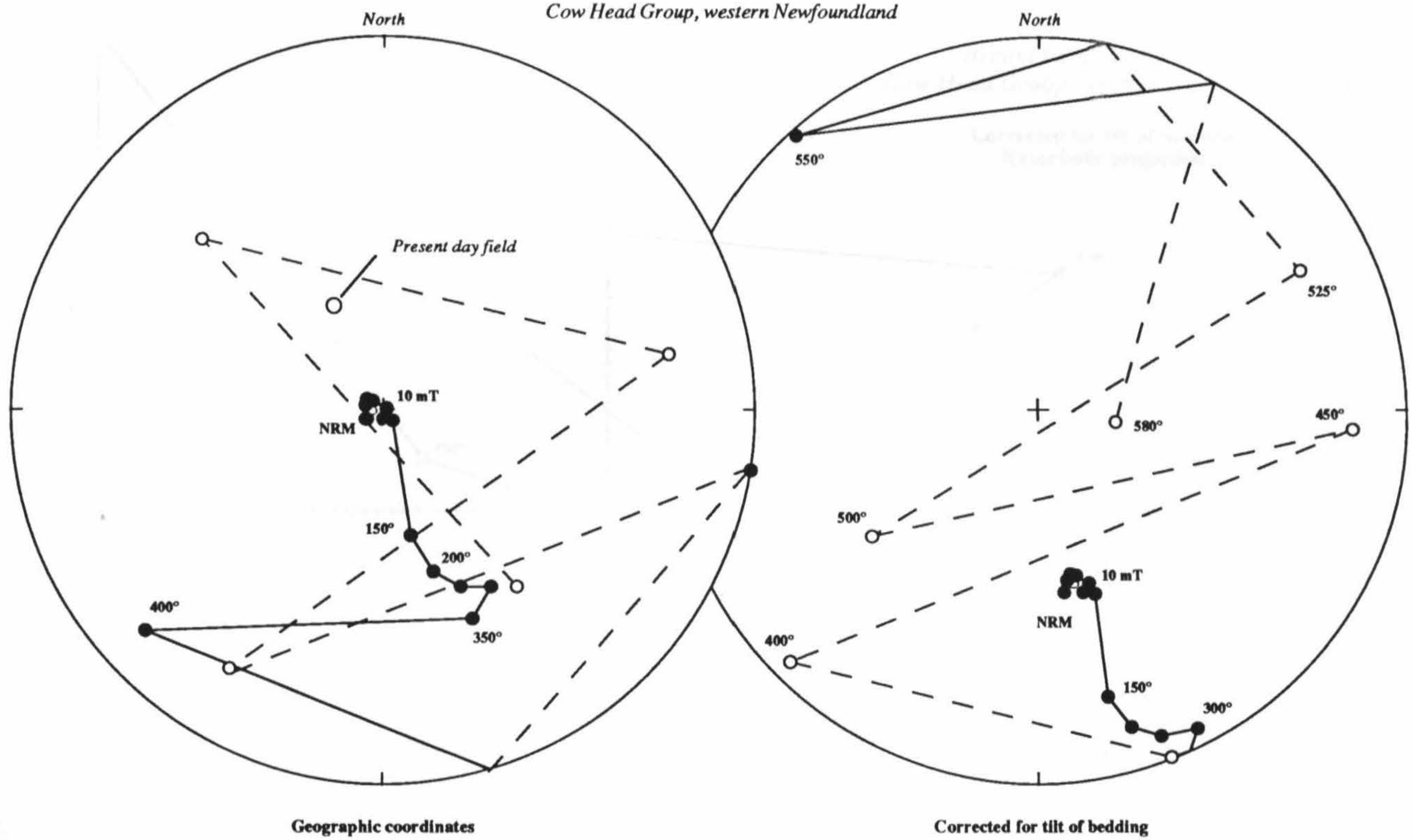

Figure 3.29.a

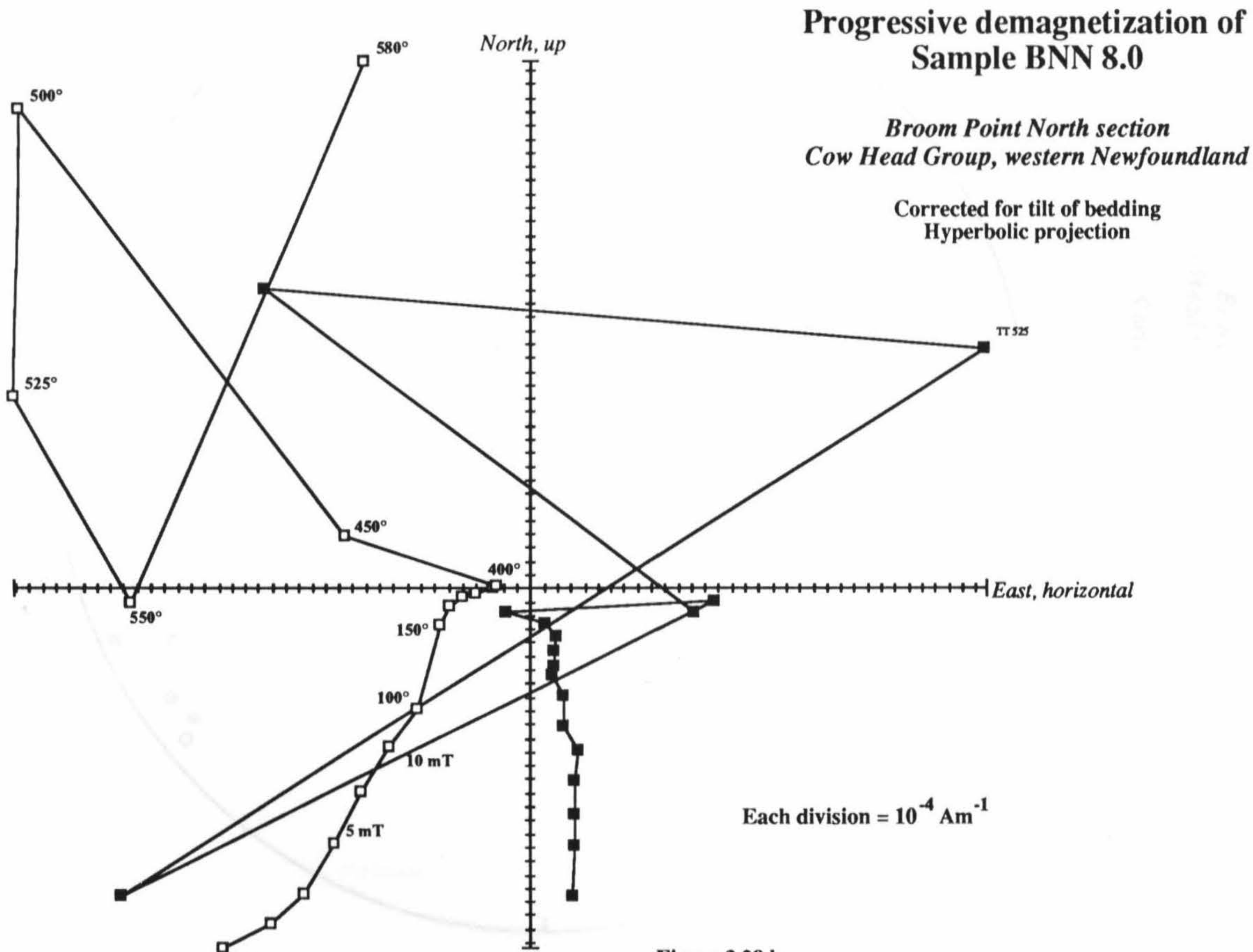
Progressive demagnetization of
Sample BNN 8.0
Broom Point North section
Cow Head Group, western Newfoundland
Corrected for tilt of bedding
Hyperbolic projection
North, up
East, horizontal
580°
500°
525°
550°
450°
400°
150°
100°
10 mT
5 mT
NRM
TT 525
Each division = 10^{-4} Am^{-1}

Figure 3.29.b

Characteristic directions

Broom Point North section
Cow Head Group, wesern Newfoundland

Corrected for tilt of bedding

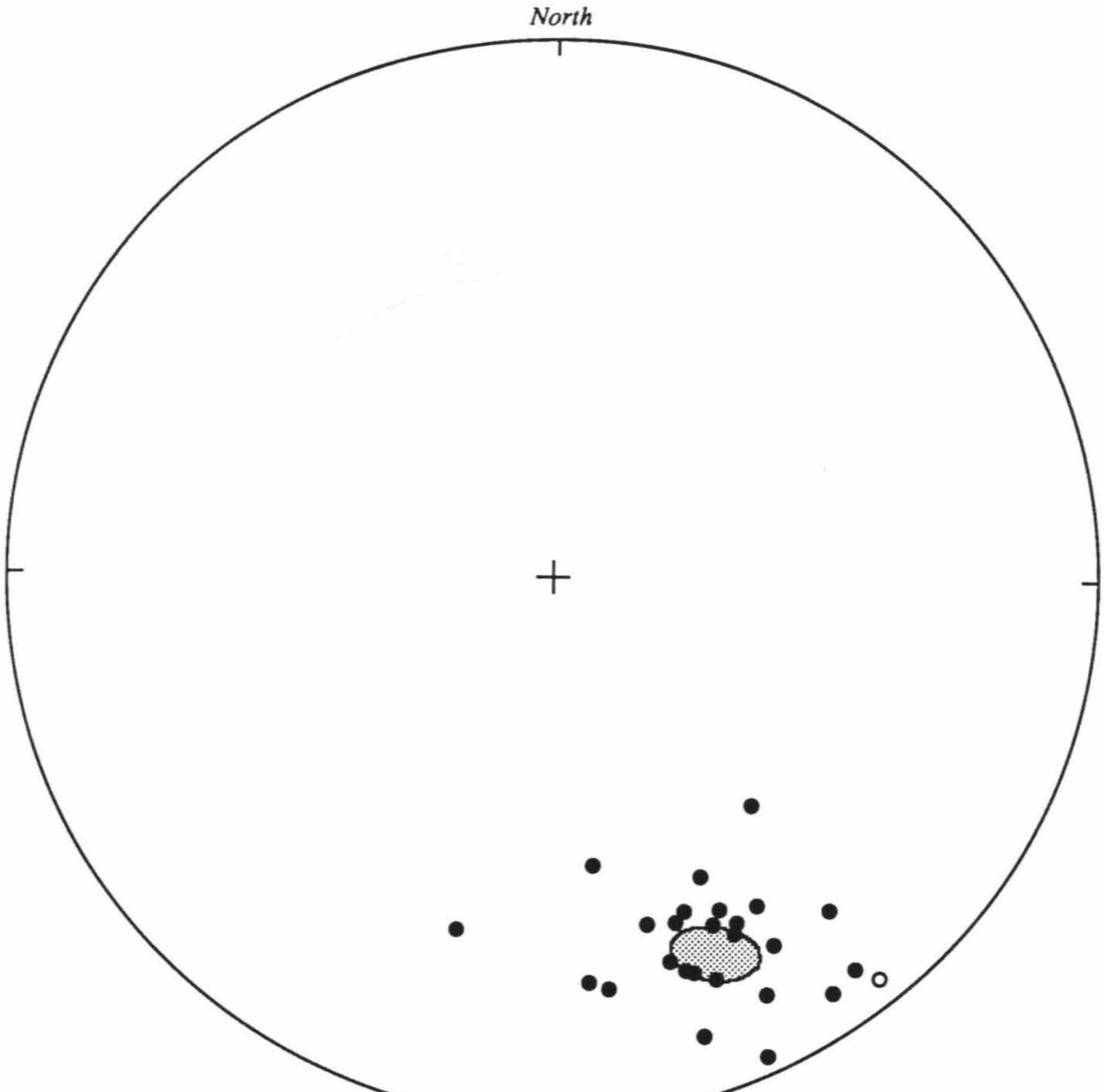

Figure 3.30

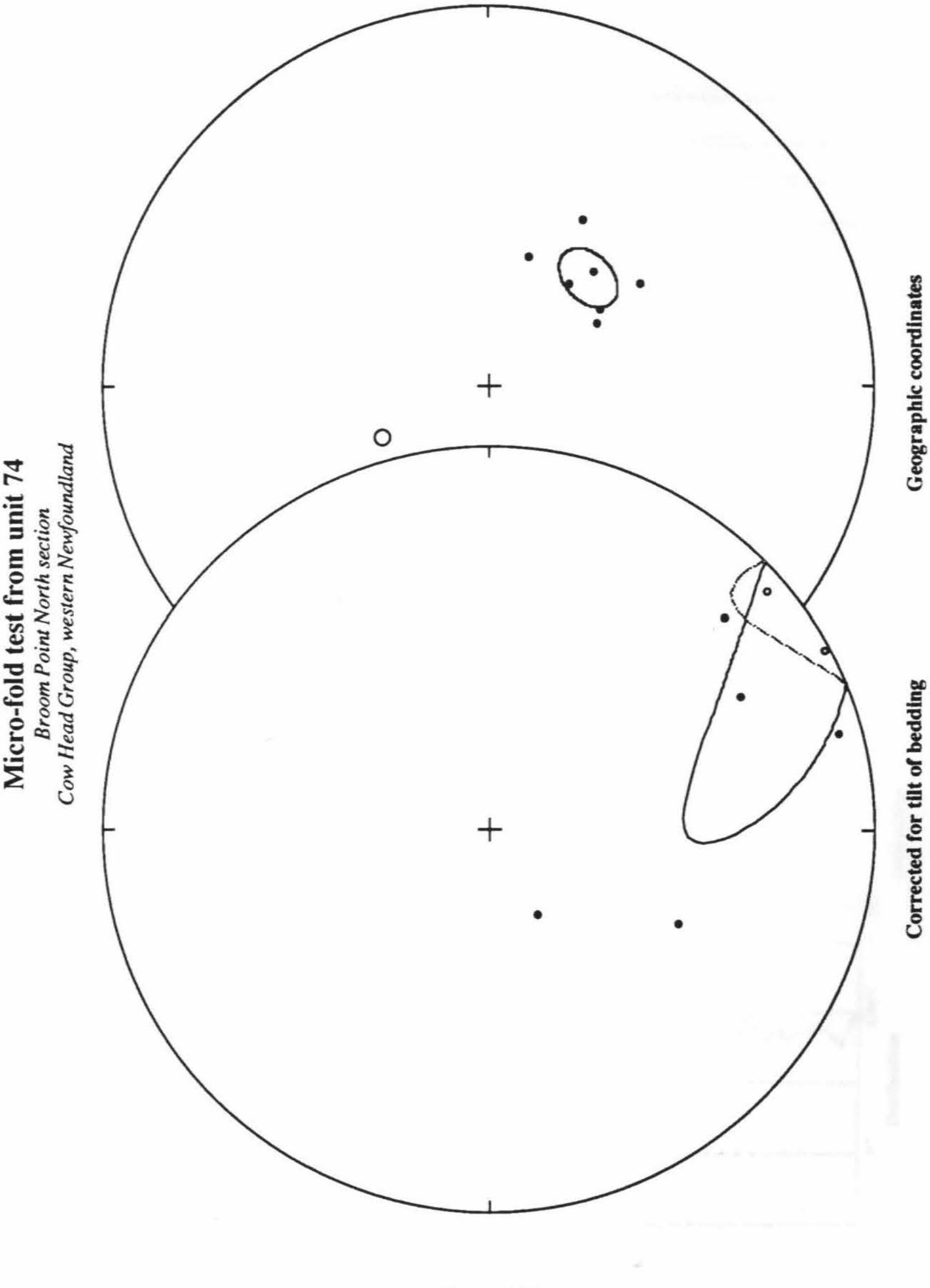
Micro-fold test from unit 74
Broom Point North section
Cow Head Group, western Newfoundland
Geographic coordinates
Corrected for tilt of bedding

Figure 3.31

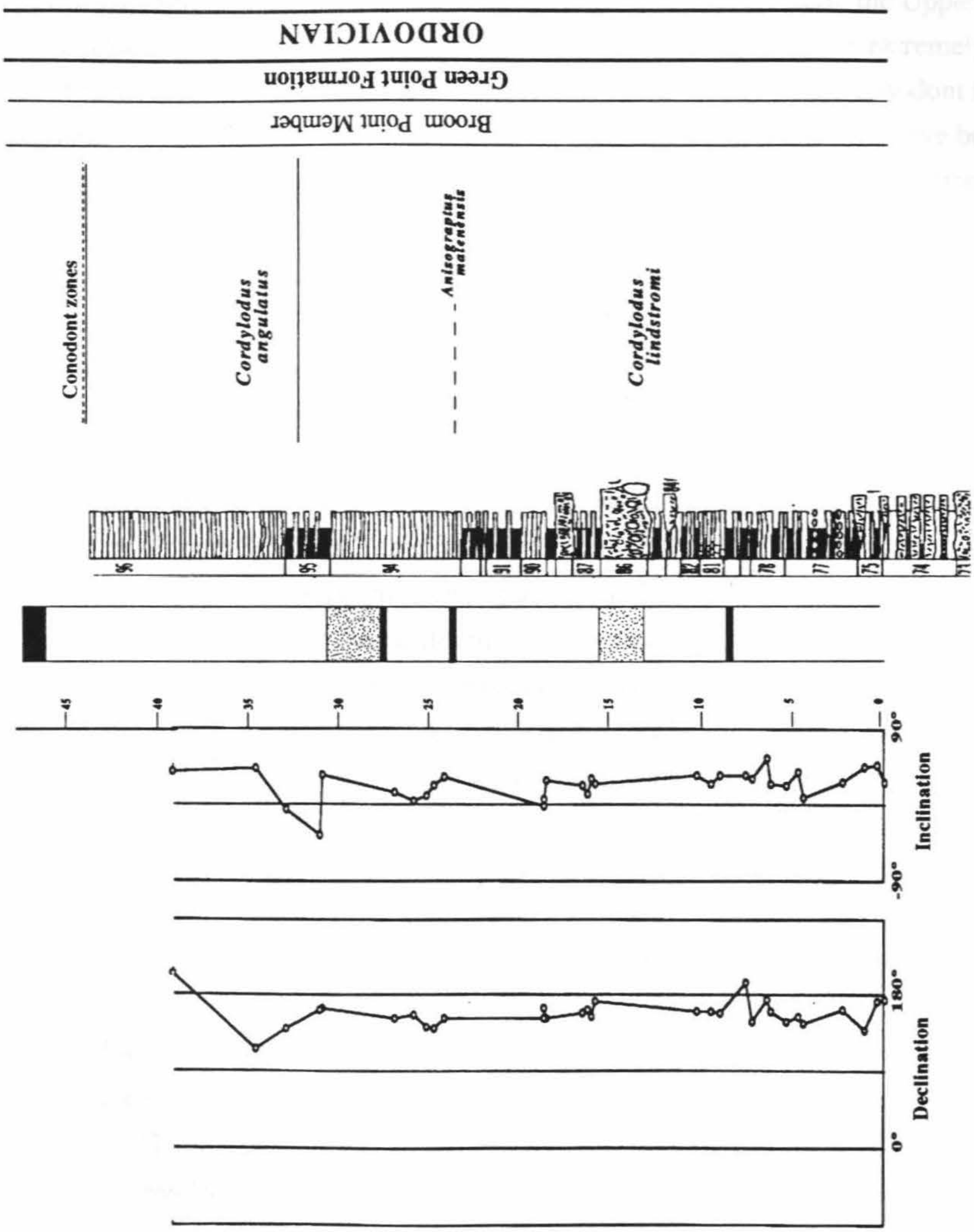
ORDOVICIAN
Green Point Formation
Broom Point Member
Conodont zones
Cordylodus angulatus
Anisograptus
Cordylodus lindstromi
96
95
94
91
90
87
86
82
81
78
77
75
74
71
45
40
35
30
25
20
15
10
5
0
90°
-90°
Inclination
180°
0°
Declination

Figure 3.32

conformities close to the Cambrian-Ordovician boundary, rendering it unsuitable as a stratotype. However, the section has the advantage over its northern counterpart of having an easily accessible Upper Cambrian sequence extending down to below the base of the Trempealeauian Series. Like most of the other sections in the Cow Head, the Upper Cambrian biostratigraphic zonations are poor or non-existent because of the extremely low number of recovered specimens. Only limited study has been done on the conodont faunas at Broom Point South, and some of the units show evidence that these faunas have been re-worked. Trilobites are relatively abundant, but their mixed faunas also raise questions as to whether they may have been re-worked.

Thermal demagnetization experiments on the samples from this section gave results very similar to those from other sections in the Cow Head Group. In most samples two components of magnetization were apparent. The first has a direction very similar to the present-day field in western Newfoundland, and is interpreted to be a VRM. This component dominates the NRM, but is removed by low levels of thermal demagnetization (Figure 3.33). The characteristic direction, which in a moderate percentage of samples is completely isolated (Figure 3.34; see Table 3.6), is similar to those from other sections, although some dispersion is apparent (see Figure 3.27). Dual polarities are present.

Fourteen samples, from four different levels within the Upper Cambrian portion of the Broom Point South section, appear to have normal polarity (Fig. 3.35). The most reasonable correlations, given the present biostratigraphic information, have the uppermost normal polarity zone, which occurs within Beds 42-45, correlative to normal polarity intervals within the *Cordylodus proavus* zone in other sections. The middle two normal zones appear to correlate well with normal polarity intervals in the *Proconodontus muelleri* and *P. posterocostatus* zones at Dayangcha, China; Black Mountain, Australia; and Threadgill Creek, Texas. Correlation of the lowest normal polarity zone is not presently possible.

4.e.4 St. Paul's Inlet quarry

Forty-six samples were collected from the section at St. Paul's Inlet quarry in August, 1988. Good conodont and graptolite faunas have been documented (Barnes 1988; James and Stevens 1986), although the number of specimens of both taxa that have been recovered is fairly small compared to the other relevant sections in the Cow Head.

Paleomagnetic directions from this section are very similar to those from the other Cow Head sections included in this study. Characteristic directions were isolated by thermal demagnetization in a few of the samples (Fig. 3.36; see Table 6), and polarity interpre-

Figure 3.33. Typical demagnetization trajectories in equal area (a) and orthogonal projection for samples with reverse polarity at Broom Point South.

Figure 3.34. Equal area projection, in tilt-corrected and geographic coordinates, of characteristic directions from the section at Broom Point South.

Figure 3.35. Magnetic polarity interpretation of the section at Broom Point South. Stratigraphic column for James and Stevens (1986); biozonation from Barnes (1988).

Figure 3.36. Equal-area (left) and orthogonal projection of a typical demagnetization trajectory for samples with normal polarity at St. Paul's Inlet quarry.

Progressive demagnetization of sample BSN 97.0

Broom Point South section
Western Newfoundland, Canada

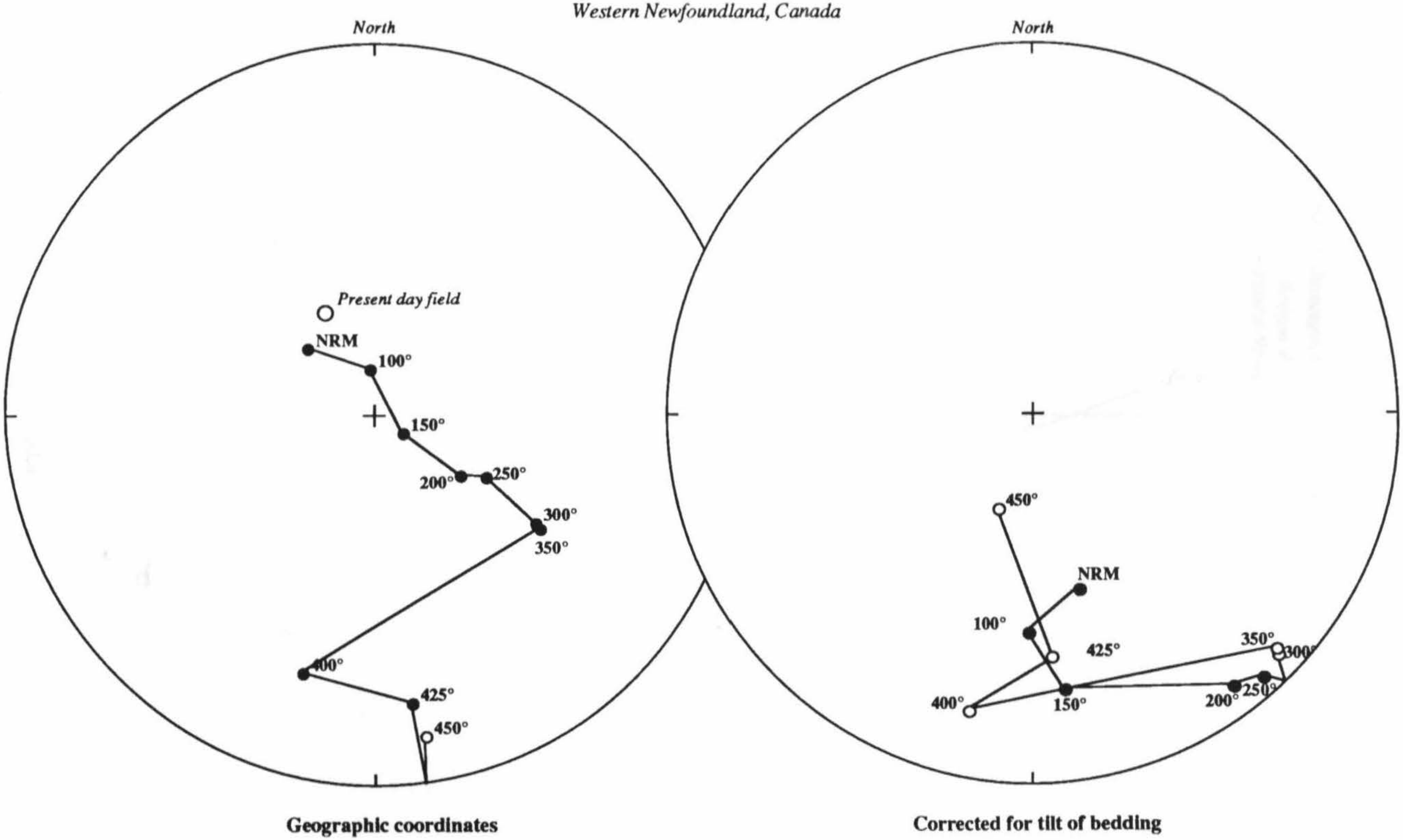

Figure 3.33.a

Progressive demagnetization of sample BSN 97.0

Broom Point South section
western Newfoundland, Canada

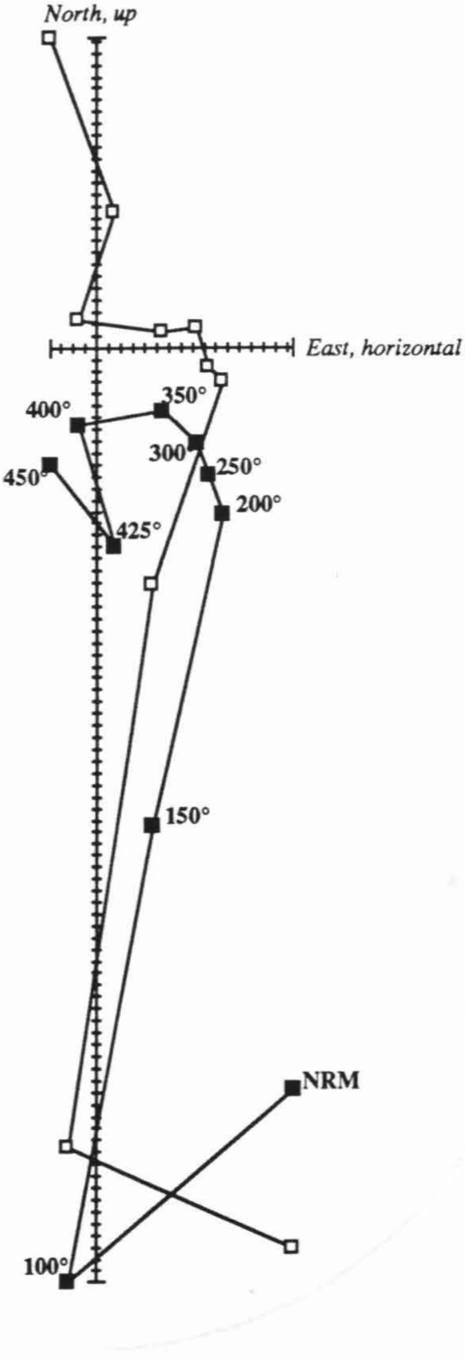

Each division = 10^{-5} Am^{-1}

Figure 3.33.b

Characteristic directions

Broom Point South section
Cow Head Group, western Newfoundland

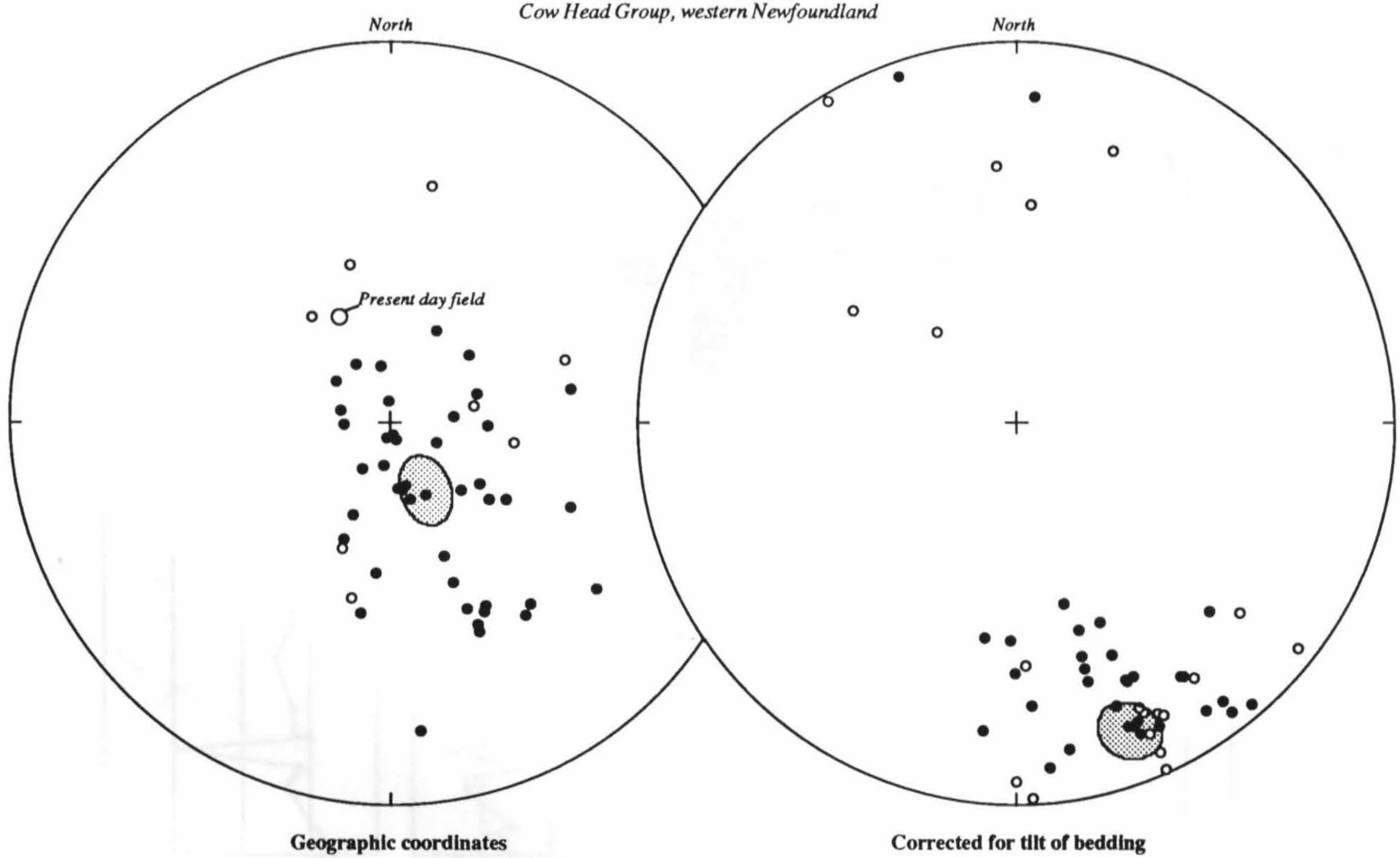

Figure 3.34

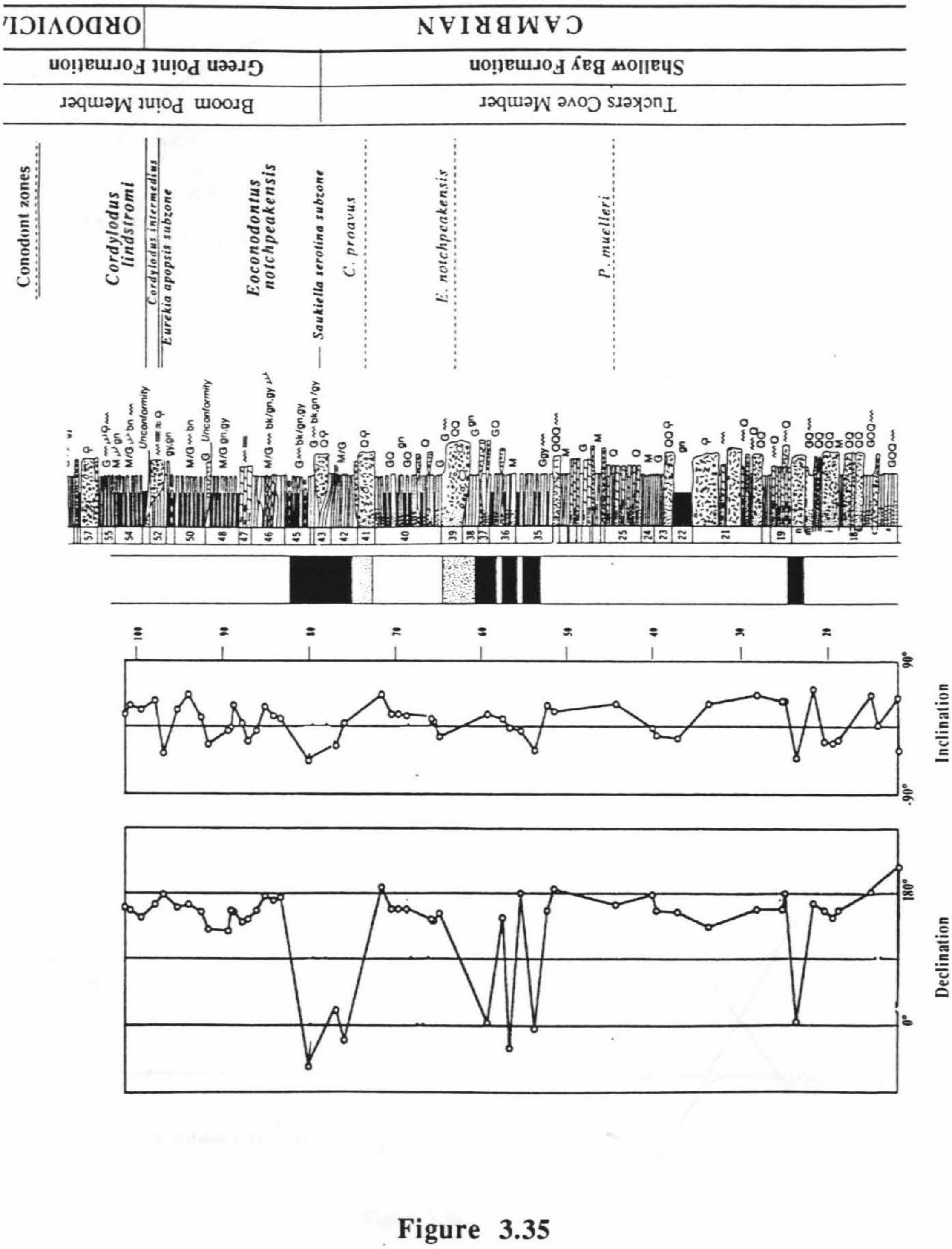
ORDOVICI
CAMBRIAN
Green Point Formation
Shallow Bay Formation
Broom Point Member
Tuckers Cove Member
Conodont zones
Cordylodus lindstromi
Cordylodus intermedius
Eurekia apopsis subzone
Eoconodontus notchpeakensis
Saukiella serotina subzone
C. proavus
E. notchpeakensis
P. muelleri
Unconformity
Inclination
Declination
90°
-90°
180°
0°

Figure 3.35

Progressive demagnetization of sample SPN 22.0

St. Paul's Inlet quarry section
Cow Head Group, western Newfoundland

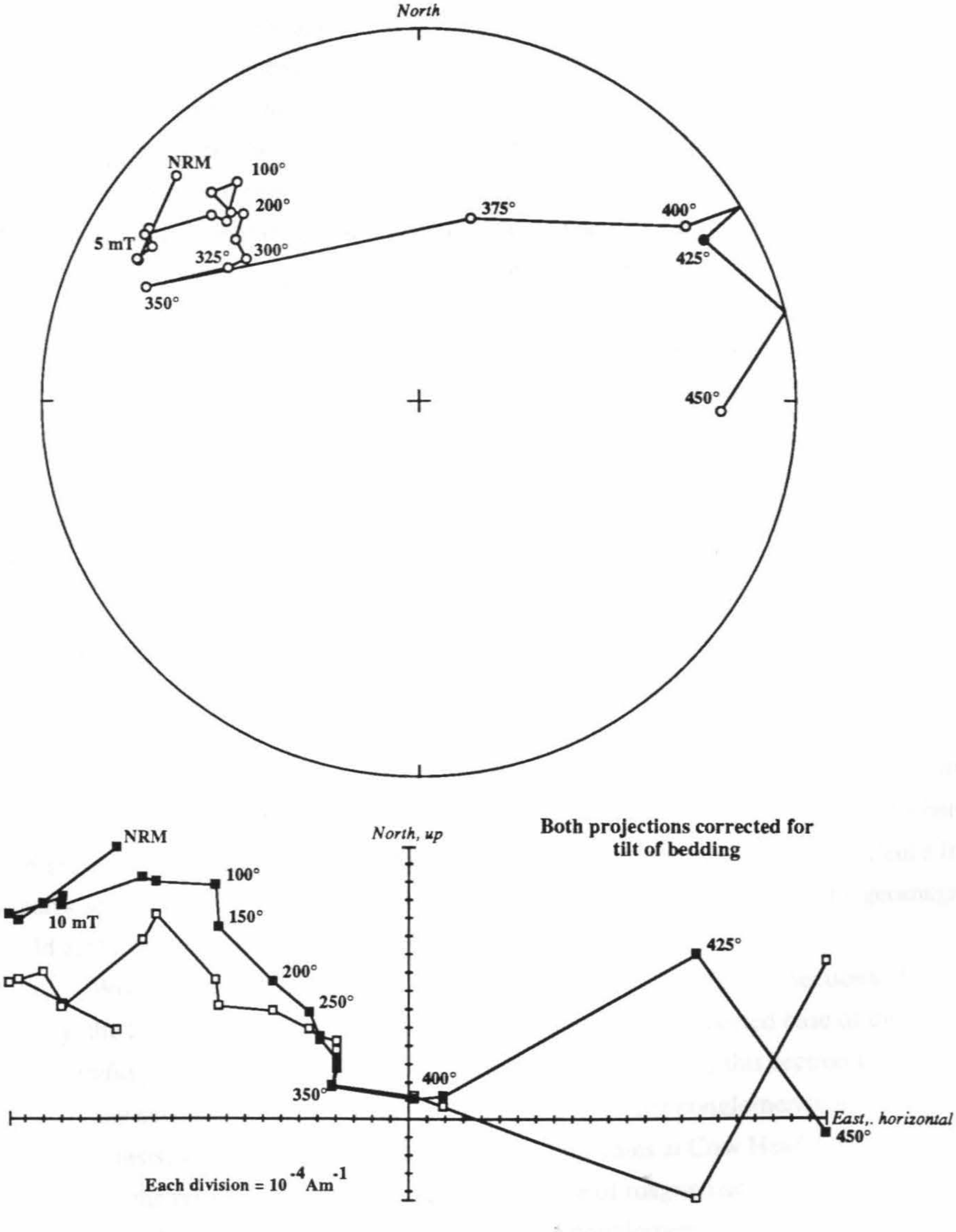

Figure 3.36

interpretation was possibly in most of the other samples from this section. Demagnetization trajectories were dominated by a VRM, which was substantially removed by low temperatures. Generally, characteristic directions isolated by this method compared favorably with those from other sections in the Cow Head (Figure 3.37).

Four levels of normal polarity were found within the section (Figure 3.38). The lower two are separated by a large conglomerate (Bed 8) and are probably the same event. Their position just below the first occurrence of *Cordylodus proavus* strongly suggests that they are correlative to normal polarity zones within the *C. proavus* zone in other sections, and that the first appearance of *C. proavus* is somewhere in Bed 5. Very low specimen yields from conodont sampling through the interval in question do not argue against this interpretation.

The youngest normal polarity zone occurs in Bed 19, just below the reported occurrence of *Anisograptus matanensis*. This position agrees well with that of a normal polarity sample in the Broom Point North section. The other sample with normal polarity occurs within Bed 12. Correlation of this level with other sections is not presently possible, although two samples with normal polarity are found at a similar level in the section at Black Mountain, Australia.

An extended form of the fold test can be performed using both characteristic (individual) directions (Figure 3.39) and site-mean directions (Figure 3.40) from the various sections. The results clearly indicate that acquisition of the characteristic component of magnetization preceded large-scale deformation of the Cow Head Group, and therefore, occurred no later than about Middle Ordovician. The similarity of polarity patterns between the sections at Green Point and Broom Point South, and possibly also the St. Paul's Inlet quarry section, further suggests this characteristic direction may represent the geomagnetic field at the time of deposition.

Work is in progress on the Cow Head Ledge and Martin Point sections. Unfortunately, the lowest sample collected at Martin Point was at the reported base of the *Cordylodus proavus* zone, and sampling intervals were larger in this section than in others, which may severely limit the utility of this section. Another conglomerate test, using non-carbone clasts, was collected from the megaconglomerates at Cow Head Ledge, and it is hoped that the results will shed more light on the age of magnetization of the Cow Head units, and perhaps also on the reasons for negative conglomerate tests from the carbonate clast-dominated conglomerates at Broom Point and Green Point.

Figure 3.37. Characteristic directions of samples from the St. Paul's Inlet quarry section.

Figure 3.38. Magnetic polarity interpretation for the section at St. Paul's Inlet quarry. Stratigraphic section from James and Stevens (1986); biozonation from Barnes (1988).

Figure 3.39. Fold test using characteristic directions from the four principal sections studied. $\kappa_{tilt}/\kappa_{geographic} = 1.57$; N=211.

Figure 3.40. Fold test using site means of the characteristic directions from the four principal sections studied. $\kappa_{tilt}/\kappa_{geographic} = 8.5$, which is significantly positive at the 95% level of confidence (McElhinny 1964). The disparity between the site-mean direction from Green Point and the site-mean directions from the other Cow Head Group sections probably represents unresolved non-horizontal axes of folding (possibly related to tectonic style), and does not significantly weaken the argument that directions at Green Point are contemporaneous with those from the other sections.

Characteristic directions

St. Paul's Inlet quarry
Cow Head Group, western Newfoundland

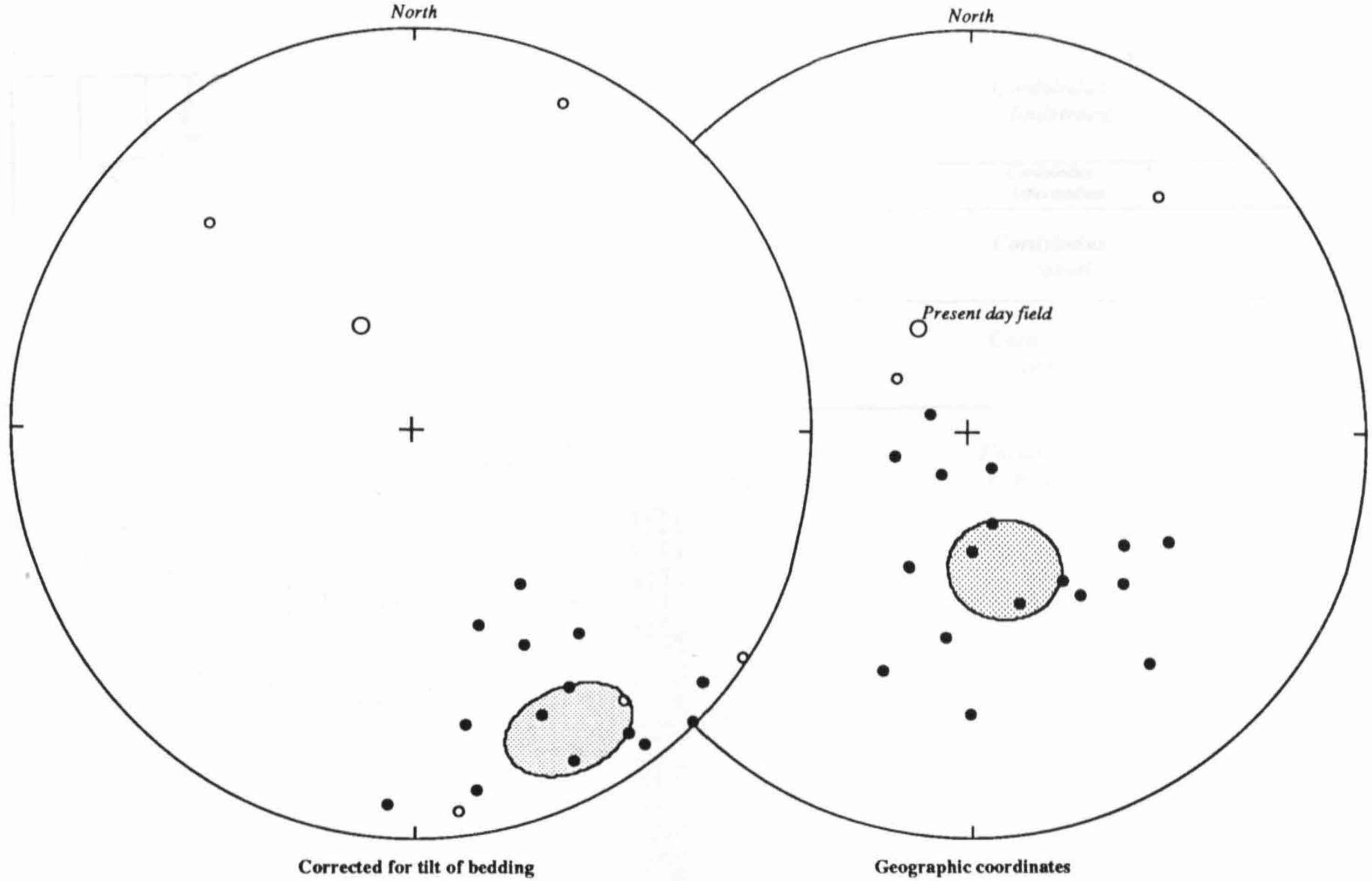

Figure 3.37

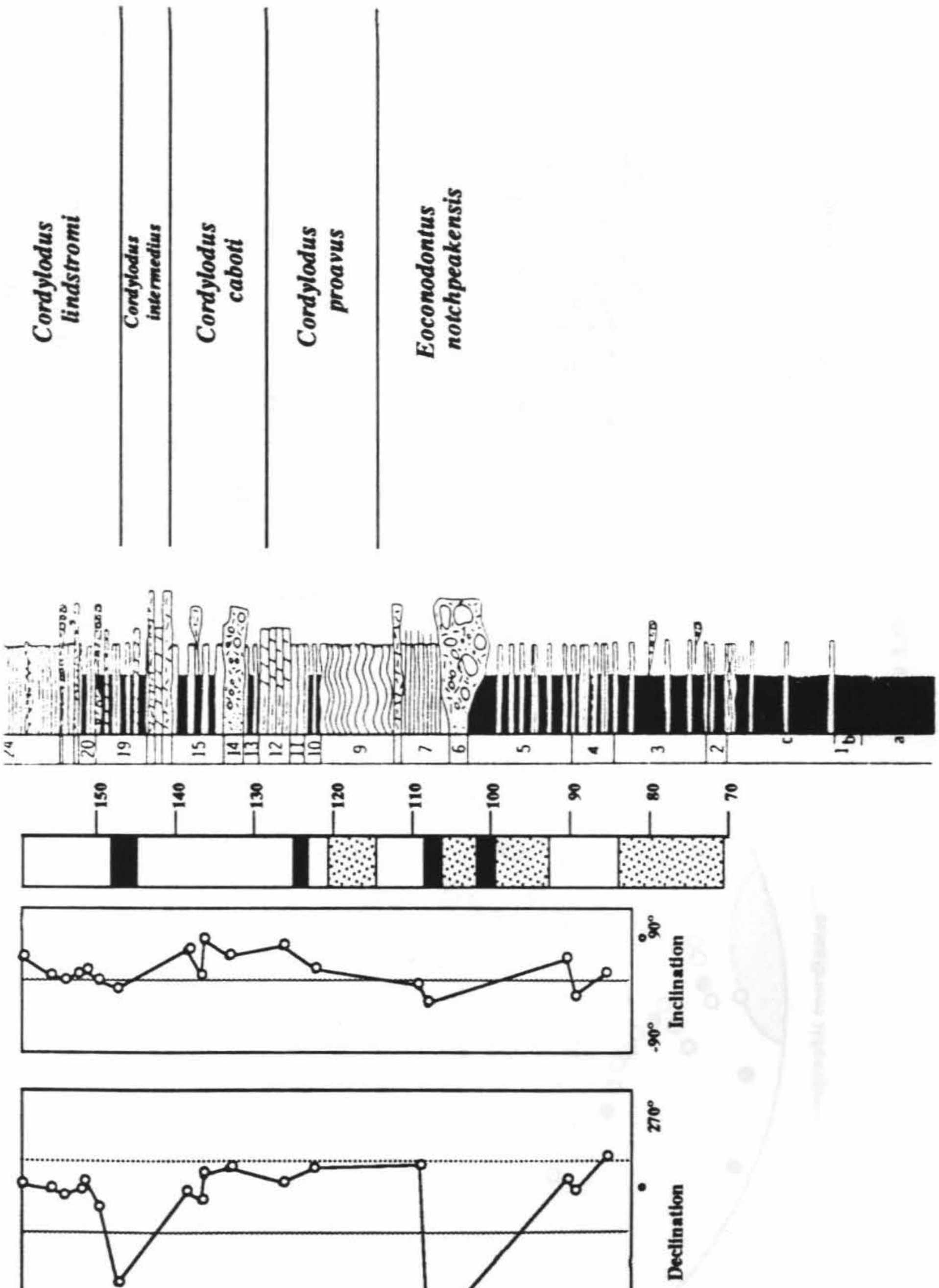
Cordylodus lindstromi
Cordylodus intermedius
Cordylodus caboti
Cordylodus proavus
Eoconodontus notchpeakensis
150
140
130
120
110
100
90
80
70
Inclination
-90°
0
90°
Declination
-90°
0
270°

Characteristic directions

Cow Head Group (total)
western Newfoundland

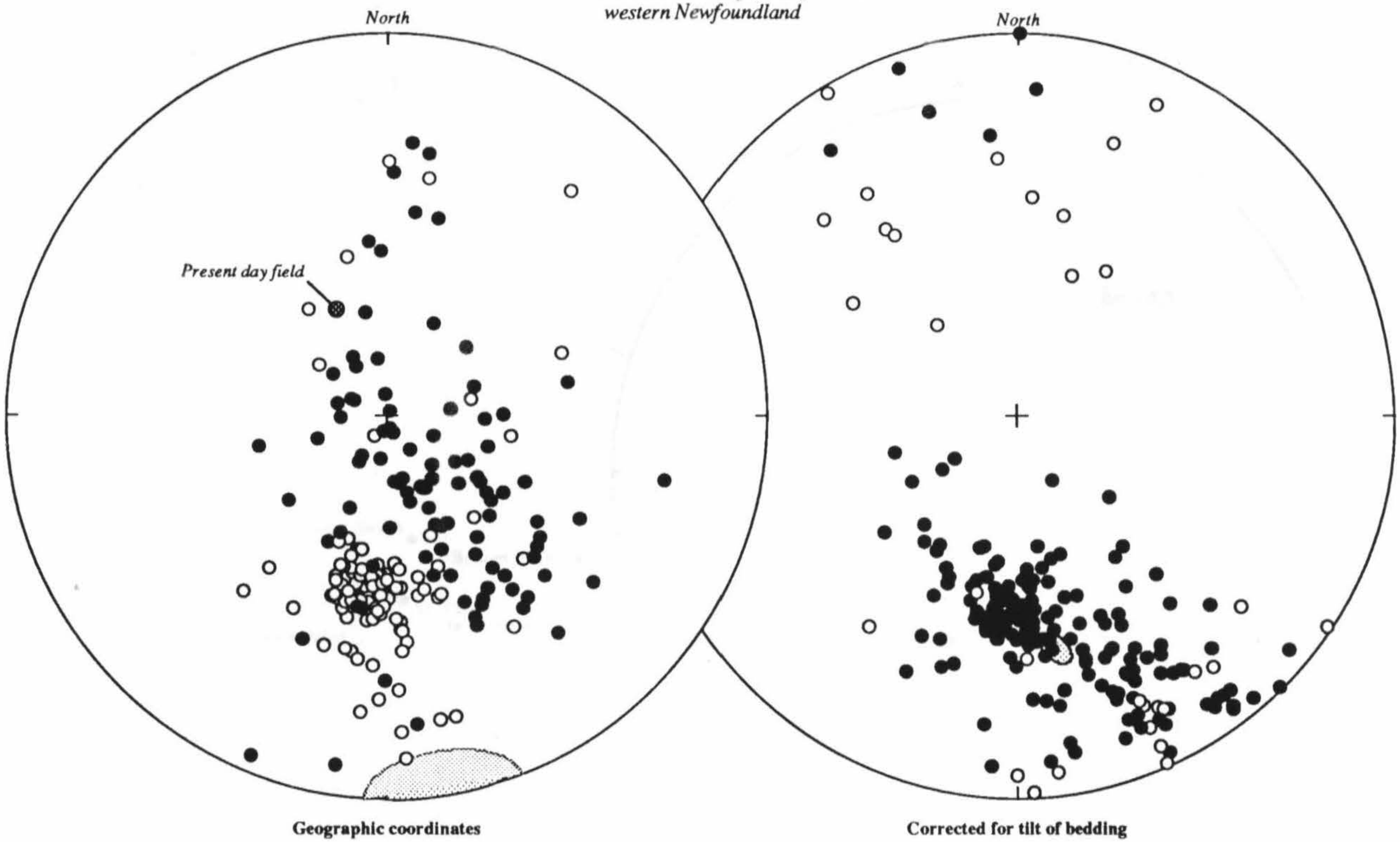

Figure 3.39

Site-mean characteristic directions
Cow Head Group

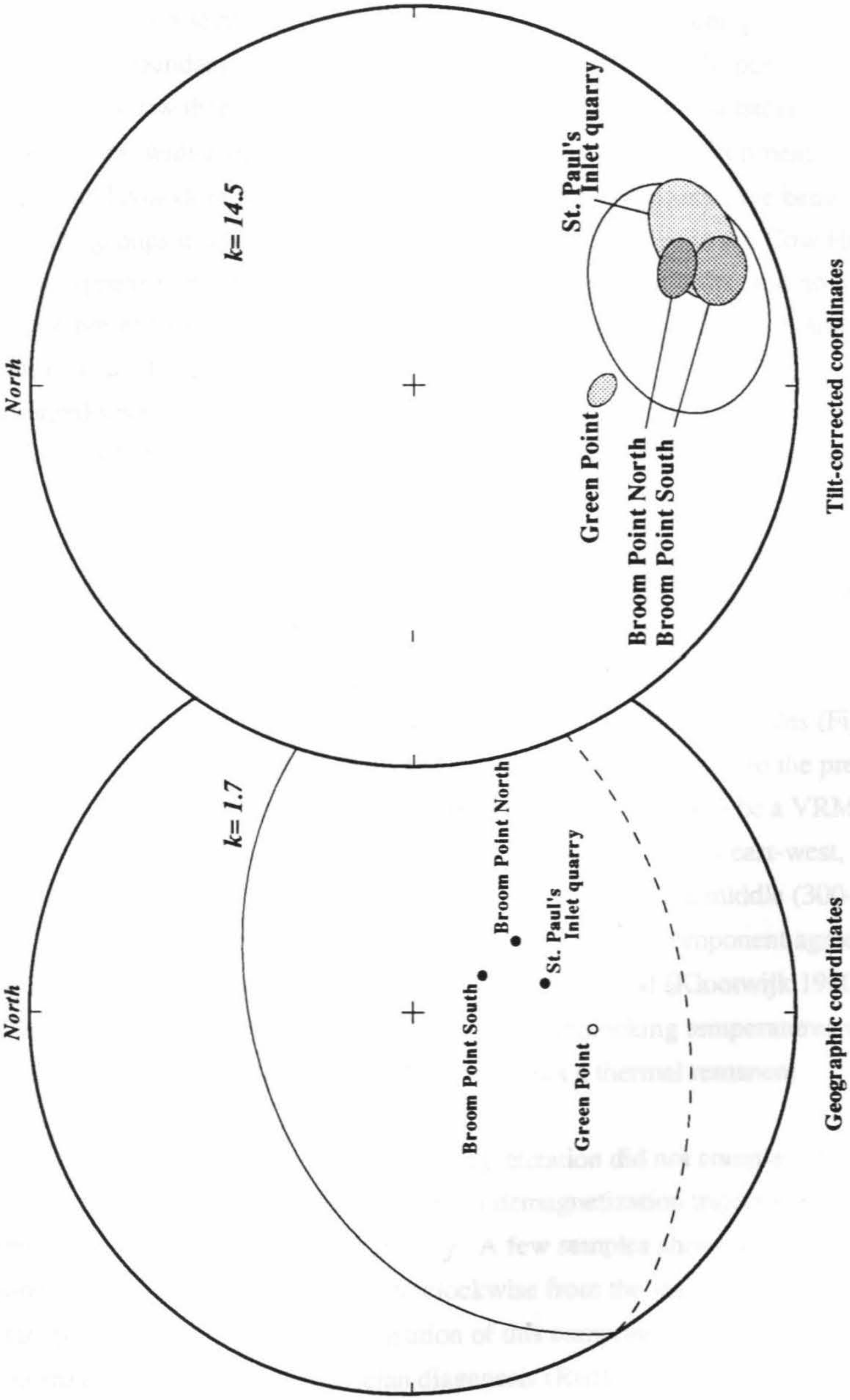

Figure 3.40

4.f. Black Mountain, western Queensland, Australia

The Black Mountain section is one of the thickest in the world encompassing the Cambrian-Ordovician boundary, and displays a CAI of 1.0-1.5 (R. Nicoll, pers. comm.), indicating an extremely low thermal maturity. Limestone, dolostone, and siltstone are the predominant lithologies, with a variety of grain sizes and depositional environments. Abundant trilobite and conodont faunas are present, and detailed zonations have been established for both groups in at least parts of the section. However, as in the Cow Head Group, conodonts appear to be sparse in some of the Upper Cambrian units, and no conodont zonation presently exists at Black Mountain for this time interval (Druce and Jones 1971; Druce *et al.* 1982).

One hundred seventeen oriented block samples were collected from 750 meters of the Upper Cambrian Chatsworth Limestone and Lower Ordovician Ninmaroo Formations in August, 1989. Samples were prepared and analyzed as previously described in this paper. The remainder of each block was dissolved for conodonts by R. Nicoll (Bureau of Mineral Resources, Canberra, Australia), allowing precise comparison of biostratigraphic and magnetostratigraphic results. (Future plans include determination of the δC^{13} stratigraphy using the end chips from core preparation.)

Thermal demagnetization revealed two components in many of the samples (Figure 3.41). One was removed by low temperatures, and was directionally similar to the present day field direction in western Queensland. This component is interpreted to be a VRM. The second component had dual-polarity directions trending approximately east-west, with very shallow inclinations (Figure 3.42, Table 3.7), that were stable in the middle (300-400° C.) and high (400-550° C.) temperature ranges. The direction of this component agrees well with other reported directions from Australia for this time period (Klootwijk 1980), and satisfies the reversal test (Figure 3.43). Comparison of unblocking temperatures with the conodont alteration index indicates that this direction is not a thermal remanent magnetization.

Fifteen other samples, for which thermal demagnetization did not completely isolate a component before unblocking, showed trends in their demagnetization trajectories which allowed unambiguous interpretation of their polarity. A few samples showed very stable second components with declinations 60° counterclockwise from the majority of samples, but with similar inclinations. The time of acquisition of this component has not yet been determined, but may possibly reflect Ordovician diagenesis (Radke 1982) during a period of rapid Australian apparent polar wander (Klootwijk 1980).

Figure 3.41. Typical demagnetization trajectories in equal area and orthogonal projections for samples with reverse (a) and normal (b) polarities from the Black Mountain section.

Figure 3.42. Characteristic directions obtained from samples taken from the Cambro-Ordovician section at Black Mountain, Australia.

Figure 3.43. Reversal test using characteristic directions presumed to be Cambro-Ordovician in age. Overlap of α_{95} ovals of confidence suggest that there is no significant difference (other than polarity) between normal and reverse polarity directions.

Progressive demagnetization of sample BMA 16.0

Black Mountain section
Western Queensland, Australia

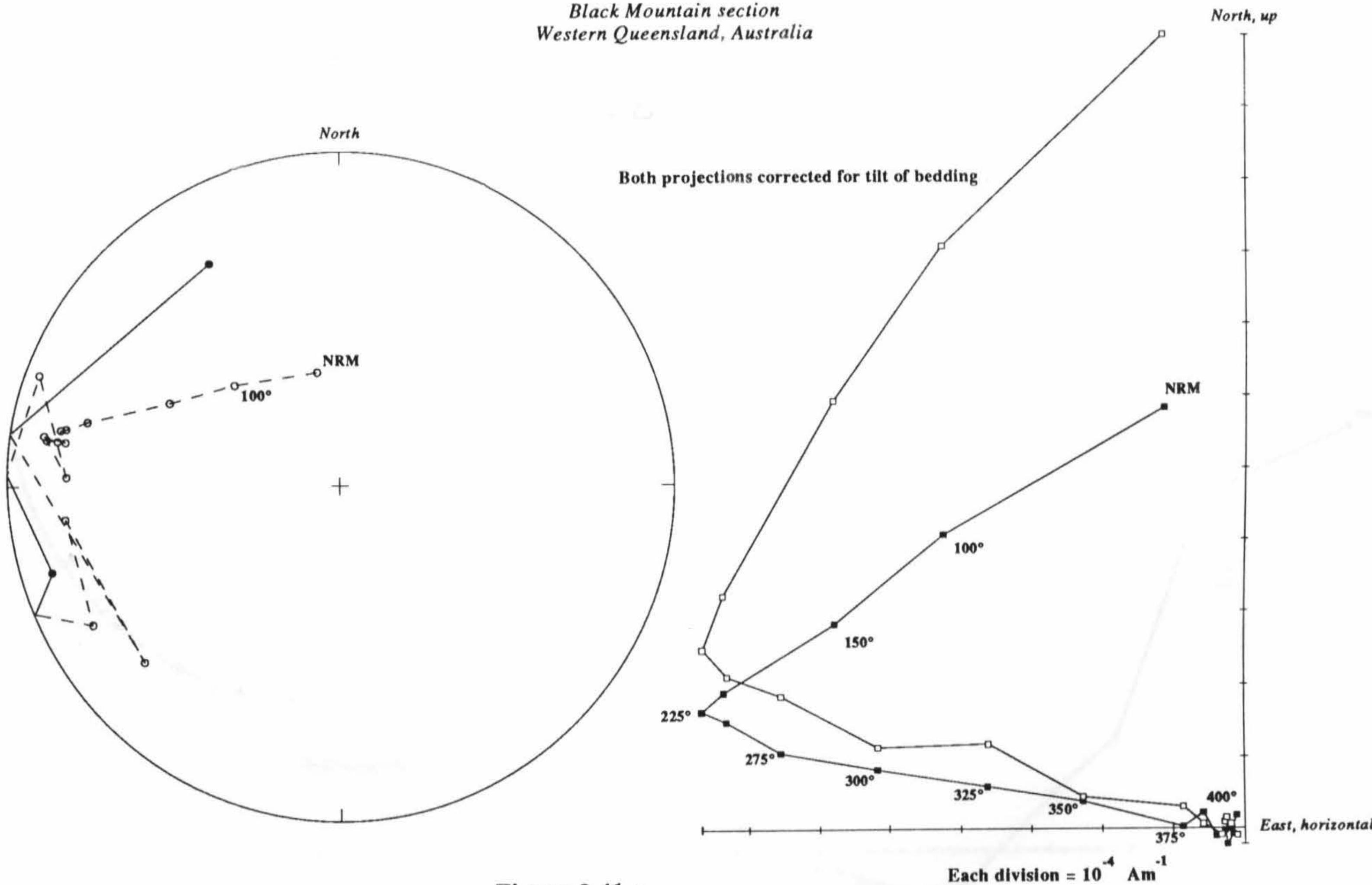

Figure 3.41.a

Progressive demagnetization of sample BMA 105.0

Black Mountain section
Western Queensland, Australia

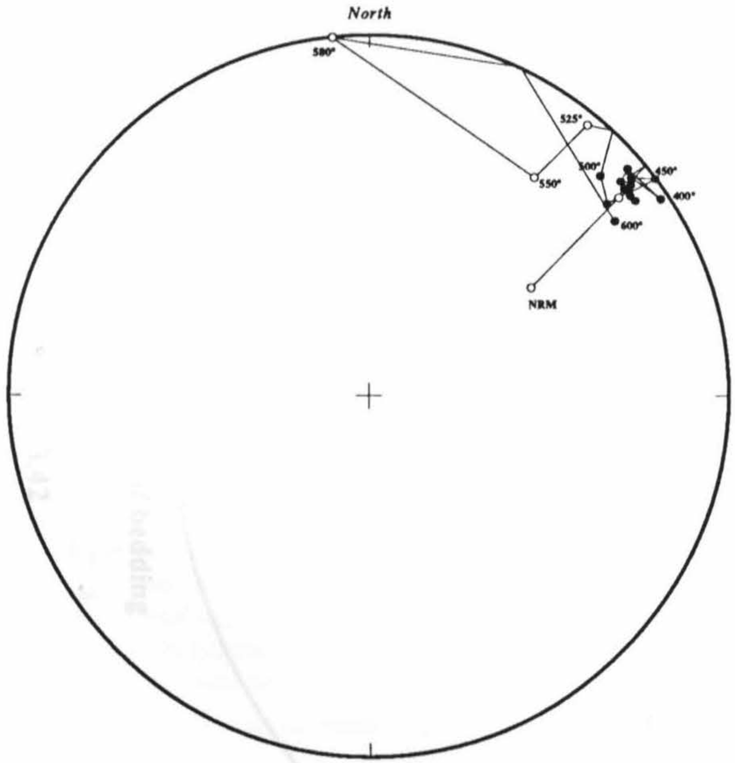

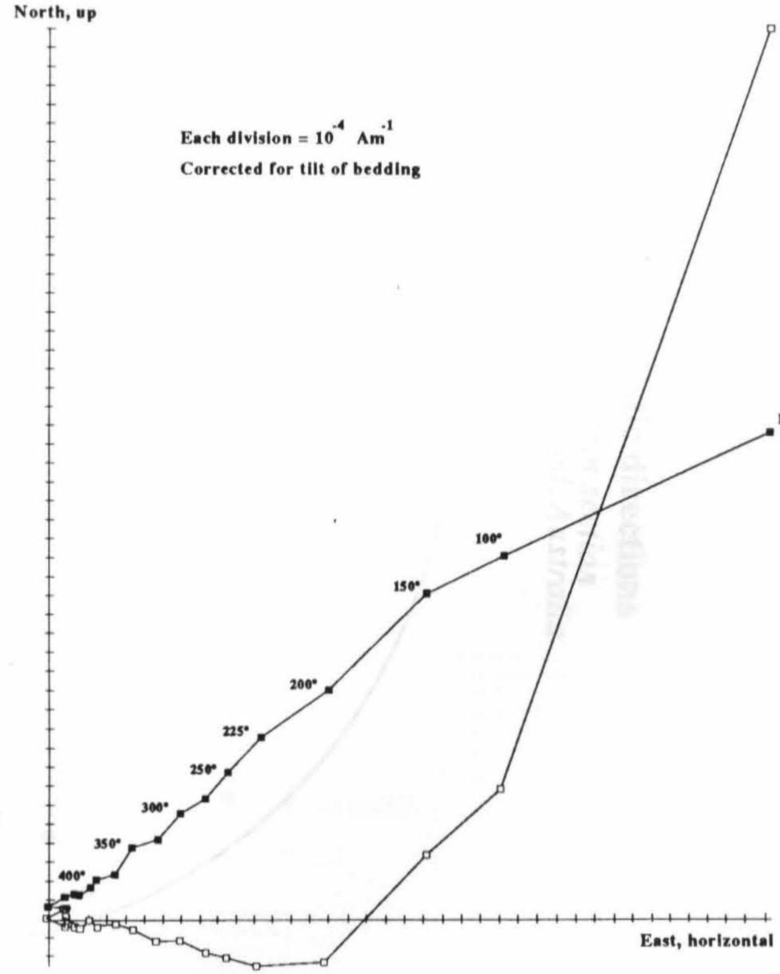

Both projections corrected for tilt of bedding

Figure 3.41.b

Characteristic directions

Black Mountain section
western Queensland, Australia

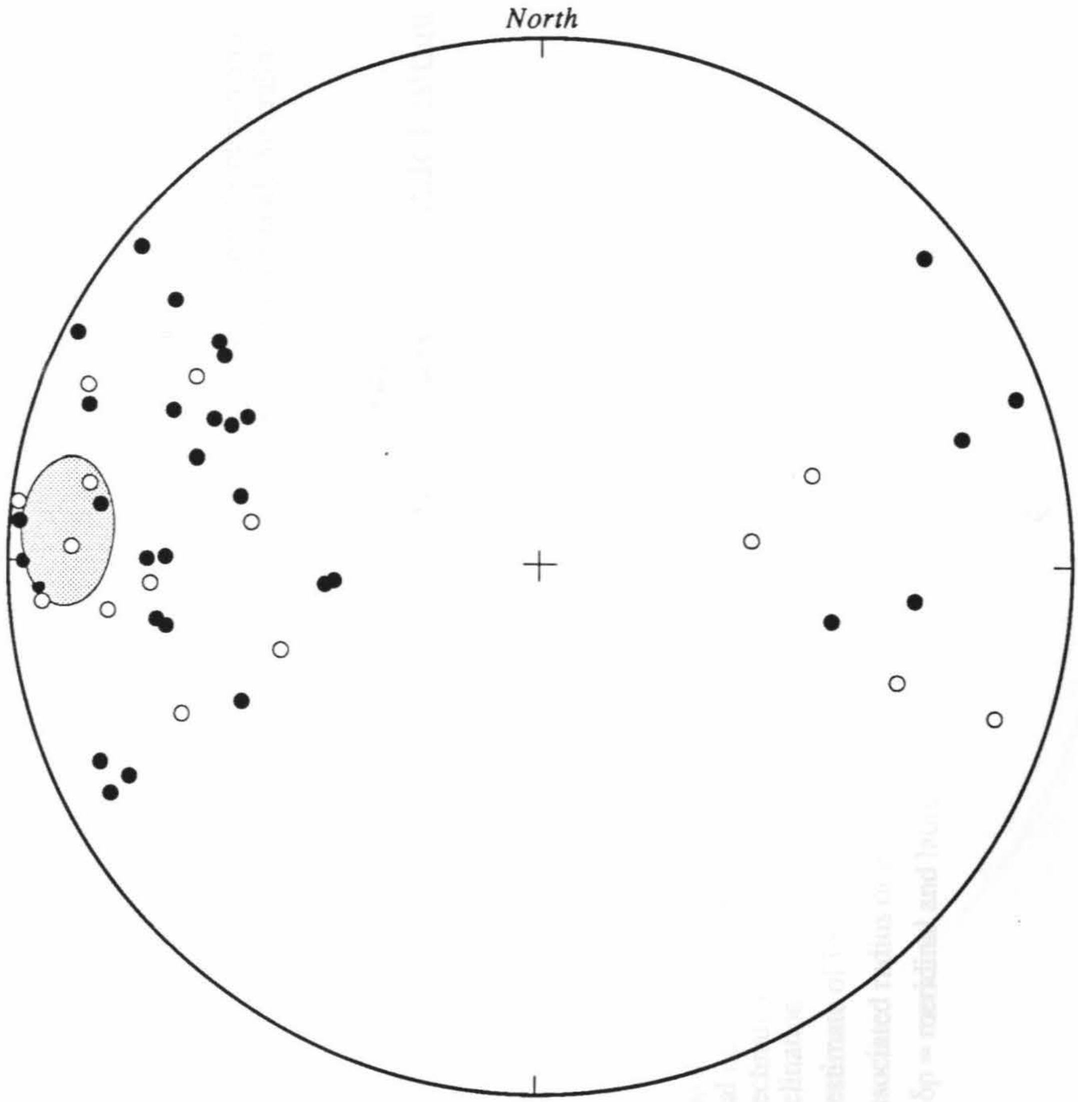

Corrected for tilt of bedding

Figure 3.42

Table 3.7. Section mean directions, statistics, and pole positions for Upper Cambrian and Lower Ordovician carbonates from Black Mountain, western Queensland, Australia.

			(Geographic)			(Tilt-corrected)							
R_t	R_s	R_p	Dec	Inc	κ	Dec	Inc	κ	α_{95}	Pole Position		δm	δp
Section located at 22.6° S., 140.3° E.													
117	47	62	269°	32°	5.5	274°	12°	6.4	9°	1° S.	123° W.	5°	9°

R_t = total number of samples analyzed
R_s = total number of samples used to calculate statistics
R_p = total number of samples used for polarity interpretation
Dec = declination
Inc = inclination

κ = the estimate of Fisher's precision parameter

α_{95} = associated radius of the cone of 95% confidence (McElhinny 1973)

δm and δp = meridinal and latitudinal axes of the oval of 95% confidence around the poles

Reversal test

Black Mountain section
western Queensland, Australia

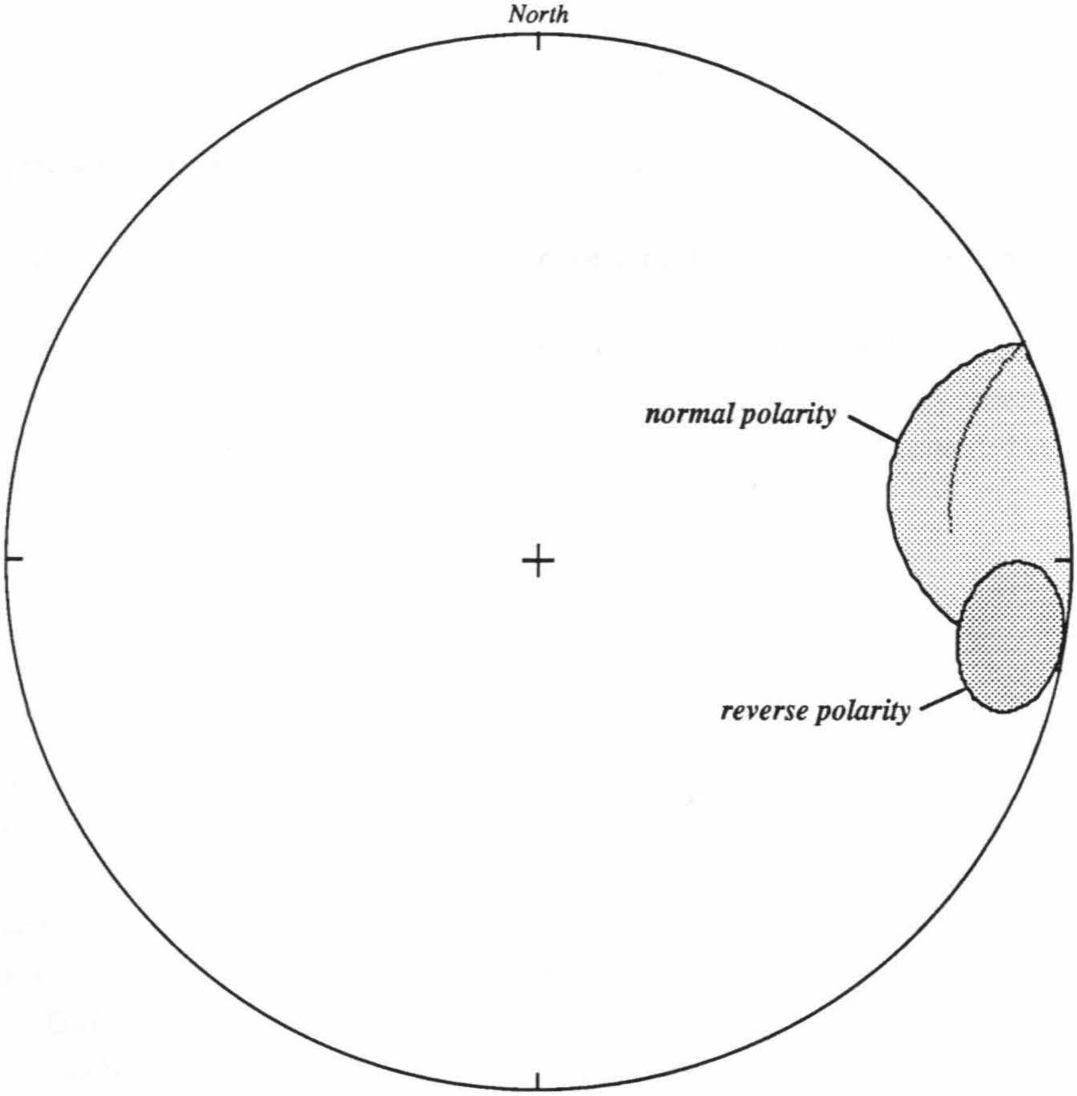

Figure 3.43

A preliminary magnetostratigraphy, based on 62 samples, indicates the presence of a 70 meter thick interval of normal polarity (6 samples) beginning at the 230m level, within the reported range of *Proconodontus muelleri* (Druce *et al.* 1982; R. Nicoll, pers. comm.) (Figure 3.44). This normal polarity interval correlates well with previously reported results from other Uppermost Cambrian sections in this study. Three shorter periods of normal polarity were identified near the 475m (3 samples), 675m (2 samples), and 750m (2 samples) levels. Correlation of these zones is problematic. Recent work by R. Nicoll indicates that the base of the *Cordylodus proavus* zone may be as much as 130 meters higher than previously reported (R. Nicoll, pers. comm.), placing it near the 550m level. Coupled with the indeterminate nature of magnetostratigraphic results from many of the samples at this level, and the observation that the base of the *C. lindstromi* zone is above our highest sample, the present interpretation of the three short periods of normal polarity is that they correlate as a group to other normal polarity intervals within the *C. proavus* zone. Intervening reverse polarity samples may be a true reflection of reverse polarity episodes that were unresolvable within the other studied sections; alternatively; they may reflect the influences of diagenesis during a period of reverse polarity. Further work is needed to confirm these interpretations.

5. Conclusions

Magnetostratigraphic results from 9 different sections indicate changes in polarity occurring throughout the studied interval, which ranges from the base of the Trempealeauian Series (or slightly below) to near the base of the Arenig Series. Relatively brief periods of normal polarity appear to be globally correlatable at no less than 3, and perhaps as many as 7, different stratigraphic levels. A compilation magnetostratigraphy, including an idealized section, is given in Figure 3.45.

Global correlation of magnetic polarity reversals occurring near the Cambrian-Ordovician boundary is complicated by the relative abundances of conodont samples obtained from the different sections. The Cow Head Group sections have severely impoverished Upper Cambrian conodont faunas (Barnes 1988), raising the possibility that the actual first occurrences of important *Cordylodus* species may be much lower, particularly in the critical Green Point section. At Black Mountain, Australia, only three species of conodonts have been reported from Unit E and Unit F of the Upper Cambrian Chatsworth

Figure 3.44. Magnetostratigraphic results from the Cambro-Ordovician boundary section at Black Mountain, western Queensland, Australia. Lithologic section and chronostratigraphy from Druce *et al.* (1982); biozonation based on R. Nicoll (pers. comm.).

Figure 3.45. Magnetostratigraphic correlation of Cambro-Ordovician boundary sections investigated in this study. Shaded intervals represent biozones. Biozonations after Barnes (1988), Miller *et al.* (1982), Chen *et al.* (1988), Druce *et al.* (1982), R. Nicoll (pers. comm.) and Apollonov *et al.* (1988). Stratigraphic height scale is the same for all sections except Black Mountain and Batyrbay ravine; scale for those two sections given with Black Mountain magnetostratigraphy. *Cordylodus caboti* and *C. oklahomensis* zones included within *C. intermedius* zone. Pinching out of a biozone is the result of no zonation present for that interval within a given section, and does not necessarily imply a depositional break.

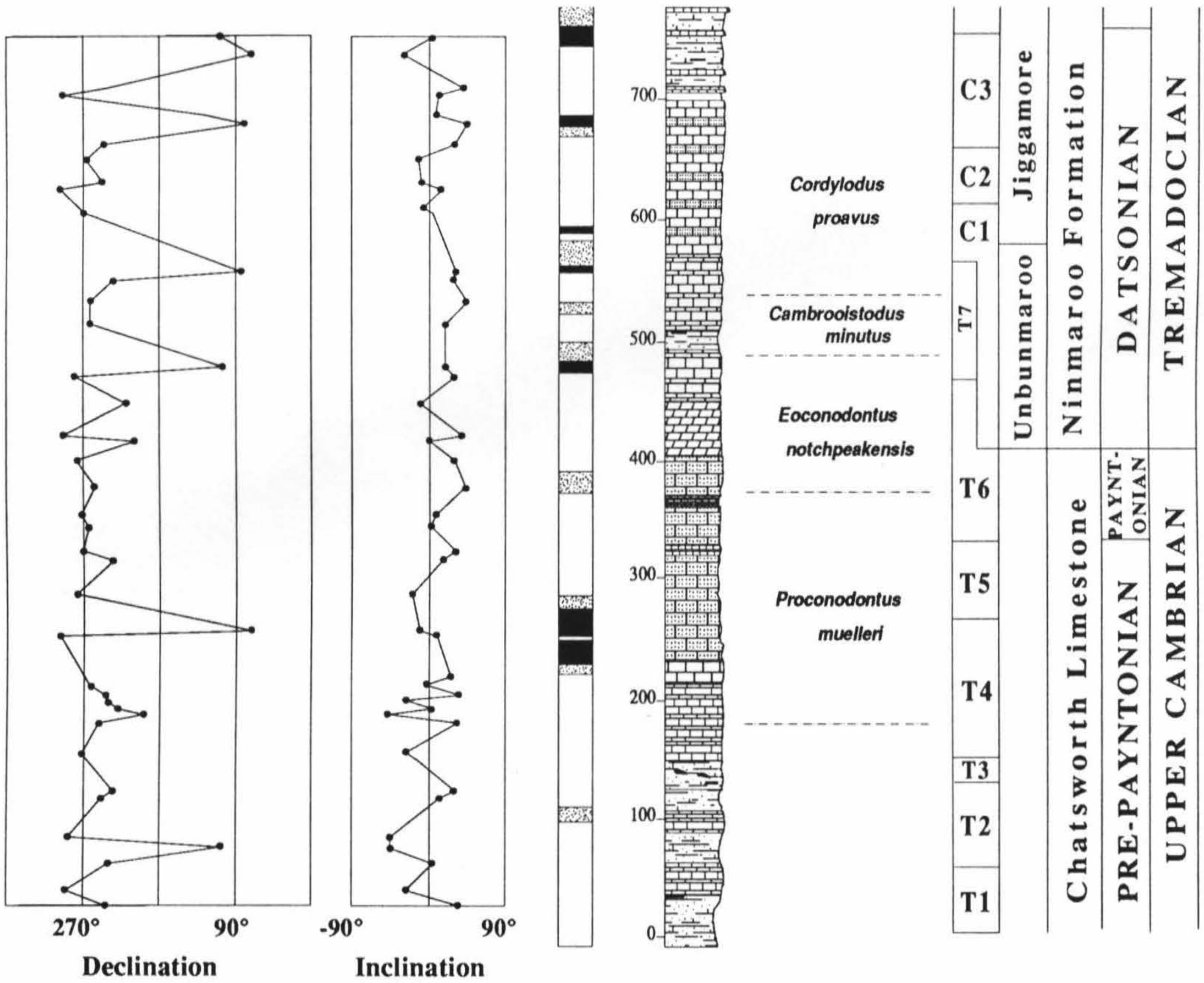
270°
90°
Declination
-90°
90°
Inclination
700
600
500
400
300
200
100
0
Cordylodus proavus
Cambrooistodus minutus
Eoconodontus notchpeakensis
Proconodontus muelleri
C3
C2
C1
T7
T6
T5
T4
T3
T2
T1
Jiggamore
Unbunmaroo
Ninmaroo Formation
Chatsworth Limestone
DATSONIAN
PAYNT-ONIAN
PRE-PAYNTONIAN
TREMADOCIAN
UPPER CAMBRIAN

Figure 3.44

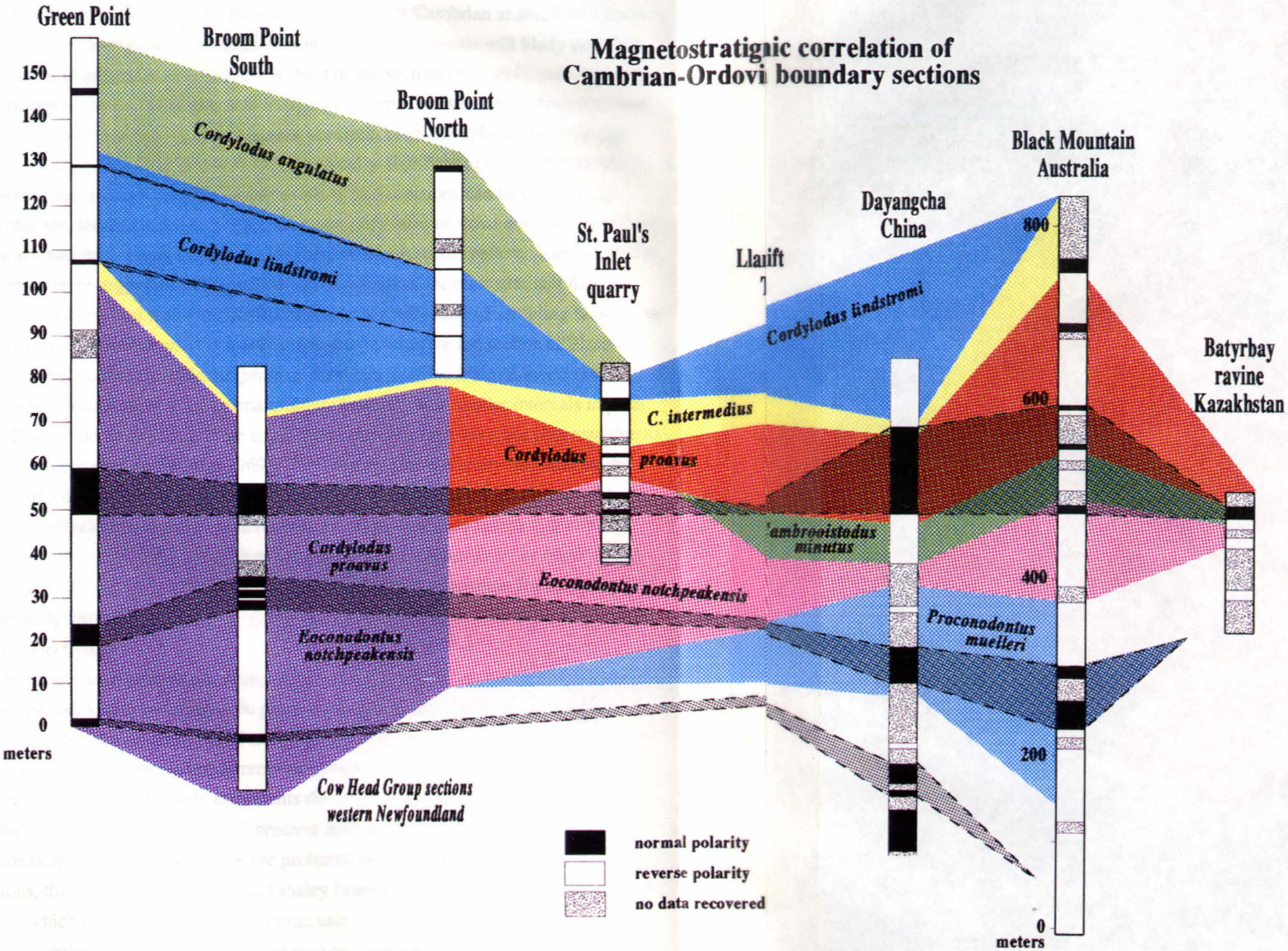

Magnetostratignic correlation of
Cambrian-Ordovi boundary sections
Green Point
Broom Point South
Broom Point North
St. Paul's Inlet quarry
Llaiift
Dayangcha China
Black Mountain Australia
Batyrbay ravine Kazakhstan
Cordylodus angulatus
Cordylodus lindstromi
C. intermedius
Cordylodus proavus
Eoconodontus notchpeakensis
Proconodontus muelleri
Cow Head Group sections western Newfoundland
normal polarity
reverse polarity
no data recovered
meters
150
140
130
120
110
100
90
80
70
60
50
40
30
20
10
0
800
600
400
200

Limestone, and only two from the overlying Lily Creek Member (Druce *et al.* 1982). As a result, there is presently no conodont zonation for the Upper Cambrian at Black Mountain. However, recent re-investigation of Black Mountain conodont faunas will likely establish more precise biostratigraphic boundaries for most of the section (R. Nicoll, pers. comm.).

It is impossible to obtain magnetostratigraphic correlations between more than two sections when assuming that the first observed occurrences of *Cordylodus proavus* and *Cordylodus lindstromi* represent chronostratigraphically-significant events. However, strong correlations between 4 (and possibly as many as 6) sections can be obtained by assuming that the documented first appearances of *Cordylodus proavus* are diachronous on a global scale, and then simply comparing the magnetostratigraphic pattern. Correlation by this method strongly suggests that the inability to make global magnetostratigraphic correlations in conjunction with *Cordylodus* biozones is a reflection of sampling bias due to insufficient specimen recovery. It is worth noting that, except for the section at Black Mountain, the base of the *Cordylodus proavus* zone required lowering in sections with few specimens in order to correlate normal polarity intervals with similar intervals in other sections. This would be expected if the significant boundary taxa were not observed due to low specimen recovery (see Sanders 1969). Furthermore, the difficulty imposed by the apparent raising of the base of *C. proavus* in the Black Mountain section is removed by the preliminary conclusions of a recent re-investigation of the conodont faunas from this section (R. Nicoll, pers. comm.), which raises the base of *C. proavus* by as much as 130 meters using only biostratigraphic criteria. (Using Nicoll's new position for the base of *C. proavus* actually implies that a small *lowering* of the base of *C. proavus* might be possible with more collection.)

The results have clear implications for selection of a globally-significant Cambrian-Ordovician period boundary horizon. In particular, the sections within the Cow Head Group, western Newfoundland, should not be candidates for consideration of a boundary based solely on the first reported occurrence of *Cordylodus proavus* until further biostratigraphic work conclusively documents this level. However, the correlations also suggest that the proposed base of the *C. proavus* zone at Green Point, if confirmed by further biostratigraphic work, would be the preferred horizon; the proposed base occurs in a continuous, thick sequence of shales and shaley limestones, as opposed to the base of *C. lindstromi* , which is near a large conglomeratic unit.

The correlations also imply that there may be large temporal differences between sections in the first appearance of *Cordylodus lindstromi*. At Dayangcha, the first appearance of *C. lindstromi* is found a few meters above the end of the normal polarity interval associated with the *C. proavus* zone. This may also be the case in the Lange Ranch section, but difficulties imposed by diagenesis allow only for speculation. In the Cow Head Group, the first appearance of *C. lindstromi* is documented to be much higher in the Broom Point South and Green Point sections than the end of the proposed *C. proavus*-correlative normal polarity zone. Differences may be due in part to the impoverished conodont faunas through the relevant intervals within the Cow Head Group, and in part to differential taxonomy between the various conodont specialists (J. Repetski, App.6, COBWG Circular 26 (1990)).

Very preliminary correlations of individual samples having normal polarity within the Cow Head Group suggest that two very short normal polarity events may have occurred in the upper part of the *Cordylodus lindstromi* zone, with the higher event occurring just below the reported first appearance of the graptolite *Anisograptus matanensis* in the Broom Point North section. Because these events are found very near the first observed appearance of an important graptolite species, they may prove to be extremely valuable indicators of the chronostratigraphic significance of this taxon within the Cow Head Group, but further work is needed.

It is noteworthy that, at the present time, a significant bias against the merits of magnetostratigraphy exists within factions of the Cambro-Ordovician Boundary Working Group. Even at this late stage in the boundary selection process, it appears important to point out that a useful Cambro-Ordovician *period* boundary requires identification of a demonstrably isochronous, globally-significant stratigraphic horizon. Placement of the boundary horizon in a section that is inaccessible to magnetostratigraphic study would define *only* the system boundary, since the global isochroneity of the boundary horizon would be impossible to demonstrate by current methods. It is hoped that the results detailed above confirm the importance of magnetostratigraphy in establishing a temporally-significant global horizon for the Cambro-Ordovician boundary, and spur renewed interest in selecting a truly chronostratigraphic boundary.

Acknowledgements

The senior author wishes to thank J.H. Shergold, C.R. Barnes, J.L. Miller, J. Laurie, R. Nicoll, J. Repetski, A. Kobayashi-Kirschvink, and C. Budney for their invaluable assistance in the field and for their extremely helpful personal communications. The authors would also like to acknowledge the extensive efforts of the Cambrian-Ordovician Boundary Working Group and its chairman, B.S. Norford. This work was supported in part by the National Science Foundation Grant EAR-8721391.

References

Chen Jun-Yuan (ed.) 1986. *Aspects of Cambrian-Ordovician Boundary in Dayangcha, China* . Beijing: China Prospect Publishing House. 410 pp.

Chen Jun-Yuan, Qian Yi-Yuan, Zhang Jun-Ming, Lin Yao-Kun, Yin Lei-Ming, Wang Zhi-Hao, Wang Zong-Zhi, Yang Jie-Dong, and Wang Yhing-Xi 1988. The recommended Cambrian-Ordovician Boundary stratotype of the Xiaoyangqiao section (Dayangcha, Jilin Province), China. *Geological Magazine* **125**: 415-444.

Cisowski, S. 1981. Interacting vs. non-interacting single domain behavior in natural and synthetic samples. *Physics of the Earth and Planetary Interiors* **26**: 56-62.

Collinson, D.W. 1983. *Methods in Rock Magnetism and Palaeomagnetism: Techniques and Instrumentation.* Chapman and Hall.

Deutsch, E.R. and Prasad, J.N. 1987. Ordovician paleomagnetic results from the St. George and Table Head carbonates of western Newfoundland. *Canadian Journal of Earth Sciences* **24**(9): 1785-1796.

Druce, E.C., Shergold, J.H., and Radke, B.M. 1982 A reassessment of the Cambrian-Ordovician boundary section at Black Mountain, Western Queensland, Australia. In *The Cambrian-Ordovician Boundary: Sections, Fossil Distributions, and Correlations* (ed. M.G. Bassett and W.T. Dean), pp. 193-209. National Museum of Wales, Geological Series no. 3, Cardiff.

Epstein, A.G., Epstein, J.B., and Harris, L.D. 1977. Conodont color alteration- an index of organic metamorphism. *Professional paper U.S. geological survey* **995**: 1-27.

Fortey, R.A., Landing, E., and Skevington, D. 1982. Cambrian-Ordovician boundary sections in the Cow Head Group, western Newfoundland. In *The Cambrian-Ordovician Boundary: Sections, Fossil Distributions, and Correlations* (ed. M.G. Bassett and W.T. Dean), pp. 95-129. National Museum of Wales, Geological Series no. 3, Cardiff.

Hall, S.A. and Evans, I. 1988. Paleomagnetic study of the Ordovician Table Head Group, Port au Port Peninsula, Newfoundland. *Canadian Journal of Earth Sciences* **25**: 1407-1419.

Harrison, C.G.A. and Somayajulu, B.L.K. 1966. Behaviour of the earth's magnetic field during a reversal. *Nature* **212**: 1193-1195.

James, N.P. and Stevens, R.K. 1986. Stratigraphy and correlation of the Cambro-Ordovician Cow Head Group, western Newfoundland. *Geological Survey of Canada, Bulletin* **366**, 143 pp.

Khramov, A.N., Rodionov, V.P., and Komissarova, R.A. 1965. New data on the Paleozoic history of the geomagnetic field in the USSR. In *The present and Past of the Geomagnetic Field*, pp. 206-213. Nauka Press, Moscow.

Kirschvink, J.L. 1980. The least squares line and plane and the analysis of palaeomagnetic data. *Geophysical Journal of the Royal astronomical Society* **62**: 699-718.

—— and Rozanov, A. Yu. 1984. Magnetostratigraphy of Lower Cambrian strata from the Siberian Platform: a palaeomagnetic pole and preliminary polarity time scale. *Geological Magazine* **121**: 189-203.

Klootwijk, C.T. 1980. Early Paleozoic paleomagnetism in Australia. *Tectonophysics* **64:** 249-332.

Lapworth, C. 1879. On the Tripartite Classification of the Lower Palaeozoic Rocks. *Geological Magazine,* New Series, Decade II **6**: 1-15.

Lowrie, W. and Fuller, M.D. 1971. On the alternating field demagnetization characteristics of multidomain thermoremanence in magnetite. *Journal of Geophysical Research* **76**: 6339-6349.

Lowrie, W. and Heller, F. 1982. Magnetic properties of marine limestones. *Reviews of Geophysics and Space Physics* **20**(2): 171-192.

McCabe, C., Van der Voo, R., Peacor, D.R., Scotese, C.R., and Freeman, R. 1983. Diagenetic magnetite carries ancient yet secondary remanence in some Paleozoic sedimentary carbonates. *Geology* **11**(4): 221-223.

McElhinny, M.W. 1964. Statistical significance of the fold test in palaeomagnetism. *Geophysical Journal of the Royal astronomical Society* **8**: 338-340.

—— 1973. *Palaeomagnetism and Plate Tectonics*. Cambridge University Press, 358 pp.

Miller, J.F. 1984. Cambrian and earliest Ordovician conodont evolution, biofacies, and provincialism. In *Conodont Biofacies and Provincialism* (ed. D.L. Clark), pp. 43-68. Geological Society of America, Special Paper **196**.

—— , Taylor, M.E., Stitt, J.H., Ethington, R.L., Hintze, L.F., and Taylor, J.F. 1982. Potential Cambrian-Ordovician boundary stratotype sections in the western United States. In *The Cambrian-Ordovician Boundary: Sections, Fossil Distributions, and Correlations* (ed. M.G. Bassett and W.T. Dean), pp. 155-180. National Museum of Wales, Geological Series no. 3, Cardiff.

Opdyke, N.D., Kent, D.V., and Lowrie, W. 1973. Details of magnetic polarity transitions recorded in a high deposition rate deep-sea core. *Earth and Planetary Science Letters* **20**: 315-324.

Pullaiah, G., Irving, E., Buchan, K.L., and Dunlop, D.J. 1975. Magnetization changes caused by burial and uplift. *Earth and Planetary Science Letters* **28**: 133-143.

Radke, B.M. 1982. Late diagenetic history of the Ninmaroo Formation (Cambro-Ordovician), Georgina Basin, Queensland and Northern Territory. *Bureau of Mineral Resources Journal of Australian Geology and Geophysics* **7**: 231-254.

Rodionov, V.P. 1966. Dipole character of the geomagnetic field in the late Cambrian and the Ordovician in the south of the Siberian Platform. *Geologiya i Geofizika* **1**: 94-101.

Sanders, H.L. 1969. Benthic marine diversity and the stability-time hypothesis. *Brookhaven Symp. Biol.* **22**: 71-81.

Watts, D.R., Van der Voo, R., and Reeve, S.C. 1980. Cambrian paleomagnetism of the Llano Uplift, Texas. *Journal of Geophysical Research* **85**(B10): 5316-5330.

Chapter Four Paleomagnetic results from Late Silurian to Middle Devonian rocks of the Barrandian area, Prague Basin, Czechoslovakia

4.1. Introduction

The Barrandian area of Prague Basin, stretching southwest from Prague in western Czechoslovakia, is one of the world's truly classic fossil localities. Middle Paleozoic strata in the area range in age from Late Silurian to Middle Devonian, and the preserved faunas are both diverse and abundant (Chlupac 1977). A number of sections have been identified as having global significance, including the Silurian-Devonian boundary global stratotype section at Klonk (near Suchomasty), the Ludlow-Pridoli stage boundary global stratotype near the Pozary quarries outside of Reporyje, and the proposed Pragian-Lochkovian boundary stratotype near Cerna Rokle. The high density of important, critically studied, and internationally-recognized sections makes the Barrandian area one of the premier places in the world to attempt to gain magnetostratigraphic information from rocks of this age.

Another important feature of the Barrandian area, which has both positive and negative aspects, is its tectonic setting. The Barrandian sits within Prague Basin, a broad synclinorium formed during the Carboniferous-aged Hercynian orogeny and trending southwest-northeast, with dips of about 30° on the limbs. Because of the shape of the basin, fold tests can be performed between sites, providing one measure of the stability of the preserved magnetic components. Deformation appears to be restricted to gentle tilting of the strata in many sections, and conodont alteration indices (CAI) for some of the studied sections are 1.5-2.0 (G. Klapper, pers. comm.), indicating only low levels of metamorphism. However, some of the sections, like the classic Silurian-Devonian boundary section at Budnany-Karlstejn, are highly deformed, confirming the acknowledged haphazard and often localized influence of the orogeny (Zwart and Dornsiepen 1978) extended to the Prague Basin.

Another strong motivation for paleomagnetic study in the Barrandian area involves its paleogeographic position during the Middle Paleozoic. The Barrandian area has been recognized as one of the elements of the Bohemian Massif, the Early and Middle Paleozoic tectonic affinities of which have been the subject of debate. Many workers consider the Bohemian Massif as part of the Armorica microplate, which has been interpreted to have accreted to Laurentia (Europe) during the Hercynian. Others have suggested that the Bohemian Massif was an independent block with unknown plate affinities. Previous paleomagnetic results from the Bohemian Massif did not encompass the critical Silurian through Devonian interval, the time periods immediately preceding a postulated Carboniferous collision of the Bohemian Massif with Laurentia (as part of the Hercynian orogeny). Resolution of this problem will rely heavily on paleomagnetic data; faunal information does not allow unique solutions to continental configurations during the Silurian and Devonian.

4.2. Results

In August of 1985 over 350 oriented core samples were collected from 6 sections within the Barrandian (Figure 4.1). Careful attention was paid to biostratigraphic relations, and all of our collecting was done with the assistance of members of the Czechoslovak Geological Survey. Except for a few minor gaps, collection spanned from the top of the Ludlow Stage to the Lochkovian-Praguean (stage) boundary.

Laboratory measurements were performed on an ScT cryogenic magnetometer under microcomputer control. Alternating-field demagnetizations were made with a Schoensted GSD-1 three-axis instrument, usually up to a maximum field of 10 millitesla. Thermal demagnetizations were done in 50° (to 350° C.) and 25° (above 350°) steps using a custom-built large-volume oven. Thermal demagnetization typically did not proceed above 450° due to the obvious development of laboratory-induced directions, probably as the result of chemical changes within the carbonate samples. Characteristic directions were isolated using the principal component techniques outlined in Kirschvink (1980).

A few samples from each of the sections were subjected to isothermal remanent magnetization (IRM) acquisition-AF demagnetization in an attempt to characterize the magnetic mineralogy. Induced IRM fields of 2 tesla were achieved using a custom-built pulse coil. Typically, the maximum AF demagnetization field used was about 1 tesla.

A recent study using three samples from the section at Klonk (Ellwood et al. 1988) suggested that siderite was present, indicating that the primary carriers of magnetization should still be intact. Their study identified a high inclination, southwest trending component, which matched well with the hypothesis that the Bohemian Massif was attached to the main body of Baltica (Europe) during the Middle Paleozoic (Briden and Duff 1981). However, two of the three samples they reported on have natural remanent magnetization (NRM) directions that are nearly equatorial, unlike the present-day-field-dominated NRM

Figure 4.1. Sample localities within the Barrandian area.

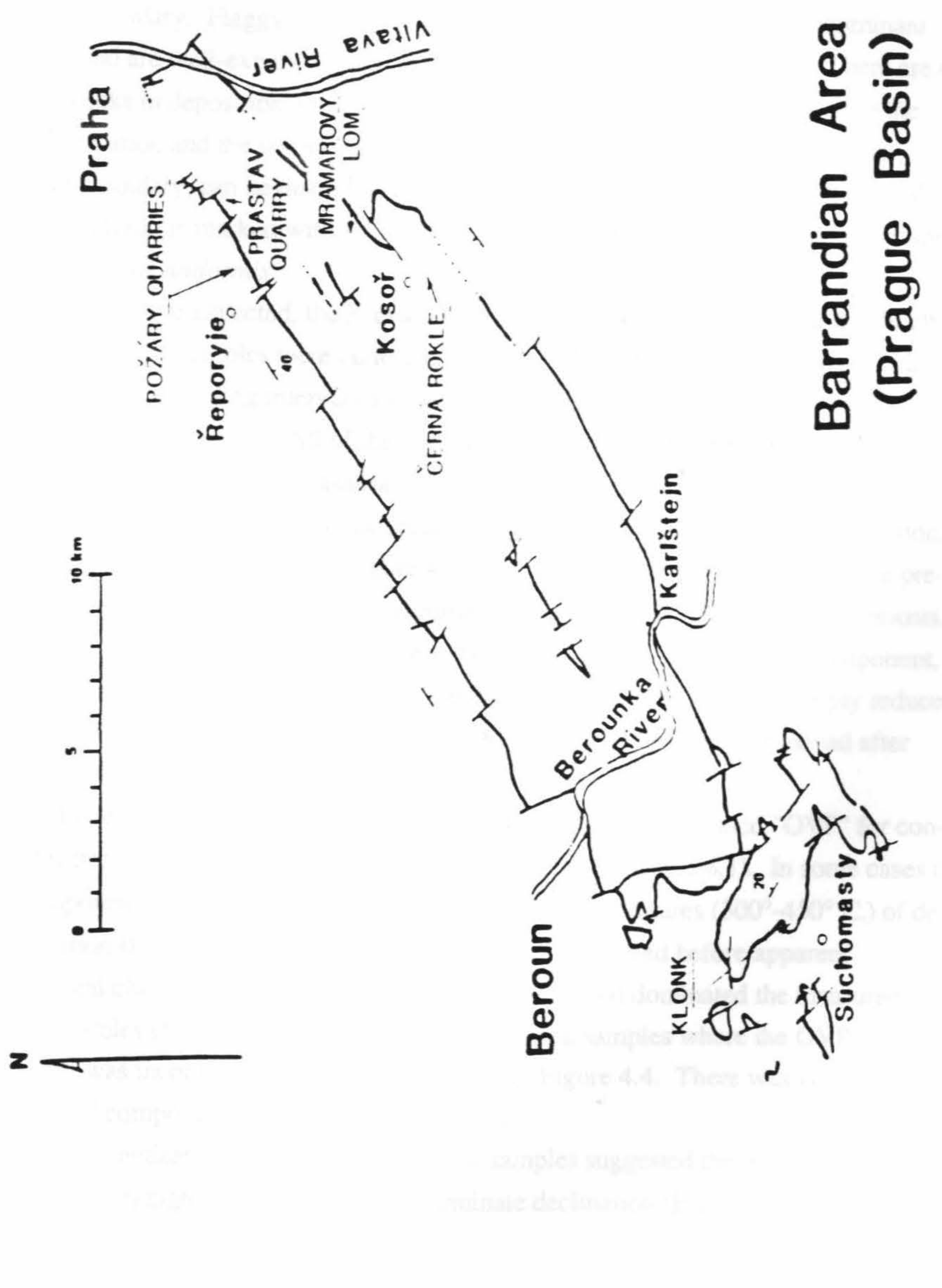
Barrandian Area
(Prague Basin)
Praha
Vltava River
POŽÁRY QUARRIES
PRASTAV QUARRY
MRAMAROVY LOM
Řeporyje
Kosoř
ČERNA ROKLE
Karlštejn
Berounka River
Beroun
KLONK
Suchomasty
40
70
0
5
10 km
N

directions obtained from most of our samples. Furthermore, the extremely low number of samples used makes it difficult to assess the reliability of their characteristic direction.

4.2.1 Klonk

The Klonk section, near Suchomasty, is the international stratotype for the Silurian-Devonian boundary. Flaggy limestones with shaley intercalations are the predominant lithology, and are well-exposed, particularly in the upper part of the section. There are no obvious breaks in deposition, or marked changes in lithology; the contact between the Pridoli Formation and the overlying Lockhov Formation, which marks the Silurian-Devonian boundary, can be distinguished only on paleontologic grounds. The official boundary horizon is marked within Bed 20, at the first observed occurrence of the graptolite *Monograptus uniformis*.

As might be expected, the Klonk section was the focus of our sampling. Ninety-four oriented core samples were collected with the help of I. Chlupac, J. Kriz, M. Krs, and M. Krsova. Sampling intervals around Bed 20 averaged about 10 cm, and about 30 cm in the rest of the section. All of the samples were subjected to progressive alternating field (AF) and thermal demagnetization.

Most of the samples from this section showed two components of magnetization; a representative example is given in Figure 4.2. One component is very similar to the present-day field, and dominated the natural remanent magnetization (NRM) measurements. It is interpreted to be a VRM from the present-day field. The influence of this component, hereafter referred to as component "PDF", on the total magnetization was sharply reduced by AF and low temperature demagnetization, and often was completely removed after heating to 200° C.

The second component found in most of the samples (designated "OVP" for convenience) trends southward, with very shallow inclinations (Table 4.1). In some cases the OVP component was completely isolated by moderate temperatures (300°-450° C.) of demagnetization (Figure 4.3), but often was incompletely resolved before apparent mineralogical changes (induced by thermal demagnetization) dominated the measured directions. Poles to the demagnetization planes of those samples where the OVP component was incompletely resolved are shown in Figure 4.4. There was no indication that the OVP component possessed dual polarities.

Demagnetization trajectories from a few samples suggested the presence of a third component, with high inclination and indeterminate declination (Figure 4.5), but the large

Figure 4.2. Typical demagnetization trajectories, in (tilt-corrected) [1]As-Zijderveld (left) and equal area projections, for samples from the Silurian-Devonian boundary stratotype section at Klonk, Czechoslovakia. In As-Zijderveld projection, solid squares represent declination, while open squares represent inclination. In equal area projection, solid circles represent positive (down) inclinations; open circles represent negative inclinations.The larger circle, situated at about 50° north in equal area projection, represents the present-day field direction in Czechoslovakia.

Figure 4.3. Equal area projection of the characteristic directions obtained using isolated OVP components. Symbols as in Figure 4.2.

Figure 4.4. Poles to planes of demagnetization of PDF and OVP components, and the associated mean demagnetization plane. Both the mean OVP and PDF component directions are constrained to lie within the mean demagnetization plane, defined by the average pole and its associated error angle.

Figure 4.5. Orthogonal and equal area projections of sample 15.0 from Klonk, showing a possible third component with high inclination. Symbols as in Figure 4.2.

---

[1]Hyperbolic projection used to facilitate viewing; in orthogonal projection (the customary format for As-Zijderveld diagrams) of this data set, declination and inclination curves collapse upon one another.

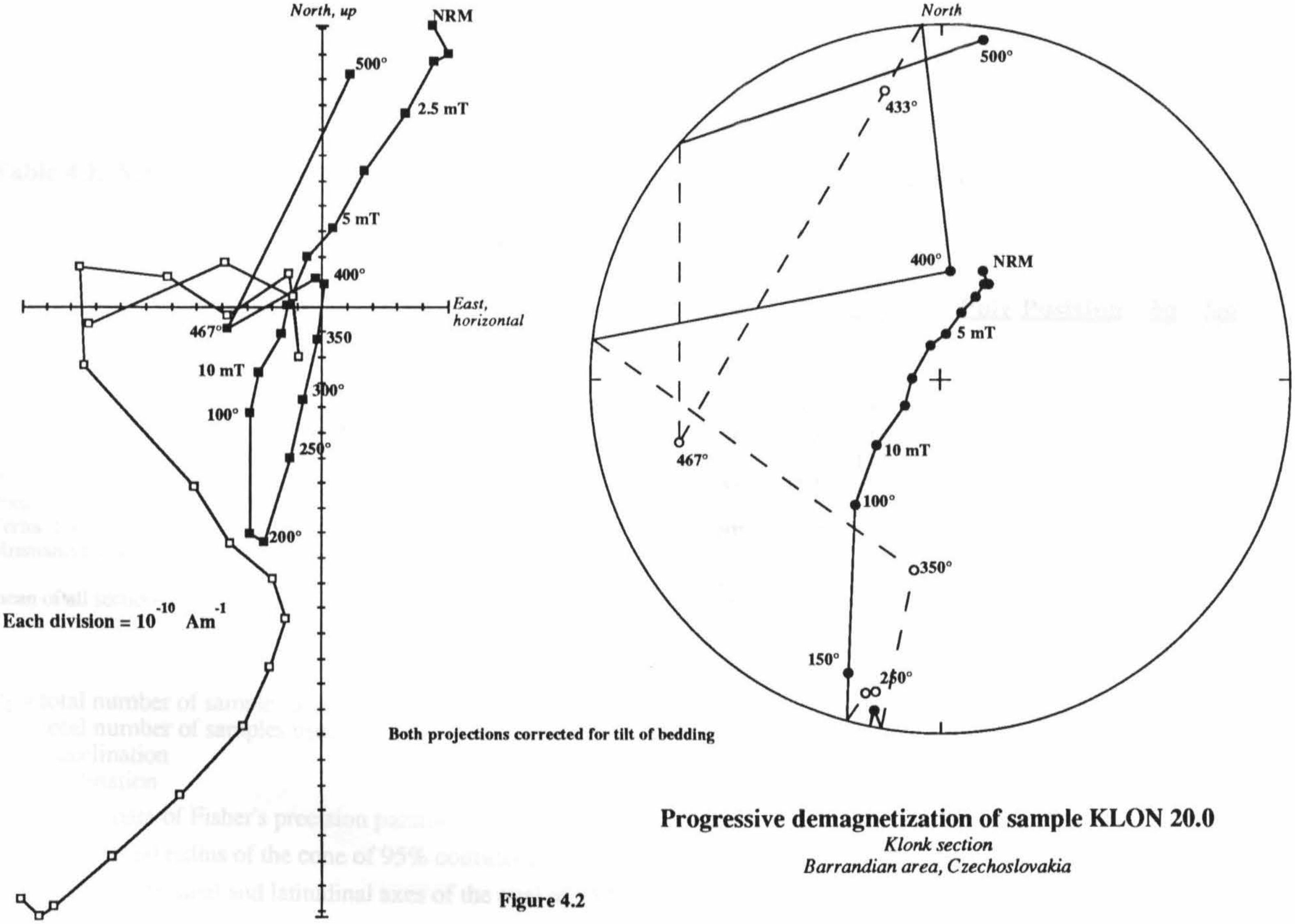

Both projections corrected for tilt of bedding

Progressive demagnetization of sample KLON 20.0

Klonk section

Barrandian area, Czechoslovakia

Figure 4.2

Table 4.1. Section mean directions for the OVP component, Barrandian area, Czechoslovakia

Section	R_t	R_s	(Geographic) Dec	Inc	κ	(Tilt-corrected) Dec	Inc	κ	α_{95}	Pole Position		δp	δm
All sections located at 50.0° N., 14.0° E.													
Klonk	94	53	202°	-24°	44.2	202°	-3°	44.3	3°	38° S.	14° W.	2°	3°
-PDF-OVP planes		(51)	118°	11°	36.7	115°	9°	36.8	3°	-	-	-	-
Pozary quarry #1	78	19	190°	31°	7.7	183°	-1°	7.9	13°	40° S.	10° E.	7°	13°
Pozary quarry #2	24	7	186°	27°	12.2	185°	-20°	15.5	15°	50° S.	6° E.	8°	16°
Prastav quarry	23	12	190°	32°	12.8	186°	-18°	12.7	12°	49° S.	5° E.	6°	11°
Cerna Rokle	35	12	201°	9°	7.7	207°	10°	7.7	16°	30° S.	17° W.	8°	16°
Mramarovy Lom	24	3	-	-	-	-	-	-	-	-	-	-	-
mean of all sections	278	106	197°	-1°	6.4	196°	-4°	12.9	4°	40° S.	7° W.	2°	4°

R_t = total number of samples analyzed
R_s = total number of samples used to calculate statistics
Dec = declination
Inc = inclination

κ = the estimate of Fisher's precision parameter

α_{95} = associated radius of the cone of 95% confidence (McElhinny 1973)

δm and δp = meridinal and latitudinal axes of the oval of 95% confidence around the poles

OVP component characteristic directions

Klonk section

Barrandian area, Czechoslovakia

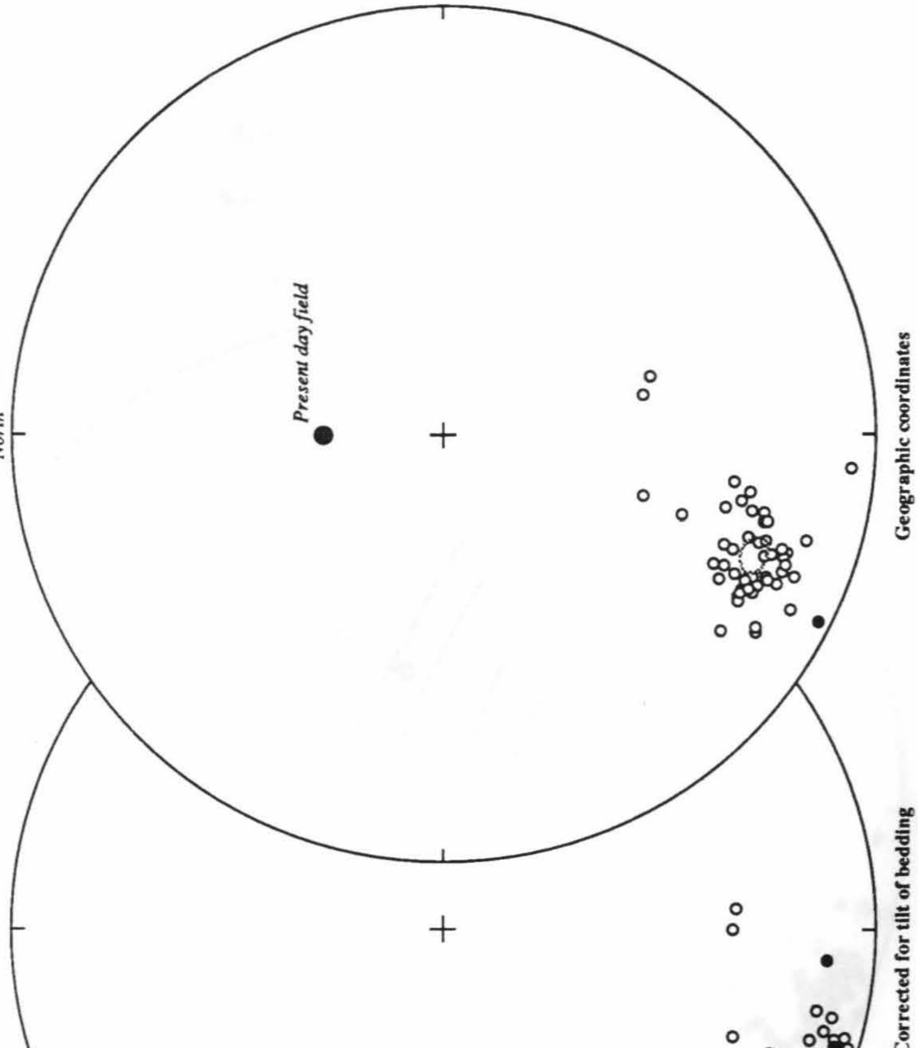

Figure 4.3

Poles to PDF-OVP demagnetization planes

Klonk section

Barrandian area, Czechoslovakia

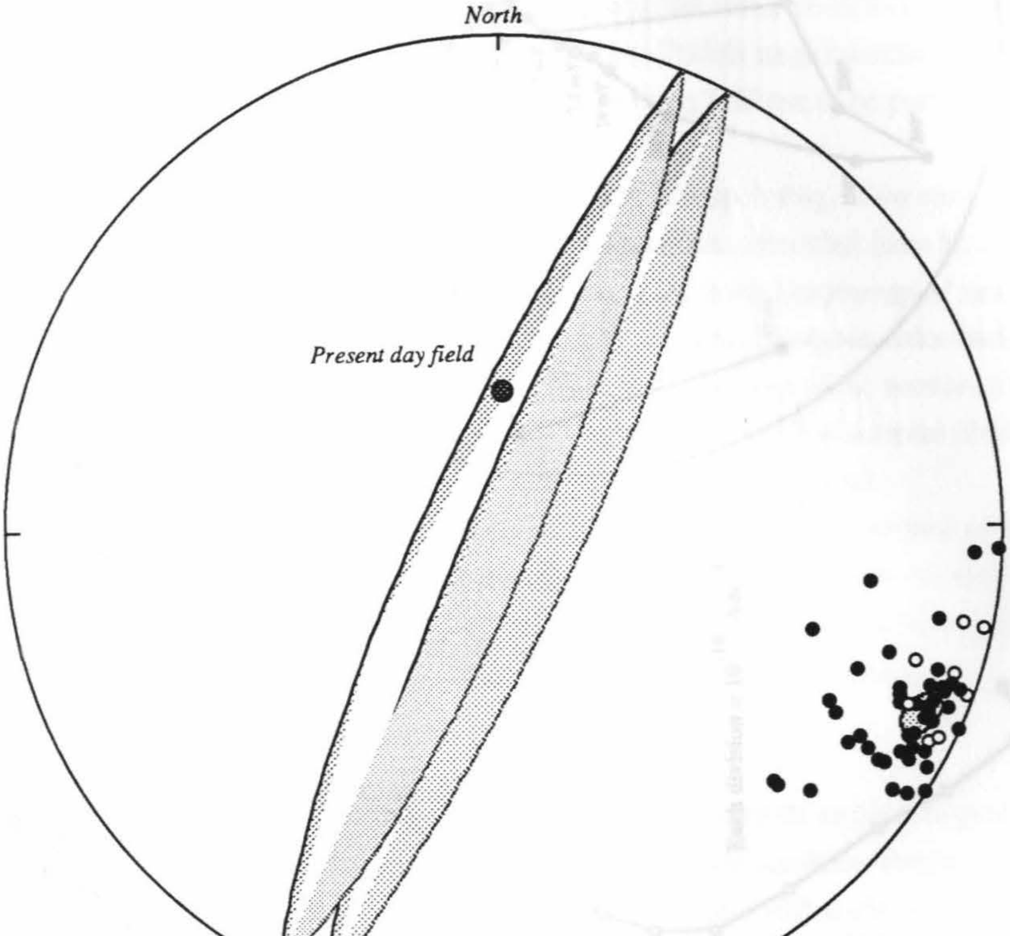

Corrected for tilt of bedding

Figure 4.4

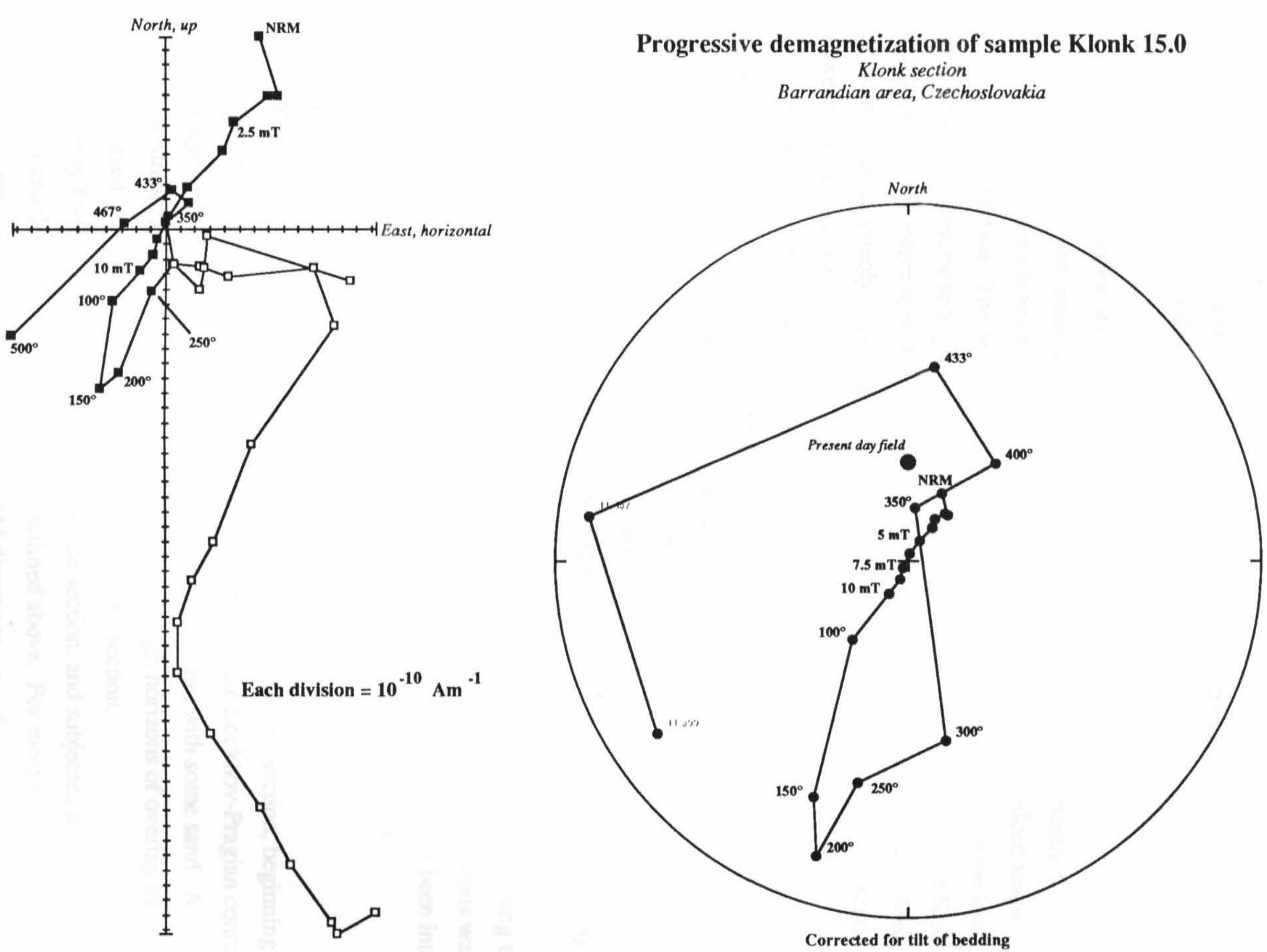
Progressive demagnetization of sample Klonk 15.0
Klonk section
Barrandian area, Czechoslovakia
North, up
East, horizontal
NRM
2.5 mT
433°
467°
350°
10 mT
100°
500°
250°
200°
150°
Each division = 10^{-10} Am $^{-1}$
North
433°
400°
Present day field
NRM
350°
5 mT
7.5 mT
10 mT
100°
300°
250°
150°
200°
Corrected for tilt of bedding

Figure 4.5

amount of scatter in the apparent direction of the component makes it impossible to confirm that the component is the same in the few samples that possess it.

4.2.2 Pozary Quarry #1

Like Klonk, the lithology of the strata in Pozary quarry #1 is dominantly flaggy limestones with shaley intercalations, becoming more massive and well-bedded towards the very top of the section. The section spans from the top of the Ludlow Stage to the lowermost Devonian, thereby stratigraphically overlapping with the lower portion of the Klonk section, and is the international stratotype for the Ludlow-Pridoli stage boundary. Also, the beds dip quite steeply in comparison to Klonk, allowing a fold test to be performed between the two sections.

Generally, the results from this section were very disappointing. Two components of magnetization, very similar to the PDF and OVP components identified from Klonk, were apparent during demagnetization (Figure 4.6). A much lower percentage of samples from this section had the OVP component completely isolated by demagnetization techniques (see Table 1). In a few samples, particularly in the lower part of the section, a third component with high inclinations is suggested (Figure 4.7), but too few samples display directions of this kind to make an accurate determination of this component.

A positive fold test (McFadden and Jones 1981) between the two sections using the OVP component (Figure 4.8) indicates that the OVP component in these two sections was acquired before deformation of the area (between these two sections), which has been interpreted to have occurred between the Middle Devonian and Late Carboniferous.

4.2.3 Pozary Quarry #2

This section is the upwards extension of the Pozary Quarry #1 section, beginning at the base of the Lockhov Stage and extending upwards to near the Lockhov-Pragian contact. The lithology in this section is predominantly massive carbonate, with some sand. A detailed biostratigraphy has not yet been established, although horizons of overlap have been recognized, tying the section to the Pozary quarry #1 section.

Twenty-five samples were collected from the section, and subjected to the same measurement and demagnetization procedures outlined above. For most samples, three components were identifiable (Figure 4.9). NRM directions were dominated by a VRM contribution from the present-day field, identifying this component as the PDF component of the sections described above. The contribution of the PDF component to the total mag-

Figure 4.6. Demagnetizaton trajectories, in orthogonal and equal-area projection, of sample DVC 86.5 from Pozary quarry #1, showing two components of magnetization. Symbols as in Figure 4.2.

Figure 4.7. Sample DVC 37.0 from Pozary quarry #1, showing three components of magnetization. Symbols as in Figure 4.2.

Figure 4.8. Equal area projection of OVP component directions from Pozary quarry #1. Symbols as in Figure 4.3.

Figure 4.9. Fold test between Klonk and Pozary quarry #1 sections using the OVP component.

Progressive demagnetization of sample DVC 86.5

Pozary quarry #1 section
Barrandian area, Czechoslovakia

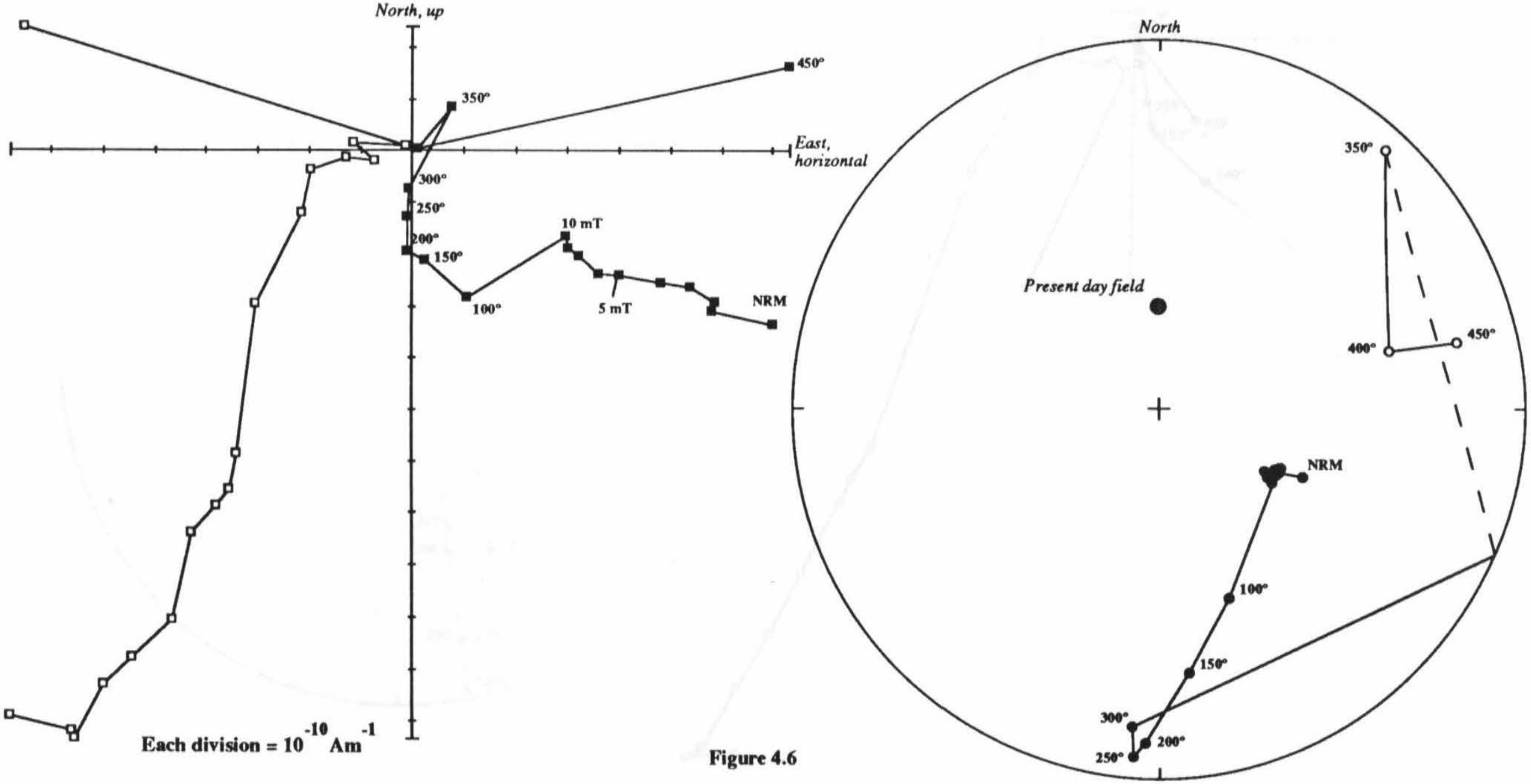

Figure 4.6

Progressive demagnetization of sample DVC 37.0

Pozary quarry #1 section
Barrandian area, Czechoslovakia

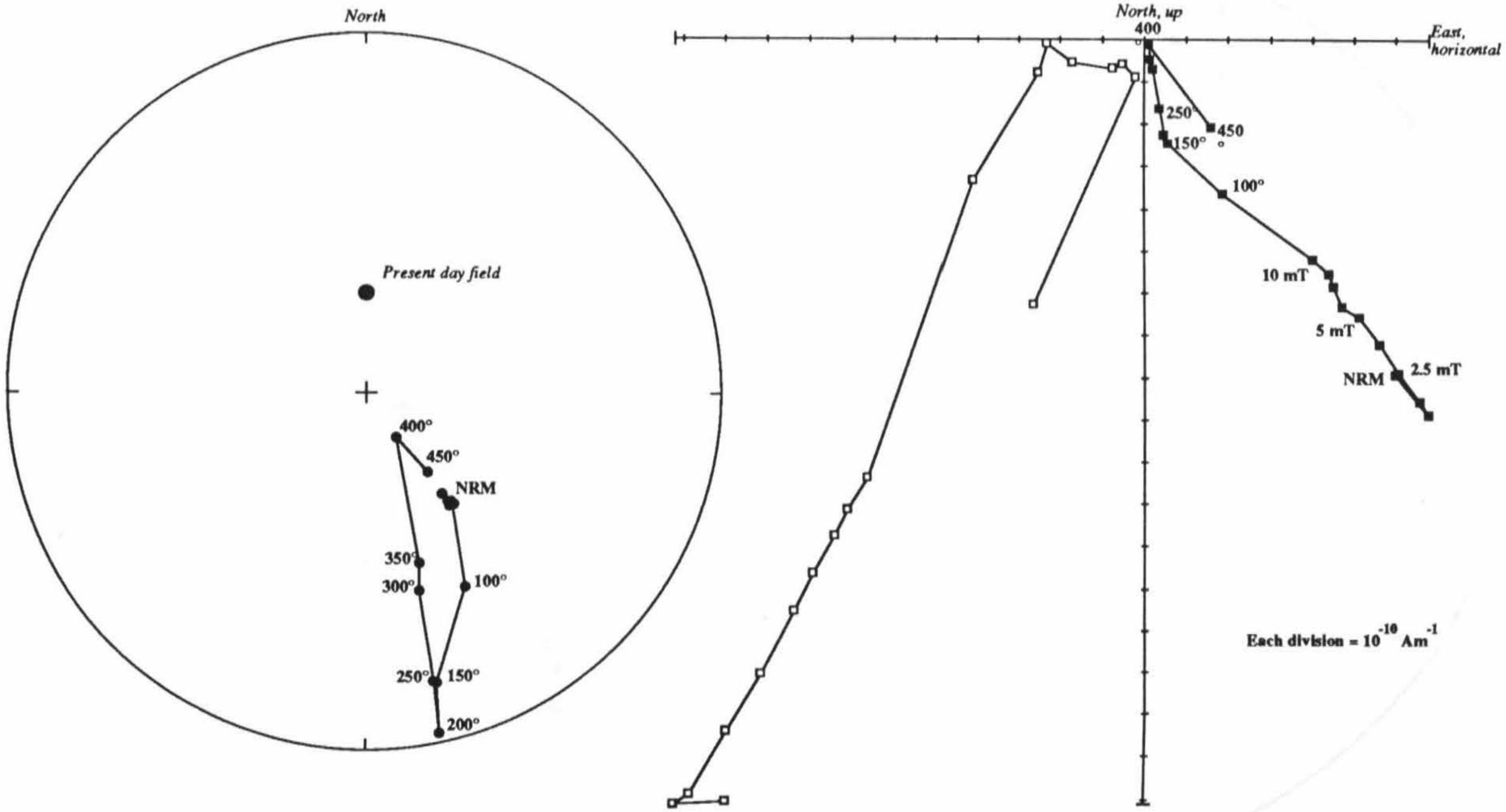

Figure 4.7

Characteristic directions of the OVP component

Pozary quarry #1 section
Barrandian area, Czechoslovakia

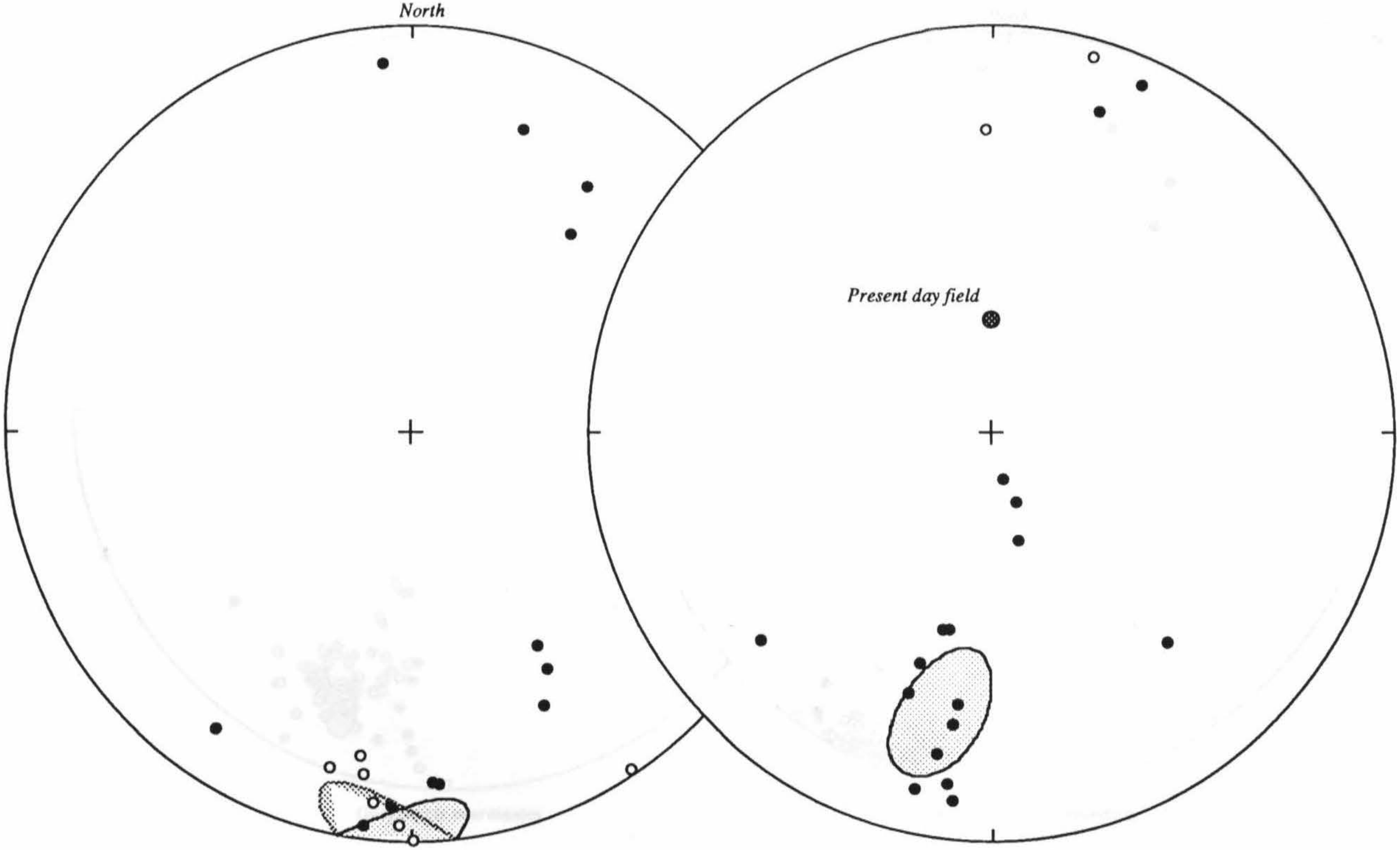

Figure 4.8

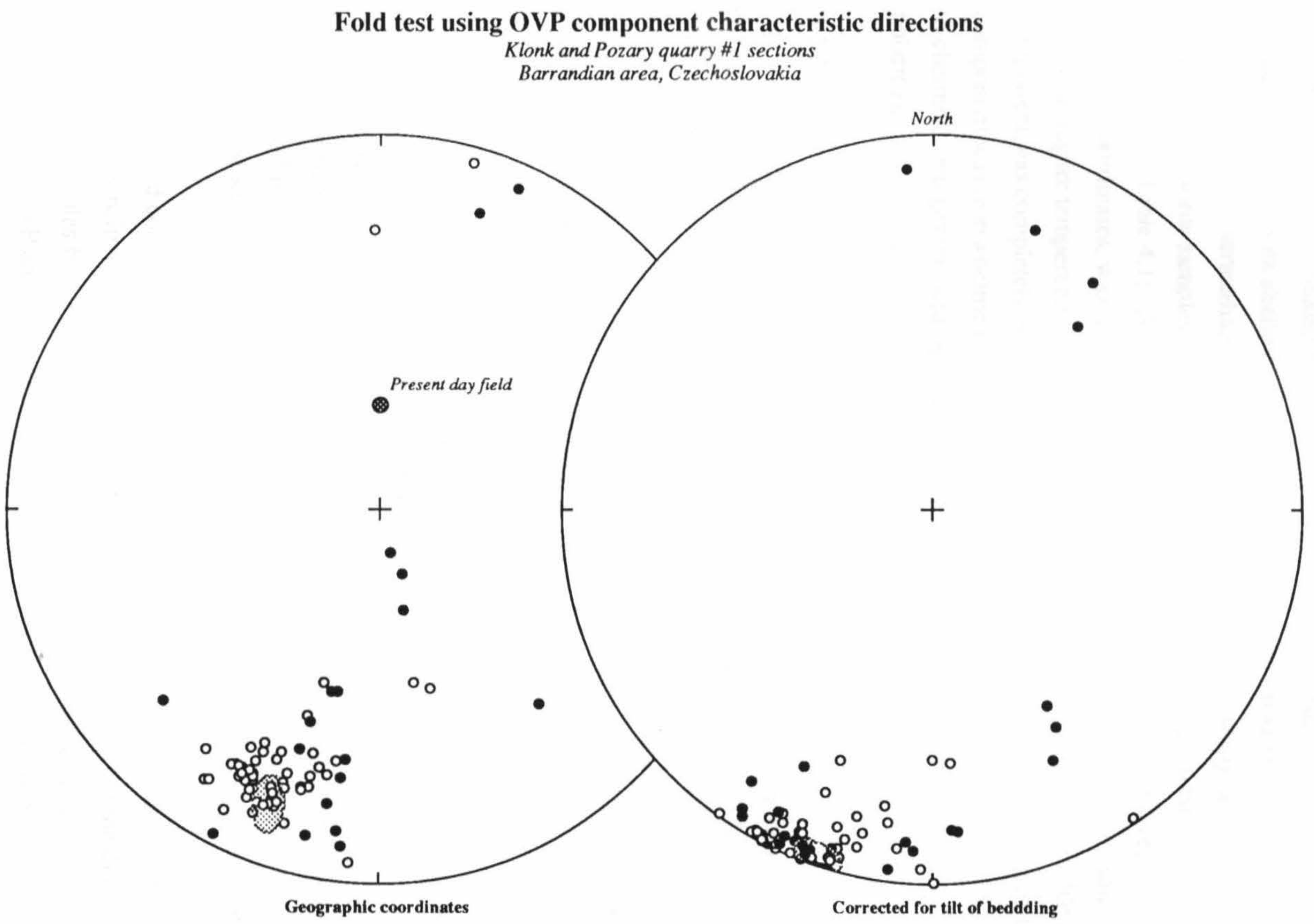
Fold test using OVP component characteristic directions
Klonk and Pozary quarry #1 sections
Barrandian area, Czechoslovakia
North
Present day field
Geographic coordinates
Corrected for tilt of beddding

Figure 4.9

netization was rapidly reduced by AF and low temperature thermal demagnetization. A second component with shallow, southern directions, identified as the OVP component, was recognized at intermediate demagnetization temperatures in many samples. This component was, in some samples, stable throughout successive demagnetization steps (Figure 4.10 and 4.11; Table 4.1). A third component, with an apparently polar direction in tilt-corrected coordinates, was found with varying levels of contribution in many samples, always at higher temperature demagnetization steps. In one sample, it appears that this component was completely isolated by thermal demagnetization, but in most cases the component was overwhelmed by development of a strong magnetization apparently related to chemical changes induced by heating. The third component appears to have dual polarities.

4.2.4 Prastav Quarry

The Prastav Quarry section at Praha-Holyne has been selected as the most suitable for definition of the Lower-Middle Devonian boundary. Particularly rich faunas of trilobites, brachiopods, crinoids, amminoids, nautiloids, bivalves, ostracods and conodonts have been identified in the section and the immediately surrounding area (Chlupac 1982). Deposition was apparently continuous, and the proposed boundary position is recognizable only on paleontological grounds. Unfortunately, the deposition rate for this section is low compared to most of the other studied sections, making sampling intervals from this section temporally large.

Twenty-three core samples were collected from the section with the help of I. Chlupac and J. Kriz. Three distinct components of magnetization can be recognized in many of the samples (Figure 4.12). The first is the PDF component seen in other sections, and is removed by alternating-field and low temperature thermal demagnetization. The second is south-directed and approximately equatorial, and is identified as the OVP component. In a few samples, the OVP component was completely isolated by demagnetization (Figure 4.13).

The third component found within this section appears to trend approximately west-east, with steep inclinations, in tilt-corrected coordinates, very similar to the third component seen in samples from Pozary quarry #2. Poles to the demagnetization planes of this component and OVP are consistent wtith similar poles from Pozary quarry #2. Dual polarities for this component appear to be preserved within this section, although in none of the samples was the component successfully isolated by demagnetization.

Figure 4.10. Demagnetization trajectories of a typical sample from Pozary quarry #2 in equal area (a) and orthogonal projection, showing three components of magnetization. Symbols as in Figure 4.2.

Figure 4.11. Equal area projection of the OVP component direction in samples from Pozary quarry #2.

Figure 4.12. Demagnetization trajectories of sample HPC 3.3, from the Prastav Quarry section, showing the OVP component dominating the NRM direction. Symbols as in Figure 4.2.

Figure 4.13. Equal area projection of characteristic directions from samples for which the OVP component was completely isolated. Symbols as in Figure 4.2.

Progressive demagnetization of sample PSC 6.0

Pozary quarry #2 section
Barrandian area, Czechoslovakia

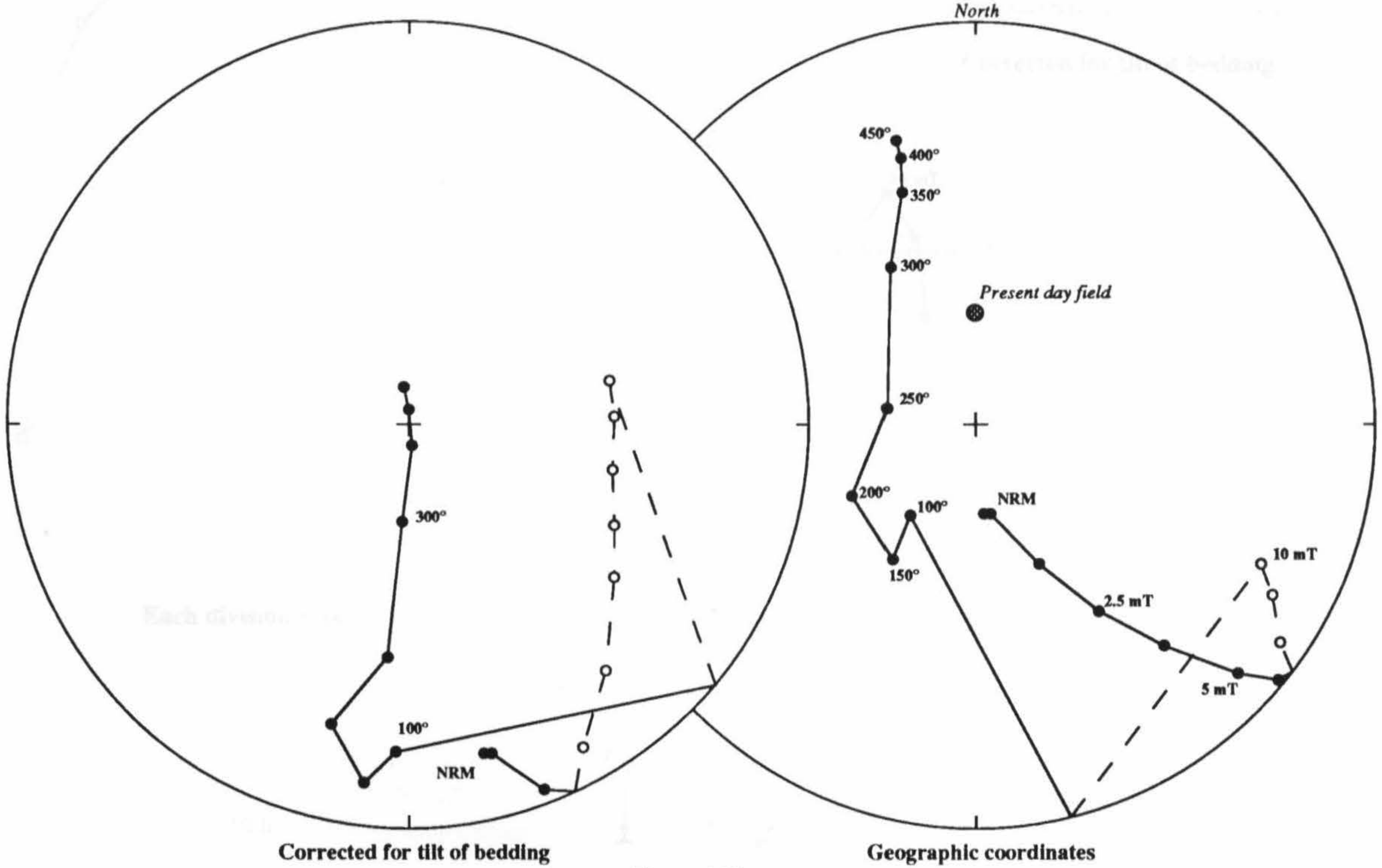

Figure 4.10.a

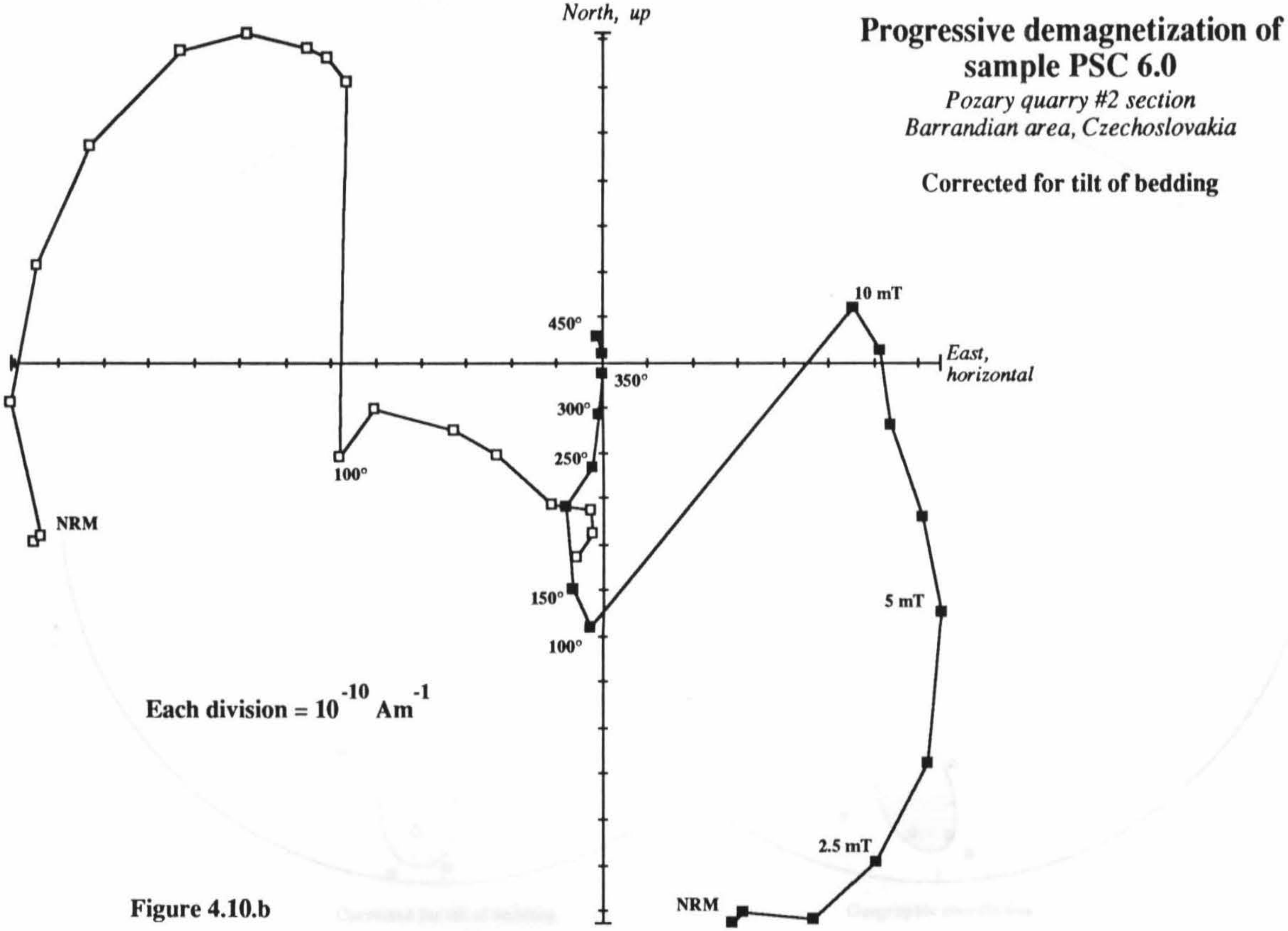
Progressive demagnetization of sample PSC 6.0
Pozary quarry #2 section
Barrandian area, Czechoslovakia
Corrected for tilt of bedding
North, up
East, horizontal
10 mT
5 mT
2.5 mT
NRM
NRM
450°
350°
300°
250°
150°
100°
100°
Each division = 10^{-10} Am^{-1}

Figure 4.10.b

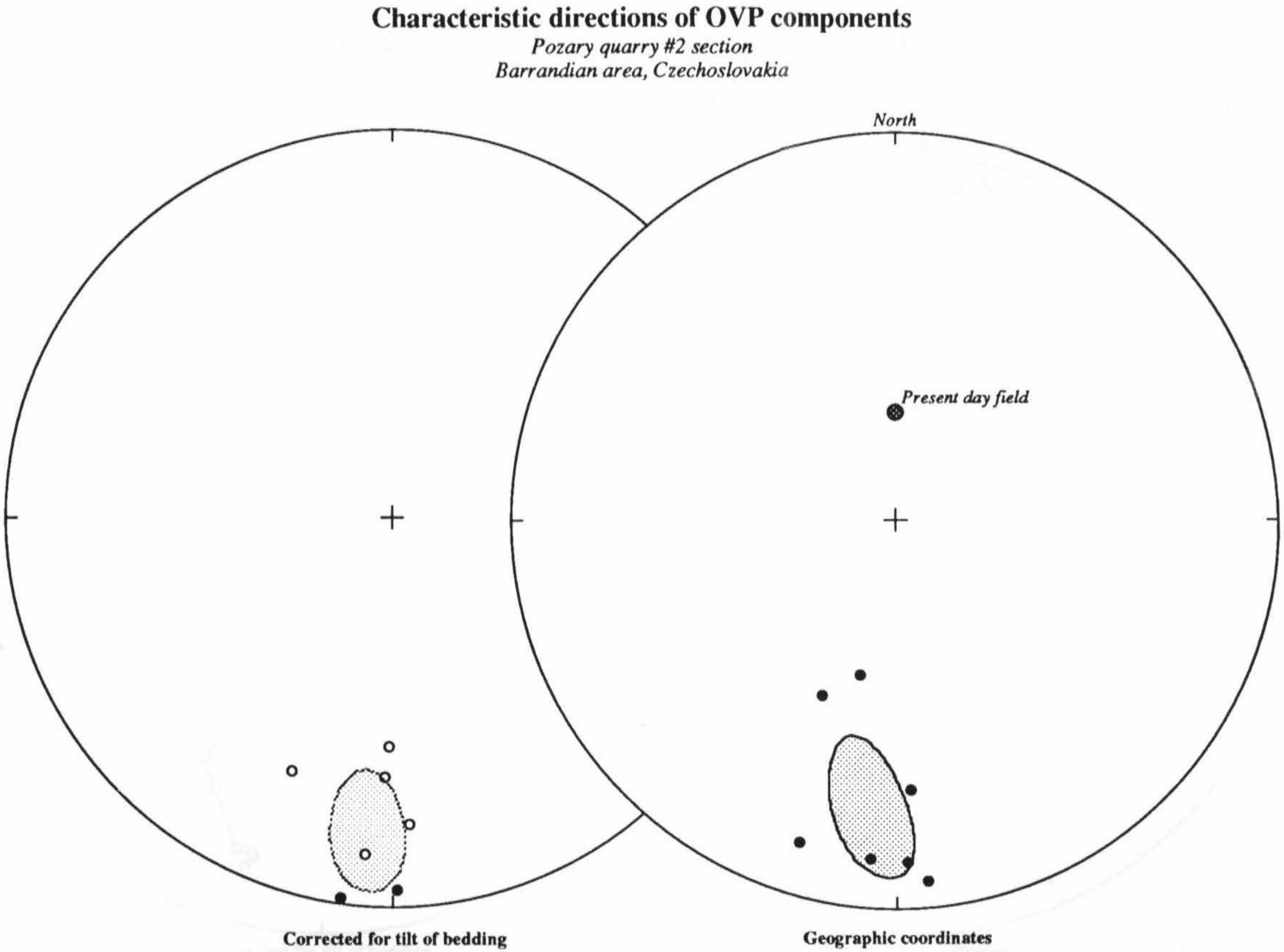
Characteristic directions of OVP components
Pozary quarry #2 section
Barrandian area, Czechoslovakia
North
Present day field
Corrected for tilt of bedding
Geographic coordinates

Figure 4.11

Progressive demagnetization of sample HPC 3.3

Prastav quarry, near Holyne
Barrandian area, Czechoslovakia

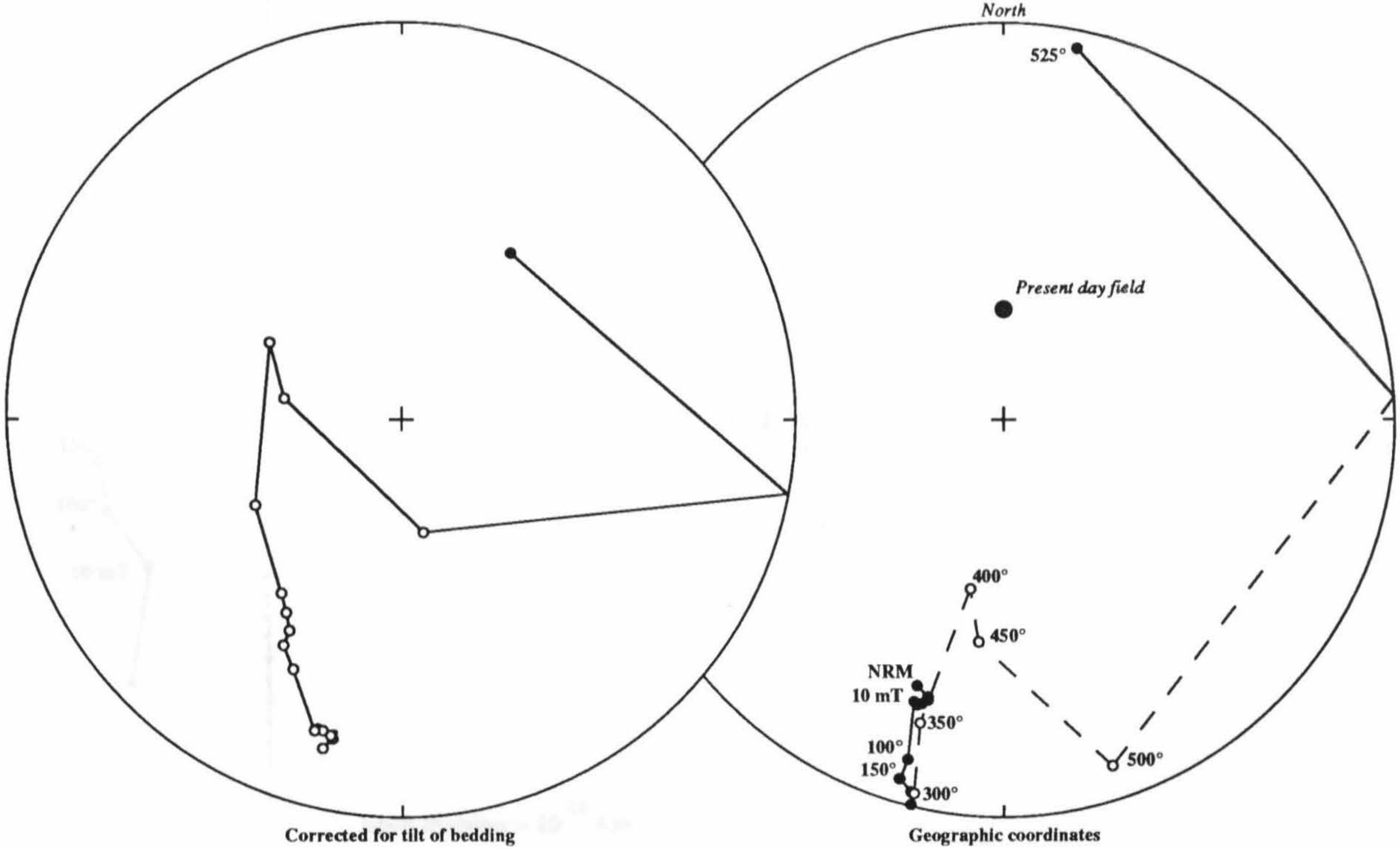

Figure 4.12.a

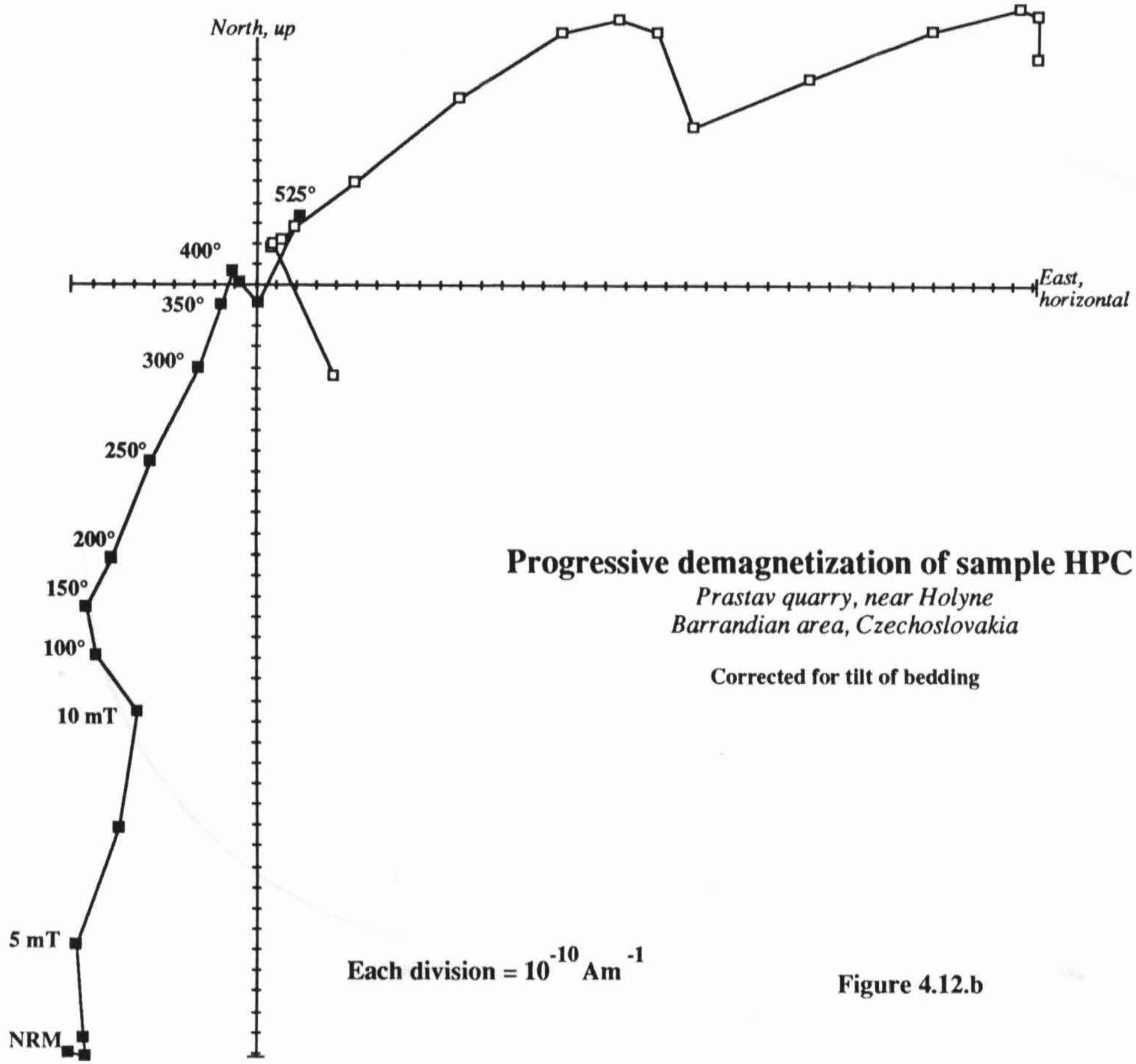

Progressive demagnetization of sample HPC 3.3

Prastav quarry, near Holyne
Barrandian area, Czechoslovakia

Corrected for tilt of bedding

Each division = 10^{-10} Am^{-1}

Figure 4.12.b

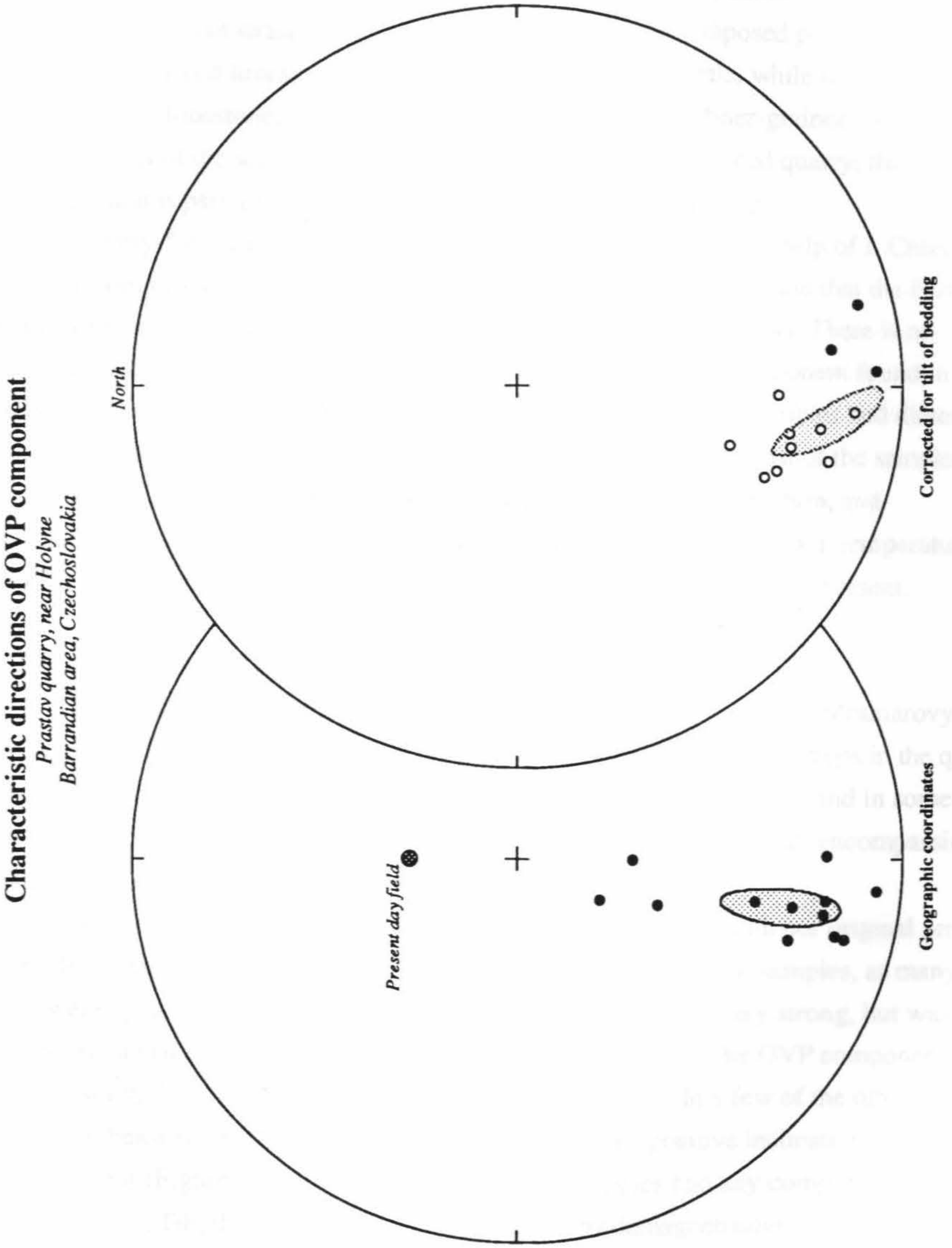
Characteristic directions of OVP component
Prastav quarry, near Holyne
Barrandian area, Czechoslovakia
North
Present day field
Geographic coordinates
Corrected for tilt of bedding

Figure 4.13

4.2.5 Cerna rokle

The Cerna rokle section, southwest of Barrande's Rock, contains upper Pridolian through Lochkovian strata. The lower part of the section is composed predominantly of flaggy, fine-grained limestones with interbedded calcareous shale, while in the upper part of the section, limestones become more definitely bedded and finer-grained. Exposures of the upper part of the section are excellent, occurring in an abandoned quarry; the lower part of the section is partially covered. The section has only a minor dip.

Thirty-five samples were collected from this section with the help of I. Chlupac. Results from this section were generally very disappointing, but indicate that the PDF and OVP components make up the bulk of the magnetization (Figure 4.14). There is no evidence that the latter component has dual polarities. The third component found in some of the other sections does not appear to be present, although a few samples had directions that may reflect the contribution of a highly-inclined component. Most of the samples from this section, however, became very weak during thermal demagnetization, and measurement errors for directions determined after higher demagnetization temperatures are large, precluding positive identification of any components that might be present.

4.2.6 Mramarovy Lom

Of all the sections studied from the Barrandian area, the quarry at Mramarovy Lom appeared to have the lowest potential for good paleomagnetic data. Outcrops in the quarry consisted primarily of marble, which in some cases were highly veined, and in some cases, diagenetically brecciated. Furthermore, the section is highly condensed, encompassing Late Silurian through Middle Devonian time.

Unfortunately, the paleomagnetic results were consistent with our original prediction. In all samples at least two components were present; in a few samples, as many as four were apparent. In most samples, the PDF component was very strong, but was rapidly removed by low temperature thermal demagnetization. The OVP component was usually south-directed and shallow, as in the other sections. In a few of the other samples third (southeast and moderately inclined) and fourth (high positive inclination) components were present (Figure 4.15). However, none of the samples had any components, including OVP and PDF, that were demonstrably isolated by demagnetization.

Figure 4.14. Demagnetization trajectories of a typical sample from Cerna rokle, showing the PDF and OVP components of magnetization. Symbols as in Figure 4.2.

Figure 4.15. Demagnetization trajectories of a sample from Mramarovy Lom quarry, showing four different components of magnetization. Symbols as in Figure 4.2.

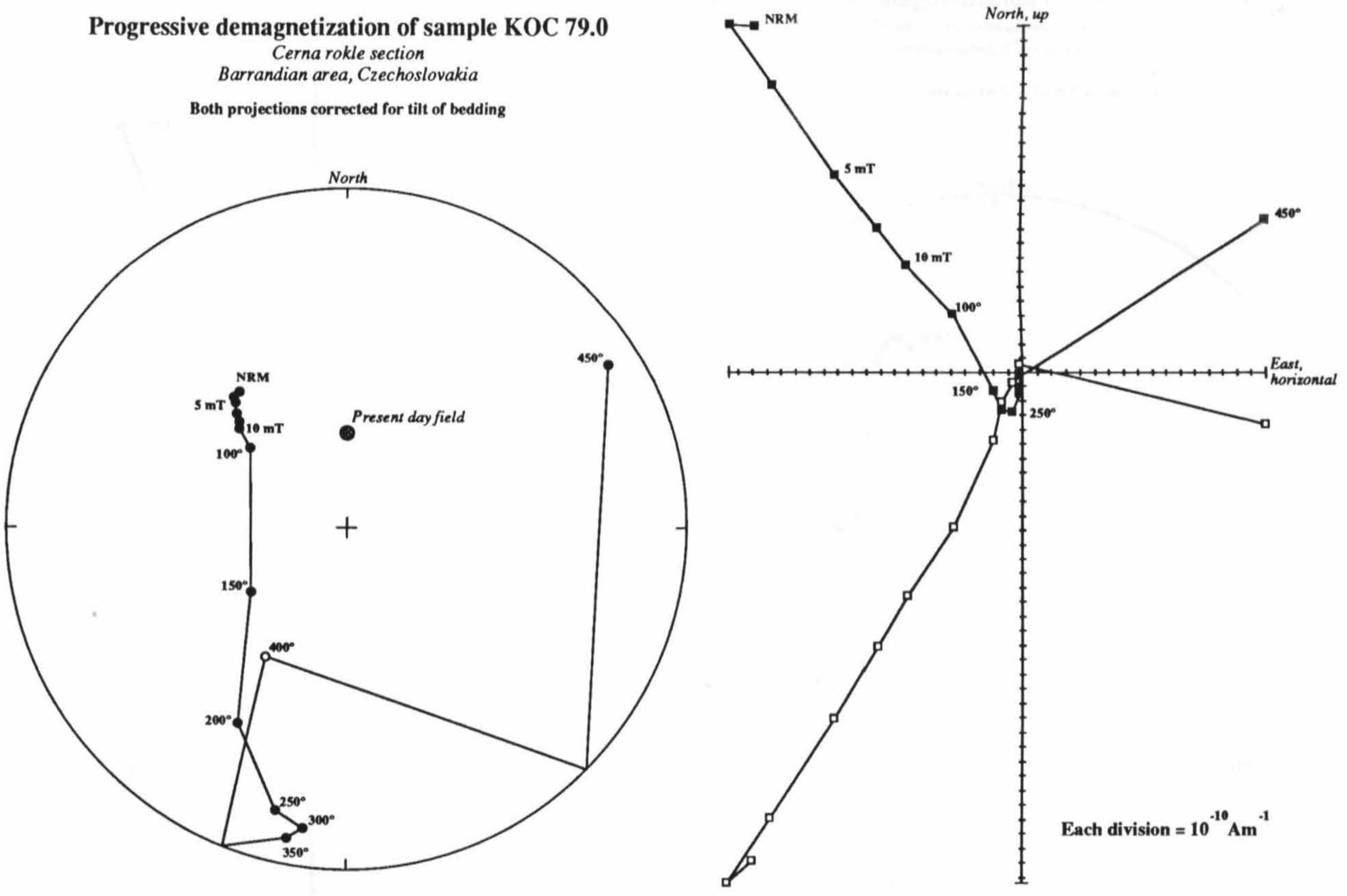
Progressive demagnetization of sample KOC 79.0
Cerna rokle section
Barrandian area, Czechoslovakia
Both projections corrected for tilt of bedding
North
NRM
5 mT
10 mT
100°
Present day field
150°
200°
250°
300°
350°
400°
450°
North, up
East, horizontal
Each division = 10^-10 Am^-1

Figure 4.14

Progressive demagnetization of sample MQC 18.0

Mramarovy Lom quarry section
Barrandian area, Czechoslovakia

Both projections corrected for tilt of bedding

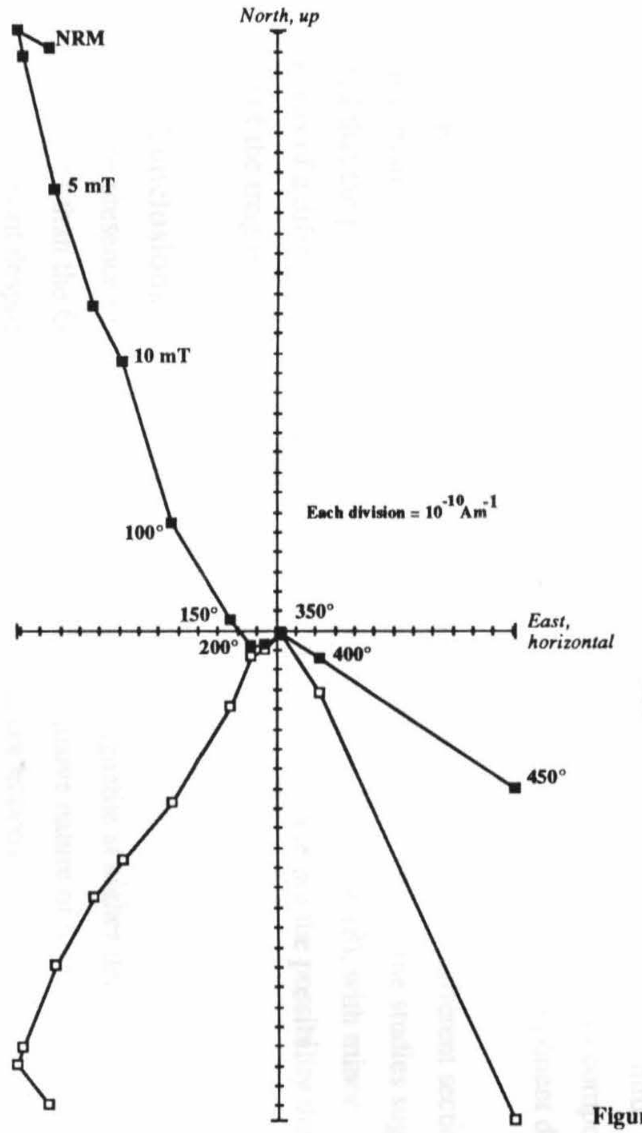

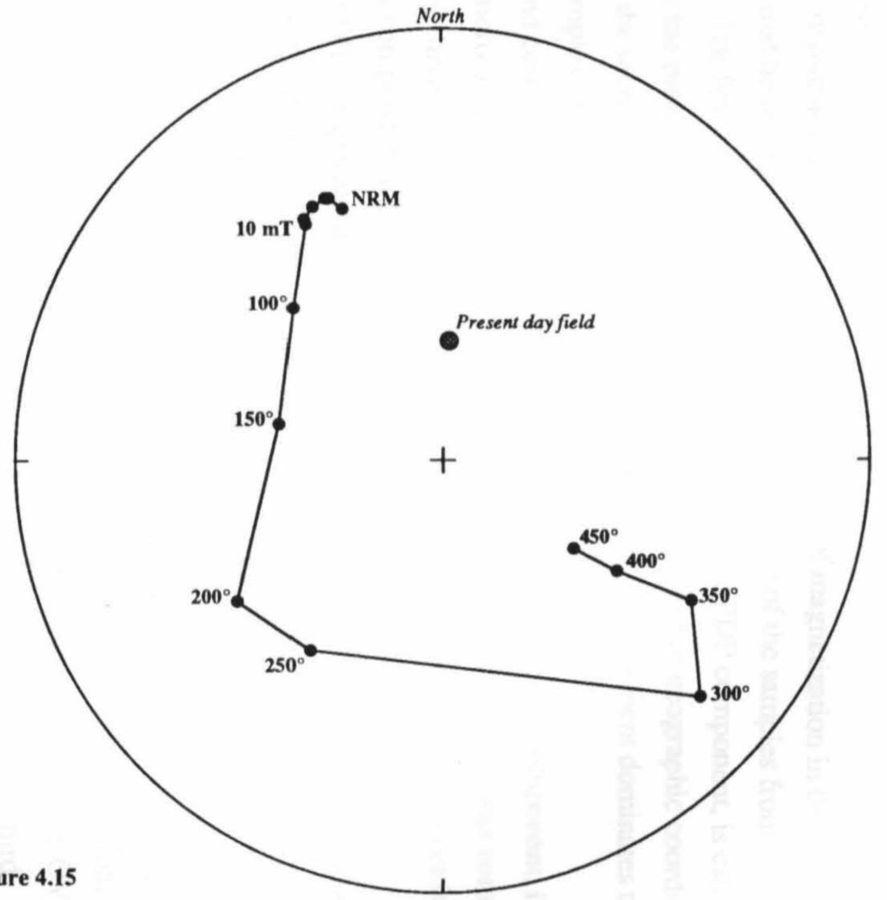

Figure 4.15

4.3. Discussion

The influence of at least three different components of magnetization in the Barrandian area is indicated by the demagnetization behavior of many of the samples from the various sections. The first component removed in all cases, the PDF component, is clearly a VRM related to the present-day field. NRM directions expressed in geographic coordinates from all of the sections (Figure 4.16) indicate that the PDF component dominates the NRM in most samples, regardless of section.

The second component removed during demagnetization, the OVP component, is present in all sections as a southerly directed, shallowly inclined direction, and was completely isolated by thermal demagnetization in some samples (Figure 4.17). A positive fold test based on this component, and encompassing all of the studied sections, strongly suggests that the OVP component was acquired after the deformational event that tilted and folded strata within the Barrandian area.

Interpretation of the demagnetization behavior of samples from some of the sections, notably those at Pozary quarry #2 and Prastav Quarry, is complicated by the presence of a third component. In all of the samples that exhibited a third (or rarely, a fourth) component, the PDF and OVP components were the first removed by demagnetization, and were usually only incompletely resolved. A provisional fold test, using poles to the OVP-third component demagnetization planes from the different sections hints that the third component was acquired before folding. Unlike the other components, the third component also exhibits dual polarities, but the low number of samples with this component does not allow magnetostratigraphic interpretation.

Rock magnetic studies indicated the magnetic mineralogies of the different sections were substantially different in size ranges, but not in mineralogy. All of the studies suggested that the primary carrier of remanence was magnetite (Figure 4.18), with minor amounts of a different, high coercivity mineral, but could not rule out the possibility that some of the magnetite might be diagenetic.

4.4. Conclusions

The presence of a third component carried by magnetite at higher demagnetization temperatures than the OVP component, and the inconclusive nature of fold tests using the OVP component despite large differences in structural corrections, indicate that the OVP component represents an overprint direction acquired either after or during deformation. The pole position derived from the direction of this component falls near the Carboniferous

Figure 4.16. Equal area projections of NRM directions of all samples, in geographic coordinates. Symbols as in Figure 4.3.

Figure 4.17. Equal area projections of directions from all samples with isolated OVP components, in a) geographic and b) tilt-corrected coordinates. $\kappa_{tilt}/\kappa_{geographic} = 2.0$; N=106. Symbols as in Figure 4.3.

Figure 4.18. Typical IRM acquisition-AF demagnetization curves for samples from the Barrandian area, Czechoslovakia. The curves indicate the primary carrier of remanence is magnetite, with a J_{50}= 35 mT. Incomplete saturation at IRM levels above 300 mT is due to the presence of high coercivity magnetic minerals, but the shape of the curve suggests the contribution of the high coercivity mineralogy to the total NRM is small.

NRM directions

Barrandian area sections, Czechoslovakia

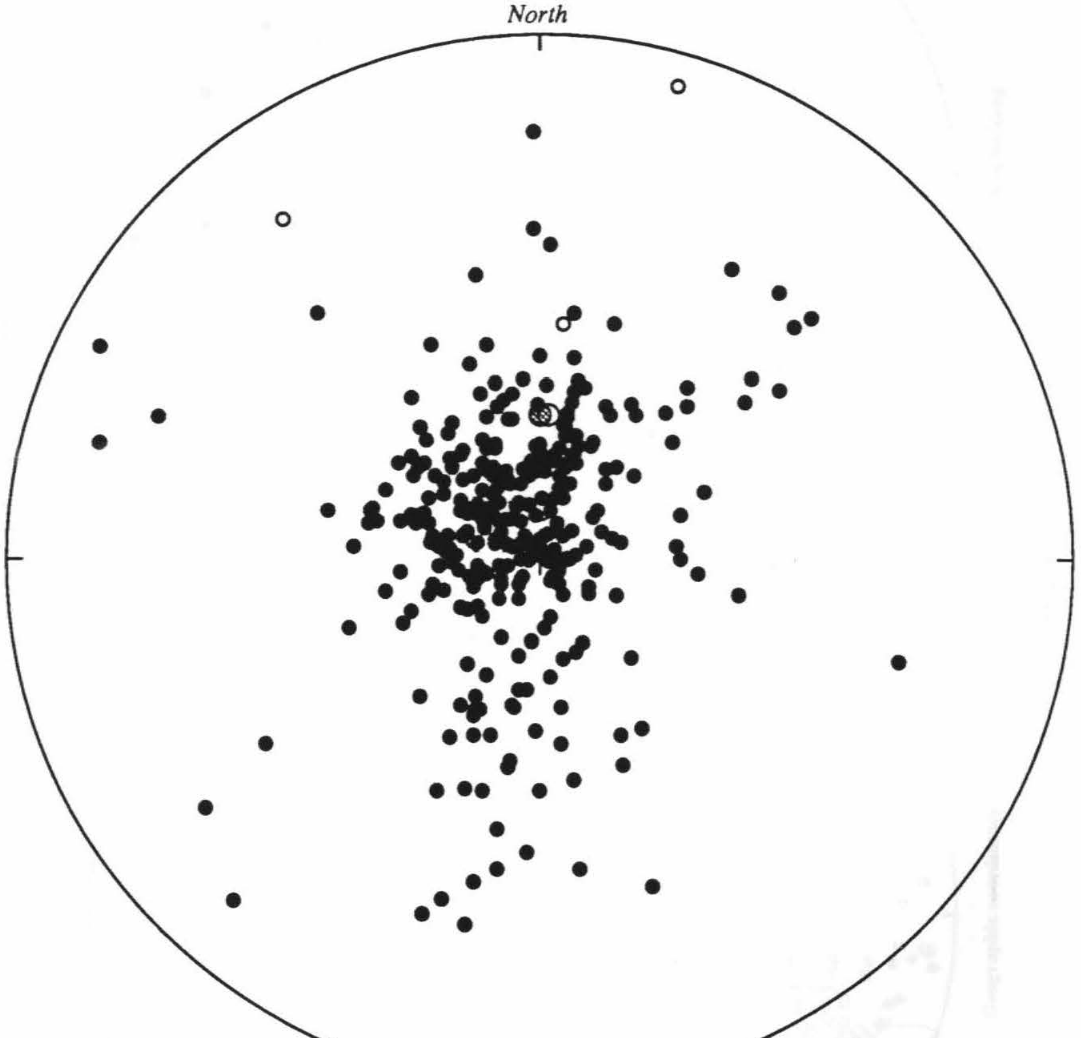

Geographic coordinates

Figure 4.16

Fold test using OVP component

All sections

Barrandian area, Czechoslovakia

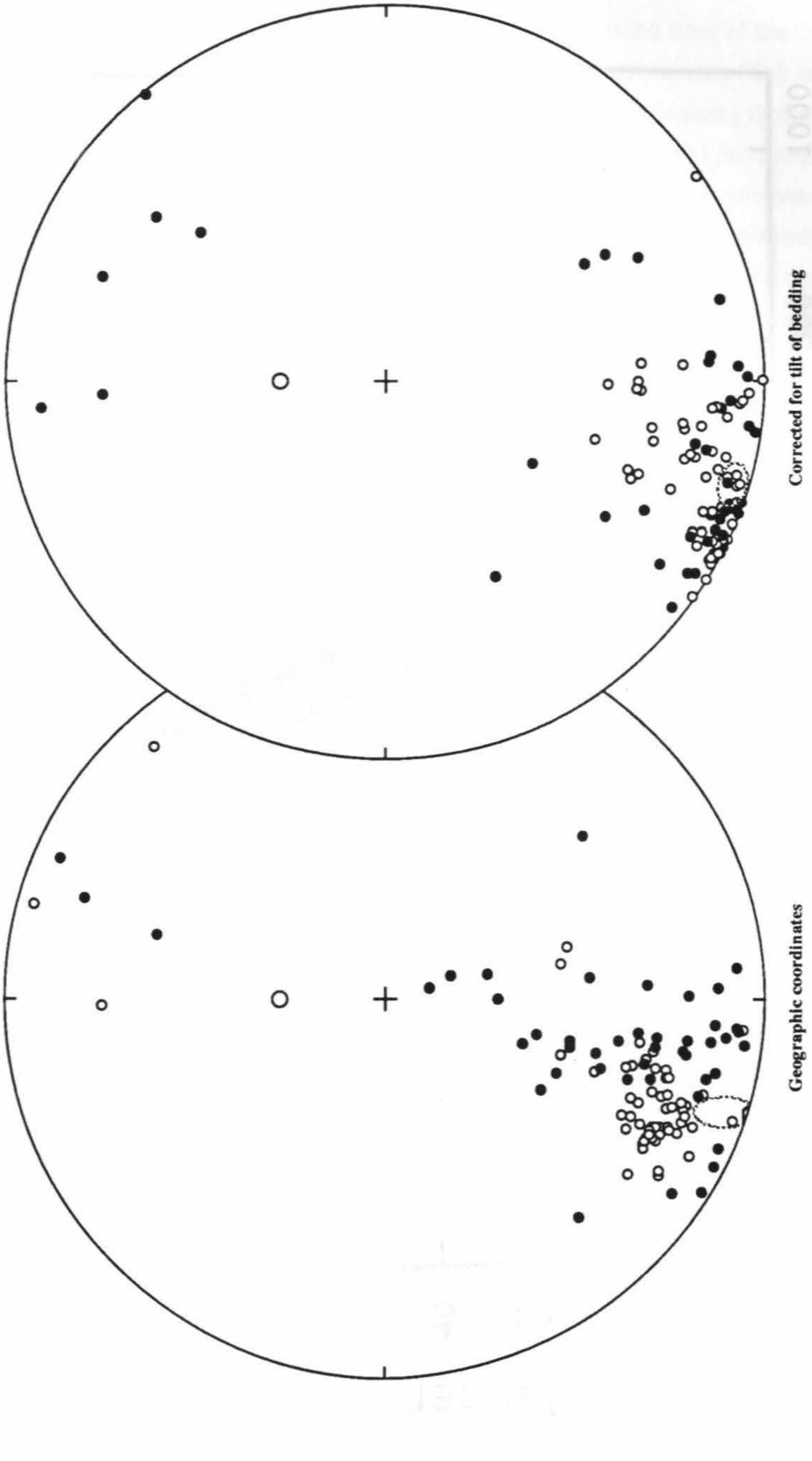

Figure 4.17

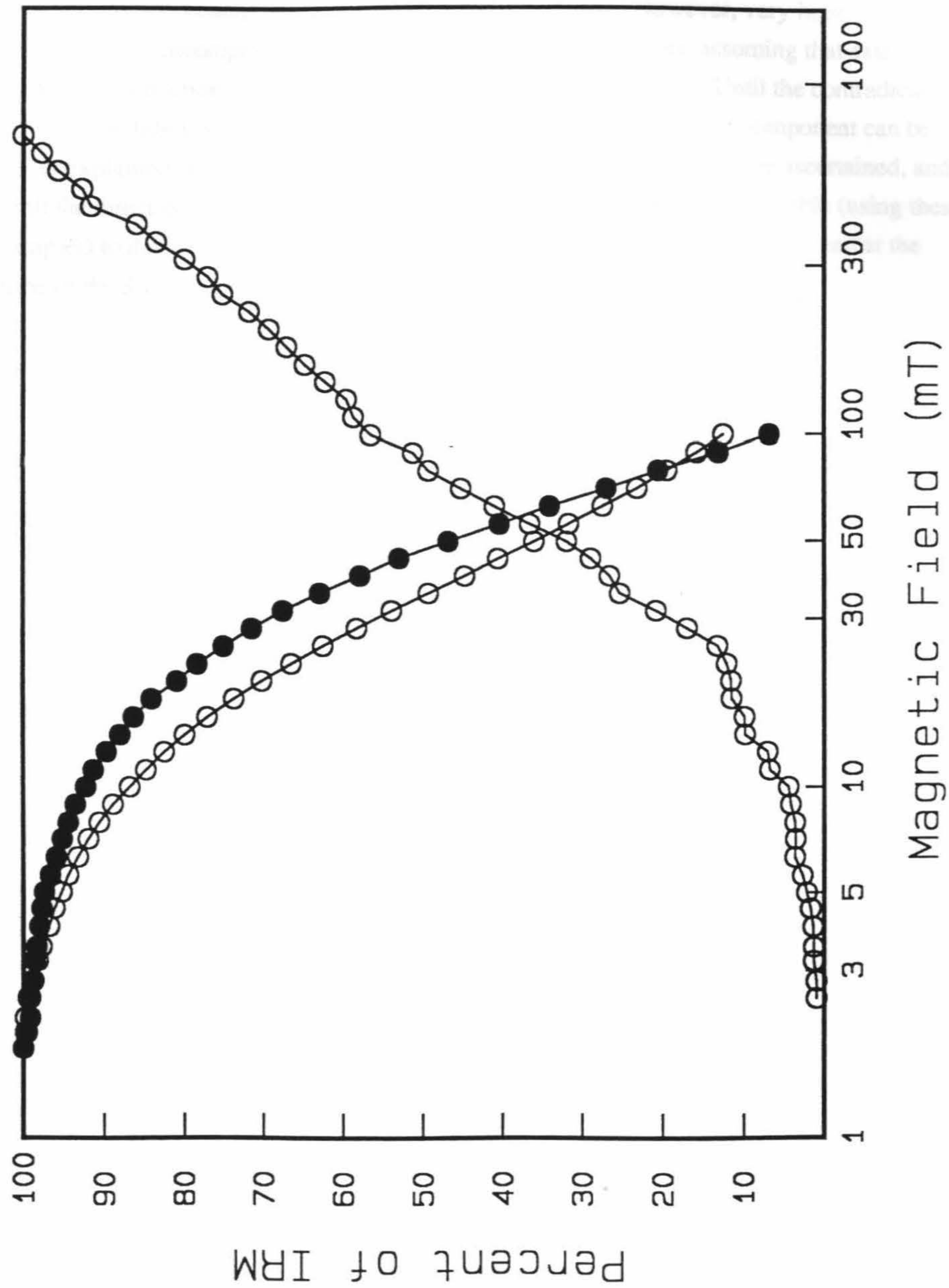
Percent of IRM
100
90
80
70
60
50
40
30
20
10
1
3
5
10
30
50
100
300
1000
Magnetic Field (mT)

portion of the APWP for Europe (Figure 4.19), corresponding to the time of the Hercynian about 60 million years), which is rapid but not impossible. However, very high latitudes are completely incompatible with the lithologic setting of the area, assuming that extensive carbonate production is restricted to tropical or temperate latitudes. Until the contradiction between the lithologic evidence and indicated high latitude of the third component can be either explained or resolved, the source of the third component can not be ascertained, and until the direction of the third component can be better defined, it is impossible (using these samples) to determine what tectonic affinities the Bohemian Massif may have had at the time of the Silurian-Devonian boundary .

Figure 4.19. Comparison of the European APW path (Briden and Duff 1981) with the pole position determined from OVP directions.

European APW for Early Paleozoic compared with OVP component

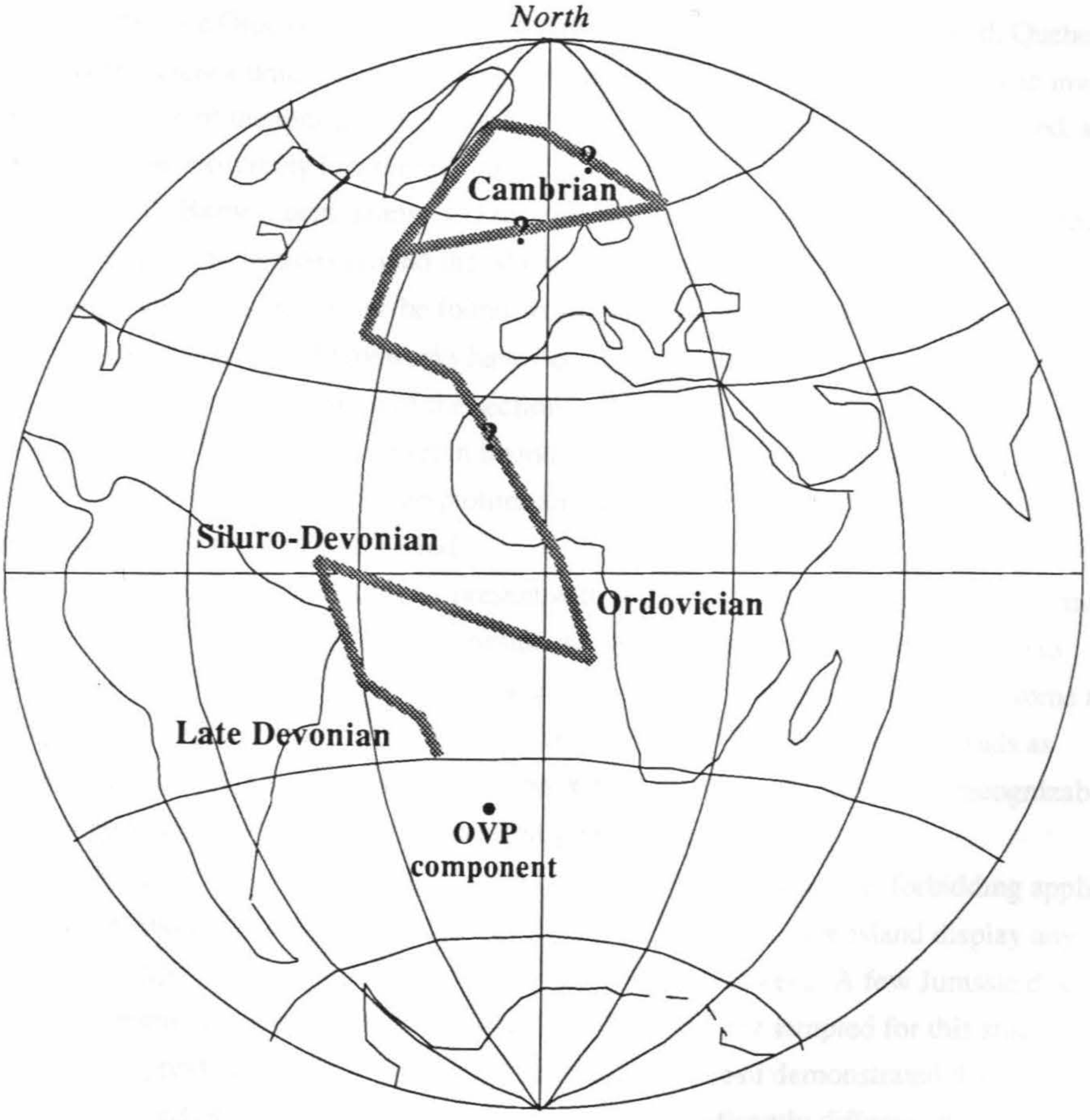

Figure 4.19

Chapter Five Paleomagnetic results from the Ordovician-Silurian boundary section at Falaise Ouest, Anticosti Island, Quebec, Canada

5.1 Introduction

The Late Ordovician and Early Silurian strata found on Anticosti Island, Quebec, Canada represent a unique opportunity for paleomagnetic and magnetostratigraphic investigation because of the unusual thickness and continuity of section for this time period, and because of the extremely low thermal maturity of the carbonates found on the island (CAI=1.0; C. Barnes, pers. comm.). Fresh exposures are guaranteed by the occurrence of extensive sea-cliff sections around the island. Exceptionally rich brachiopod, trilobite, coral, and conodont faunas can be found within various sections around the island, and detailed biostratigraphic frameworks have been established for many of the sections. The primary reason for designation of the section at Dob's Lin, Scotland as the international stratotype for the Ordovician-Silurian boundary , rather than on Anticosti Island, was the lack of graptolites at Anticosti; graptolites are far superior to any other group for biostratigraphic zonations of this time period.

The predominant lithologies present within the Falaise Ouest section are lime mudstones and thin-to-medium-bedded limestones, and coarser-grained equivalents up to packstones and wackestones. Near the boundary horizon, prominent bioherms, some as much as 3 meters high, can be found with cateniporid corals and stromatoporoids as framebuilders (IUGS Field meeting guidebook Vol. 1; 1981). A few easily-recognizable marker beds are also present within the stratigraphic column.

An unfortunate aspect of the island is the total lack of structure, forbidding application of the fold test. None of the sections on the western half of the island display any significant dip; generally, dips were less than 5° to the southwest. A few Jurassic dykes are also present, permitting a baked contact test, but were not sampled for this study. However, a previous investigation using rocks from Anticosti demonstrated that the site-mean directions of the De Puyjalon Cliff dykes were significantly different from Lower Paleozoic directions obtained from Anticosti carbonates (Seguin and Petryk 1984). Additionally, a few intraclastic conglomerate units are available, particularly on the eastern shores of the island[1].

Two problems that could be addressed using paleomagnetic data from the Anticosti sections bear on the magnetostratigraphic relationships across the boundary interval, and comparison of any pole positions obtained from Anticosti Island with the North American APW path. The Late Ordovician through Early Silurian portion of the North American APW path is poorly-constrained. Furthermore, most of the poles presently used come from the Appalachian Mts., an area known to have widespread remagnetization. The possibility of obtaining a reliable pole position from undeformed, unmetamorphosed strata is also attractive in terms of shedding new light on the paleogeographic position of Anticosti Island.

5.2. Results

The Falaise Ouest section is located on the western shore of Baie Ellis, stretching for about 3 km north from Pointe Aux Ivrognes, to the Baie Jolliet swamp at the northern end of the bay (Figure 5.1). The Ordovician-Silurian boundary is near the south end of the section, within the Becscie Formation. The Upper Ordovician Ellis Bay Formation has its top 15 meters below the boundary, and stretches northward to the north end of the section. Exposures along the shore of Baie Ellis are excellent, and access can be made via boat from Port-Menier, or by 4-wheel drive vehicle along the coast.

Ninety-three oriented core samples were collected from the section in August of 1986, prepared using standard procedures outlined elsewhere (see Chapter 2), and measured on an ScT cryogenic magnetometer using SQUID devices interfaced to a microcomputer. Both alternating-field (AF) and thermal demagnetizations were performed. Typically, the peak AF intensity used was 20 mT; thermal demagnetizations often were done up to 650° C.

Unfortunately, the results from the Falaise Ouest section were very disappointing. In virtually all samples, a strong VRM component of the present-day field dominated the natural remanent magnetization (NRM) (Figure 5.2). In many cases, alternating-field demagnetization to 20 mT did not change the preserved direction. Significant departures from NRM directions were obtained using thermal demagnetization, but a consistent

---

[1]Work is in progress on samples recently provided by D.G.F. Long from one of these units.

Figure 5.1. Map showing the location of the Falaise Ouest section on Anticosti Island, Quebec, Canada.

Figure 5.2. Equal area projection of NRM directions of samples from Falaise Ouest, showing the strong influence of a present-day field VRM component. Positive inclinations are denoted by filled circles.

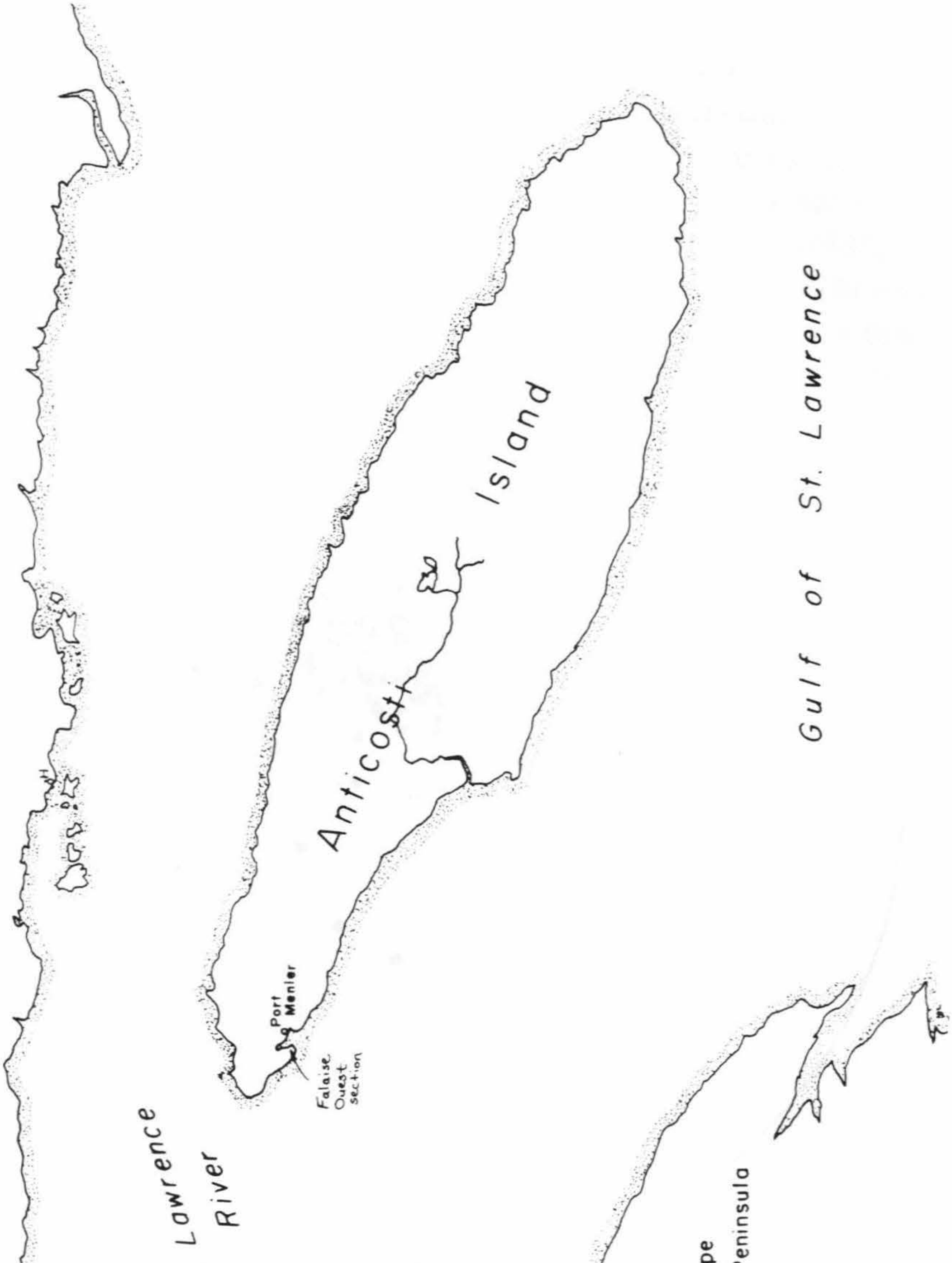
QUEBEC
St. Lawrence
River
Anticosti
Island
Port
Menier
Falaise
Ouest
section
Gulf of St. Lawrence
Gaspe
Peninsula

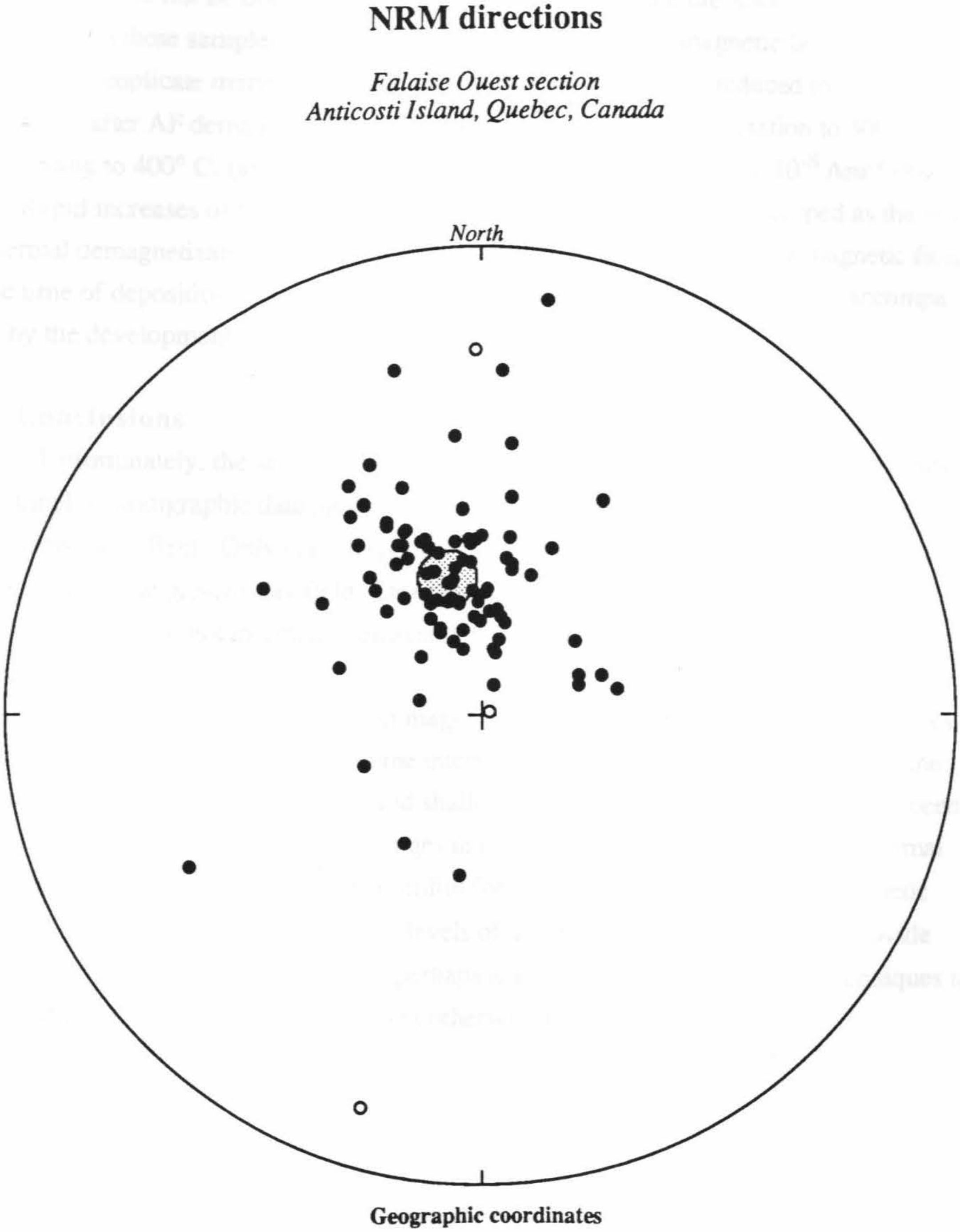
NRM directions
Falaise Ouest section
Anticosti Island, Quebec, Canada
North
Geographic coordinates

Figure 5.2

component could not be obtained. Figures 5.3-5.5 demonstrate the 'shotgun pattern' obtained from these samples, which is characteristic of unstable magnetic behavior.

To complicate matters further, magnetizations were usually reduced to around 1 x 10^{-10} Am^{-1} after AF demagnetization to 20 mT and thermal demagnetization to 300° C., but after heating to 400° C. (and often at 350° C.), typically increased to 1 x 10^{-8} Am^{-1} (Figure 5.6). Rapid increases of this kind often are due to chemical changes developed as the result of thermal demagnetization, and do not yield information relevant to the geomagnetic field at the time of deposition. In many samples, marked increases in intensity were accompanied by the development of a red tint.

5.3. Conclusions

Unfortunately, the section at Falaise Ouest does not appear to have preserved any directional or stratigraphic data providing knowledge of the Ordovician-Silurian boundary-age geomagnetic field. Only one component can be clearly identified- the VRM component that dominates the present-day field. Directions obtained after higher temperatures of demagnetization are not internally consistent, and cannot presently be used for any sort of interpretation.

The unusually large increases in magnetization induced by moderate temperatures of thermal demagnetization may be of some interest, however, in terms of investigating the rock magnetic properties of platform and shallow water carbonate rocks. It has long been recognized that carbonates undergo changes in their magnetic mineralogy during thermal demagnetization, often hampering their utility for paleomagnetic study. Rock magnetic studies of samples subjected to different levels of thermal demagnetization may provide clues as to what these changes are, and perhaps lead to development of better techniques to recover directional information that might otherwise be obscured.

Figure 5.3. Directions obtained from Falaise Ouest samples after thermal demagnetization at 100° C.; the strong influence of the VRM component is still evident. Symbols as in Figure 5.2.

Figure 5.4. Directions obtained after thermal demagnetization at 250° C. The VRM component has been effectively removed, but no directional grouping is apparent.

Figure 5.5. Directions obtained after thermal demagnetization at 350° C. There is no apparent trend visible in this representation.

Figure 5.6. Typical demagnetization trajectories of samples from Falaise Ouest. In orthogonal projection, filled squares denote declination; unfilled squares represent inclination. In equal area projection, symbols as in Figure 5.2.

Directions after heating at 100° C. for 1 hour

Falaise Ouest section
Anticosti Island, Quebec, Canada

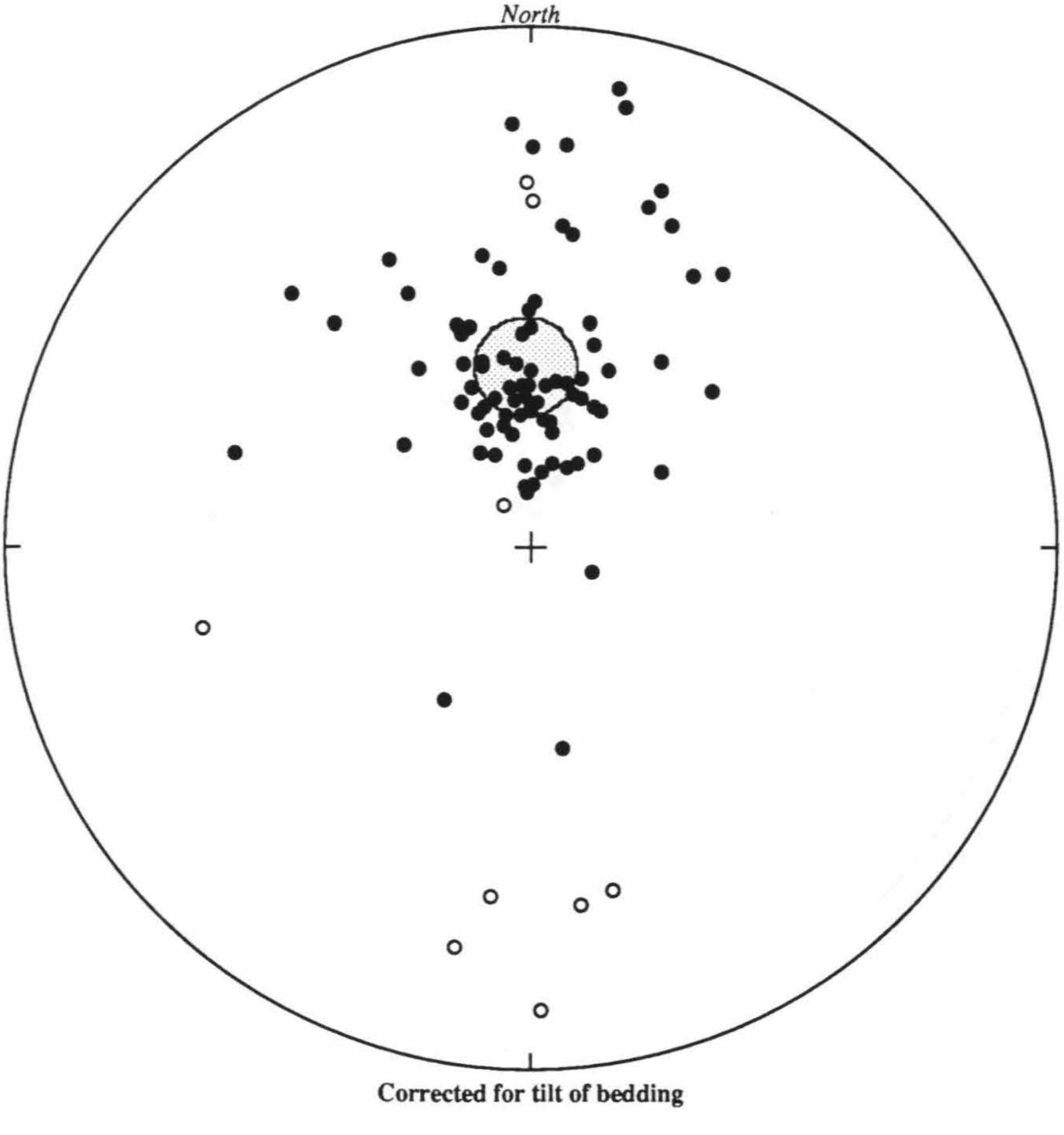

Figure 5.3

Directions after heating at 250° C. for 1 hour

Falaise Ouest section
Anticosti Island, Quebec, Canada

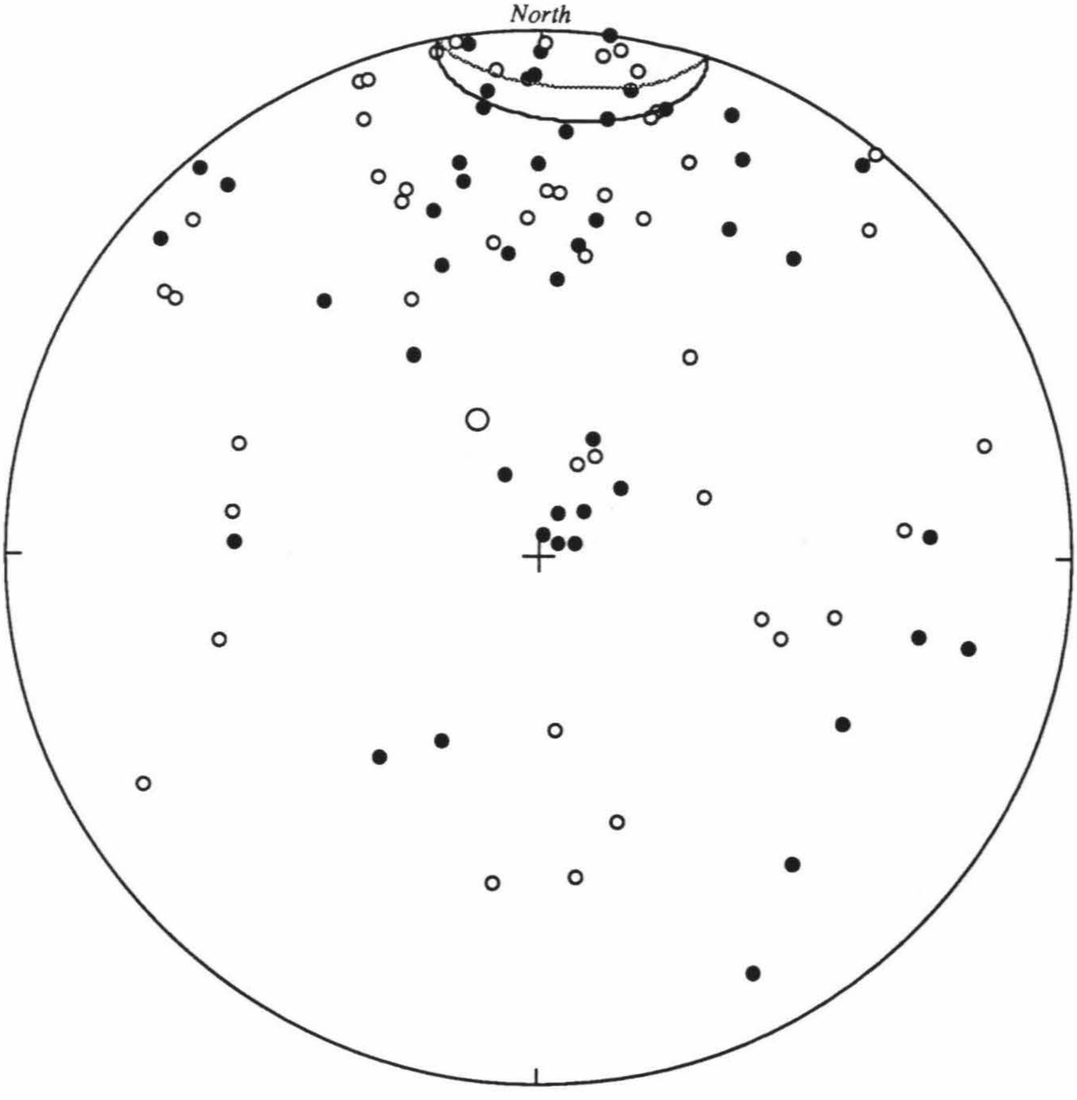

Corrected for tilt of bedding

Figure 5.4

Directions after heating at 350° C. for 1 hour

Falaise Ouest section
Anticosti Island, Quebec, Canada

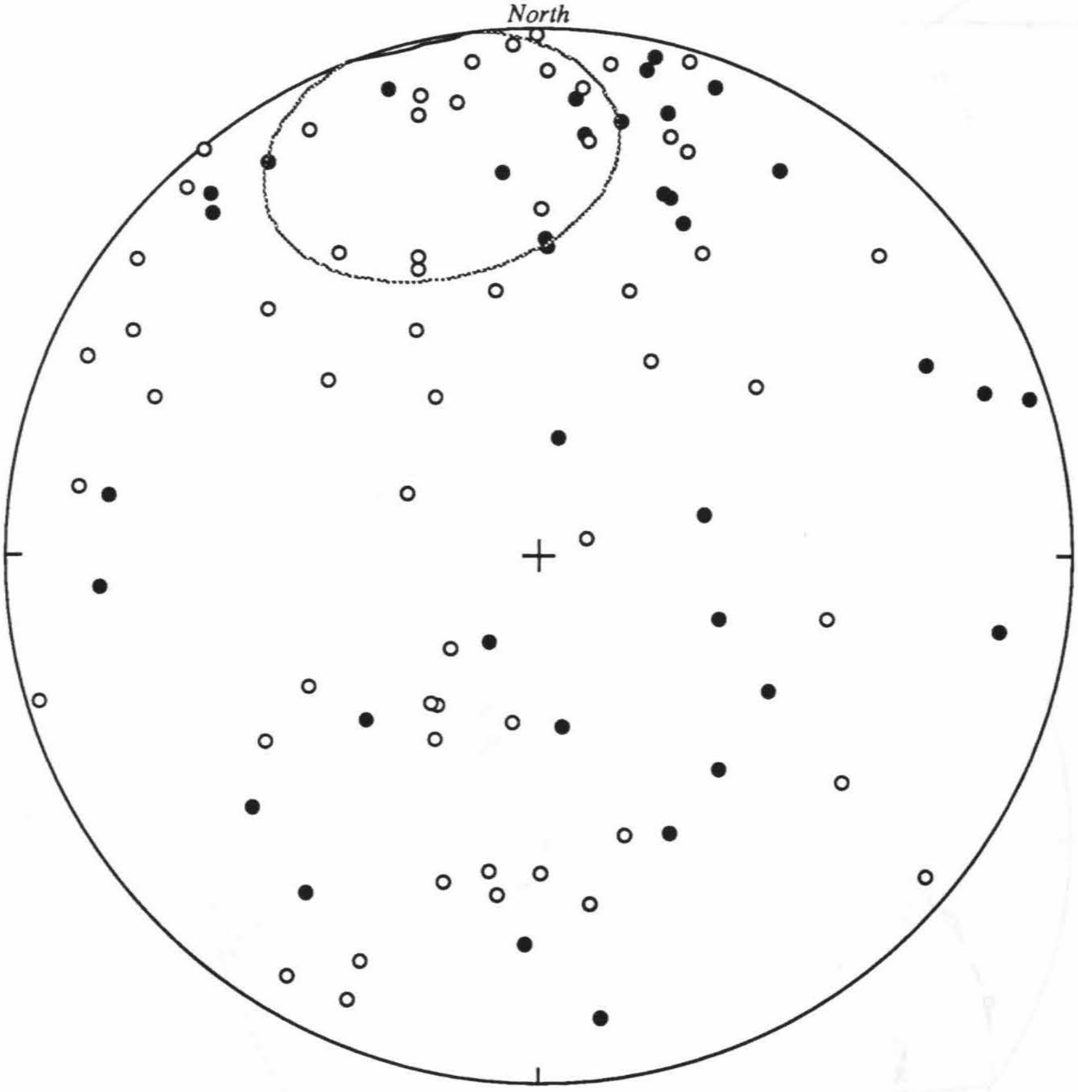

Corrected for tilt of bedding

Figure 5.5

Progressive demagnetization of sample AQC 12.0

Falaise Ouest section

Anticosti Island, Quebec, Canada

Corrected for tilt of bedding

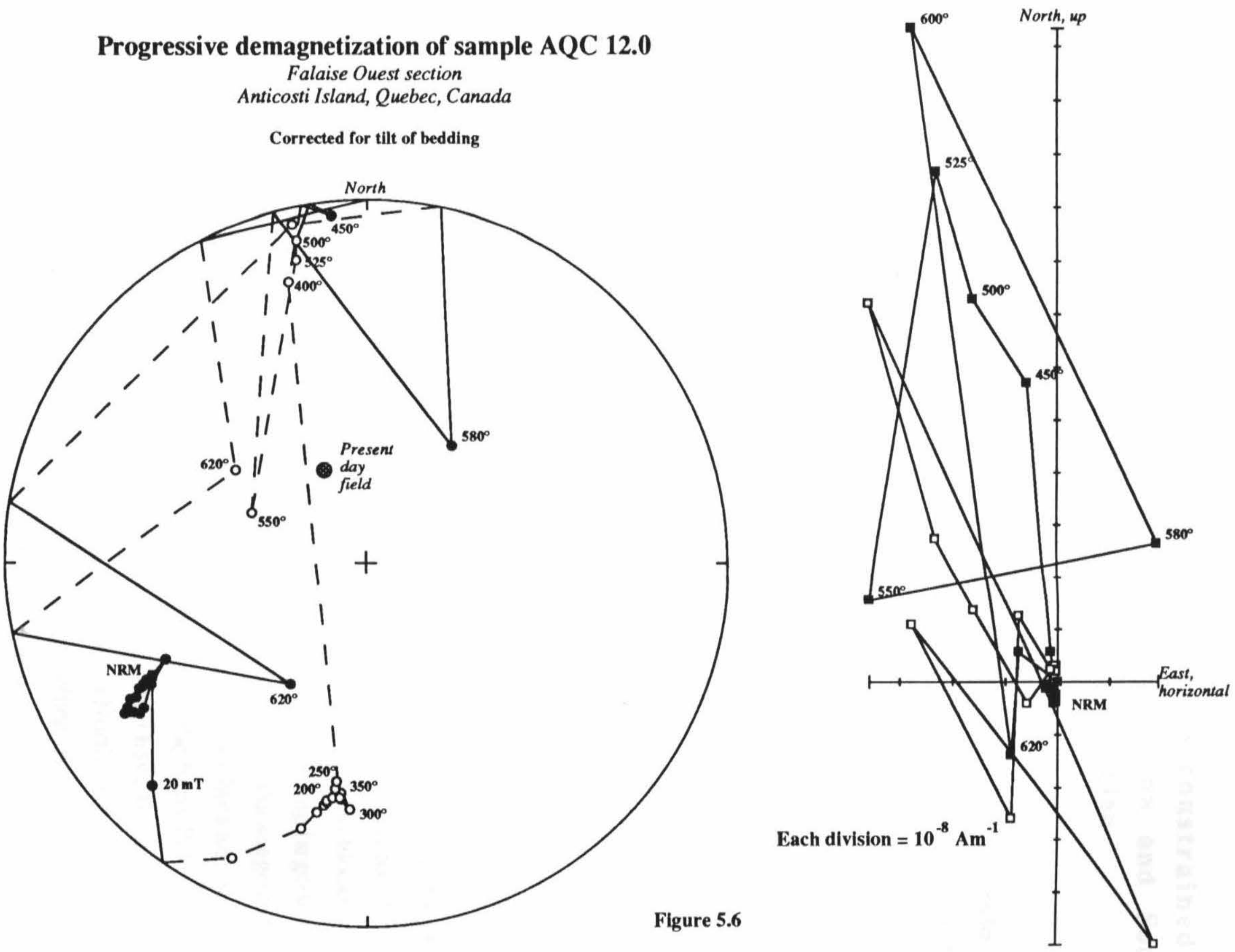

Figure 5.6

Chapter Six Magnetostratigraphically-constrained paleogeographic positions of the North China and South China Blocks during the Cambrian-Ordovician boundary interval

This study represents the first application of magnetostratigraphic techniques to Paleozoic paleogeographic reconstructions. It is, in some respects, a fortuitous fact that there has been a great deal of controversy generated over paleogeographic reconstructions for the late Cambrian and Early Ordovician; it provides a ready forum for testing the paleomagnetic data from this study against available data of various kinds.

Paleogeographic reconstructions for Latest Cambrian and Earliest Ordovician time involving 'East Gondwana' (Australia, Antarctica, India, and 'proto-Asian' fragments) have been at odds with each other, dependent on the data base being used. Previous paleomagnetic results from the North China and South China blocks (Lin 1984) allowed preliminary paleolatitude determinations (Lin *et al.* 1985) (Figure 6.1), but the hemispheric ambiguity inherent within paleomagnetic data was not resolved by their correlation techniques or through development of a continuous apparent polar wander path. Instead, the authors based their polarity interpretation on the assumption that large-scale rotations (of approximately 180°) for the two blocks were implausible.

Paleogeographic reconstructions by Burrett and Stait (1986) for the Early Cambrian to the Middle Ordovician, using faunal associations, arrived at much different conclusions than those of Lin *et al.* for the positions of the North China and South China blocks (Burrett and Stait 1986). They concluded that both blocks were undergoing large-scale rotations in conjunction with the 90° counterclockwise rotation of Australia suggested by Klootwijk (1980). The faunal associations also suggested that North China and South China must have been very close to Australia throughout much of the Early Paleozoic.

The magnetostratigraphic correlations outlined in Chapter 3 have allowed definition of polarity for Cambrian-Ordovician boundary-aged samples in North China through correlation with sections from Australia and North America. When the data sets of Lin *et al.* (1985) and Lin (1984) are inverted, 90° of counterclockwise rotation during the Cambrian is apparent, identical to the apparent rotation experienced by Australia during the same time period. This observation strongly suggests that previous polarity interpretations

Figure 6.1. (a) Early Cambrian time paleogeographic reconstruction of Lin *et al.* (1985), showing North China in the southern hemisphere at about 30° latitude and oriented in approximately its present day orientation. Note the position of the South China block with respect to North China. (b).Late Cambrian paleogeographic reconstruction of Burrett and Stait (1986), showing North China and South China next to the present-day northern coast of Australia, and oriented about 90° clockwise from their current position.

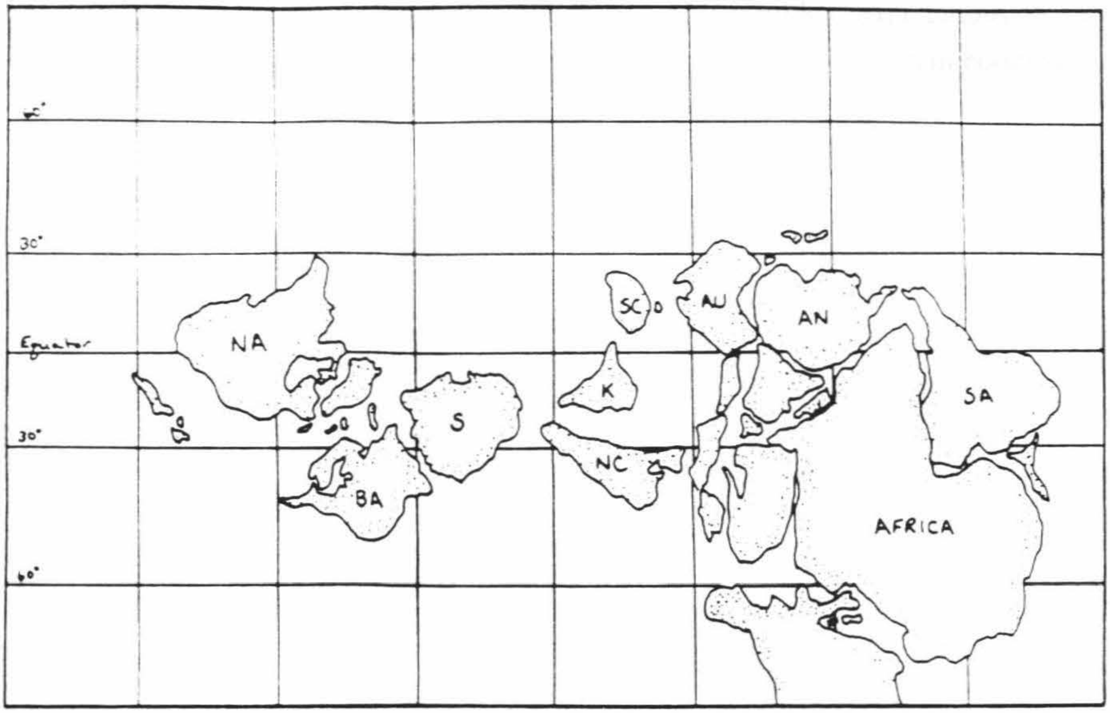
30°
Equator
30°
60°
NA
BA
S
K
NC
SC
AU
AN
SA
AFRICA

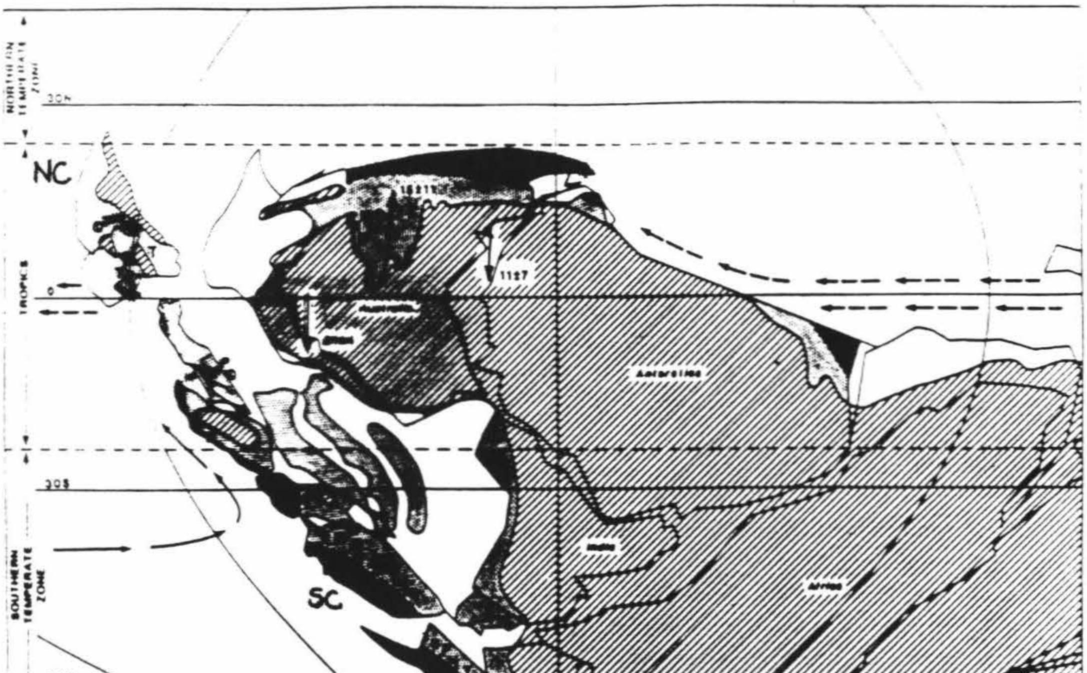
NORTHERN TEMPERATE ZONE
30N
NC
TROPICS
0
30S
SOUTHERN TEMPERATE ZONE
SC
1127
Australia
India
Africa
60S
270
0
90

were inverted, and that the Burrett and Stait models are reasonable interpretations of the paleogeography of 'East Gondwana' at the time of the Cambrian-Ordovician boundary.

Magnetostratigraphically-constrainted positions of the North China and South China Blocks during the Cambrian-Ordovician boundary interval

R.L. Ripperdan and J.L. Kirschvink
Division of Geological and Planetary Sciences 170-25
California Institute of Technology
Pasadena, California U.S.A. 91125

Several paleogeographic reconstructions for Early and Late Cambrian time have had strikingly different solutions for the positions of 'proto-Asiatic' microcontinental blocks near what is now the northern margin of Australia.[1,2,3] Those based primarily on paleomagnetic results[1,2] have neither resolved the hemispheric ambiguity inherent in the data, nor addressed the question of whether the blocks strewn along the margin were connected to or moving independently of a postulated Austral-Asian supercontinent during the Cambrian. Our results, based on magnetostratigraphic correlations in Upper Cambrian carbonates from North America, Kazakhstan, China, and Australia,[4] resolve the Late Cambrian paleogeographic position of the North China block, constraining it to the northern hemisphere for most of the Cambrian period. Comparison of Early and Late Cambrian and Late Precambrian-age pole positions from the North China[4,5,6] and South China blocks[1,4,5,7] and Australia[4,8,9,10,11,12] suggest that they simultaneously underwent about 90° of counterclockwise rotation during Cambrian time. These results support the hypothesis that the North China and South China blocks were an integral part of an Austral-Asia supercontinent throughout the entire Cambrian period, although the observation is made that true polar wander could account for the similarity of rotations.

Introduction

The composition and integrity of the northern and western margins of an Early Paleozoic Austral-Asian supercontinent, and the orientations of the constituent blocks, have been the subjects of sharp disagreements between paleogeographic reconstructions based on paleomagnetic data and those relying on faunal relationships. In particular, the positions of the North China and South China blocks with respect to each other and to Australia have been given markedly different solutions. Lin et al.[1] placed the North China block at 30° S. and the South China block at the equator in the Early Cambrian, basing the positions primarily on their own paleomagnetic results[1,5] and a preliminary interpretation of polarity. In their reconstruction, North China is in approximately the same orientation as today, while South China is rotated 90° counterclockwise from the present. Both are distinctly separated from Australia.

Burrett and Stait[3] based their paleogeographic reconstructions primarily on faunal associations. They placed the North China Block in northern sub-tropical latitudes at the beginning of the Cambrian, adjacent to what is now the northern margin of Australia. Their reconstructions have the North China Block rotating counterclockwise with Australia beginning in the Early Cambrian, and by the end of the period, oriented about 60° clockwise from its modern orientation and separated slightly from Australia. In their model the South China Block is also close to Australia, also moving into more southerly latitudes in the Early Cambrian, and also oriented about 90° clockwise from the present by the end of the period. They further concluded that the distributions of faunas required that the relative positions of microcontinents with respect to Australia be roughly maintained throughout the Cambrian. Another reconstruction based primarily on paleomagnetic data, by Scotese[2], places the North China block near the equator and north of South China in the Late Cambrian, but rotated 180° from the present and essentially independent of Australia.

Fundamental to establishing a reliably-constrained configuration for the western Austral-Asian margin at the end of the Cambrian is resolution of the hemispheric ambiguity inherent in paleomagnetic data. There are essentially two strategies for accomplishing this objective. The method used in virtually all previous studies is construction of an apparent polar wander path (APWP) for the continental unit, using a large number of closely-spaced pole positions with well-constrained ages. Such data are presently available only for a few of the larger cratons. A second method, applied here for the first time to Early Paleozoic reconstructions, utilizes magnetostratigraphic correlations where one of the sections has known polarity (through use of the first method). This strategy has a decided advantage when working in areas from which there are few or no previous results, or where there are large gaps in the stratigraphic record, both of which are true for the North China and South China blocks in Early Paleozoic time.

Magnetostratigraphic constraints

Magnetostratigraphic results from Cambrian-Ordovician boundary-aged sections in the North China block, Newfoundland, Kazakhstan, Texas, and Australia have identified correlatable normal polarity events preserved within the Upper Cambrian conodont subzones *Proconodontus posterocostatus* and *P. muelleri,* and possibly also within the Upper Cambrian/Lower Ordovician conodont zone *Cordylodus proavus*, following a long interval of predominantly reverse polarity during the Late Cambrian[4,13] (Figure 1). Geomagnetic polarities for the North China, western Newfoundland, and Kazakhstan sections were established through magnetostratigraphic correlation with results from Upper Cambrian sections in central Texas and Australia. Geomagnetic polarities for the latter were established by comparison with the APWP of their respective cratons.

Only one of the sample localities, Kazakhstan, yields results that conclusively satisfy standard paleomagnetic criteria for reliability; they pass the fold test. The sections from North China provisionally pass the reversal test, but the results are statistically not reliable because many samples possess multiple, overlapping components. Pole positions obtained from western Newfoundland sections approximately pass fold tests between sites, but substantial differences in site mean directions exist that are probably related to deformation of the Cow Head Group during emplacement as the northern element of the Humber Allochthon. Only about one-fourth of the central Texas samples yield results that are consistent with those from Watt et al.[13]; the other samples demonstrate serious overprinting through diagenesis and/or complete viscous remagnetization by the present geomagnetic field. Results from the Australian samples are very consistent, with half of the samples showing stable components during thermal demagnetization, but the low number of samples with normal polarity render the positive reversal test insignificant.

The major argument for the reliability of the results from each of the above-mentioned sections is the consistency in stratigraphic position of Late Cambrian normal polarity events with the Upper Cambrian *Proconodontus muelleri* conodont zone. It seems highly unlikely that stratigraphically-equivalent diagenetic overprinting could occur within sections from such widely-spaced localities as Texas, Newfoundland, Australia, and North China. A more logical explanation would be that the polarities preserved within these sections represent the Late Cambrian geomagnetic field, even though standard paleomagnetic reliability tests may not be applicable or completely satisfied.

Another estimate of the reliability of our results can be gained through comparison of pole positions with the previous results from the area. Our pole from Black Mountain, western Queensland fits well with similar-aged poles from Australia (Table 1). Likewise, our results from the Llano Uplift area, central Texas, compare favorably with the directions determined by Watts et al. for the same area and time period.

Figure 1. Magnetostratigraphic correlations for Cambrian-Ordovician boundary-aged sections in (a) Australia, China, and Texas, and (b) western Newfoundland (from Ripperdan et al., in review). Shaded regions represent conodont biozones.

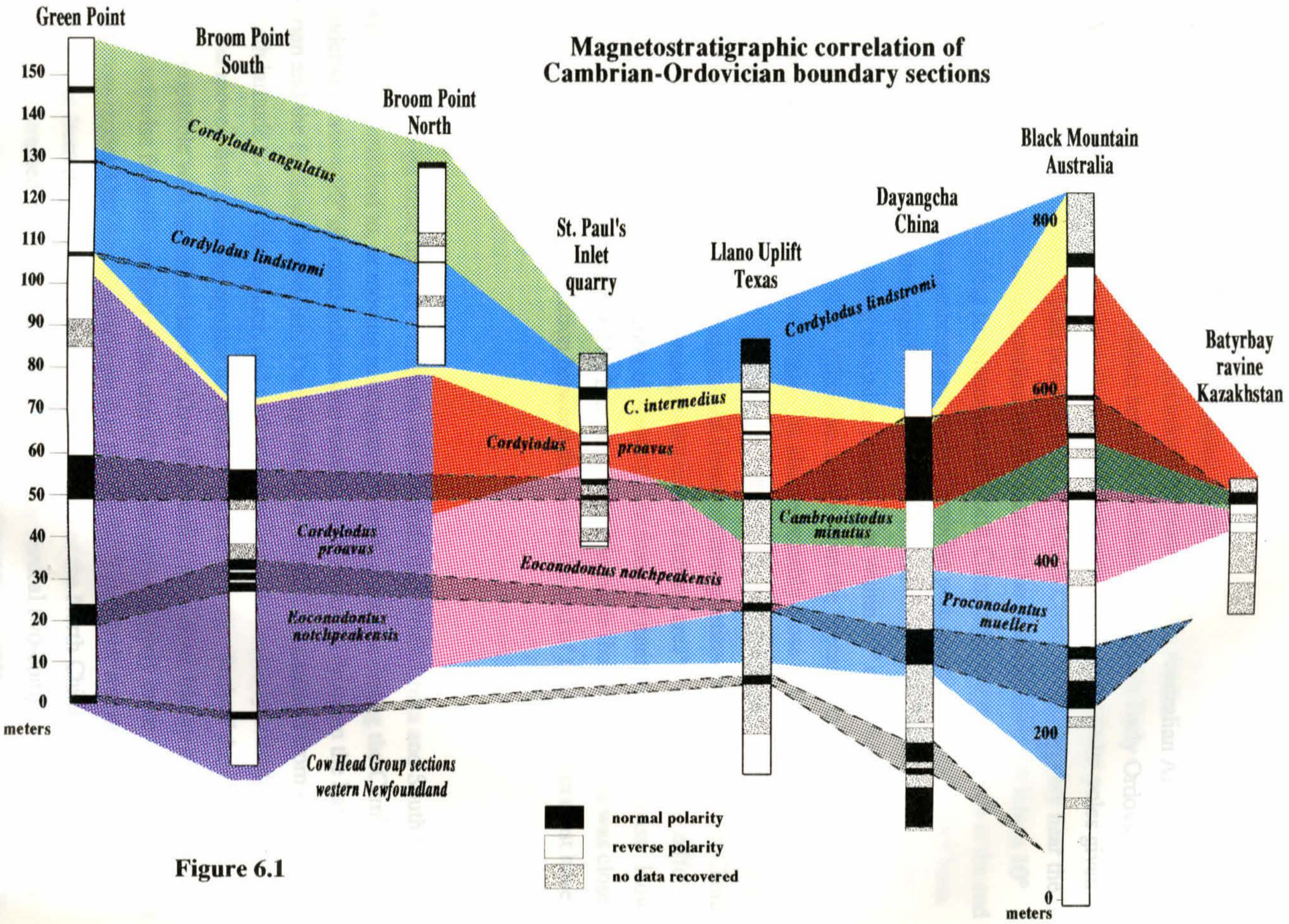
Magnetostratigraphic correlation of
Cambrian-Ordovician boundary sections
Green Point
Broom Point South
Broom Point North
St. Paul's Inlet quarry
Llano Uplift Texas
Dayangcha China
Black Mountain Australia
Batyrbay ravine Kazakhstan
Cordylodus angulatus
Cordylodus lindstromi
Cordylodus proavus
Eoconodontus notchpeakensis
C. intermedius
Cordylodus
proavus
Cambrooistodus minutus
Proconodontus muelleri
Cow Head Group sections
western Newfoundland
150
140
130
120
110
100
90
80
70
60
50
40
30
20
10
0
meters
800
600
400
200
0
meters
normal polarity
reverse polarity
no data recovered

Figure 6.1

Comparisons of apparent polar wander paths

The Late Precambrian to Early Ordovician portion of the Australian APWP indicates about 90° of counterclockwise rotation between Vendian time and the Early Ordovician (Figure 2). When recalculated for a Burrett and Stait-type fit using the Euler poles given in Figure 2, our Late Cambrian pole position from the North China Block lies very near the Late Cambrian portion of the Australian APWP (and can be placed directly on it by a 10° shift in paleolatitude), arguing for placement of North China adjacent to Australia at the end of the Cambrian. Late Precambrian and Early Cambrian pole positions from North China also lie on the corresponding-aged portions of the Australian APWP. Our pole from the South China block, recalculated in similar fashion, lies within 30° of the Late Cambrian portion of the Australian APWP. Likewise, a pole from the Precambrian-Cambrian boundary section at Meischucun, South China[7] is also reasonably close to the Australian APWP, but does not lie directly upon it. Differences between the Australian and South China poles may reflect a pervasive Late Mesozoic and Cenozoic remagnetization event in South China, based on recent paleomagnetic investigations in the Yichang area[14]. Alternatively, differences may also be due to separation of South China from the main continental mass. However, the faunal associations used by Burrett and Stait indicate that South China was close to Australia, so that any separation between the two at the end of the Cambrian must have been minor.

Conclusions

Based on these lines of evidence, we conclude that North China and South China were either attached to, or moving in conjunction with, Australia during the Cambrian, and underwent about 90° of counterclockwise rotation with Australia between the Late Precambrian and the Earliest Ordovician. During that time, North China moved from about 30° north latitude to near the equator, and perhaps even into low southerly latitudes. South China moved from near the equator to about 20° south latitude. Both of these conclusions are compatible with faunal evidence. Also, the North China block had an orientation about 90° clockwise from the present at the end of the Cambrian, slightly more than in the Burrett and Stait model. Our data also indicate that the South China block was oriented about 70° clockwise from its present position. The orientation of the North China block is more highly constrained than the paleolatitude; the nearly vertical two-component least-squares planes of the samples from Xiaoyangqiao allowed for very accurate determination of declination, but less reliable estimates of inclination. Unlike the results from the North China

Table 1. Virtual geomagnetic poles used to construct Vendian to Ordovician portion of apparent polar wander paths for Australia and the North China and South China blocks.

Locality	Symbol	Age	Lat.	Long.	Source
Australia					
Black Mountain	AU13	C/O	-1°	237°	Ripperdan *et al.*[4]
Aroona Dam Fm.	AU12	late C	36°	212°	Klootwijk 1980[8]
Lake Frome Gp.	AU11	mid to late C	31°	207°	Klootwijk 1980[8]
Giles Creek Dolo.	AU10	middle C	40°	210°	Klootwijk 1980[8]
Billy Crk Fm. (Flinders)	AU9	upper early C	37°	200°	Klootwijk 1980[8]
Billy Crk Fm. (Kang.Is)	AU8	upper early C	29°	196°	Klootwijk 1980[8]
Hawker Gp. (top)	AU7	mid-early C	13°	211°	Klootwijk 1980[8]
Hawker Gp. (base)	AU6	earliest C	27°	182°	Klootwijk 1980[8]
Todd River Dol.	AU5	early C	43°	160°	Kirschvink 1978b[9]
Upper Arumbera Ss.	AU4	latest PreC	47°	157°	Kirschvink 1978b[9]
Lower Arumbera Ss.	AU3	latest PreC	44°	162°	Kirschvink 1978b[9]
Elatina Fm.	AU2	Cryogenian	51°	152°	Embleton and Williams 1986[10]
Yilgarn craton dykes	AU1	~750 my	20°	102°	Giddings 1976[11]
North China block					
Xiaoyangqiao section	NC6	C/O	-12°	39°	*Ripperdan et al.[4]
Maozhuang Fm.	NC5	early C	-19°	120°	†Lin[5]
Jing'eryu Fm. (10c)	NC4	late Prot.	5°	139°	Elston *et al.*[6]
Jing'eryu Fm. (10b)	NC3	late Prot.	3	146°	Elston *et al.*[6]
Jing'eryu Fm. (10a)	NC2	late Prot.	-12°	170°	Elston *et al.*[6]
Xiamaling Fm.	NC1	late Prot.	-22°	209°	Elston *et al.*[6]
Souh China block					
Huanghuachang sec.	SC3	C/O	-27°	11°	Ripperdan et al.[4]
Tianheban Fm.	SC2	early C	-7°	10°	†Lin et al.[1]
Meischucun sec.	SC1	PC/C	-68°	91°	†Van der Voo and Wu[7]

Ages: O) Ordovician; C) Cambrian; PC) Precambrian; Prot.) Proterozoic
*Estimated pole position.
†Interpreted polarity has been inverted from the original reference.

Figure 2. Precambrian to Earliest Ordovician apparent polar wander paths for Australia and the North and South China blocks, after re-fitting of North and South China to Australia (based in part on Burrett and Stait model) using the following Euler poles: North China 22° N. 120.5° E., 179.3° rotation; South China 5.8° N. 111.0° E., 162.8° rotation.

Late Precambrian to Earliest Ordovician Apparent Polar Wander Paths for Australia and the North and South China Blocks

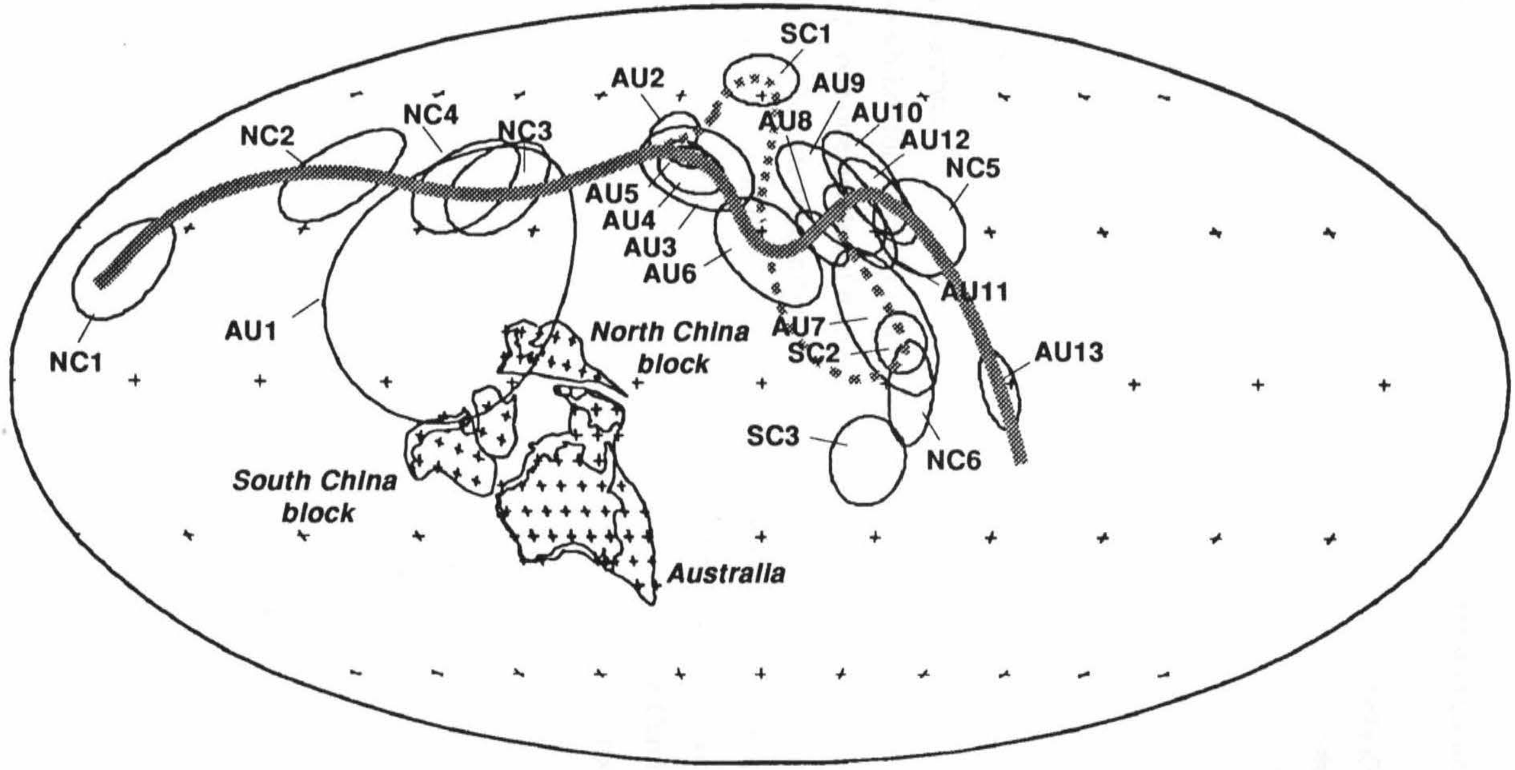

block, obtained from the Yangtze Gorges area have much smaller deviations in inclination, allowing a more precise determination of paleolatitude than of orientation.

Our paleogeographic reconstructions of 'East Gondwana' for Middle Early Cambrian and Cambrian-Ordovician boundary times are given in Figure 3. Both show the present northern margin of Australia as inboard from an amalgamation of microcontinental blocks which apparently remained coherent with Austral-Asia throughout the Cambrian, similar to the Burrett and Stait model. In their reconstructions they slightly separated the various continental fragments from Australia, basing their reasoning in part on the interpretation that the Early Cambrian Antrim Plateau basalts in northern Australia are the result of rifting of a continental block[15]. Any separation must have been minimal, however, since the paleomagnetic data argue for coordinated rotational motion of the Chinese blocks and Australia throughout the Cambrian.

An alternative possibility for the congruent rotations of the Chinese microcontinents and Australia is that an episode or episodes of true polar wander occurred during the Cambrian. The dashed portion of the Late Precambrian to Earliest Ordovician APWP shown in Figure 2 reflects the assumption that all of the data used are equally reliable. Three sharp hairpins are present; one around the time of the Precambrian-Cambrian boundary, one occurring around the end of the Early Cambrian, and one in the Middle to Late Cambrian. Midpoints of the APWP between the cusps of hairpins approximately trace out a smooth arc reflecting counterclockwise rotation of Australia, but the presence of the hairpins creates the impression that rapid and erratic plate motion was occurring. Others have noted that Australia, during the Latest Precambrian and throughout the Cambrian, underwent rotation at discrete intervals, interspersed with periods of quasi-stasis[8]. One possible explanation for this type of 'apparent plate motion' is that Australia was undergoing continual counterclockwise rotation, with a slowly wandering rotational (and magnetic) axis superimposing alternatingly additive and subtractive shifts of as much as 45 degrees. A curious coincidence is that, during the Cambrian, perhaps as much as 95% of the global continental mass may have been in the southern hemisphere[16].

When assuming that true polar wander did not occur, the simplest explanation for the equivalent rotations is that North and South China were attached to Australia during the Cambrian, which in turn, makes it reasonable to compare isochronous pole positions from Australia and North and South China. Permitting the possibility that true polar wander was responsible for the similarities in rotation removes the constraint that North and South China must have been tectonically associated with Australia to have had identical rotations.

Figure 3. Paleogeographic reconstructions of an Austral-Asian supercontinent (East Gondwana) for (a) the Middle Early Cambrian, and (b) the Cambrian-Ordovician boundary.

Early Cambrian paleogeographic reconstruction for East Gondwana

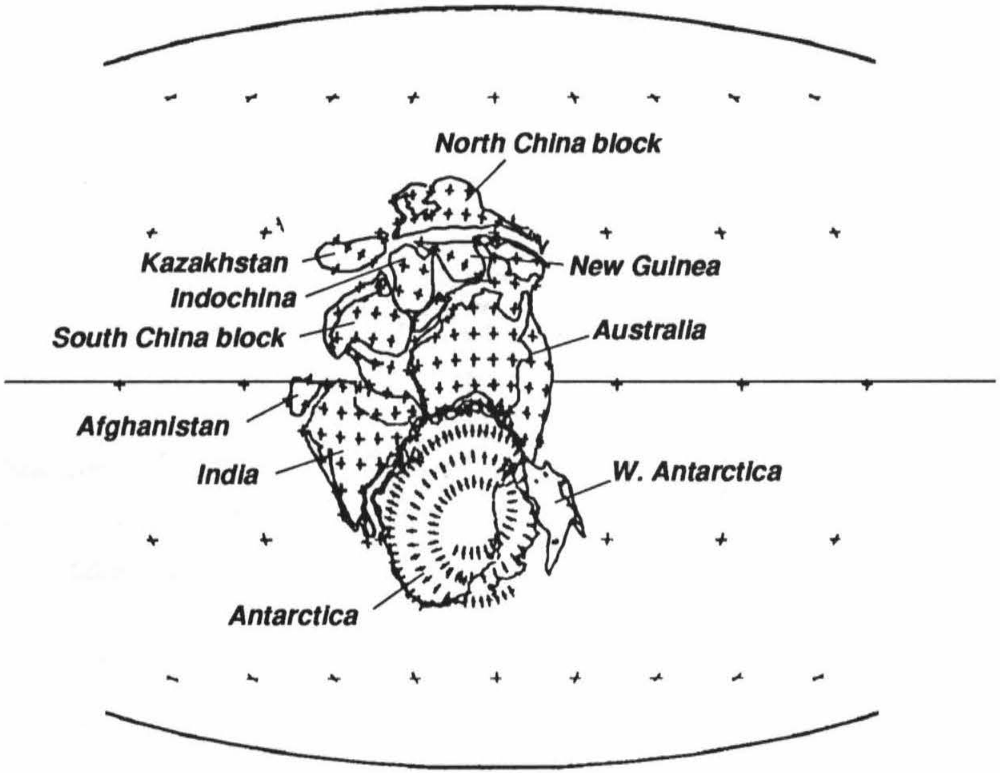

Cambrian-Ordovician boundary paleogeographic reconstruction for East Gondwanaland

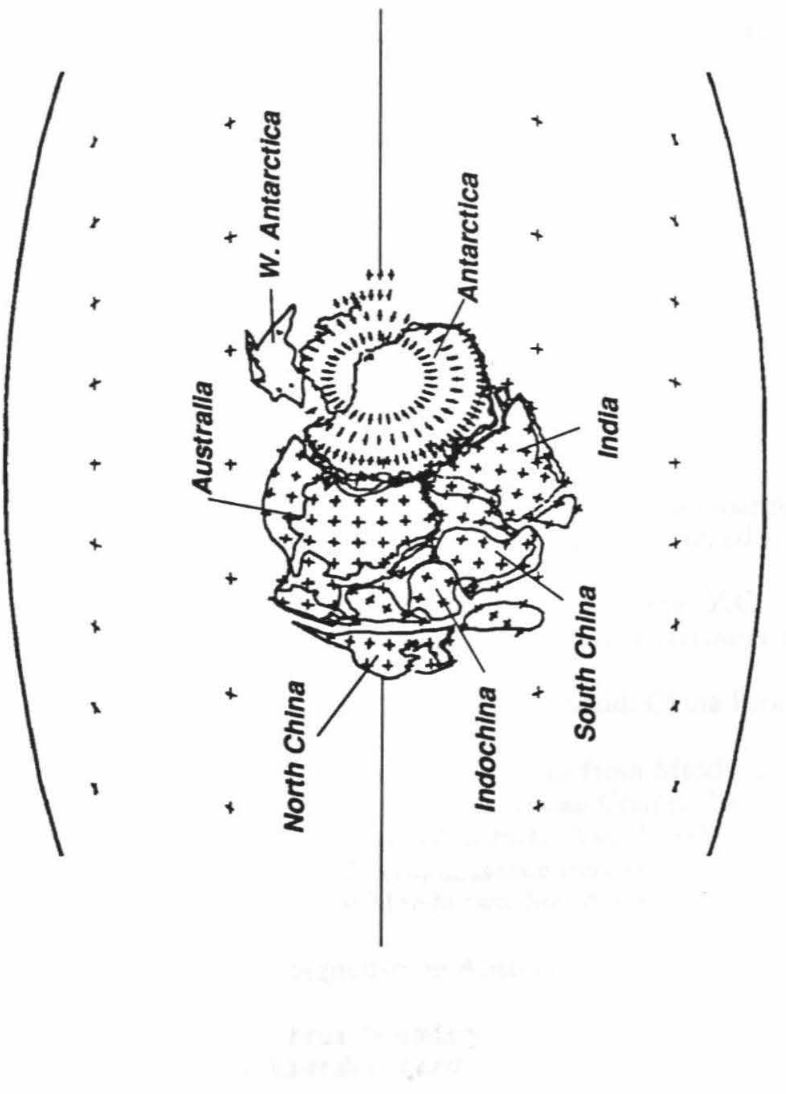

However, even if true polar wander were responsible for the observed rotations, it seems unlikely that the similarities between Early and Late Cambrian pole positions from the North and South China blocks (after recalculation to accomodate a fit against Australia), and corresponding-aged segments of the Australian APWP, are coincidental. The most logical interpretation for the existing paleomagnetic data is that North and South China were either very near or attached to Australia throughout the Cambrian, and rotated about 90° counterclockwise with Australia during that time.

Acknowledgements

This study was supported by National Science Foundations grant EAR-8721391. The authors wish to thank A.K. Kirschvink and C. Budney for their assistance with sample collection and analysis, and A. Boucot, J. Shergold, A.R. Palmer, and B. Stait for helpful discussions.

References

[1]Lin, J.-l., Fuller, M., and Zhang, W.-y. 1985. Paleogeography of the north and south China blocks during the Cambrian. *Journal of Geodynamics* **2**: 91-114.

[2]Scotese, C.R. 1987. Plate tectonic development of the Circum-Pacific (Panthallasic Ocean) during the Early Paleozoic. In *Circum-Pacific Orogenic Belts and the Evolution of the Pacific Ocean Basin* (J.W. Monger and J. Francheteau, eds.), American Geophysical Union Geodynamics Series **18**:49-57.

[3]Burrett, C. and Stait, B. 1986. China and southeast Asia as part of the Tethyan margin of Cambro-Ordovician Gondwanaland. In *Shallow Tethys 2* (K.G. McKenzie, ed.), pp. 65-77. International Symposium on Shallow Tethys 2, Wagga Wagga.

[4]Ripperdan, R.L., Kirschvink, J.K., Apollonov, M.K., Ma, G.G., and Zhang, Z.C. Magnetostratigraphy across the Cambrian-Ordovician boundary. In review (*Geological Magazine*).

[5]Lin, J.-l. 1984. The apparent polar wander paths for the North and South China Blocks. Ph.D. thesis, University of California, Santa Barbara. 248 pp.

[6]Elston, D.P., Zhang, H., and Zhang, W. 1989. Paleomagnetic poles from Middle and Late Proterozoic Changcheng, Jixian, and Qingbaikou Groups, Jixian County, North China [abstract], 28th International Geological Congress Abstracts, Vol. 1, 448-449.

[7]Wu, F., Van der voo, R., and Liang, Q.Z. 1989. Reconnaissance magnetostratigraphy of the Precambrian-Cambrian boundary section at Meishucun, Southwest China. *Cuadernos de Geologia Iberica* **12**: 205-222.

[8]Klootwijk, C.T. 1980. Early Paleozoic paleomagnetism in Australia. *Tectonophysics* **64:** 249-332.

[9]Kirschvink, J.L. 1978. The Precambrian-Cambrian boundary problem: Paleomagnetic directions from the Amadeus Basin, Central Australia. *Earth and Planetary Science Letters* **40**:91-100.

[10]Embleton, B.J.J. and Williams, G.E. 1986. Low palaeolatitude of deposition for Late Precambrian periglacial varvites from South Australia: Implications for palaeoclimatology. *Earth and Planetary Science Letters* **58**: 383-394.

[11]Giddings, J.W. 1976. Precambrian palaeomagnetism in Australia I: basic dykes and volcanics from the Yilgarn Block. *Tectonophysics* **30**: 91-108.

[12]Duff, B.A., and Embleton, B.J.J. 1976. Palaoemagnetic directions in Precambrian basic intrusives of the Mount Isa province, Australia. *Earth and Planetary Science Letters* **28**:418-426.

[13]Watts, D.R., Van der Voo, R., and Reeve, S.C. 1980. Cambrian paleomagnetism of the Llano Uplift, Texas. *Journal of Geophysical Research* **85**(B10): 5316-5330.

[14]Kent, D.V., Zeng, X., Zhang, W.Y., and Opdyke, N.D. 1987. Widespread late Mesozoic to Recent remagnetization of Paleozoic and lower Triassic sedimentary rocks from South China. *Tectonophysics* **41**:113-133.

[15]Veevers, J.J. (ed.) 1984. Phanerozoic earth history of Australia. Oxford: Clarendon Press.

[16]Kirschvink, J.L. in review.

Chapter Seven Summary

The past 100 years have seen major changes in the way geologists think about global geological phenomenon. As biostratigraphic correlations have become more refined, questions concerning the timing and mechanism of global events have come to the forefront. Especially in today's philosophical environment, which has retained elements of the old ideology of earth history as punctuated by globally significant events providing natural demarcations of geologic time, it becomes especially important that global correlations be done within a globally isochronous framework. Magnetic polarity reversal stratigraphy provides that framework by utilizing globally simultaneous events with transition times on the order of 10,000 years.

The application of magnetostratigraphic techniques to problems concerning definition of a globally applicable Cambrian-Ordovician boundary indicate that temporal differences exist between the major conodont biozones suggested as boundary horizons. In particular, correlations between North China, Australia, North America, and Kazakhstan suggest that the first observed occurrence of*Cordylodus proavus* may provide a suitably isochronous horizon, but that sampling bias (due to extremely low specimen recovery) may be obscuring the 'real' first occurrence of *Cordylodus proavus* within the important western Newfoundland sections. They also confirm that problems exist in correlating the level of the first observed specimens of *Cordylodus lindstromi*, that may stem from observer-dependent taxonomic assignments.

Application of magnetostratigraphic techniques is not always successful. Results from several important Silurian-Devonian boundary interval sections within the Barrandian area of Prague Basin, Czechoslovakia do not yield a polarity stratigraphy. It appears likely that many of the characteristic directions isolated using samples from the international Silurian-Devonian boundary stratotype section at Klonk, and from stratotype sections within the Daleje Valley at Reporyje, were acquired immediately before or contemporaneous with Hercynian folding of the Prague Basin during the Carboniferous, so that stratigraphic information has been lost. Some samples preserve a component which may record the geomagnetic field at the time of deposition, but intervals between these samples are too great to make stratigraphic relationships meaningful. Important paleogeographic information can be inferred from these results, however, suggesting major latitudinal transport for the Bohemian Massif during the Devonian. Future work is needed to confirm the time of acquisition of the observed components before conclusions about plate motion can be constrained.

Some magnetostratigraphic investigations yield neither useful stratigraphic nor directional information because of magnetically-unstable lithologies. Directions from the Ordovician-Silurian boundary parastratotype section at Falaise Ouest, Anticosti Island, Quebec, are essentially random during thermal demagnetization experiments, and no useful conclusions concerning the paleogeographic position of the section can be gleaned from them.

Successful application of magnetostratigraphic techniques within magnetically-stable lithologies, however, can yield important paleogeographic information, especially from continental entities from which little or no previous paleomagnetic data has been obtained. Magnetostratigraphic correlations around the Cambrian-Ordovician boundary, and comparisons with the Australian apparent polar wander path, indicate that North China (and probably South China) were rotating with Australia during the Cambrian. Future work may reveal whether this observed coordinated rotation was the result of plate motion or translocation of the earth's magnetic pole in the form of true polar wander.

References

Briden, J.C. and Duff, B.A. 1981. Pre-Carboniferous paleomagnetism of Europe north of the Alpine orogenic belt. In *Paleoreconstruction of the Continents* (ed.M.W. McElhinny and D.A. Valencio), pp. 137-150. American Geophysical Union, Washington, D.C.

Burrett, C. and Stait, B. 1986. China and southeast Asia as part of the Tethyan margin of Cambro-Ordovician Gondwanaland. In *Shallow Tethys 2* (K.G. McKenzie, ed.), pp. 65-77. International Symposium on Shallow Tethys 2, Wagga Wagga.

Chen Jun-Yuan (ed.) 1986. *Aspects of Cambrian-Ordovician Boundary in Dayangcha, China* . Beijing: China Prospect Publishing House. 410 pp.

—— , Qian Yi-Yuan, Zhang Jun-Ming, Lin Yao-Kun, Yin Lei-Ming, Wang Zhi-Hao, Wang Zong-Zhi, Yang Jie-Dong, and Wang Yhing-Xi 1988. The recommended Cambrian-Ordovician Boundary stratotype of the Xiaoyangqiao section (Dayangcha, Jilin Province), China. *Geological Magazine* **125**: 415-444.

Chlupac, I. 1972. The Silurian-Devonian boundary in the Barrandian. *Bulletin of Canadian Petroleum Geology* **20**(1): 104-174.

—— 1982. Preliminary submission for Lower-Middle Devonian boundary stratotype in the Barrandian area. *Cour. Forsch.-Inst. Senckenberg* **55**: 85-96.

Cisowski, S. 1981. Interacting vs. non-interacting single domain behavior in natural and synthetic samples. *Physics of the Earth and Planetary Interiors* **26**: 56-62.

Collinson, D.W. 1983. *Methods in Rock Magnetism and Palaeomagnetism: Techniques and Instrumentation*. Chapman and Hall.

Deutsch, E.R. and Prasad, J.N. 1987. Ordovician paleomagnetic results from the St. George and Table Head carbonates of western Newfoundland. *Canadian Journal of Earth Sciences* **24**(9): 1785-1796.

Druce, E.C., Shergold, J.H., and Radke, B.M. 1982 A reassessment of the Cambrian-Ordovician boundary section at Black Mountain, Western Queensland, Australia. In *The Cambrian-Ordovician Boundary: Sections, Fossil Distributions, and Correlations* (ed. M.G. Bassett and W.T. Dean), pp. 193-209. National Museum of Wales, Geological Series no. 3, Cardiff.

Duff, B.A., and Embleton, B.J.J. 1976. Palaoemagnetic directions in Precambrian basic intrusives of the Mount Isa province, Australia. *Earth and Planetary Science Letters* **28**: 418-426.

Ellwood, B.B., Chrzanowski, T.H., Hrouda, F., Long, G.J. and Buhl, M.L. 1988. Siderite formation in anoxic deep-sea sediments: a synergetic bacterially controlled process with important implications for paleomagnetism. *Geology* **16**(11):980-982.

Elston, D.P., Zhang, H., and Zhang, W. 1989. Paleomagnetic poles from Middle and Late Proterozoic Changcheng, Jixian, and Qingbaikou Groups, Jixian County, North China [abstract], 28th International Geological Congress Abstracts, Vol. 1, 448-449.

Embleton, B.J.J. and Williams, G.E. 1986. Low palaeolatitude of deposition for Late Precambrian periglacial varvites from South Australia: Implications for palaeoclimatology. *Earth and Planetary Science Letters* **58**: 383-394.

Epstein, A.G., Epstein, J.B., and Harris, L.D. 1977. Conodont color alteration- an index of organic metamorphism. *Professional paper U.S. geological survey* **995**: 1-27.

Fortey, R.A., Landing, E., and Skevington, D. 1982. Cambrian-Ordovician boundary sections in the Cow Head Group, western Newfoundland. In *The Cambrian-Ordovician Boundary: Sections, Fossil Distributions, and Correlations* (ed. M.G. Bassett and W.T. Dean), pp. 95-129. National Museum of Wales, Geological Series no. 3, Cardiff.

Giddings, J.W. 1976. Precambrian palaeomagnetism in Australia I: basic dykes and volcanics from the Yilgarn Block. *Tectonophysics* **30**: 91-108.
Hall, S.A. and Evans, I. 1988. Paleomagnetic study of the Ordovician Table Head Group, Port au Port Peninsula, Newfoundland. *Canadian Journal of Earth Sciences* **25**: 1407-1419.
Harrison, C.G.A. and Somayajulu, B.L.K. 1966. Behaviour of the earth's magnetic field during a reversal. *Nature* **212**: 1193-1195.
Henningsmoen, G. 1973. The Cambro-Ordovician boundary. *Lethaia* **6**: 423-439.
James, N.P. and Stevens, R.K. 1986. Stratigraphy and correlation of the Cambro-Ordovician Cow Head Group, western Newfoundland. *Geological Survey of Canada, Bulletin* **366**, 143 pp.
Kent, D.V., Zeng, X., Zhang, W.Y. and Opdyke, N.D. 1987. Widespread late Mesozoic to Recent remagnetization of Paleozoic and lower Triassic sedimentary rocks from South China. *Tectonophysics* **139**: 133-143.
Khramov, A.N., Rodionov, V.P., and Komissarova, R.A. 1965. New data on the Paleozoic history of the geomagnetic field in the USSR. In *The present and Past of the Geomagnetic Field*, pp. 206-213. Nauka Press, Moscow.
Kirschvink, J.L. 1978. The Precambrian-Cambrian boundary problem: Magnetostratigraphy of the Amadeus Basin, Central Australia. *Geological Magazine* **115**: 139-150.
—— 1980. The least squares line and plane and the analysis of palaeomagnetic data. *Geophysical Journal of the Royal astronomical Society* **62**: 699-718.
—— and Rozanov, A. Yu. 1984. Magnetostratigraphy of Lower Cambrian strata from the Siberian Platform: a palaeomagnetic pole and preliminary polarity time scale. *Geological Magazine* **121**: 189-203.
Klootwijk, C.T. 1980. Early Paleozoic paleomagnetism in Australia. *Tectonophysics* **64:** 249-332.
Lapworth, C. 1879. On the Tripartite Classification of the Lower Palaeozoic Rocks. *Geological Magazine,* New Series, Decade II **6**: 1-15.
Lin, J.-l. 1984. The apparent polar wander paths for the North and South China Blocks. Ph.D. thesis, University of California, Santa Barbara. 248 pp.
——, Fuller, M., and Zhang, W.-y. 1985. Paleogeography of the north and south China blocks during the Cambrian. *Journal of Geodynamics* **2**: 91-114.
Lowrie, W. and Fuller, M.D. 1971. On the alternating field demagnetization characteristics of multidomain thermoremanence in magnetite. *Journal of Geophysical Research* **76**: 6339-6349.
—— and Heller, F. 1982. Magnetic properties of marine limestones. *Reviews of Geophysics and Space Physics* **20**(2): 171-192.
McCabe, C., Van der Voo, R., Peacor, D.R., Scotese, C.R., and Freeman, R. 1983. Diagenetic magnetite carries ancient yet secondary remanence in some Paleozoic sedimentary carbonates. *Geology* **11**(4): 221-223.
McElhinny, M.W. 1964. Statistical significance of the fold test in palaeomagnetism. *Geophysical Journal of the Royal astronomical Society* **8**: 338-340.
—— 1973a. *Palaeomagnetism and Plate Tectonics*. Cambridge University Press, 358 pp.
Miller, J.F. 1984. Cambrian and earliest Ordovician conodont evolution, biofacies, and provincialism. In *Conodont Biofacies and Provincialism* (ed. D.L. Clark), pp. 43-68. Geological Society of America, Special Paper **196**.
——, Taylor, M.E., Stitt, J.H., Ethington, R.L., Hintze, L.F., and Taylor, J.F. 1982. Potential Cambrian-Ordovician boundary stratotype sections in the western United

States. In *The Cambrian-Ordovician Boundary: Sections, Fossil Distributions, and Correlations* (ed. M.G. Bassett and W.T. Dean), pp. 155-180. National Museum of Wales, Geological Series no. 3, Cardiff.

Opdyke, N.D., Kent, D.V., and Lowrie, W. 1973. Details of magnetic polarity transitions recorded in a high deposition rate deep-sea core. *Earth and Planetary Science Letters* **20**: 315-324.

Pullaiah, G., Irving, E., Buchan, K.L., and Dunlop, D.J. 1975. Magnetization changes caused by burial and uplift. *Earth and Planetary Science Letters* **28**: 133-143.

Radke, B.M. 1982. Late diagenetic history of the Ninmaroo Formation (Cambro-Ordovician), Georgina Basin, Queensland and Northern Territory. *Bureau of Mineral Resources Journal of Australian Geology and Geophysics* **7**: 231-254.

Rodionov, V.P. 1966. Dipole character of the geomagnetic field in the late Cambrian and the Ordovician in the south of the Siberian Platform. *Geologiya i Geofizika* **1**: 94-101.

Sanders, H.L. 1969. Benthic marine diversity and the stability-time hypothesis. *Brookhaven Symp. Biol.* **22**: 71-81.

Scotese, C.R. 1987. Plate tectonic development of the Circum-Pacific (Panthallasic Ocean) during the Early Paleozoic. In *Circum-Pacific Orogenic Belts and the Evolution of the Pacific Ocean Basin* (J.W. Monger and J. Francheteau, eds.), American Geophysical Union Geodynamics Series **18**:49-57.

Seguin, M.K. and Petryk, A.A. 1984. A paleomagnetic study of Upper Ordovician-Lower Silurian strata of Anticosti Island, Quebec. *Northeastern Geology* **6**(1): 25-37.

Veevers, J.J. (ed.) 1984. Phanerozoic earth history of Australia. Oxford: Clarendon Press.

Watts, D.R., Van der Voo, R., and Reeve, S.C. 1980. Cambrian paleomagnetism of the Llano Uplift, Texas. *Journal of Geophysical Research* **85**(B10): 5316-5330.

Wu, F., Van der voo, R., and Liang, Q.Z. 1989. Reconnaissance magnetostratigraphy of the Precambrian-Cambrian boundary section at Meishucun, Southwest China. *Cuadernos de Geologia Iberica* **12**: 205-222.

Zwart, H.J. and Zornsiepen, U.F. 1978. The tectonic framework of Central and Western Europe. *Geol. Mijnb.* **57**: 627-654.